

091696

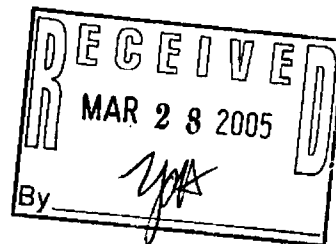
107

LA-UR-05-6397  
December 2005  
ER2005-0580

**Decision Analysis for  
Addressing Groundwater  
Contaminants from the Radioactive  
Liquid Waste Treatment Facility  
Released into Mortandad Canyon**



14266

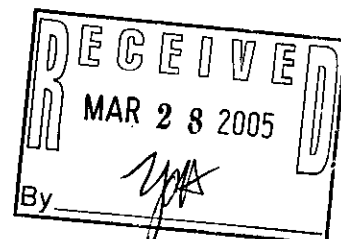


091696

107

LA-UR-05-6397  
December 2005  
ER2005-0580

**Decision Analysis for  
Addressing Groundwater  
Contaminants from the Radioactive  
Liquid Waste Treatment Facility  
Released into Mortandad Canyon**



**Disclaimer**

This document contains data on radioactive materials, including source, special nuclear, and by-product material. The management of these materials is regulated under the Atomic Energy Act and is specifically excluded from regulation under the Resource Conservation and Recovery Act and the New Mexico Hazardous Waste Act. Information on radioactive materials and radionuclides, including the results of sampling and analysis of radioactive constituents, is voluntarily provided to the New Mexico Environment Department in accordance with US Department of Energy policy.

Prepared by  
Environmental Stewardship Division—Environmental Remediation and Surveillance  
Program

Los Alamos National Laboratory, an affirmative action/equal opportunity employer, is operated by the University of California for the United States Department of Energy under contract W-7405-ENG-36.

This report was prepared as an account of work sponsored by an agency of the United States Government. Neither the Regents of the University of California, the United States Government nor any agency thereof, nor any of their employees make any warranty, express or implied, or assume any legal liability or responsibility for the accuracy, completeness, or usefulness of any information, apparatus, product, or process disclosed, or represent that its use would not infringe privately owned rights. Reference herein to any specific commercial product, process, or service by trade name, trademark, manufacturer, or otherwise does not necessarily constitute or imply its endorsement, recommendation, or favoring by the Regents of the University of California, the United States Government, or any agency thereof.

Los Alamos National Laboratory strongly supports academic freedom and a researcher's right to publish; as an institution, however, the Laboratory does not endorse the viewpoint of a publication or guarantee its technical correctness. By acceptance of this article, the publisher recognizes that the US Government retains a nonexclusive, royalty-free license to publish or reproduce the published form of this contribution, or to allow others to do so, for US Government purposes. Los Alamos National Laboratory requests that the publisher identify this article as work performed under the auspices of the US Department of Energy.

# Decision Analysis for Addressing Groundwater Contaminants from the Radioactive Liquid Waste Treatment Facility Released into Mortandad Canyon

December 2005

<u>Chris Echohawk</u>	<u></u>	<u>Project Leader</u>	<u>EES-9</u>	<u>3/28/06</u>
Printed Name	Signature	Title	Organization	Date

<u>Jean Dewart</u>	<u></u>	<u>Program Manager</u>	<u>ENV-ERS</u>	<u>3/28/06</u>
Printed Name	Signature	Title	Organization	Date

## CONTENTS

<b>1.0</b>	<b>INTRODUCTION AND BACKGROUND .....</b>	<b>1</b>
1.1	Background on Risk Assessment and Risk-Based Decision Making .....	1
1.2	Background on Mortandad Canyon .....	4
1.3	Relationship of this Document to Mortandad Canyon Decisions.....	4
1.4	Content and Format of This Document.....	5
<b>2.0</b>	<b>PROBLEM FORMULATION.....</b>	<b>5</b>
2.1	RLTWF Contaminant Source .....	7
2.2	Groundwater Contaminant Distribution in Mortandad Canyon .....	8
2.2.1	Observations .....	8
2.2.2	Pathways.....	13
2.3	Geology in Mortandad Canyon .....	17
2.4	Hydrology in Mortandad Canyon .....	18
2.4.1	Surface Water .....	18
2.4.2	Alluvial Groundwater .....	19
2.4.3	Vadose Zone.....	19
2.4.4	Intermediate-Depth Perched Aquifer .....	20
2.4.5	Regional Aquifer .....	20
2.5	Water-Supply Wells near Mortandad Canyon .....	21
2.6	Generalized Conceptual Site Model .....	21
<b>3.0</b>	<b>RISK-ASSESSMENT METHODOLOGY AND RESULTS .....</b>	<b>23</b>
3.1	Risk-Assessment Approach.....	24
3.2	Summary of Tier-1 Risk Assessment.....	25
3.3	Tier-3 Groundwater Transport Simulation .....	31
3.3.1	Tier-3 Source Term.....	31
3.3.2	Alluvial Groundwater Distribution and Infiltration .....	34
3.3.3	Unsaturated Transport.....	40
3.3.4	Saturated Transport .....	48
3.4	Tier-3 Human-Health Risk Assessment.....	58
3.4.1	Risk-Assessment Results for a Continuous Release Scenario, Assuming Regional-Aquifer Model A .....	64
3.4.2	Risk-Assessment Results for a Continuous-Release Scenario, Assuming Regional-Aquifer Model B .....	69
3.4.3	Risk-Assessment Results for a Discontinued Release Scenario .....	70
3.4.4	Risk-Assessment Results for Alternative Perchlorate Limits.....	71
<b>4.0</b>	<b>IDENTIFICATION AND EVALUATION OF POTENTIAL RISK-MANAGEMENT ACTIVITIES.....</b>	<b>73</b>

4.1	Identifying Potential Risk-Management Activities .....	74
4.2	Evaluation Process .....	74
4.2.1	Parameter Screening .....	74
4.2.2	Correlation Analysis .....	74
4.2.3	Linear Regression Analysis .....	76
4.2.4	Uncertainty-Reduction Analysis .....	80
4.3	Additional Risk-Reduction Possibilities .....	81
4.3.1	Conceptual Model Uncertainty .....	81
4.3.2	Discontinuing Discharges into Mortandad Canyon.....	81
4.3.3	Management of Pumping Rates .....	82
4.4	Summary .....	84
<b>5.0</b>	<b>CONCLUSIONS AND RECOMMENDATIONS .....</b>	<b>84</b>
5.1	Summary of Results .....	84
5.1.1	Baseline Risk-Assessment Results .....	85
5.1.2	Potential Risk-Reduction Activities Analyzed .....	86
5.2	Integration with Ongoing Mortandad Canyon Efforts .....	86
5.2.1	Integration with Field and Laboratory Characterization Activities.....	86
5.2.2	Use of the Risk-Based Decision-Support Process for Groundwater Monitoring Network Design.....	87
5.2.3	Potential Use of the Risk-Based Analysis in Cleanup .....	87
5.2.4	Potential Use of the Risk-Based Analysis for Monitored Natural Attenuation or Defense of Technical Impracticability .....	87
5.3	Concluding Remarks.....	88
<b>6.0</b>	<b>REFERENCES .....</b>	<b>88</b>

**Figures**

Figure 1.1-1.	EPA's tiered risk-assessment process described in RAGS3.....	2
Figure 2.2-1.	Locations of alluvial (MCO-), intermediate (MCOBT-), and regional (R-) groundwater wells in Mortandad Canyon and water supply wells (O- and PM-) near Mortandad Canyon .....	11
Figure 2.2-2.	Concentrations of nitrate (as nitrogen), perchlorate and tritium in the regional wells in the vicinity of Mortandad Canyon (after Longmire 2002, 72614; figure created by D. Broxton)....	15
Figure 2.2-3.	Conceptual model of transport of contaminants from RLWTF in groundwater in Mortandad Canyon (LANL 2004, 82613) .....	16
Figure 2.3-1.	Generalized stratigraphy along Mortandad Canyon.....	17
Figure 2.4-1.	Comparison of time-histories of liquid discharges from the RLWTF to surface water volumes from sources other than the RLWTF for the E200 stream gage near the RLWTF ...	18

Figure 2.6-1.	Generalized conceptual model of contaminant transport and fate from the RLWTF to drinking-water supply wells .....	22
Figure 3.2-1.	Annual average estimates of perchlorate concentration ( $\mu\text{g/L}$ ) releases based on recorded concentrations of nitrate ( $\text{mg/L}$ ) releases. The perchlorate releases represent an estimated 95% upper-confidence limit for the Tier-1 source.....	26
Figure 3.2-2.	Illustration of three 1-D columns used for the Tier-1 unsaturated-zone groundwater transport simulations.....	28
Figure 3.2-3.	Illustration of the relationship between the three unsaturated-zone columns and the grid elements used in the saturated-zone model.....	28
Figure 3.2-4.	Tier-1 concentrations of perchlorate from (a) upper, (b) middle, and (c) lower Mortandad Canyon and (d) for all three sections combined in water pumped from PM-4 and PM-5 (Time = 0 represents 1964).....	29
Figure 3.3-1.	Perchlorate and nitrate (as nitrate) concentrations in pore water from core samples from boreholes in Mortandad Canyon.....	32
Figure 3.3-2.	First 10 realizations of 1000 of infiltration in the upper and lower sections of Mortandad Canyon for the upper/middle-canyon-dominated infiltration model .....	36
Figure 3.3-3.	Comparison of infiltration rates in the upper, middle, lower, and bottom sections of Mortandad Canyon, calculated using the upper/middle-canyon-dominated infiltration model ("Base" in legend) and the lower-canyon-dominated infiltration model ("Case 2" in legend).....	37
Figure 3.3-4.	Results of resistivity survey in Mortandad Canyon, showing several zones of relatively high electrical conductivity (green to blue).....	38
Figure 3.3-5.	Comparison of relative infiltration rates in the upper, middle, and lower sections of Mortandad Canyon using the lower-canyon-dominated uniform infiltration model (solid lines with markers) and the fast-path infiltration model (fast paths represented by solid lines, adjacent nonfast paths represented with dashed lines).....	39
Figure 3.3-6.	Illustration of the 38 1-D columns used in the Tier-3 unsaturated transport model, with three columns that are discussed in text.....	40
Figure 3.3-7.	Comparison of perchlorate total fluxes exiting the base of the unsaturated zone for the Tier-1 point estimates and 10 realizations of Tier-3 upper/middle-canyon-dominated infiltration simulations. The left figure shows results from the upper-canyon column(s), and the right figure shows results from the lower-canyon column(s).....	42
Figure 3.3-8.	Comparison of historical nitrate concentrations in alluvial wells MCO-4 and MCO-6 to simulated input nitrate concentrations for the first ten stochastic realizations.....	43
Figure 3.3-9.	Comparison of the first 100 stochastic calculations of water content as a function of elevation, using the upper/middle-canyon-dominated uniform infiltration model, to measured water content from core samples. The simulation column is located between MCOBT-4.4 and R-15 in the lower canyon section.....	44

Figure 3.3-10. Comparison of 100 stochastic calculations of perchlorate concentration as a function of elevation and measured perchlorate concentrations from core samples. The simulation column is located between MCOBT-4.4 and R-15 in the lower canyon section. ....45

Figure 3.3-11. Comparison of 100 stochastic calculations of nitrate concentration as a function of elevation with measured nitrate concentrations from core samples. Simulation results are for a column between MCOBT-4.4 and R-15 in the lower canyon section and use the upper/middle-canyon-dominated uniform infiltration model. ....46

Figure 3.3-12. Comparison of 6 of 1000 stochastic calculations of perchlorate mass fluxes exiting the base of the unsaturated zone (Column 14 in the lower canyon) for discontinued (solid lines) and continued (dashed lines) releases from the RLWTF.....48

Figure 3.3-13. Alternative conceptual models of the saturated zone .....49

Figure 3.3-14. Comparison of Tier-1 (left; green curve) and Tier-3 (right; aquifer Model A and lower-canyon-dominated infiltration model with fast paths in the upper and middle canyons sections) perchlorate concentrations [ppb] in PM-5. (Time = 0 is 1964) .....53

Figure 3.3-15. 1000 perchlorate concentration [ppb] histories at water supply wells (a) PM-1, (b) PM-3, and (c) PM-5 for simulated fast-path infiltration in upper and middle Mortandad Canyon and uniform infiltration in lower Mortandad Canyon and regional-aquifer Model A (Time = 0 is 1964). ....55

Figure 3.3-16. Peak nitrate concentrations [ppm] and peak arrival times [a] at the water supply wells for fast-path (left) and lower-canyon-dominated uniform infiltration (right) conceptual models with regional-aquifer Model A.....56

Figure 3.3-17. Comparison of perchlorate concentrations [ppb] in PM-3 well water with continuous perchlorate releases (left) and discontinued perchlorate releases (right) for the lower-canyon-dominated uniform infiltration model and regional-aquifer Model A. (Time = 0 is 1964.).....57

Figure 3.3-18. Portion of the 27,000,000 particles (all 27 release locations, all realizations) captured by the water-supply wells and springs/Rio Grande within 1000 yr for alternative regional aquifer conceptual models: Model A (left) and Model B (right). ....58

Figure 3.3-19. Perchlorate concentrations [ppb] as a function of time at PM-3 (left) and springs (right) for aquifer Model B (note the different concentration scales) (Time = 0 is 1964). ....58

Figure 3.4-1. General equation for calculating human-health risk through drinking water .....59

Figure 3.4-2. Comparison of complementary cumulative distribution functions of HI as a result of perchlorate and nitrate in PM-5 for alternative conceptual infiltration models and a 1000-yr simulation period. All simulations shown assume regional-aquifer Model A.....66

Figure 3.4-3. The CCDF of HI calculated for 1000 equally probable nitrate and perchlorate exposure-point concentrations in water-supply wells for the 1000-yr simulation period for (top) upper/middle-canyon-dominated uniform infiltration model and (bottom) lower-canyon-dominated uniform infiltration model. Both assume regional-aquifer Model A. ....67

Figure 3.4-4. Percentage of 1000 HI calculations that exceed an HI of 1 for perchlorate during any given year of the 1000-yr risk simulation. Lower-canyon-dominated infiltration with fast paths in the upper, middle, and lower canyons for perchlorate and nitrate with regional-aquifer Model A. ....68

Figure 3.4-5. Complementary cumulative distribution functions of dose calculated for 1000 equally probable tritium exposure-point concentrations in supply wells for (top) lower-canyon-dominated uniform infiltration and (bottom) lower-canyon-dominated infiltration with fast paths in the upper, middle, and lower canyons. Both assume regional-aquifer model A. ....69

Figure 3.4-6. Complementary cumulative distribution functions of HI values calculated for 1000 equally probable perchlorate exposure-point concentrations in supply wells over 1000 yr, assuming that RLWTF discharges cease in 2006 (Lower-canyon-dominated uniform infiltration model with regional-aquifer model A).....70

Figure 3.4-7. Fraction of 1000 simulations with HI >1 for perchlorate at supply-well PM-3, discontinued release source term, lower-canyon-dominated uniform infiltration model and regional-aquifer Model A.....71

Figure 4.2-1. Linear-regression analysis results for PM-3 for perchlorate using the upper/middle-canyon-dominated uniform infiltration model and regional-aquifer Model A .....77

Figure 4.2-2. Probability plot of residuals for the linear regression of PM-3 data for perchlorate, using the upper/middle-canyon-dominated uniform infiltration model and regional-aquifer Model A.....78

Figure 4.2-3. Linear regression analysis results for PM-5 for perchlorate, using the upper/middle-canyon-dominated uniform infiltration model and regional-aquifer Model A. ....79

Figure 4.3-1. Observed and predicted values of the logarithm of the summed averages of HI values for PM-3 and PM-5 for the upper/middle-canyon-dominated uniform infiltration for perchlorate with regional-aquifer Model A.....83

**Tables**

Table 2.1-1 Annual Discharges Recorded from the RLWTF .....7

Table 2.4-1 Permeability and Hydraulic Conductivity Data for Hydrostratigraphic Units in Regional Aquifers (LANL 2003).....21

Table 3.2-1 Infiltration Estimates from the Alluvial Aquifer to the Unsaturated Zone for Three Sections of Mortandad Canyon (Purtymun 1967, 11785).....27

Table 3.2-2 Tier-1 Mean-Mass Contaminant Travel Times .....30

Table 3.3-1 Parameters and Distribution Attributes Used in the Tier-3 Infiltration Models (See Appendix B for Full Distribution.).....35

Table 3.3-2 Minimum Fraction of Volumetric Flow between Canyon Sections .....36

Table 3.3-3 Physical and Hydraulic Parameters and Distributions Used in the Tier-3 Unsaturated Transport Model.....40

Table 3.3-4	Permeabilities of Aquifer Materials Evaluated in the Tier-1 and Tier-3 Saturated Transport Model.....	51
Table 3.3-5	Variable Well Production Rate (kg/s) Evaluated in the Tier-3 Saturated Transport Models ....	52
Table 3.3-6	Aquifer Distributions Evaluated in the Tier-3 Saturated Transport Models .....	53
Table 3.4-1	Results of the Nitrate and Perchlorate Risk Assessment for a 1000-yr Period.....	61
Table 3.4-2	Statistics of HI Distributions Calculated for Perchlorate in Water Pumped from PM-3 over a 1000-yr Period with Regional-Aquifer Model A and a Continuous Source .....	64
Table 3.4-3	Statistics of HI Distributions Calculated for Perchlorate for 1000 Yr in Water Pumped from PM-5 with Regional-Aquifer Model A and a Continuous Source .....	65
Table 3.4-4	Probability of Exceeding HI of 1 over 1000 Yr for Several Assumed MCL for Perchlorate .....	72
Table 4.2-1	Correlation Coefficients Calculated for Input Parameters and Model-Calculated HI Values for Regional-Aquifer Model A.....	75
Table 4.2-1	Results of Uncertainty-Reduction Analysis for PM-5 .....	81
Table 4.3-1	Partial Coefficient of Correlation.....	82

**ACRONYMS**

AT	averaging time
BW	body weight
CCDF	complementary cumulative distribution function
CDF	cumulative distribution function
CDI	chronic daily intake
CERCLA	Comprehensive Environmental Response, Compensation, and Liability Act
CR	contact rate
CTE	central tendency exposure
DCF	dose conversion factor
DCG	dose concentration guideline
DOE	Department of Energy
ED	exposure duration
EF	exposure frequency
EPA	Environmental Protection Agency
FEHM	Finite Element Heat and Mass transfer code
HEAST	Health Effects Assessment Summary Tables
HI	hazard index
HQ	hazard quotient
HSWA	Hazardous and Solid Waste Amendments
ICR	incremental cancer risk
IRIS	Integrated Risk Information System
LHS	Latin hypercube sampling
MCL	maximum concentration limits
MCO	Mortandad Canyon Observation
MCOBT	Mortandad Canyon Observation Bandelier Tuff
MDA	material disposal area
MNA	monitored natural attenuation
NMED	New Mexico Environment Department
MW	molecular weight
NOEL	no-observed-effect levels
O	Otowi
PM	Pajarito Mesa
PRA	probabilistic risk assessment
RCRA	Resource Conservation and Recovery Act
RfD	reference doses
RLWTF	Radioactive Liquid Waste Treatment Facility
RME	reasonable maximum exposure
RPF	Records Processing Facility
TA	technical area
TDS	total dissolved solids
TEDE	total effective dose equivalent
TI	technical impracticability
YMP SQAP	Yucca Mountain Project Software Quality Assurance Program

## 1.0 INTRODUCTION AND BACKGROUND

This report documents the results of a project to develop and demonstrate analytical tools necessary to implement a risk-based decision-support system to help managers cost-effectively invest resources. Although Los Alamos National Laboratory's cleanup program has always conducted risk assessments as part of the corrective-action process, this task extends the traditional role of risk assessment to the use of decision analysis. Decision-analysis methods incorporate concepts from management science, operations research, and economics, providing a useful way to analyze the relative value of alternative actions under conditions of uncertainty. The "risk" in "risk-based decision analysis" highlights the central role uncertainty plays in the decision-analysis process.

Risk refers to the probability of adverse outcome. In this context, environmental contamination poses a risk to human health when there is a potential for people to be exposed to unsafe amounts of contaminants under unprotected conditions of exposure. The potential for such exposures often depends upon many variables, such as dynamic environmental conditions that affect the fate and transport of contaminants from one location to another over time. Risk-based decision analysis uses the uncertainty in conditions affecting the probability of unsafe exposures (i.e., risk) to evaluate actions that are likely to reduce the probability of such exposures (i.e., reduce risk).

Accordingly, risk-based decision analysis requires that risk assessments be conducted in a way that objectively quantifies uncertainties that may affect exposure conditions. Monte Carlo analysis is widely used to combine (or propagate) multiple uncertain or variable elements in a probabilistic risk assessment. Monte Carlo methods are especially useful in computer simulations that calculate potential contaminant distributions at various locations and times, resulting from dynamic environmental processes. Although Monte Carlo analysis was developed in 1946 (at the Laboratory), it has not been widely used in human-health risk assessments, here or elsewhere, to support corrective-action decisions. However, there is a growing number of advocates for this application, including the U.S. Environmental Protection Agency (EPA).

This effort was intended as a demonstration of this approach and not as a corrective-measures evaluation study. Although this approach could be used to great benefit in the final remedy selection process, that is outside the scope of the work documented in this report.

### 1.1 Background on Risk Assessment and Risk-Based Decision Making

According to the EPA, the goal of its cleanup programs is to avoid or minimize risks (defined as the likelihood that humans or ecological receptors will experience health problems) from the generation and management of hazardous wastes. It follows that the success of the Laboratory's cleanup project should, ultimately, be judged in terms of the reduction or minimization of the probability that human or ecological health will be harmed by environmental contaminants. Corrective actions will be implemented as necessary to protect human health and the environment from *current* and *potential* threats posed by releases of contaminants. Current threats are identified largely by characterization data from known points of exposure. Potential threats are identified through risk assessment, which is conducted in accordance with EPA guidance (EPA 1989, 08021; EPA 2001, 85534). Risk assessments are used to calculate human-health impacts represented by the total effective dose equivalent (TEDE) for radionuclides, hazard index (HI) for simultaneous exposures to multiple noncarcinogenic chemicals, hazard quotient (HQ) for exposures to single noncarcinogenic chemicals, and incremental cancer risk (ICR) for exposures to carcinogenic chemicals.

Since the enactment of the Comprehensive Environmental Response, Compensation, and Liability Act (CERCLA) in 1980 the risk assessment policies and guidance documents have evolved to reflect advances in science and changes in federal regulations. (EPA 2001, 85534, p. 1-4, Section 1.1, paragraph 1)

In 2001, EPA published Risk Assessment Guidance for Superfund, Volume III, Part A: Process for Conducting Probabilistic Risk Assessment (RAGS3; EPA 2001, 85534), which describes a tiered risk-assessment process that “promotes an efficient allocation of resources and improved decision making” (EPA 2001, 85534, p. 1-7, Section 1.1.3). This tiered process is shown in Figure 1.1-1, which is taken directly from RAGS3.

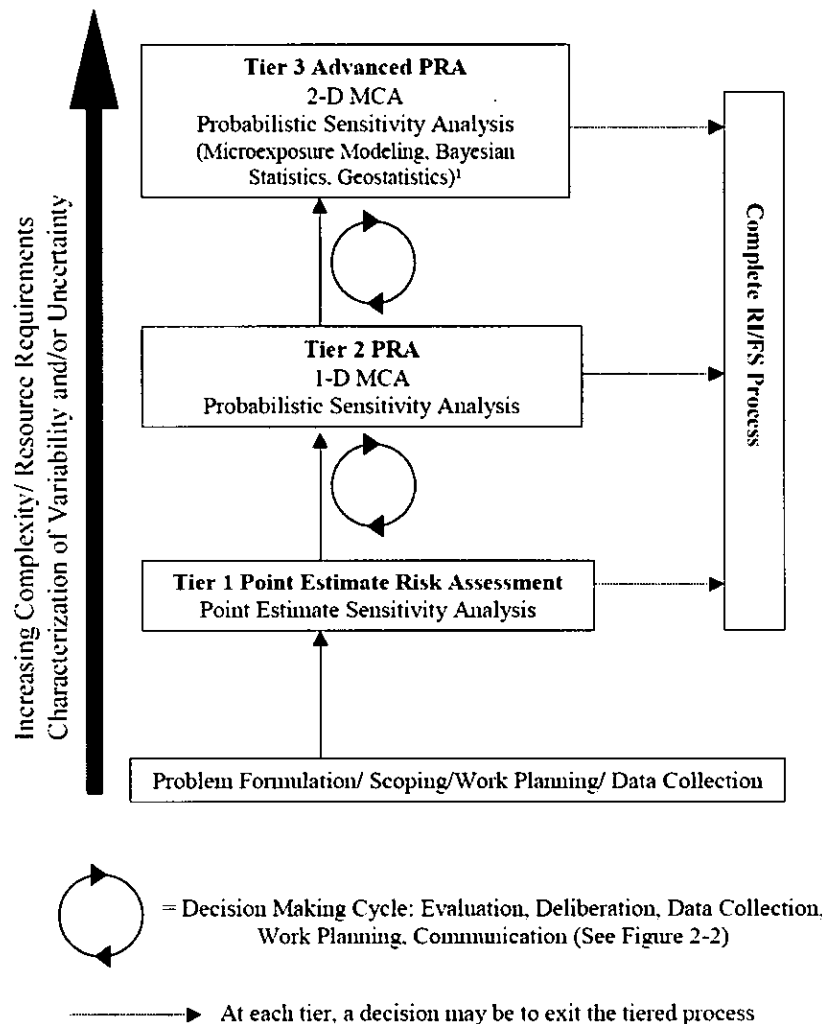


**Figure 1.1-1. EPA's tiered risk-assessment process described in RAGS3**

The first tier in the EPA's RAGS3 process begins with a point-estimate approach to risk assessment. Guidance on conducting point-estimate risk assessments is provided in EPA's Risk Assessment Guidance for Superfund, Volume 1, Part A: Baseline Risk assessment (EPA 1989, 08021). "Point estimate risk assessments use single values (point estimates) to represent variables in the risk equation. The output of the risk equation in a point-estimate risk assessment is, therefore, a point estimate of risk, which can be a central tendency exposure (CTE) estimate of risk (i.e., the average expected risk) or reasonable maximum exposure (RME) estimate of risk (e.g., the risk expected if the RME was to occur),

depending on the input values used in the risk equation" (RAGS3, EPA 2001, 85534, pp. 1–6, Section 1.1.4). In the RAGS3 process, Tier 1 is a point estimate of RME risk that is used primarily to determine *if* corrective action is required to protect human health and the environment from potential threats. Higher-tier probabilistic risk assessments (PRAs) are conducted to provide information that is helpful in deciding *what* actions are necessary and sufficient to ensure protection.

Risk assessment performed using probabilistic methods is very similar in concept to the point-estimate method, with the main difference being the methods used to incorporate variability and uncertainty into the risk estimate.... Probabilistic risk assessment uses probability distributions for one or more variables in the risk equation in order to quantitatively characterize variability and/or uncertainty. The output of a PRA [probabilistic risk assessment] is a probability distribution of risks that reflects the combination of the input probability distributions. (EPA 2001, 85534, pp. 1-8 and 1-9)

A primary benefit of PRA, which is not available with point-estimate risk assessment, is that sensitivity analysis can be used to establish quantitative correlations between input and risk. If input probability distributions that reflect uncertainty because of a lack of knowledge correlate with high risk, then sensitivity analysis identifies what additional knowledge is needed. If input distributions that reflect variability (not lack of knowledge) correlate with high risk, the sensitivity analysis identifies variability that must be addressed in remedy selection.

Because both uncertainty (lack of knowledge) and variability (natural heterogeneity) affect the Laboratory's ability to assess *potential* threats posed by contaminants in the environment, PRA is a valuable tool. In PRA, the probability of risk directly reflects uncertainty and variability in processes that control the fate and transport of contaminants in the environment. The potential for harm in the future depends upon the potential for contaminants to migrate to locations where exposures are likely and in concentrations that are considered harmful under the same conditions of exposure.

The Laboratory has conducted numerous risk assessments that meet the EPA's definition of a Tier-1 risk assessment in RAGS3. As stated previously, Tier 1 estimates the risk that would be expected *if* the RME were to occur. That is, Tier 1 assumes that exposures will occur without addressing uncertainty in that assumption. This report describes the Laboratory's first Tier-3 probabilistic risk assessment, which was conducted to evaluate whether RME exposures through drinking water are likely to occur as a result of contaminants in groundwater resulting from waste water discharged from the Radioactive Liquid Waste Treatment Facility (RLWTF) at Technical Area (TA) 50 into Mortandad Canyon. Then, this report describes how the results of the Tier-3 PRA were used as input to a decision analysis developed to identify and evaluate alternative actions that will reduce the likelihood of RME exposures.

Mortandad Canyon was chosen for the demonstration of this risk-based decision analysis for several reasons, including

- relatively short estimated groundwater travel times, and
- the presence of mobile, soluble, and potentially harmful contaminants.

It is intended that similar decision analyses be developed for the other canyons where similar conditions exist. The resulting decision-support tools are expected to be used by project managers in focusing investigations, evaluating alternative corrective measures, optimizing performance monitoring, and designing watershed-scale groundwater monitoring programs.

## **1.2 Background on Mortandad Canyon**

Mortandad Canyon and its tributaries have received effluents from Laboratory facilities since the early 1950s. These effluents have contained a variety of contaminants, including nitrate, perchlorate, tritium, cesium-137, strontium-90, americium-241, and several isotopes of uranium and plutonium (LANL 1997, 56835). Most contaminants found in Mortandad Canyon are associated with discharges from TA-50, except for strontium-90 (LANL 1997, 56835), which was also from TA-35. The RLWTF is still discharging treated wastewater into Mortandad Canyon, although at historically low contaminant concentrations as demonstrated through the facility's [nonradioactive wastes] National Pollution Discharge Elimination System permit (LANL 2002, 71301).

The Laboratory began monitoring sediments, surface water, and groundwater in Mortandad Canyon and its tributaries in the early 1960s. Contaminants have been identified in sediments, alluvial and perched intermediate groundwater, and in the regional aquifer beneath Mortandad Canyon. Historically, the following constituents have been detected in surface water, alluvial groundwater, and sediments: americium-241; cesium-137; plutonium-238 and plutonium-239/240; strontium-90; tritium; uranium-234/235/236/238; nitrate; perchlorate; chloride; sulfate; fluoride; and total dissolved solids ([TDS] LANL 2002, 71301). The EPA conducted independent groundwater and surface water monitoring in the canyon in 1999, 2001, and 2002 that confirmed the presence of contaminants observed by the Laboratory.

Field investigations are underway in Mortandad Canyon to determine the nature and extent of contamination as part of the Laboratory's corrective action program mandated by the 1976 Resource Conservation and Recovery Act (RCRA), as amended by the 1984 Hazardous and Solid Waste Amendments (HSWA) under the administration of the New Mexico Environment Department (NMED) (LANL 1997, 56835; LANL 2004, 82613). Data available from previous investigations and monitoring (including data from several alluvial groundwater wells, two intermediate groundwater wells, and three regional-aquifer wells) show elevated concentrations of tritium, nitrate, and perchlorate in alluvial groundwater, pore water, perched intermediate water, and the regional aquifer. Concentrations of these solutes measured in alluvial, pore, perched, and regional groundwater in Mortandad Canyon are elevated above those measured in supply wells. Current investigations include alluvial monitoring wells, intermediate-depth wells, and regional aquifer wells. Groundwater samples will be analyzed for metals and anions, including perchlorate, radionuclides, organic compounds, and stable isotopes.

## **1.3 Relationship of this Document to Mortandad Canyon Decisions**

The Mortandad Canyon Groundwater Workplan defines the nature and extent of contamination "as bounding spatial and temporal (100 yrs) uncertainties in contaminant concentrations and distributions. Information obtained from determining the nature and extent of contamination will assist in making decisions regarding characterization, regulatory compliance, pathway analysis, risk assessment, remediation and monitoring" (LANL 2004, 71301). Chapters 2 and 3 of this report describe a preliminary pathway analysis and risk assessment for groundwater contamination in Mortandad Canyon based on the current state of knowledge (as of the study initiation in 2004). Chapter 4 of this report describes a decision process to determine the need for revising the preliminary pathway analysis and risk assessment and to determine the need for additional specific characterization. Chapter 5 of this report provides recommendations on how the risk assessment and decision analysis can be used to aid in the design of a groundwater monitoring program in Mortandad Canyon that, through adaptive management, will be cost effective before, during, and after the implementation of corrective actions.

## 1.4 Content and Format of This Document

This report includes information that addresses the eight conditions for acceptance for PRA as defined by the EPA in RAGS3 (RAGS3, EPA 2001, 85534), which are paraphrased for applicability as follows:

- The purpose and scope of the assessment should be clearly articulated in a problem formulation, including the questions that the risk assessment attempts to answer and assessment endpoints (provided in Section 2 of this report).
- The methods used for the analysis include sufficient information to allow the results of the analysis to be independently reproduced (provided in Section 3 of this report).
- The techniques and results of sensitivity analyses are to be presented and discussed (provided in Section 4 of this report).
- The presence or absence of moderate-to-strong correlations or dependencies between the input variables is to be discussed and accounted for in the analysis, along with the effects these have on the output distribution (provided in Section 4 of this report).
- Information for each input and output distribution is to be provided in the report, including tabular and graphical representations of the distributions (e.g., probability density function and cumulative distribution function plots) that indicate the location of any point estimates of interest (e.g., mean, median, 95th percentile), and the selection of distributions is to be explained and justified (provided in Sections 3 and 4 of this report, and in supporting appended materials).
- The numerical stability of the central tendency and the higher end (i.e., tail) of the output distributions are to be presented and discussed (provided in Sections 3 and 4 of this report, and in supporting appended materials).
- Calculations of exposures and risks using deterministic (e.g., point estimate) methods are to be reported if possible to allow comparisons between the probabilistic analysis and screening-level risk assessments (provided in Section 3 of this report).
- Because fixed exposure assumptions (e.g., exposure duration, body weight) are sometimes embedded in the toxicity metrics (e.g., reference doses, reference concentrations, cancer risk factors), the exposure estimates from the probabilistic output distribution are to be aligned with the toxicity metric (provided in Section 3 of this report).

## 2.0 PROBLEM FORMULATION

The RLWTF has released treated wastewater containing varying quantities of chemical and radiological constituents since 1963. These releases may pose a potential risk to human health and the environment.

Operational practices and natural processes have resulted in a variable distribution of contaminants in groundwater in Mortandad Canyon. Current risks resulting from groundwater contamination are low because concentrations of constituents are low or absent where exposures are most likely to occur. However, constituents will continue to move through the hydrologic system. The potential for future exposures to contamination within the hydrologic system depends upon future contaminant concentrations at future exposure points.

For the near future, existing water-supply wells will continue to provide domestic water to local residents. A baseline risk assessment is conducted to analyze whether potentially harmful contaminants might cause future health risks to users of water pumped from the existing supply wells.

The risk-management question addressed in the baseline risk assessment (Section 3) is graded, consistent with EPA's tiered risk-assessment process,

- Tier-1 Point-Estimate Risk Assessment: Is there a potential for drinking water to be contaminated at unsafe levels because of releases from the RLWTF?
- Tier-3 Probabilistic Risk Assessment: What is the potential for drinking water to be contaminated at unsafe levels because of releases from the RLWTF?

The decision analysis can use the results of the probabilistic risk assessment to provide information such as

- when contaminants are expected to reach drinking-water supply wells,
- what parameters in the probabilistic risk assessment are highly correlated with high probabilities of unsafe drinking water,
- what additional information regarding risk-significant parameters can be collected to reduce the probability of predicted unsafe drinking-water concentrations because of uncertainty in input parameters,
- what general remedial approaches would be cost effective at reducing the probability of unsafe drinking water, and
- where monitoring should be conducted to provide a high probability that contaminants will be detected in time to act to prevent exposures to unsafe drinking water.

In the present analysis, safe drinking water is the assessment endpoint. *Unsafe drinking water* is defined here as water that contains levels of

- noncarcinogenic chemicals that would result in an HQ or HI greater than 1 (EPA 1989, 08021);
- carcinogenic chemicals that would result in an estimated ICR greater than 1-in-100,000 (EPA 1989, 08021); and
- radionuclides that would result in an estimated TEDE greater than 4 mrem (EPA 1989, 08021).

These values are calculated for a 1000-yr period using EPA's recommended methodology for drinking-water exposures.

Depending on the potential for (and timing of) unsafe drinking water, various actions may be suggested to reduce the likelihood of harmful exposures. A decision analysis (see Chapter 4) is conducted to identify and evaluate alternative actions based on risk reduction.

The remainder of Chapter 2 describes the history and the current conditions associated with the RLWTF discharges in Mortandad Canyon.

## 2.1 RLWTF Contaminant Source

Several Laboratory TAs are located along Mortandad Canyon, many of which influence surface water directly (through discharge) or indirectly (through runoff). From 1951 to 1963, the TA-35 wastewater treatment plant discharged into Ten-Site Canyon, a tributary of Mortandad Canyon. Since 1963, radioactive liquid wastes from Laboratory operations have been collected and treated at the RLWTF at TA-50. Treated wastewater from the RLWTF is discharged into Effluent Canyon, which drains into Mortandad Canyon. Discharge volumes from the TA-35 treatment plant (total life-time discharge volume on the order of  $10^7$  L; LANL 1997, 56835) were small compared to those from the TA-50 treatment plant (annual discharge volumes greater than  $10^7$  L). Therefore, this assessment focuses on the treated effluent coming from the RLWTF. (Other possible discharge locations are the springs, but they are not used for water supply and are not considered.)

Table 2.1-1 summarizes the discharge volumes as well as the masses and concentrations of nitrate and tritium recorded as being released from the RLWTF beginning in 1964. This information was collected as part of the historical monitoring of the outfall (LANL, 2002, 71301). Discharge volumes have ranged from  $1.10 \times 10^7$  L/yr in 2002 to a high of  $6.03 \times 10^7$  L/yr in 1968. Generally, greater volumes were discharged until about 1981. In 2002, the discharge volume was 20% of the 1981 volume. The average discharge volume between 1963 and 1981 was approximately  $5 \times 10^7$  L/yr, and discharge volumes since 1982 have been less than  $4 \times 10^7$  L/yr.

**Table 2.1-1  
Annual Discharges Recorded from the RLWTF**

Year	Discharge Volume (L)	Average Discharge Concentration NO <sub>3</sub> as N (mg/L)	Total NO <sub>3</sub> as N (kg)	Average Discharge Concentration Tritium (nCi/L)	Total Tritium (Ci)
1964	5.14E+07	21.9	1126	na <sup>a</sup>	na
1965	4.90E+07	29.6	1450	na	na
1966	5.28E+07	11.3	596	na	na
1967	5.97E+07	12.4	741	na	na
1968	6.03E+07	14.2	858	na	na
1969	5.45E+07	29.6	1612	na	na
1970	5.32E+07	124.5	6618	na	na
1971	4.57E+07	84.0	3838	na	na
1972	5.71E+07	173.0	9875	104.6	5.97
1973	5.37E+07	70.0	3762	325.2	17.47
1974	4.06E+07	65.5	2660	99.8	4.05
1975	3.97E+07	na	3000 <sup>b</sup>	1661.6	66.00
1976	3.99E+07	na	3000 <sup>b</sup>	4687.9	187.00
1977	4.21E+07	99.8	4199	867.2	36.50
1978	4.05E+07	90.0	3649	303.4	12.30
1979	4.86E+07	156.0	7578	673.1	32.70
1980	5.28E+07	176.0	9298	849.9	44.90
1981	5.53E+07	262.0	14,496	307.2	17.00
1982	3.98E+07	335.0	13,320	357.1	14.20
1983	3.45E+07	384.0	13,248	252.2	8.70
1984	3.50E+07	331.0	11,595	371.1	13.00
1985	2.86E+07	376.0	10,754	2426.6	69.40
1986	3.05E+07	410.0	12,505	2377.0	72.50

Table 2.1-1 (continued)

Year	Discharge Volume (L)	Average Discharge Concentration NO <sub>3</sub> as N (mg/L)	Total NO <sub>3</sub> as N (kg)	Average Discharge Concentration Tritium (nCi/L)	Total Tritium (Ci)
1987	2.66E+07	476.0	12,662	3759.4	100.00
1988	2.93E+07	384.0	11,251	716.7	21.00
1989	2.28E+07	488.0	11,126	701.8	16.00
1990	2.11E+07	297.0	6267	568.7	12.00
1991	2.19E+07	164.0	3592	484.0	10.60
1992	1.99E+07	204.0	4060	534.2	10.63
1993	2.17E+07	360.0	7821	122.4	2.66
1994	2.08E+07	45.5	948	107.0	2.23
1995	1.76E+07	81.6	1440	41.5	0.73
1996	1.65E+07	76.4	1260	61.7	1.02
1997	1.75E+07	69.6	1220	76.3	1.33
1998	2.32E+07	61.1	1420	52.8	1.23
1999	2.00E+07	24.2	486	24.3	0.49
2000	1.86E+07	2.5	47	48.7	0.91
2001	1.36E+07	3.9	53	9.3	0.13
2002	1.10E+07	na	na	na	na

<sup>a</sup> na = Data not available.

<sup>b</sup> Estimated NO<sub>3</sub> release for simulations.

Table 2.1-1 indicates the variability in discharge volumes and concentrations over time. These reflect contemporaneous Laboratory operations whose wastewater was treated at the RLWTF, new wastewater treatment methods, and evolving regulatory requirements. Treatment technologies and regulatory requirements generally result in reduced contaminant concentrations in effluent. For example, a new reverse-osmosis and ultrafiltration system began operating at the RLWTF in 2000 to remove additional radionuclides from the effluent and to ensure that the discharges meet the Department of Energy (DOE) public dose guidelines. Also in 2000, the RLWTF instituted a program to restrict the discharge of nitrogenous wastes into the facility's collection system, and since then, nitrate (nitrate as nitrogen) concentration of effluent discharge from the RLWTF has been less than 10 mg/L; the average 2001 effluent nitrate concentration was 3.9 mg/L. The RLWTF began measuring perchlorate in liquid effluent discharged into Mortandad Canyon in 2000. That year, the RLWTF discharged 4.74 kg of perchlorate, for an average concentration of 254 µg/L in the effluent. In 2001, 2.29 kg of perchlorate were released, resulting in an average concentration of 169 µg/L. In 2002, the RLWTF installed ion-exchange resins to reduce perchlorate in effluent to below 4 ppb (4 µg/L).

## 2.2 Groundwater Contaminant Distribution in Mortandad Canyon

### 2.2.1 Observations

Contaminants have been detected in surface water, on sediments, in near-surface perched alluvial groundwater, in vadose-zone pore water, in intermediate perched groundwater, and in the regional aquifer in Mortandad Canyon. This section summarizes these findings with particular emphasis on observations of nitrate, perchlorate, and tritium.

The alluvial groundwater in Mortandad Canyon has been monitored since 1960 using alluvial wells (Mortandad Characterization Observation [MCO] -wells, shown in Figure 2.2-1). Also, systematic monitoring of sediments, surface water, and groundwater has been conducted there since 1970 as part of the Laboratory's site-wide environmental surveillance program. Historically, the following constituents have been detected in unfiltered samples of surface water and alluvial groundwater: americium-241; cesium-137; plutonium-238 and plutonium-239/240; strontium-90; tritium; uranium-234/ 235/236/238; nitrate; perchlorate; chloride; sulfate; fluoride; and TDS (LANL 2002, 71301). Filtered water samples typically contain tritium, nitrate, perchlorate, chloride, sulfate, fluoride, and TDS, indicating that the balance of contaminants detected in unfiltered samples is bound (or sorbed) to sediments.

This page intentionally left blank.

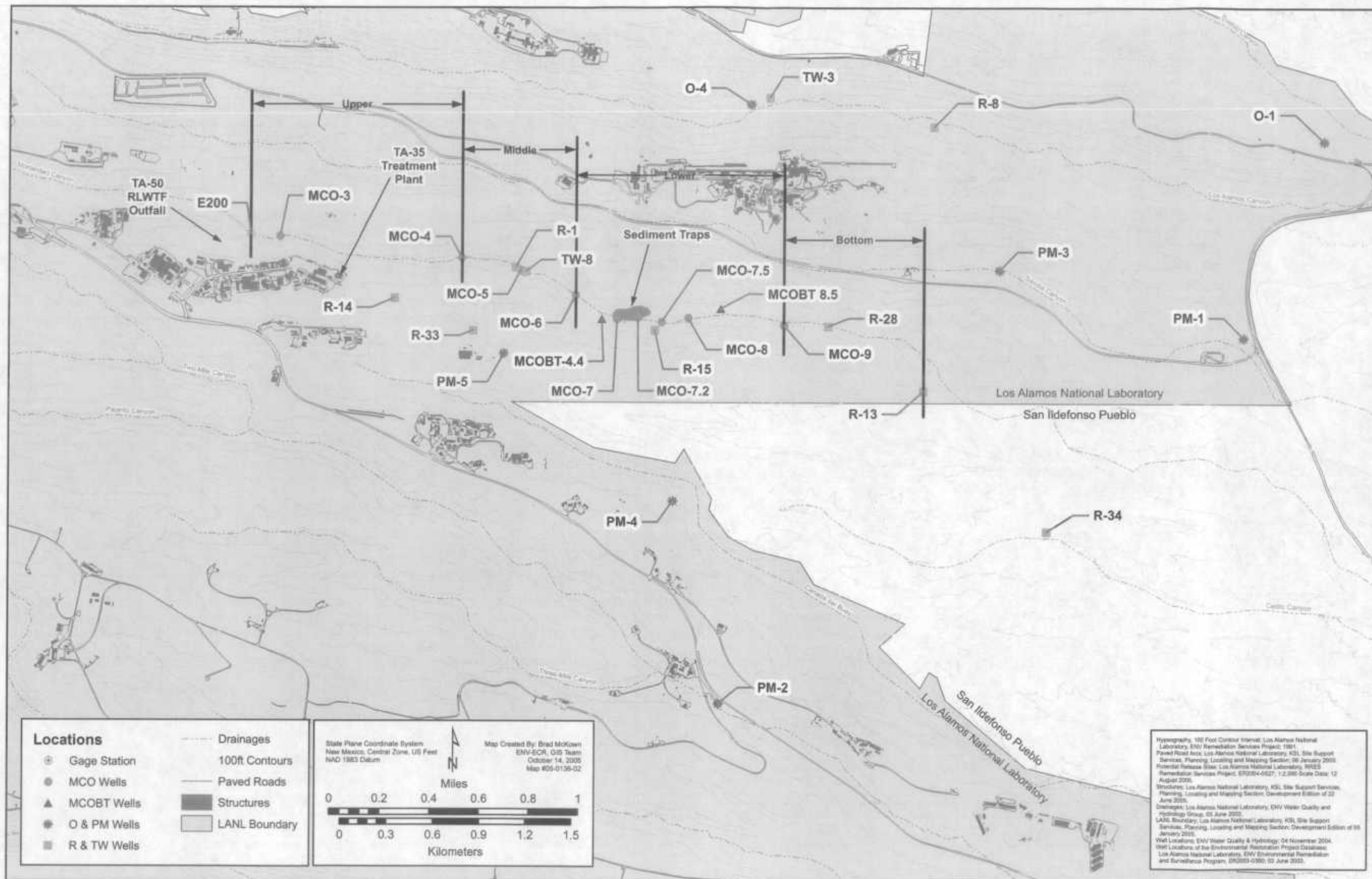


Figure 2.2-1. Locations of alluvial (MCO-), intermediate (MCOBT-), and regional (R-) groundwater wells in Mortandad Canyon and water supply wells (O- and PM-) near Mortandad Canyon

This page intentionally left blank.

Pore water within core and cuttings samples collected from the upper vadose zone during drilling of wells in and around Mortandad Canyon (Figure 2.2-1) since 1998 provides evidence of vadose-zone migration at various locations. Regional well R-1, located downstream of the confluence of Effluent Canyon with Mortandad Canyon, has vadose-zone perchlorate concentrations as high as 629 µg/L and nitrate (as nitrate) as high as 919 mg/L, but these drop to nondetectable concentrations in the lower portion of the Otowi Member (Qbo). Below the confluence of Mortandad Canyon with Ten Site Canyon, alluvial well Mortandad Canyon Observation (MCO)-7.2, intermediate wells MCOBT-4.4 and MCOBT-8.5, and regional well R-15 had perchlorate concentrations ranging from less than 2 to 840 µg/L either near the alluvium/Bandelier Tuff contact or within the Bandelier Tuff (Broxton et al. 2002, 76006; Longmire et al. 2001, 70103). Pore-water concentrations of nitrate (as nitrate) in the Bandelier Tuff range from less than 0.01 to 272 mg/L in these four wells. In regional well R-28, located about 2000 ft west of the Laboratory boundary, perchlorate was only detected in 2 of 16 pore water samples at concentrations of 33 µg/L or less; nitrate (as nitrate) concentrations ranged from less than 0.01 to 111 mg/L. Finally, in regional well R-14, located in Pratt Canyon below the historic TA-35 outfall, perchlorate was not detected, and nitrate concentrations ranged from below 0.01 to a maximum of 6.7 mg/L (as nitrate). This last result further supports the choice to focus only on the TA-50 RLWTF source rather than to include the TA-35 source.

Intermediate perched groundwater was encountered in wells MCOBT-4.4 and R-15. Analytical results from intermediate perched groundwater samples collected from intermediate observation well MCOBT-4.4 showed 12,797 pCi/L tritium, 13.2 mg/L nitrate plus nitrite (as N), and 142 µg/L perchlorate (Broxton et al. 2002, 76006). The well has a single screen set in a perched zone within the upper Puye Formation/Cerros del Rio basalt at a depth of 524 ft, approximately 450 ft above the regional water table. Perched groundwater encountered at a depth of 646 ft during the drilling of regional characterization well R-15 contained 3770 pCi/L tritium and 12 parts per billion (ppb) perchlorate (Longmire et al. 2001, 70103).

Figure 2.2-2 presents the measured concentrations of nitrate (as N), perchlorate, and tritium in regional-aquifer water samples collected at regional wells in the vicinity of Mortandad Canyon. Many of the samples are characterized as nondetects (<0.01 ppm NO<sub>3</sub> [as N], <2 ppb ClO<sub>4</sub>), with the majority of perchlorate samples characterized this way. When more than one sample is available, the data are shown as a range. For example, samples of the regional aquifer taken from characterization well R-15 at a depth of 1019 ft contained concentrations of from 2.2 to 2.4 mg/L nitrate (as N) (Longmire 2002, 72614). The highest nitrate concentration is observed at R-28. The highest perchlorate concentration is observed at R-15. Both wells are located along Mortandad Canyon. The highest tritium concentration is observed at R-12 in Sandia Canyon, which may reflect the impact of contaminant sources other than the RLWTF.

### 2.2.2 Pathways

Taken as a group, the contaminant distribution data indicate that liquids discharged from the RLWTF flowed laterally along the ephemeral streambed and the underlying alluvial aquifer in Mortandad Canyon. With time, the liquids have infiltrated to various depths into the unsaturated rock beneath the alluvium. The observed distribution of contaminants shows that the vast majority of the contaminants are located within the unsaturated zone beneath Mortandad Canyon, predominantly in porewater of the bedrock located beneath the alluvial groundwater. These observations, along with supporting geologic and hydrologic data (presented in the upcoming sections), provide the basis for the conceptual model of groundwater transport of contaminants in Mortandad Canyon shown in Figure 2.2-3, which was first presented in the Mortandad Canyon Groundwater Workplan, Revision 1 (LANL 2004, 82613).

The conceptual model identifies likely groundwater-transport processes that explain the distribution of contaminants within the different groundwater bodies and porewater beneath Mortandad Canyon. The TA-50 effluent is discharged into Effluent Canyon and flows into the upper portion of Mortandad Canyon, which is a steep, narrow canyon with thin, locally discontinuous alluvium. Effluent from TA-50 combines

with other effluent discharges from cooling towers up-canyon and infrequent storm water and snowmelt runoff to generate surface water flow down-canyon. The down-canyon extent of surface-water flow varies, depending on effluent discharge rates and contributions from the other water sources, but flow generally disappears before reaching TW-8 (Figure 2.2-1). During large storm-runoff events, surface flow collects in sediment traps below the confluence with Ten Site Canyon.

Nonsorbing contaminants (tritium, nitrate, and perchlorate) are transported as dissolved species in the surface water. The surface water infiltrates the alluvial aquifer down to where the canyon widens and surface-water flow disappears. Flow in the alluvial aquifer is down-canyon and highly variable with an estimated velocity within an order of magnitude of 1 km/yr (Purtymun 1974, 05476).

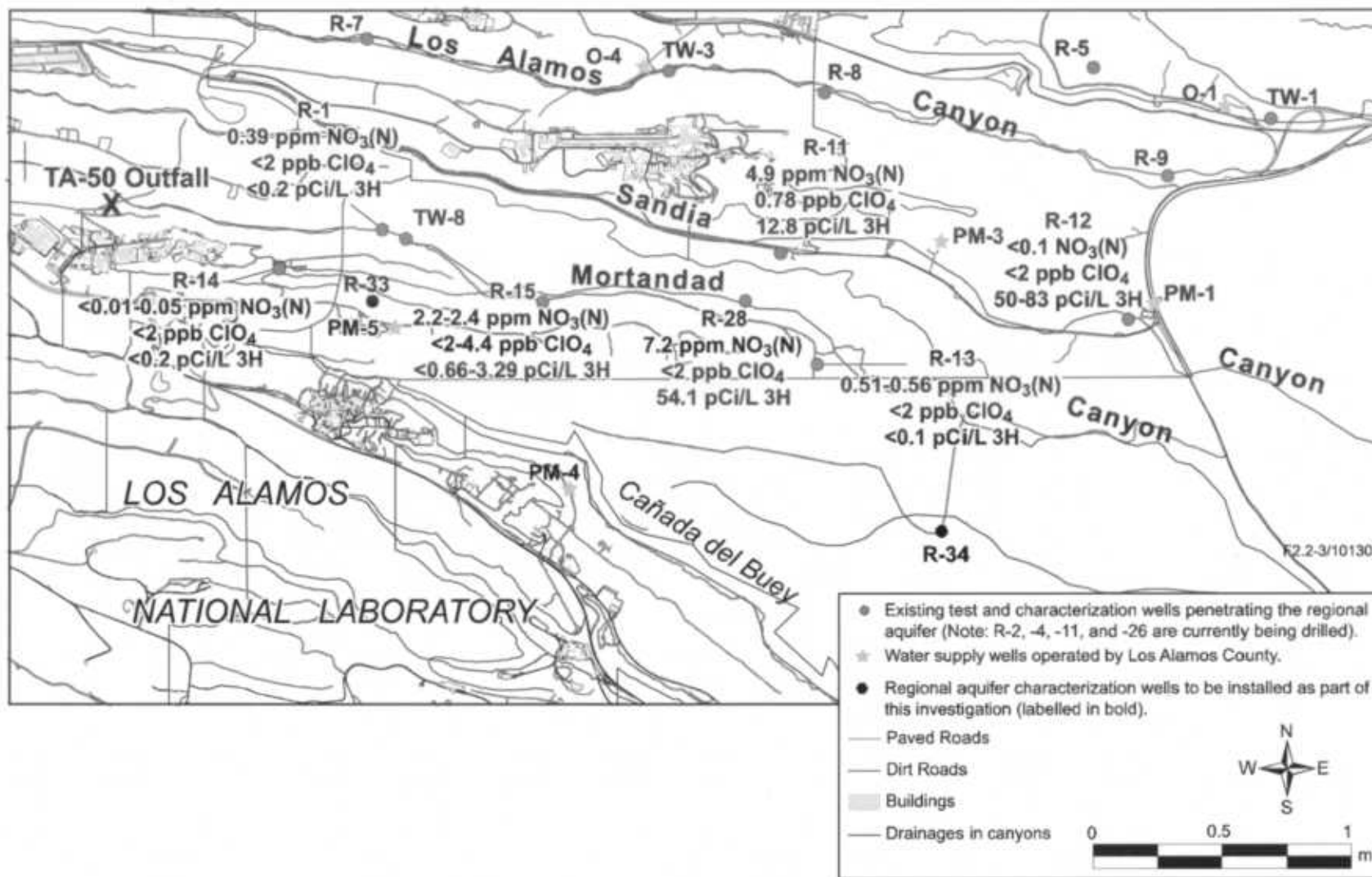


Figure 2.2-2. Concentrations of nitrate (as nitrogen), perchlorate, and tritium in the regional wells in the vicinity of Mortandad Canyon (after Longmire 2002, 72614; figure created by D. Broxton)

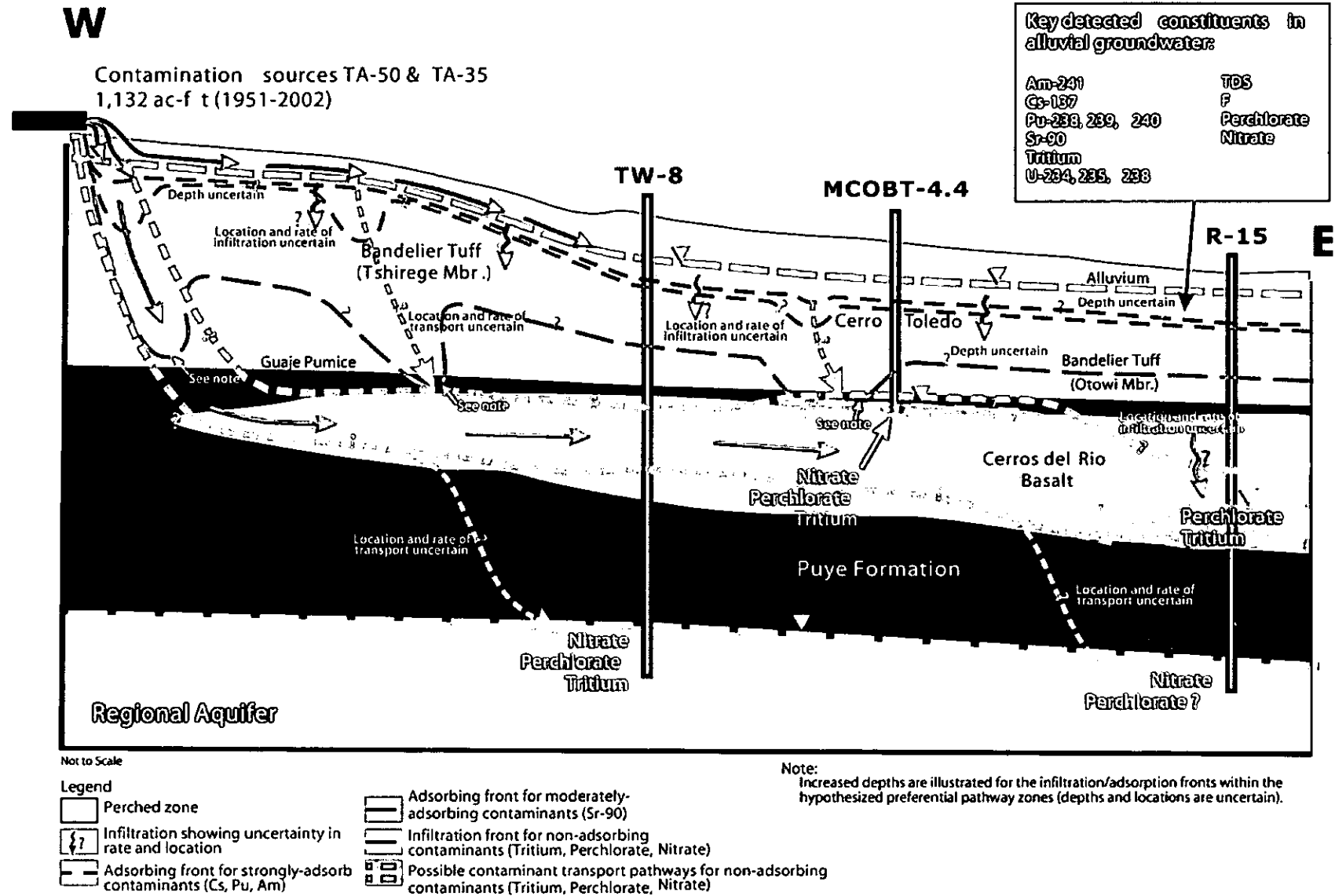


Figure 2.2-3. Conceptual model of transport of contaminants from RLWTF in groundwater in Mortandad Canyon (LANL 2004, 82613)

Nonsorbing contaminants in alluvial groundwater move downward into pores in the unsaturated tuff beneath the alluvium and into localized pockets of perched intermediate groundwater. Measurements of tritium, perchlorate, and nitrate in the pore water and intermediate perched water in concentrations exceeding those found in the regional aquifer and in water-supply wells indicate that most of the contaminant mass of nonsorbing contaminants resides in the unsaturated region.

The distributions of water-soluble contaminants discharged from the RLWTF are a result of hydrologic processes and geologic features present within Mortandad Canyon. These are described below.

### 2.3 Geology in Mortandad Canyon

The generalized stratigraphy of Mortandad Canyon is shown in the cross section of Figure 2.3-1 (LANL 2004, 82613). This stratigraphy is derived from mapped contacts in canyon walls and borehole drilling logs. In descending order, the vadose zone beneath Mortandad Canyon is made up of Quaternary rocks of Qbt 2, Qbt 1v, and Qbt 1g of the Tshirege Member of the Bandelier Tuff, Cerro Toledo interval, the Otowi Member of the Bandelier and its basal Guaje Pumice Bed, and of Pliocene rocks of the upper Puye Formation, Cerros del Rio lavas, and the lower Puye Formation. The top of the regional zone of saturation occurs within the Miocene rocks that include pumice-rich volcanoclastic rocks, river gravels, sands and older fanglomerate. Detailed descriptions of these units can be found in Broxton and Vaniman (2005, 90038).

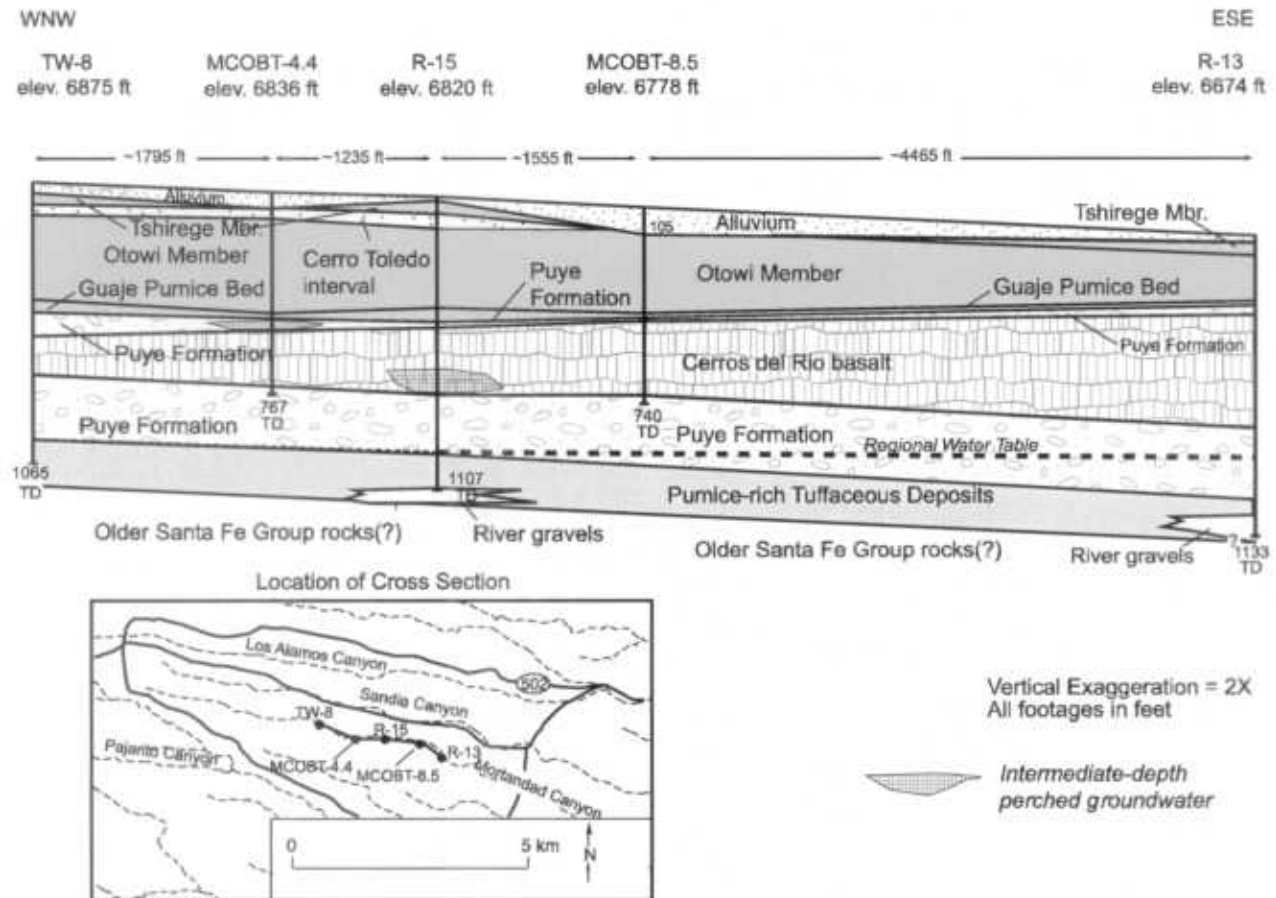


Figure 2.3-1. Generalized stratigraphy along Mortandad Canyon

The alluvium in Mortandad Canyon is less than 1.5 m thick in the upper western portion and thickens to about 30 m at the easternmost extent of Laboratory lands. The canyon is narrowly incised in strongly to partly welded tuffs of Qbt 2 and Qbt 1v in the reach between Effluent Canyon and TW-8. The canyon floor becomes much broader east of TW-8 where increasingly thicker deposits of alluvium overlie nonwelded tuffs of Qbt 1g and the poorly consolidated sediments of the Cerro Toledo interval. Near the eastern Laboratory boundary, thick deposits of alluvium overlie nonwelded tuffs of the Otowi Member.

The upper Puye Formation and Cerros del Rio basalt are geologic units of particular interest because they host the known occurrences of intermediate-depth perched groundwater in Mortandad Canyon. The Cerros del Rio basalt (Tb4) is a wedge-shaped stack of lava flows that thicken eastward. The maximum thickness of these lava flows beneath Mortandad Canyon is 427 ft at well R-13, and the minimum thickness is 145 ft at TW-8. Perched water is typically associated with coarse sands and gravels of the Puye Formation atop the Cerros del Rio basalt and with interflow breccias and highly fractured basalt flows in the lower part of the Cerros del Rio basalt (Broxton and Vaniman 2005, 90038).

**2.4 Hydrology in Mortandad Canyon**

This section summarizes current understanding about the hydrologic system in Mortandad Canyon as it relates to the potential for nonsorbing contaminants to be transported to water-supply wells in the regional aquifer.

**2.4.1 Surface Water**

There are no natural sources of continuously flowing water in the Mortandad watershed. Surface water occurs intermittently because of storm runoff, snowmelt runoff, and discharges from several permitted outfalls, including that at the RLWTF. Surface water flow is measured at gaging station E200 or its predecessor GS-1 in Mortandad Canyon.

Figure 2.4-1 compares surface water volumes from sources other than the RLWTF measured at gaging station E200/GS-1 in Mortandad Canyon (just downstream of the RLWTF) to effluent volumes released from the RLWTF. The comparison shows that, while variable, the RLWTF discharge contributes significantly to the total surface water flow in Mortandad Canyon.

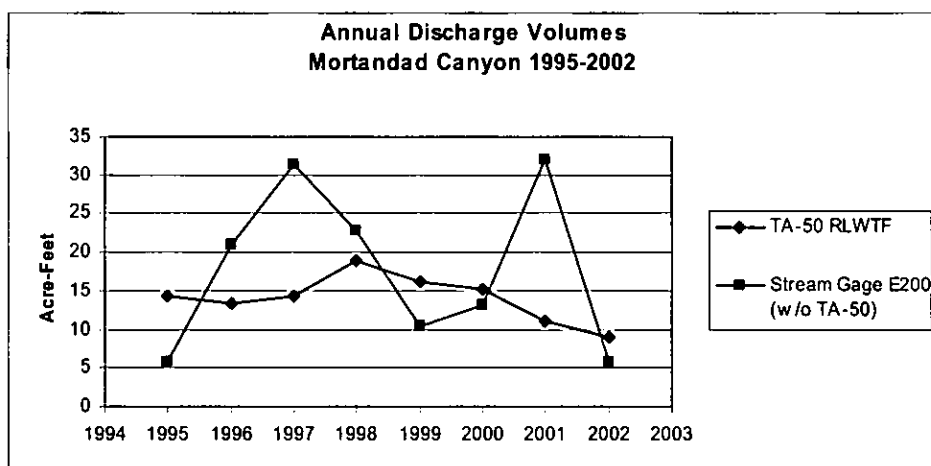


**Figure 2.4-1. Comparison of time-histories of liquid discharges from the RLWTF to surface water volumes from sources other than the RLWTF for the E200 stream gage near the RLWTF**

Surface water in Mortandad Canyon on Laboratory land generally infiltrates into the alluvium that fills the streambed, although some is also lost to evaporation. Currently, surface water flow generally disappears upstream of TW-8 (Figure 2.2-1). Since 1976 when sediment traps were constructed below the confluence with Ten Site Canyon (Figure 2.2-1), surface flow beyond the sediment traps has only been observed once. In the 1960s, before construction of the sediment traps, surface water reached the eastern portion of the canyon near the Laboratory boundary on very rare occasions. (LANL 1997, 56835).

#### 2.4.2 Alluvial Groundwater

Alluvial groundwater flows down Mortandad Canyon toward the east-southeast and infiltrates into the underlying Bandelier Tuff and Cerro Toledo interval. The horizontal and vertical extent of the alluvial groundwater is limited by depletion through evapotranspiration and movement into the underlying rocks (Purtymun et al. 1977, 11846). A tracer study conducted by Purtymun (1974, 05476) indicated that approximately half of the volume of liquid discharged from the RLWTF appears as alluvial groundwater 3 km downstream within about a year (388 days). Some portion of the other approximately half of the volume of liquid evaporates, and the remainder infiltrates beneath the canyon alluvium. Purtymun (1974, 05476) estimated the velocity of alluvial groundwater flow ranges from about 6.7 km/yr in the upper reach or Mortandad Canyon to about 0.78 km/yr in the lower reach of the canyon and along the gradient at the base of the alluvium. Purtymun (1974, 05476) determined field-scale hydraulic conductivity values for several zones of different texture within the alluvium, which were identified by Baltz et al. (1963, 08402). Chloride and tritium tracer measurements were used to estimate the hydraulic conductivities. The results of the tracer study indicated the following hydraulic conductivities in alluvium in Mortandad Canyon:

- 50 km/yr between MCO-5 and MCO-6,
- 18 km/yr between MCO-6 and MCO-7.5, and
- 2.7 km/yr between MCO-7.5 and MCO-8.

In core obtained during the drilling of MCOBT-4.4, the moisture content in the alluvium is 2% to 10% gravimetric near the surface and increases (with substantial variability) to a maximum of 28% in the zone of perched alluvial groundwater (35 ft to 50 ft depth). The moisture content is as high as 37% in core from MCOBT-8.5, corresponding with two separate zones of saturation between 94.4 ft to 112.5 ft depth (LANL 2002, 71301).

#### 2.4.3 Vadose Zone

Core samples were taken through to depths of about 310 feet in MCOBT-4.4 and to depths of about 350 ft in MCOBT-8.5 (LANL 2002, 71301). Gravimetric moisture content measured in those samples ranges from 13% to 40% in the Cerro Toledo interval, encountered in MCOBT-4.4. Rogers and Gallaher (1995, 55334) report volumetric moisture content values from about 17% to about 56% for samples of the Tsankawi Pumice/Cerro Toledo interval collected in Mortandad Canyon. Gravimetric moisture content in Mortandad Canyon for the Otowi Member ranges from 15% to 22% in samples collected in boreholes MCOBT-4.4, MCOBT-8.5, R-15, and MCM5.9 (LANL 2002, 71301; Longmire et al. 2001, 70103 [R-15 report]). In general, the moisture content in the Otowi Member is less variable than in the alluvium or Cerro Toledo interval. The low variability of moisture in the Otowi Member probably reflects the relative homogeneity of the ash-flow tuffs that make up this unit compared to the stratified sedimentary deposits that make up the alluvium and Cerro Toledo interval. Rogers and Gallaher (1995, 55334) report volumetric moisture content values from 20% to 23% for Otowi tuff samples from Mortandad Canyon.

Eighteen sidewall core samples were taken from depths between 272 to 735 ft in the MCOBT-4.4 borehole, and nine sidewall samples were collected between 405 and 709 ft in the MCOBT-8.5 borehole. These samples were used to determine gravimetric moisture contents in the units beneath the Otowi Member. The moisture content measured in the single sample of the Guaje Pumice Bed (Qbog) taken from MCOBT-4.4 was 46% (at a depth of 470 ft). The average gravimetric moisture content in three samples of the Puye Formation in MCOBT-4.4 was about 20%, higher than the 5.8% moisture content measured in the single sample of Puye in MCOBT-8.5. The average moisture content measured in eight samples of interflow breccia zones in the Cerros del Rio basalt from MCOBT-4.4 was 14%, which closely matched the average moisture content measured in seven basalt samples taken in MCOBT-8.5. However, the gravimetric moisture content data for the basalt are highly variable and range between 4% and 45% in the sidewall core samples (LANL 2002, 71301, Table 11.1-2).

The direction and flux of water through the unsaturated zone have been examined in several studies. Rogers and Gallaher (1995, 55334) tabulated Bandelier Tuff core hydraulic properties from several boreholes at the Laboratory to estimate recharge rates beneath the Pajarito Plateau. Rogers et al. (1996, 55543) used hydraulic properties from seven boreholes that had sufficient data to evaluate the movement of water in the unsaturated bedrock. The seven boreholes were from mesa top and canyon bottom locations, which represent two of the distinct hydrologic regimes on the Pajarito Plateau. For wells MCM-5.1 and MCM-5.9A in Mortandad Canyon, they estimate downward Darcy fluxes ranging from 0.13 to 1.5 mm/yr (Rogers et al. 1996, 55543). More recently, Kwicklis et al. (2005, 90069) estimated infiltration rates in Mortandad Canyon at 176 mm/yr based on average stream flow data for the years 1995 through 2000. They acknowledged that rates were likely higher before 1995 when greater effluent volumes were released into the canyon.

#### **2.4.4 Intermediate-Depth Perched Aquifer**

Perched intermediate groundwater was encountered during the drilling of regional aquifer well R-15, within the Cerros del Rio basalt and in intermediate well MCOBT-4.4 within the Puye formation. Perched water was not encountered in regional wells R-1, R-13, R-14, or R-28. Broxton and Vaniman (2005, 90038) give a more complete listing of perched water occurrences for Mortandad Canyon.

#### **2.4.5 Regional Aquifer**

The regional aquifer was encountered in the Puye Formation in regional wells R-1, R-13, R-14, R-15 and R-28 in the Mortandad watershed. At a larger scale, the regional aquifer is primarily made up of several sedimentary hydrostratigraphic units of varying thickness, lateral extent, and permeability (Broxton and Vaniman 2005, 90038; Keating et al. 2005, 90039). Groundwater flow in the regional aquifer is generally eastward (Purtymun 1984, 06513; LANL 2003, 76059). The hydraulic conductivity of aquifer rocks is heterogeneous and averages approximately 140 m/yr at a regional scale, with spatial variations on the order of 10 m/yr. In the western portions of the Laboratory, the hydraulic gradient (which controls the direction of flow) is generally downwards, and groundwater generally flows east/southeast towards the Rio Grande.

Permeability and conductivity measurements measured in the regional aquifer in wells across the Pajarito Plateau are listed in Table 2.4-1. Data in this table demonstrate variability in hydraulic conductivity and, to a lesser extent, permeability derived from wells near Mortandad Canyon. Across the Pajarito Plateau, however, permeability data show greater variability (LANL 2003, 76059, Table 4.3-4).

**Table 2.4-1**  
**Permeability and Hydraulic Conductivity Data for Hydrostratigraphic Units in Regional Aquifers (LANL 2003)**

Stratigraphic Unit	Well	Permeability (log m <sup>2</sup> )	Hydraulic Conductivity (m/yr)
Santa Fe Group (Tsf)	O-1	-12.64	70.11
Older fanglomerate (Tsfuv)	O-4	-11.84	447.35
	PM-4	-11.94	358.32
Puye (Tpf)	TW-8	-11.92	372.79
	R-15	-12.14	223.67
	R-15	-11.92	369.45
Cerros del Rio Basalt (Tb)	PM-5	-12.59	79.01

The Rio Grande is the main discharge area for the regional aquifer. Stream flow data indicate that the river potentially gains about 490 kg/s, or 12,500 acre ft/yr, from the regional aquifer near Pajarito Plateau (Keating et al. 1999, 88746).

## 2.5 Water-Supply Wells near Mortandad Canyon

Water-supply wells extract water from deep within the regional aquifer for residential and commercial use in Los Alamos County as well as for the Laboratory. The pumping wells are screened over 200 to 500 m, beginning about 50 to 70 m below the water table. The water-supply wells nearest to (and potentially impacted by contaminants in) Mortandad Canyon are located in the Pajarito Mesa (PM-1, PM-2, PM-3, PM-4, and PM-5) and Otowi (O-1 and O-4) well fields (Figure 2.2-1), which together provide about half of the water supply for the County.

The total rate of pumping of the O series and PM series wells has increased over time [Koch and Rogers 2003, 88425]. The first wells to start pumping were PM-1, PM-2, and PM-3, between 1965 and 1968. After that, PM-4 (1982) and PM-5 (1986) were added. The latest wells to start pumping were O-4 (1993) and O-1 (1996). Annually averaged pumping rates vary among these supply wells. The greatest variability in pumping rates is for PM-2 and PM-4.

The supply wells pump during irregular periods within a given year, but wells pump at a relatively constant rate when they are working. The wells typically are pumped about 30% of the time each year.

To date, no contaminants have been detected in water from wells supplying drinking water in concentrations that exceed EPA's safe drinking-water standards.

## 2.6 Generalized Conceptual Site Model

The descriptive information presented above provides the basis for the generalized conceptual model shown in Figure 2.6-1. This figure generalizes the transport processes for the conceptual model shown in Figure 2.2-3 and includes the potential exposure pathway provided by the water-supply wells. The conceptual model incorporates several component processes, namely source term, infiltration, unsaturated transport, saturated transport, and exposure. This conceptual model is the general framework for the risk assessments described in Chapter 3 of this document.

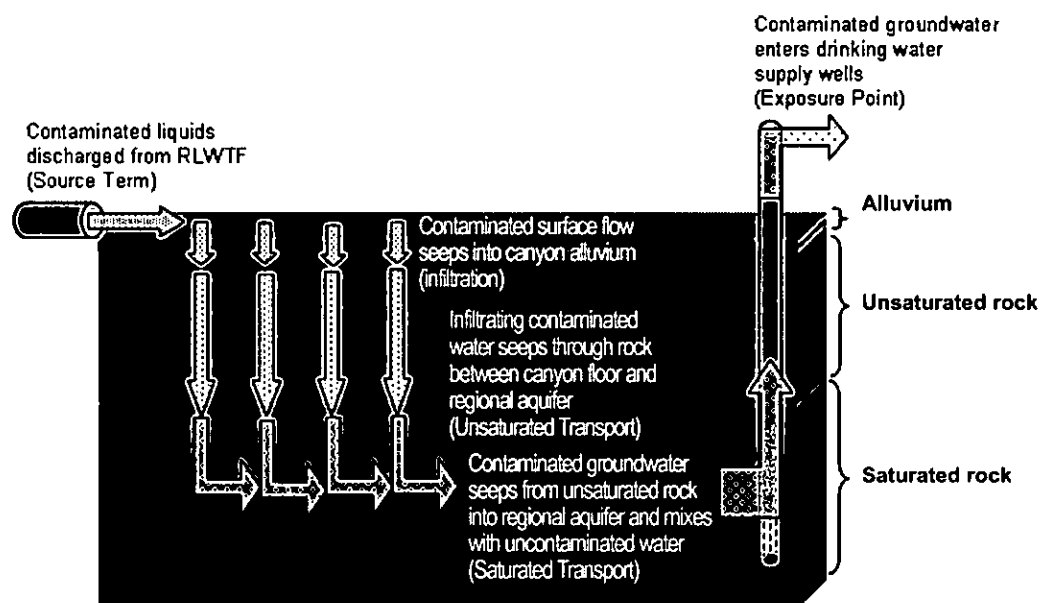


**Figure 2.6-1. Generalized conceptual model of contaminant transport and fate from the RLWTF to drinking-water supply wells**

The conceptual model is a simplified representation of the various and variable processes that influence the transport of soluble, nonsorbing contaminants within the groundwater system between the point of release (the RLWTF) and the point of exposure (drinking water). Again, the focus is on nonsorbing contaminants because these will migrate most quickly through the unsaturated zone and toward water supply wells. Currently, exposure-point concentrations are not high enough to present an imminent human-health impact, but because contaminants are present in the groundwater system, there is a need to evaluate the potential for future human-health impacts associated with exposure from produced water. This will follow the risk-management question(s) presented at the beginning of this chapter. To conduct a risk assessment for future exposures, each of the processes identified in the generalized conceptual model is analyzed with mathematical models, which are discussed in Chapter 3.

The following items describe the conceptual model, which is based on several simplifying assumptions.

- Contaminated water from the RLWTF is discharged into Mortandad Canyon, where it is mixed with and diluted by uncontaminated surface water from other upstream locations.
- Some of the well-mixed surface water infiltrates into the alluvial system along the canyon, but some continues downstream. The surface flow is assumed to eventually infiltrate into the alluvial system. However, evapotranspiration of surface water and alluvial water in the upper reach of the canyon occurs because the alluvial system is near the surface in that reach (Purtymun 1967, 11785).
- Contaminated water mixes throughout the alluvial groundwater system and acts as a line source of water and nonsorbing contaminants to the deeper unsaturated bedrock. The nonsorbing contaminants are assumed to be well mixed in alluvial groundwater, based on observations of both rapid travel times through the alluvium (reported by Purtymun 1974, 05476), and on nitrate and tritium concentrations measured regularly in alluvial wells since the early 1960s (LANL 1997, 56835; LANL 2001, 70346).

- Some degradation of nitrate (and lesser degradation of perchlorate) occurs throughout the unsaturated zone as a result of microbial activity.
- Infiltration from the alluvial groundwater to the deeper unsaturated zone is assumed to be a function of the discharge volume from the RLWTF. This infiltration process is variable and uncertain in space and time, but the majority of the alluvial groundwater is assumed to infiltrate within the Laboratory boundary because alluvial monitoring wells downstream from well MCO-8 (Figure 2.2-1) rarely contain perched alluvial water (LANL 1997, 56835).
- Groundwater infiltrates predominantly downward through the unsaturated bedrock, primarily through the pore spaces in the rock matrix. Some fracture flow may occur in some of the more welded units of the Bandelier Tuff. Flow through the Cerros del Rio basalt is assumed to be fracture dominated. Perched intermediate groundwater within the Puye Formation and Cerros del Rio basalt may either be relatively stagnant, resulting in a retardation of vertical flow, or may provide a lateral pathway, depending on geometric constraints and permeability contrasts (LANL 2004, 82613; Broxton and Vaniman 2005, 90038).
- Groundwater moving through the vadose zone recharges the regional groundwater that might be contaminated by upstream Mortandad Canyon columns at the water table.
- Municipal water supply wells extract water over large screened intervals deep within the regional aquifer. Pumping of supply wells creates transient pressure gradients (and flow directions) in the regional aquifer.
- Individual members of the public receive drinking water pumped directly from a specific supply well, which is their only source of drinking water.

The Laboratory will continue to treat liquid wastes at the RLWTF for the near future. The future volume and composition of treated wastewater is not known, but if recent trends continue, the net volume and concentration of many contaminants could be reasonably expected to decrease. It is also unknown if treated wastewater will be discharged into Mortandad Canyon for the operational lifetime of the facility. The containment of treated wastewater has been proposed.

The risk assessment discussed in Section 3.0 considers the impacts that the numerous uncertainties in operations, environmental processes, water-supply pumping, and the potential past and future releases from the RLWTF could have on the local public drinking-water supply.

### 3.0 RISK-ASSESSMENT METHODOLOGY AND RESULTS

The conceptual model presented in Section 2.6 of this document identifies several sequential dynamic processes that affect the groundwater transport of contaminants released from the RLWTF into Mortandad Canyon and the concentrations of those contaminants at production wells. To date, no contaminants have been detected in groundwater supply wells at concentrations that exceed EPA's safe drinking water standards.<sup>\*</sup> However, alluvial and intermediate groundwater in Mortandad Canyon contains tritium and nitrate at concentrations exceeding their maximum concentration limits (MCLs), and perchlorate exceeding its EPA health advisory level. Although neither alluvial nor intermediate groundwater is used for municipal purposes, both are hydrologically connected to the regional aquifer; therefore, the contaminants in alluvial and intermediate groundwater are expected to move into the

---

<sup>\*</sup> Perchlorate has been detected in samples from O-1 in concentrations near 4 ppb; O-1 is not currently being used as a source of drinking water.

regional aquifer in the future. Above-background concentrations of nitrate, perchlorate, and tritium have been detected in the regional aquifer at Mortandad Canyon in a few of the monitoring wells, which indicates that some contamination has already entered the aquifer. The rate of contaminant transport and the concentration of contaminants (which together describe the flux of contaminants) are important factors in determining corrective actions to ensure that members of the public are not exposed to unsafe drinking water. Data obtained through (ongoing) site investigations provide information about how contaminants have moved. These data also provide information that is used to construct and calibrate simulation models that provide information regarding how contaminants are expected to move in the future. Simulation models are used to estimate unknown future contaminant fluxes and concentrations in water pumped from the regional aquifer. This information is used in exposure and toxicity assessments to evaluate the potential for unsafe drinking water concentrations to occur over time.

In the analysis described in this paper, groundwater transport and supply-well pumping simulations were conducted over a period of 1000 yr, a time frame that captured maximum potential concentrations in production wells. In general, baseline risk assessments for cleanup sites consider a time horizon of up to 100 yr. This time period is the objective of the Mortandad Canyon Groundwater Workplan to characterize the nature and extent of contamination in terms of "bounding spatial and temporal (100 yr) uncertainties in contaminant concentrations and distributions" to provide input to risk assessment (LANL 2004, 82613).

This chapter describes the groundwater transport simulations and exposure and toxicity assessments conducted to aid in decision making for potential corrective actions in Mortandad Canyon. Because the Tier-1 risk assessment established the need for a higher-tier risk assessment, the Tier-1 analysis is briefly summarized here and presented more fully in Appendix A. In the subsequent sections of this chapter, the Tier-3 groundwater transport simulations and risk-assessment methodology are described to facilitate an understanding of the decision analysis described in the next chapter.

### **3.1 Risk-Assessment Approach**

The approach to this human-health risk assessment is based on EPA's Risk Assessment Guidance for Superfund Volume III, Process for Conducting Probabilistic Risk Assessment (Part A) (RAGS3; EPA 2001, 85534). The first step in the risk assessment process is a simple Tier-1 calculation of risk (Figure 1.1-1). Depending on the results of the Tier-1 risk assessment, relatively more complex, higher-tier calculations are conducted to provide decision makers and decision stakeholders with information to support high-confidence decisions. For Mortandad Canyon, a Tier-1 and a Tier-3 risk assessment were conducted.

The Tier-1 risk-assessment results indicated a potential for contamination of regional groundwater at a production well, as summarized below in Section 3.2. Because of this result, a Tier-3 assessment was conducted to provide more detailed information regarding the likelihood that groundwater standards would be exceeded and the factors associated with that occurrence. The Tier-2 risk assessment described in RAGS3 (RAGS3; EPA 2001, 85534) (Fig. 1.1-1) examines the importance of uncertainty in a single variable in the risk assessment, but the Tier-3 risk assessment examines the importance of multiple uncertainties at once. Given the high degree of cumulative uncertainty in groundwater transport processes and future pumping scenarios, the Tier-3 risk assessment was most appropriate for Mortandad Canyon assessment and decision support.

In RAGS3 (EPA 2001, 85534), EPA states that Tier-3 human-health risk assessments should reflect variability or uncertainty in exposure. For Mortandad Canyon, variability and uncertainty in exposure is accomplished by using groundwater-transport models to calculate contaminant concentrations at wells, each time using a different set of values for parameters in the models from each parameter distribution (Sections 3.3 and 3.4). The results of the groundwater transport simulations described in Section 3.3 are

used as input to a probabilistic risk assessment described in Section 3.4. The risk assessment is probabilistic because it evaluates the probability (which is a measure of the cumulative uncertainty) that contaminants will reach production wells in concentrations that may result in unacceptable exposures.

Over 750,000,000 Tier-3 transport and risk-assessment calculations were conducted; therefore, the meaning of the cumulative results will be discussed rather than the individual simulations. These results, as presented in Sections 3.3 and 3.4, are a summary of the detailed information reported by Birdsell et al. (2005, in progress) and in Appendix C.

The unsaturated-zone and saturated-zone flow and transport simulations for both the Tier-1 and Tier-3 analyses were run using the Finite Element Heat and Mass (FEHM) transfer code (Zyvoloski et al. 1997, 70147). FEHM was developed by researchers at the Laboratory and is particularly suited for addressing the unique characteristics of the Pajarito Plateau, including 3-D saturated and unsaturated multiphase flow and the transport of multiple contaminants within complex geologic media. FEHM simulates three-dimensional, time-dependent, multiphase, nonisothermal flow and multicomponent reactive groundwater transport through porous and fractured media. The software is mature, has users throughout the world and has been certified through the Yucca Mountain Project Software Quality Assurance Program (YMP SQAP). Other advantages are that the software is locally developed, and local users have extensive experience with the code. FEHM can be used for probabilistic simulations when run in multiple realization mode using the software package FEHM2POST, which is also certified through the YMP SQAP. The parameter estimation code PEST can also be used with FEHM. Both FEHM2POST and PEST were used in these analyses.

### 3.2 Summary of Tier-1 Risk Assessment

This section summarizes the Tier-1 risk assessment. It demonstrates the incorporation of the component models illustrated in Figure 2.6-1 into a deterministic analysis. The simulations consider the movement of contaminants from their source at the RLWTF outfall, through the alluvium in Mortandad Canyon, through the unsaturated bedrock beneath the alluvium, through the regional aquifer and into water-supply wells. The resultant water-supply well concentrations are input to calculations of human-health indicators. More detail about the Tier-1 assessment is given in Appendix A.

Source Term: The Tier-1 groundwater transport simulations address annual discharges of wastewater from the RLWTF into Mortandad Canyon between 1964 and 2104. Annual tritium and nitrate releases were based on the discharge records presented previously in Table 2.1-1, with discharges for the 102 yr beyond 2002 held constant at the 2002 rate. Because the full reported masses released for nitrate and tritium were used in the simulations, the sources are considered to represent upper bounds. Because perchlorate discharge data are not available for the period between 1964 and 2002 (when a treatment process was added at the RLWTF to eliminate perchlorate from discharged effluent), annual perchlorate releases for this time period were inferred from correlations of nitrate and perchlorate measurements in core samples, as reported in Appendix A and by Birdsell et al. (2005, in progress). The 95% upper-confidence limit from a linear regression of nitrate and perchlorate core data was used with the RLWTF nitrate data to estimate the perchlorate source, as shown in Figure 3.2-1.

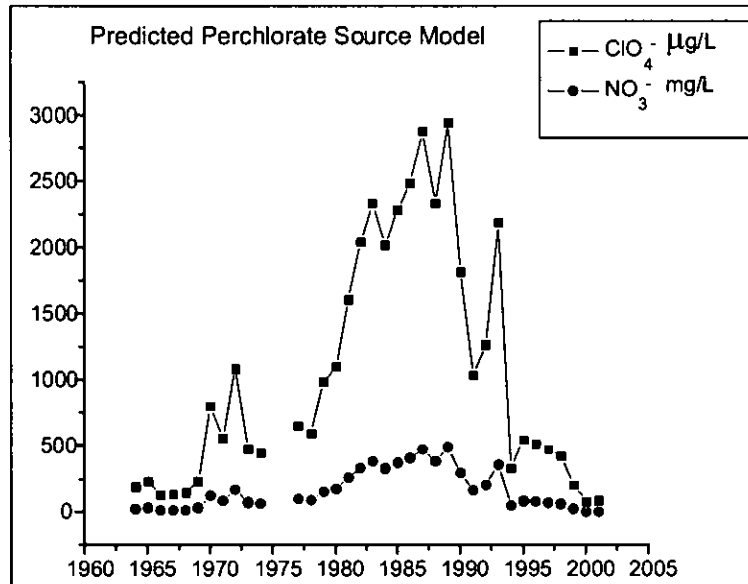


**Figure 3.2-1. Annual average estimates of perchlorate concentration ( $\mu\text{g/L}$ ) releases based on recorded concentrations of nitrate ( $\text{mg/L}$ ) releases. The perchlorate releases represent an estimated 95% upper-confidence limit for the Tier-1 source.**

The annual masses of tritium, nitrate, and perchlorate released into Mortandad Canyon in RLWTF surface-water effluent were assumed to homogeneously mix with other surface water in the canyon, to infiltrate into the alluvium, and then flow along the canyon floor within the alluvial aquifer. Flow within the alluvial aquifer is assumed to be rapid and to result in uniform concentrations that are generally lower than the RLWTF source concentration. These assumptions are supported by gaging station data, which indicate higher surface water flow rates than RLWTF release rates, and also by alluvial nitrate concentration data, which are fairly uniform (i.e., well mixed) throughout the alluvial aquifer on an annual basis.

**Infiltration:** A portion of the combined surface water flowing along Mortandad Canyon infiltrates into alluvial material, creating alluvial groundwater distributed along the canyon. The distribution of alluvial groundwater used in the Tier-1 groundwater transport simulations was based on a study conducted in the early 1960s (Purtymun 1967, 11785). That study used monthly data from gaging stations and alluvial observation wells along Mortandad Canyon to estimate the volume of water infiltrating in three sections along the canyon, which were designated upper, middle, and lower Mortandad Canyon. The spatial delineations established in the Purtymun study are shown in Table 3.2-1, along with the estimates of the interface areas between the base of the alluvium and the underlying tuff, and the rates and volumes of infiltration for each section. These conservative assumptions are designed to provide a worst-case estimate of transport.

**Table 3.2-1**  
**Infiltration Estimates from the Alluvial Aquifer to the Unsaturated Zone**  
**for Three Sections of Mortandad Canyon (Purtymun 1967, 11785)**

Canyon Section	Location Markers (see Figure 2.2-1)	Volume of Infiltrating Water ( L/yr)	Effective Infiltration Rate (m/yr)	Area of Section (m <sup>2</sup> )
Upper	TA-50 outfall to MCO-4	$6.0 \times 10^7$ (60%)	6.0	9987
Middle	MCO-4 to MCO-6	$1.8 \times 10^7$ (18%)	1.5	12077
Lower	MCO-6 to Laboratory boundary	$2.2 \times 10^7$ (22%)	0.6	37161

The estimated effective annual infiltration rates in the upper, middle, and lower portions of Mortandad Canyon (i.e., 6.0, 1.5, and 0.6 m/yr, respectively) are the highest among several independent analyses. What is more, the infiltration rates listed in Table 3.2-1 result in a cumulative infiltration volume ( $10 \times 10^7$  L/yr) that exceeds the recorded discharge volumes (Table 2.1-1). Consistent with the intention of Tier-1 analyses, the Purtymun infiltration rates were used as point-estimates of infiltration at the alluvium/bedrock interface in the Tier-1 analysis to minimize transport times through the unsaturated tuff and are held constant throughout the entire Tier-1 analysis.

Unsaturated-zone transport: Unsaturated-zone flow and transport calculations were run with the FEHM computer code (Zyvoloski et al. 1997, 70147). In the Tier-1 model, the upper, middle, and lower portions of Mortandad Canyon described by Purtymun (Table 3.2-1) were represented as three one-dimensional (1-D) columns, as illustrated in Figure 3.2-2. As the figure indicates, each column was divided into layers representing the appropriate geologic strata between the base of the alluvium and the top of the regional aquifer using data from the site-wide geologic model (Carey et al. 1999, 66782).

The Tier-1 analysis used mean-value estimates of hydrologic properties (according to van Genuchten 1980, 63542) derived from site-specific data (LANL 2002, 73113). Fractured strata were assigned very low porosity values to ensure rapid contaminant transport, consistent with the Tier-1 approach.

The cross-sectional area of each column in the Tier-1 unsaturated transport model was equal to the appropriate area in Table 3.2-1, and the corresponding effective infiltration rate provided the steady upper-boundary condition for each column. The total annual contaminant mass discharged from the RLWTF and entering the alluvial groundwater was mixed with uncontaminated surface water and entered the unsaturated columns the same year that it was released, assuming short residence time in the alluvium. Contaminant transport was simulated from 1964 through 2104. Time-dependent contaminant mass flux from the three columns was input into the saturated-zone model.

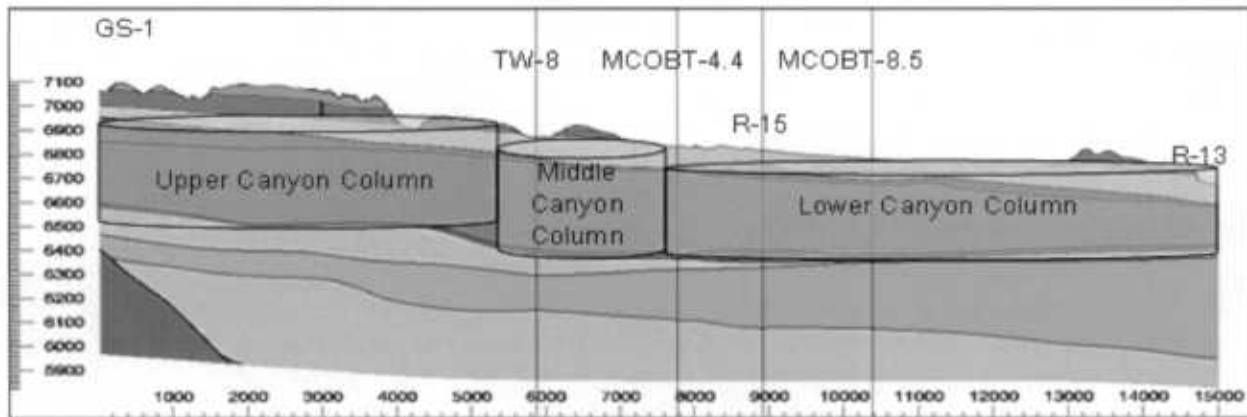


Figure 3.2-2. Illustration of three 1-D columns used for the Tier-1 unsaturated-zone groundwater transport simulations

**Saturated flow and transport/pumping scenario:** The Tier-1 saturated transport model uses the site-scale version of the three-dimensional (3-D) regional-aquifer model described in the Groundwater Annual Status Report for Fiscal Year (FY) 2002 (Nylander et al. 2003, 76059). The saturated transport simulations were conducted using the FEHM code (Zyvoloski et al. 1997, 70147). The Tier-1 analysis assumed that the pumping wells control the spatial distribution of the contaminants entering the regional aquifer at the water table. In addition, the basalts have a very low porosity (0.0001) to represent rapid fracture transport in those units. This conceptual model ensures that most of the contaminants will be captured by the water-supply wells. The contaminant fluxes exiting the base of the three Tier-1 unsaturated model columns provide input into three cells at the top surface of the 3-D saturated transport grid, shown in Figure 3.2-3.

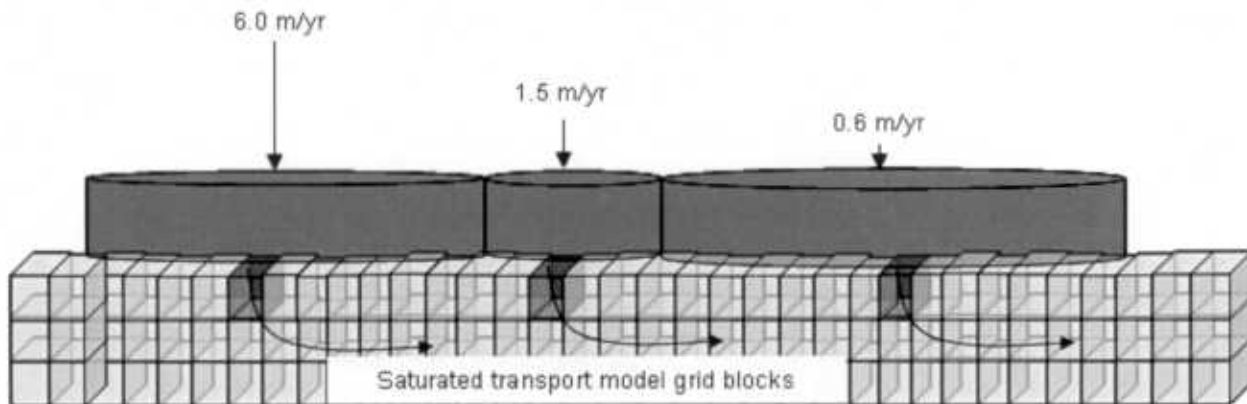
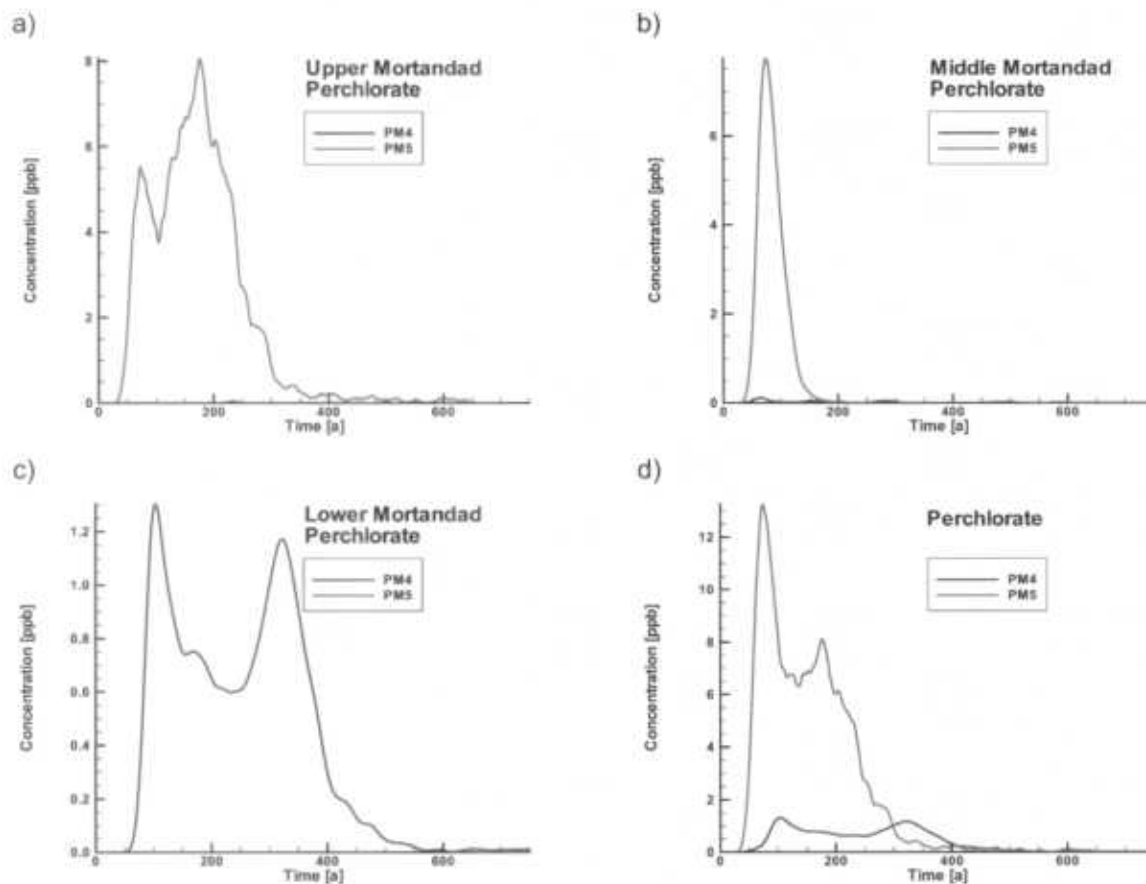


Figure 3.2-3. Illustration of the relationship between the three unsaturated-zone columns and the grid elements used in the saturated-zone model

The saturated-zone simulation starts in 1946 to create a transient flow condition that is influenced by pumping wells, and it runs for a 1000-yr period to capture the full tails of the breakthrough curves to water-supply wells. The model simulates pumping of water according to water-supply, well-production data for both the Los Alamos County supply wells, and the Buckman well field. These data are averaged over 5-yr time periods, starting in 1946, as shown in Appendix A. Pumping rates beyond the final 1996 to 2000 period of record are held constant at that 5-yr average rate because of unknown, expected future pumping rates.

Pumping of the regional supply wells, especially the PM wells, has a strong control on contaminant flow rate and direction. In fact, the assumed steady pumping rates used after 1996 are highest for wells PM-2, PM-4, and PM-5, which are south of Mortandad Canyon. In that scenario, wells PM-1 and PM-3, to the east of Mortandad Canyon, have relatively low pumping rates. Figure 3.2-4 shows the calculated concentrations of perchlorate in water pumped from PM-4 and PM-5 over the first 750 yr of a 1000-yr simulation period, for perchlorate originating from the upper-, middle-, and lower-canyon columns, and the cumulative concentration from the three columns. Contaminants entering the saturated-zone transport model after 1996 from the upper-canyon column of the unsaturated transport model flow almost directly to PM-5 and do not reach the other PM wells over the simulated time frame. Contaminants from the lower-canyon column flow directly toward PM-4 and do not reach PM-5. Contaminants from the middle-canyon column reach both PM-5 and PM-4. In the Tier-1 groundwater transport simulations, PM-1, PM-2, PM-3, O-1, and O-4 are not impacted by contaminants from the RLWTF released into Mortandad Canyon because the flow direction is so strongly dominated by pumping of the wells to the south.



**Figure 3.2-4.** Tier-1 concentrations of perchlorate from (a) upper, (b) middle, and (c) lower Mortandad Canyon and (d) for all three sections combined in water pumped from PM-4 and PM-5 (Time = 0 represents 1964)

Table 3.2-2 gives contaminant travel-time information for the Tier-1 assessment. The unsaturated-zone travel times represent mean-mass transport times through the upper-, middle-, and lower-canyon columns in the unsaturated transport model. The saturated-zone travel times are mean-mass arrival times for contaminants to reach a supply well upon arrival in the regional aquifer at the water table. The total mean-mass travel time is reflected in the arrival of the peaks in the perchlorate breakthrough curves for PM-4 and PM-5, given in Figure 3.2-4.

**Table 3.2-2**  
**Tier-1 Mean-Mass Contaminant Travel Times**

	Unsaturated-zone Travel Time (yr)	Saturated-zone Travel Time (yr)	Total Travel Time (yr)
Upper canyon to PM-5	12	152	164
Middle canyon to PM-5	35	33	68
Lower canyon to PM-4	67	7	74

In the Tier-1 groundwater transport simulations, most of the perchlorate reaching the supply wells originates from the upper-canyon column in the unsaturated transport model, causing relatively high concentrations in water pumped from PM-5 for about 200 yr (Figure 3.2-4[a]). Releases from the middle-canyon column create equally high concentrations in PM-5, but these concentrations are shorter-lived relative to those resulting from the upper-canyon column (Figure 3.2-4(b) and [a]). These relative concentrations reflect the distribution of contaminants input into each column in the unsaturated transport model. Perchlorate concentrations at PM-4 from the lower-canyon column are about an order of magnitude lower than those at PM-5. Nitrate concentrations at wells PM-4 and PM-5 are over 100 times greater than perchlorate concentrations are, yet scaled nitrate breakthrough curves mimic the time-dependent behavior of the perchlorate breakthrough curves because of the correlation of the perchlorate source to the nitrate source (Figure 3.2-1).

**Human-Health Risk Assessment:** The concentrations of nitrate and perchlorate calculated for supply-well water in the saturated transport model were used in the Tier-1 exposure and toxicity assessment calculations. For nitrate, separate HQ values were calculated for infant and adult exposures, using the applicable reference doses (RfDs) from EPA (EPA Integrated Risk Information System [IRIS]). For perchlorate, HQ values were calculated for hypothetical adult exposures, using an RfD of 0.00003 mg/kg/day, which is equivalent to an MCL of 1 ppb. Adult HI values were calculated for cumulative exposures to both nitrate and perchlorate.

Adult HQ and HI values were calculated for chronic 70-yr exposures to 2 L/day of contaminated drinking water. The maximum concentrations calculated in any individual well over any continuous 70-yr period were used in the chronic adult-exposure toxicity assessments. This implies that a hypothetical member of the public drinks 2 L/day of water drawn exclusively from a single well continuously for 70 yr. All sources of contamination were included in the exposure and toxicity assessment.

Infant HQ values for nitrate also were calculated according to EPA guidance. The infant toxicity assessment assumed a 0.64 L/day ingestion rate over a period of one year, using the maximum annual concentration of nitrate calculated in any single supply well. Appendix C provides additional information on the exposure and toxicity assessment calculations.

Tritium exposures were not explicitly calculated for the Tier-1 assessment because radioactive decay during the estimated saturated-zone transport time to wells PM-4 and PM-5 was sufficient to reduce tritium concentrations exiting the unsaturated zone to values of less than 20,000 pCi/L, which is equivalent to the 4-mrem/yr dose threshold for safe drinking water using EPA's toxicity and exposure methodology. The maximum concentration of tritium in pumped water is calculated to be 8000 pCi/L.

In the Tier-1 risk assessment, tritium doses remain well below the 4 mrem/yr safe drinking water standard throughout the Tier-1 simulation period. Similarly, the HQ and HI values for hypothetical exposures to calculated concentrations of nitrate and perchlorate in waters pumped from PM-4 never exceed 1.0, and

HQ values for hypothetical exposures to calculated nitrate concentrations in waters pumped from PM-5 are essentially zero. The Tier-1 HQ for hypothetical infant exposures to nitrate concentrations calculated in well water from PM-4 and PM-5 never exceeds the threshold value of 1.0. In contrast, the Tier-1 HQ values for hypothetical exposures to perchlorate concentrations in PM-5 are well above 1.0, reaching a maximum of about 8.0. The HI values calculated for both PM-4 and PM-5 exposures are due entirely to perchlorate.

### 3.3 Tier-3 Groundwater Transport Simulation

The groundwater transport simulations developed to calculate contaminant concentrations as input to the risk assessment integrates mathematical models of the components illustrated in Figure 2.6-1 and summarized with the Tier-1 discussion as follows:

- Source Term: Annual releases of contaminants into Mortandad Canyon from the RLWTF.
- Alluvial Transport: Discharges from the RLWTF flow along the streambed and into alluvial groundwater in Mortandad Canyon.
- Deep Infiltration: Contaminated alluvial groundwater seeps downward into the unsaturated bedrock (Bandelier Tuff and Cerro Toledo interval).
- Unsaturated Transport: Contaminated groundwater moves downward through unsaturated bedrock under the forces of gravity and capillary suction.
- Saturated Transport: Contaminated groundwater moves from unsaturated rock into saturated rocks (basalts) and sediments (Puye Formation/Santa Fe Group) and is transported in directions established by natural and induced hydraulic gradients.
- Pumping: Contaminated groundwater in the regional aquifer is drawn into supply wells.

The Tier-3 models for source term, infiltration, unsaturated transport, saturated transport, and pumping incorporates uncertainties in hydrologic and transport parameters and in conceptual understanding were bounded, but not quantified, in Tier-1 models. The groundwater transport simulations do not explicitly account for perching at intermediate depths in the unsaturated zone, which is known to occur at some discrete locations in Mortandad Canyon. However, the unsaturated transport model does implicitly account for the effects of perching on vertical transport insofar as it is conditioned to bound measured moisture content and contaminant concentrations.

#### 3.3.1 Tier-3 Source Term

The Tier-3 groundwater transport simulations address annual discharges of wastewater from the RLWTF into Mortandad Canyon between 1964 and 3002. The simulations are run for 1000 yr into the future so that maximum calculated concentrations are captured.

Annual tritium and nitrate releases were based on the discharge records in Table 2.1-1, with discharges for the 1000 yrs beyond 2002 held constant at the 2002 rate. Annual perchlorate releases between 1964 and 2002 (when a treatment process was added at the RLWTF to eliminate perchlorate from discharged effluent) were inferred from correlations of nitrate and perchlorate measurements in core samples, as reported by Birdsell et al. (2005, in progress). Both nitric and perchloric acids were used extensively in radiochemistry activities at the Laboratory. Waste waters containing the spent acids were processed through the RLWTF, and these acids represent the major source of nitrate and the only source of perchlorate, in the canyon. Full details of the development of the source term are given by Birdsell et al. (2005, in progress).

Figure 2.2-1 shows the locations of the boreholes from which core samples were analyzed for nitrate and perchlorate pore water concentrations. In order of their proximity to the RLWTF outfall, these boreholes are intermediate characterization wells MCOBT-4.4 and MCO-7.2, regional characterization well R-15, and intermediate observation well MCOBT-8.5. Samples from these locations were used to derive a basis for estimating historic perchlorate releases from the RLWTF.

Figure 3.3-1 shows plots of perchlorate and nitrate pore water concentrations from core samples from boreholes MCOBT-4.4, MCO-7.2, R-15, and MCOBT-8.5. The plots indicate a correlation between perchlorate and nitrate concentrations in the vadose zone at all locations except intermediate observation well MCOBT-8.5. The preferential denitrification of nitrate (rather than perchlorate) is thought to occur at the site. Because MCOBT-8.5 is farther from the source of contamination at the RLWTF outfall than MCOBT-4.4, MCO-7.2, and R-15, nitrate in pore water at the location of MCOBT-8.5 has had more time to undergo denitrification, and this may explain why there is less correlation between perchlorate and nitrate concentration at that location. Denitrification also helps to explain the decrease in nitrate concentration relative to perchlorate at deeper locations in MCOBT-4.4 and R-15.

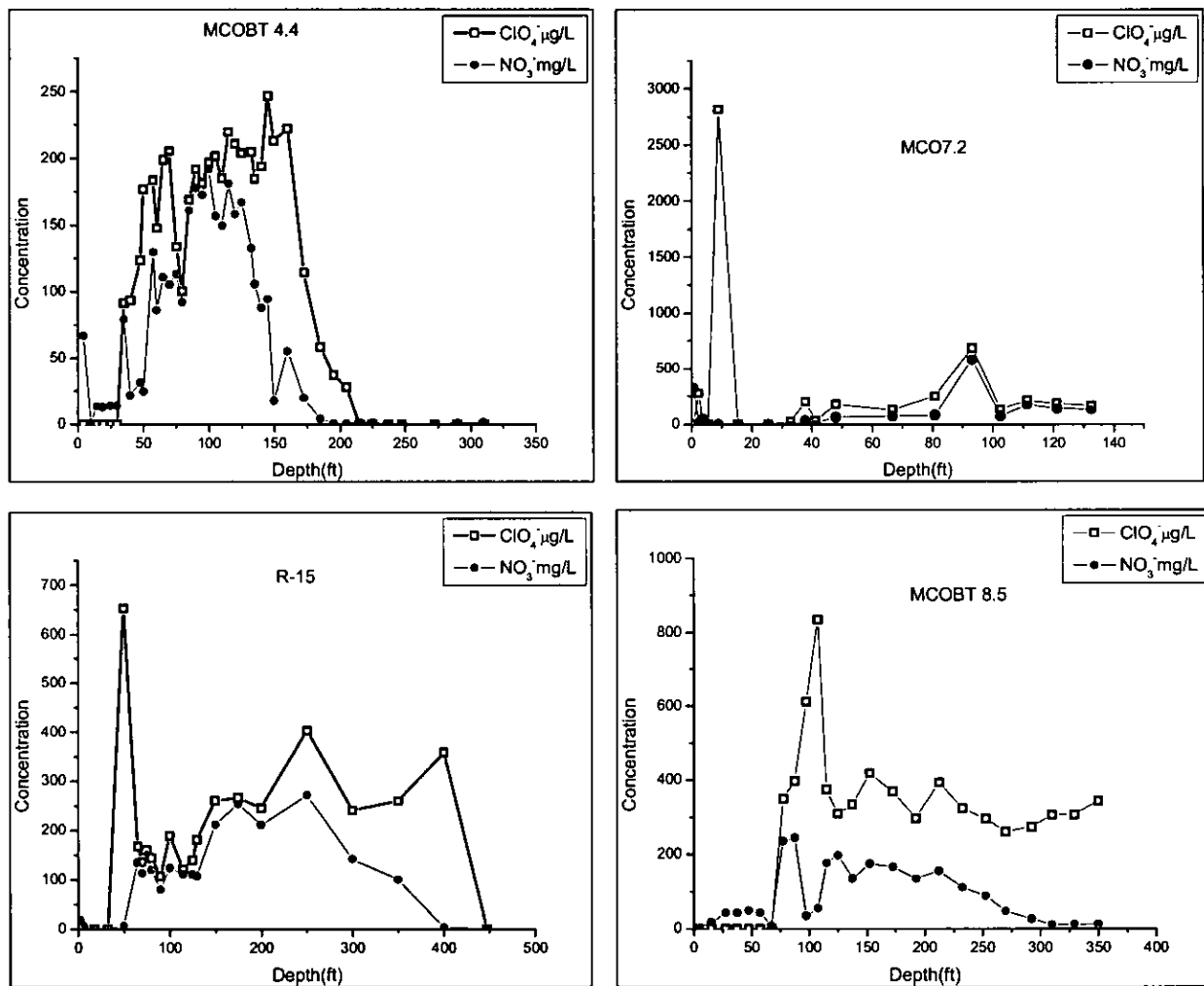


Figure 3.3-1. Perchlorate and nitrate (as nitrate) concentrations in pore water from core samples from boreholes in Mortandad Canyon

Data shown in Figure 3.3-1 were used in a regression analysis to establish a basis for estimating the time history of perchlorate releases. The data associated with core samples from intermediate borehole MCOBT-4.4 revealed the best statistical relationship between nitrate and perchlorate. Therefore, that data set was used to develop a relationship to estimate perchlorate releases based on the nitrate releases listed in Table 2.1-1. In the case of the Tier-1 analysis, the entire nitrate source term from the RLWTF was used to estimate the 95% upper confidence limit for the source term for perchlorate, as described in Section 3.2.

The Tier-3 analysis also used the data of nitrate releases from the RLWTF and the correlation between perchlorate and nitrate at borehole MCOBT-4.4 to develop a perchlorate source term. However, in Tier 3, the nitrate and perchlorate sources were varied to account for the potential effects of denitrification throughout the simulation period. In addition, Tier 3 was used to evaluate the impact of eliminating all discharges from the RLWTF, beginning in 2005. These Tier-3 variations for the nitrate and perchlorate source term are summarized in the next two sections and by Birdsell et al. (2005, in progress).

The Tier-3 analysis used recorded tritium discharge data for the period after 1972, as shown in Table 2.1-1. The tritium source was estimated for the years between 1964 and 1971 by comparing alluvial well concentrations for that time period to the period after 1972. Although tritium is lost through evapotranspiration, these losses are not included in the study. The tritium source is described in Birdsell et al. (2005, in progress).

### 3.3.1.1 Denitrification of Nitrate

Based on site-specific data and literature review, nitrate degradation is likely to occur in alluvial groundwater. However, the degradation rate is not well known. The Tier-1 analysis did not account for denitrification of nitrate, which results in a potential overestimate of the inventory of perchlorate because the nitrate-perchlorate correlation derived for this analysis is based on the entire mass of nitrate released from the RLWTF, rather than on a degraded nitrate inventory.

The Tier-3 analysis incorporated uncertainty in nitrate degradation rates, which impacts both the nitrate and perchlorate source terms. In the Tier-3 analysis, a range of degradation rates was used to derive the source-term model. The primary assumption in this degradation analysis is that the denitrification of nitrate is the only source of nitrite in the vadose zone in Mortandad Canyon. Nitrite is relatively rare in the vadose zone on the Pajarito Plateau; therefore, any nitrite present may be from nitrate degradation (although nitrite can form from reactions other than nitrate degradation). Two methods were used to estimate the relative degree of denitrification of nitrate, consistent with this assumption. First, the approximate percentage of nitrogen as nitrite was evaluated using the ratio of nitrite pore water concentrations to the sum of nitrate and nitrite concentrations detected in specific groundwater and core samples. Second, the ratio of cumulative nitrite mass to cumulative nitrate plus nitrite mass over the entire depth of the borehole was evaluated. The results indicated that nitrate degradation estimates in the range of 2% to 30% were justified, although larger percentages of degradation could even be assumed.

To adjust the perchlorate release estimates in accordance with this range of nitrate degradation estimates, the nitrate data from borehole MCOBT-4.4 (cf. Figure 3.3-1) were increased by 2% and 30%, as detailed in Birdsell et al. (2005, in progress), using the following adjusted regression equations, which represent the average regression equations rather than the 95% upper-confidence limit, as in the Tier-1 analysis:

$$\begin{aligned} 2\% \quad \text{Perchlorate (mg/L)} &= 0.001046 * (\text{Nitrate mg/L as Nitrate}) + 0.037304 \\ 30\% \quad \text{Perchlorate (mg/L)} &= 0.000821 * (\text{Nitrate mg/L as Nitrate}) + 0.037304 \end{aligned}$$

The "2%" equation above represents the upper bound for the perchlorate source, and the "30%" equation gives the lower bound for the perchlorate source. For the nitrate source, the upper-bound source simply uses 98% of the nitrate inventory listed in Table 2.1-1, and the lower bound source uses 70% of the nitrate inventory. For the Tier-3 analysis, any source within (and including) these bounds is considered to be equally likely. The Tier-3 source then linearly interpolates between these two bounding source terms based on a scaling factor chosen for a particular realization, as described by the parameter "source interpolation factor" in Appendix B.

### **3.3.1.2 Discontinued Releases**

The Laboratory is evaluating alternatives that would allow for the elimination of discharges from the RLWTF into Mortandad Canyon. To evaluate how this action would impact the transport of contaminants already in the groundwater system, groundwater transport calculations for perchlorate were conducted using the Tier-3 source-term model described in the previous section with the following changes to represent the elimination of future discharges:

- From 2002 through 2005, the 2002 discharge volume is used ( $1.1E + 07$  L/yr), and the perchlorate source is assumed to vary randomly along a uniform distribution resulting in a release concentration of between 1 and 4 µg/L.
- From 2006 through 2010, the RLWTF discharge volume is maintained at 50% of the 2002 value to account for residual water in the alluvial system. No perchlorate is released with this water because effluent releases are assumed to cease in 2006.
- In 2010 and for the remainder of the simulation, the infiltration rate throughout the entire canyon (38 1-D columns) is reduced to a steady value of 50 mm/yr, which is consistent with infiltration rates for canyons with ephemeral surface water cited in the Groundwater Annual Status Report for FY 2002 (Nylander et al. 2003, 76059). No contamination is included in this infiltrating water.

### **3.3.2 Alluvial Groundwater Distribution and Infiltration**

The annual point-estimates of tritium, nitrate, and perchlorate released into Mortandad Canyon in RLWTF surface-water effluent were assumed to homogeneously mix with other surface water in the canyon, then to flow along the canyon floor before infiltrating into alluvium. This assumption is supported by gaging-station data, which indicate higher surface-water flow rates than RLWTF release rates, and also by alluvial nitrate concentration data, which are fairly uniform (i.e., well mixed) throughout the alluvial aquifer on an annual basis. The Tier-3 analysis used a distribution of values to account for a cumulative effect of variable discharge rates, surface water mixing, and evaporation/transpiration, as described in Appendix B and in Birdsell et al. (2005, in progress).

Three conceptual models of infiltration from the alluvial aquifer to the deeper vadose zone were developed for the Tier-3 analysis. The specifics of each alternative conceptual model are summarized in the next subsections, although much more information is provided by Birdsell et al. (2005, in progress). The following statements apply to all three infiltration models:

- The time-history of RLWTF discharges represents the volume and constituency of contaminated water entering the alluvium in Mortandad Canyon.
- RLWTF discharge volumes are scaled by a variable factor that is used to calculate the volume of water that enters the canyon as surface flow and ultimately ends up as the volume of water that can infiltrate into the deep vadose zone. For any single simulation, the value of the conversion factor is randomly sampled from an input distribution (see "TA-50 flow-to-surface-flow conversion factor" in Appendix B). The conversion factor accounts for the combined effect of both dilution by other sources of surface water in Mortandad Canyon and concentration by evapotranspiration.

- Mortandad Canyon, between the confluence with Effluent Canyon and the Laboratory boundary, is split into four sections, called the upper, middle, lower, and bottom sections, as shown in Figure 2.2-1. These sections are similar to those defined in Table 3.2-1, with the lower section split into two at well MCO-8. That is, for Tier 3, the lower canyon section is between wells MCO-6 and MCO-8; the bottom canyon section is between MCO-8 and the Laboratory boundary. Time-dependent infiltration is then defined in terms of these four canyon sections, as described below.
- For a given simulation, the maximum infiltration rate for the upper and middle canyon sections is constant, but the value of the constant is randomly sampled from an input distribution (see "Infiltration rate for the upper canyon," Appendix B; the same constant applies for both sections). The infiltration rate is, however, constrained to maintain at least a minimum of lateral alluvial flow from one canyon section to the next section, as represented in the model and described in detail in the following sections.

Table 3.3-1 characterizes the distributions used in the Tier-3 analyses to account for uncertainty in the maximum value of the upper and middle-canyon infiltration rate (represented as  $I_{upper}$ ) at the alluvium/tuff interface, and the cumulative effects (TA-50 Conversion Factor) that other sources of surface water and evapotranspiration have on the volume of and the concentrations of contamination in infiltrating water. Distributions developed for these parameters are based on data sets described by Birdsell et al. (2005, in progress) and in Appendix B, which gives justification for a lower maximum value of  $I_{upper}$  than was used in the conservative Tier-1 analysis.

**Table 3.3-1**  
Parameters and Distribution Attributes Used in the Tier-3 Infiltration Models  
(See Appendix B for Full Distribution.)

Parameter	Distribution	Min	Max	Mean	Standard Deviation
$I_{upper}$ , infiltration rate for the upper canyon (m/yr)	Normal, truncated at lower end	0.05	4.47	1.31	0.79
TA-50 flow to surface flow conversion factor	Normal, truncated at lower end	0.30	1.27	0.65	0.21

### 3.3.2.1 Upper/Middle-Canyon-Dominated Infiltration

The upper/middle-canyon-dominated infiltration model is the Tier-3 conceptual model for infiltration that is most like the Tier-1 infiltration model. With this model, many of the realizations yield preferentially higher infiltration rates in the upper and middle canyon sections than in the lower and bottom canyon sections (Figure 2.2-1). The maximum infiltration rate defined for the upper and middle canyon sections, shown in Table 3.3-1, is held constant, provided there is a sufficient volume of flow to meet that maximum infiltration rate and send a defined minimum percentage of alluvial water to the next canyon section. Table 3.3-2 lists the minimum percentage of alluvial water that is forced to flow from one canyon section to another for the upper/middle-canyon-dominated infiltration model, as well as for the lower-canyon-dominated infiltration model, which is discussed in the following section. If for the upper/middle-canyon-dominated infiltration model, there is an insufficient volume of water entering the upper canyon to satisfy both the maximum infiltration rate and allow 70% of that water to flow into the middle canyon section, then the infiltration rate for the upper canyon will be decreased to meet the minimum volume constraint.

**Table 3.3-2**  
**Minimum Fraction of Volumetric Flow between Canyon Sections**

Infiltration Model	Canyon Sections		
	Upper to Middle	Middle to Lower	Lower to Bottom
Upper/middle-canyon-dominated infiltration (Base case)	70%	40%	5%
Lower-canyon-dominated infiltration (Case 2)	80%	60%	0%

Figure 3.3-2 illustrates the upper/middle-canyon-dominated Tier-3 infiltration model by showing 10 of the 1000 infiltration rate histories calculated in the upper and lower canyon sections. (The figure refers to this conceptual model as “base case” because it is most consistent with the Tier-1 conceptual model.)

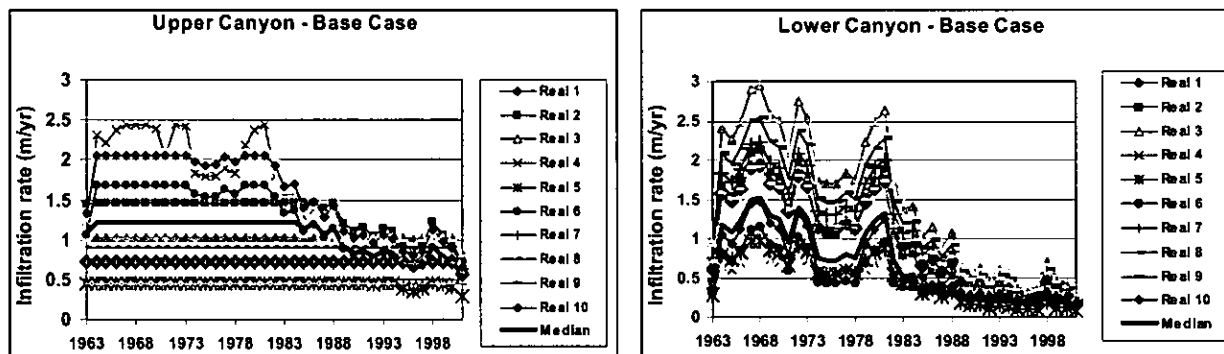


**Figure 3.3-2. First 10 realizations of 1000 of infiltration in the upper and lower sections of Mortandad Canyon for the upper/middle-canyon-dominated infiltration model**

For a given simulation, the time-dependent, upper and middle (not shown) canyon infiltration rates are similar because these sections are primarily controlled by the maximum value for the upper/middle-canyon infiltration rate,  $I_{upper}$ , which is automatically and randomly selected from the distribution represented in Table 3.3-1. When the initial infiltration rate is sufficiently low for the relative infiltration volumes flowing to each section of the canyon to be maintained (Table 3.3-2),  $I_{upper}$  remains constant throughout a given simulation. Conversely, when the maximum infiltration rate is too high to maintain the infiltration distribution among the canyon sections, then the upper- and middle-canyon infiltration rate varies within a given simulation until that balance is achieved. The infiltration rates in the lower (and bottom, not shown) canyon section are controlled simply by the volume of water that bypasses the upper- and middle-canyon sections through the alluvial system. Overall, 95% of the water that enters the lower-canyon alluvial system infiltrates within the lower canyon, but 5% infiltrates within the bottom, based on the fraction defined in Table 3.3-2.

### 3.3.2.2 Lower-Canyon-Dominated Infiltration

The lower-canyon-dominated infiltration model changes the spatial distribution of infiltration relative to the upper/middle-canyon-dominated model. This model is based on recent water content and contaminant distribution data gathered in cores at boreholes in the lower section of the canyon. The data indicate relatively deep contaminant transport (greater than 350 ft) in the lower canyon at the location of boreholes R-15 and MCOBT-8.5, but not in the bottom canyon section at the location of borehole R-28.

In this alternative infiltration model, a lateral flow of alluvial water is assumed to allow a greater volume of water to reach and then infiltrate the lower portion of the canyon. This is accomplished by forcing a greater percentage of water to enter the lower section of the canyon from the upper- and middle-canyon

sections, and by forcing all of the water that enters the lower canyon to infiltrate rather than to flow to the bottom section of the canyon. Table 3.3-2 gives the minimum percentages of flow that must pass on to the next section. The same distribution for the upper-canyon infiltration rate (Table 3.3-1) is used as for the lower canyon-dominated infiltration rate. However, because a greater percentage of flow is passed laterally down the canyon, this infiltration model acts to limit the highest rates that might occur in the upper- and middle-canyon sections. Birdsell et al. (2005, in progress) provide a more comprehensive description of this infiltration model.

To illustrate the differences in the two uniform infiltration models (i.e., upper/middle-canyon dominated and lower-canyon dominated), Figure 3.3-3 shows an example of time-dependent (median) infiltration rates calculated for the four canyon sections for both models. For these examples,  $I_{upper}$  has a value of 1.22 m/yr, and the upper and middle canyon sections maintain this value as long as there is a sufficient volume of water available to send the required percentage of entering flow (Table 3.3-2) on to the next canyon section. Recall that the volume of water entering the entire canyon decreases as RLWTF discharge volumes decrease. For this reason, the upper- and middle-canyon infiltration rates drop off the steady maximum value after about 1981 for both models because discharge volumes fell. However, the drop is more significant for the lower-canyon-dominated model because that model requires a larger percentage of flow to pass on to the lower canyon section. With the lower-canyon-dominated model, the lower canyon has a higher infiltration rate for the entire time. Although the upper- and middle-canyon sections maintain a constant infiltration rate, the difference is due only to that volume of water that is not going to the bottom canyon section. (The lower-canyon-dominated infiltration model sends no water to the bottom canyon section, as shown in Table 3.3-2.) When the  $I_{upper}$  value is not maintained in the upper and/or middle sections, the difference is greater. In general, the lower-canyon infiltration rate closely mimics the time dependency of the RLWTF annual discharge volumes (Table 2.1-1).

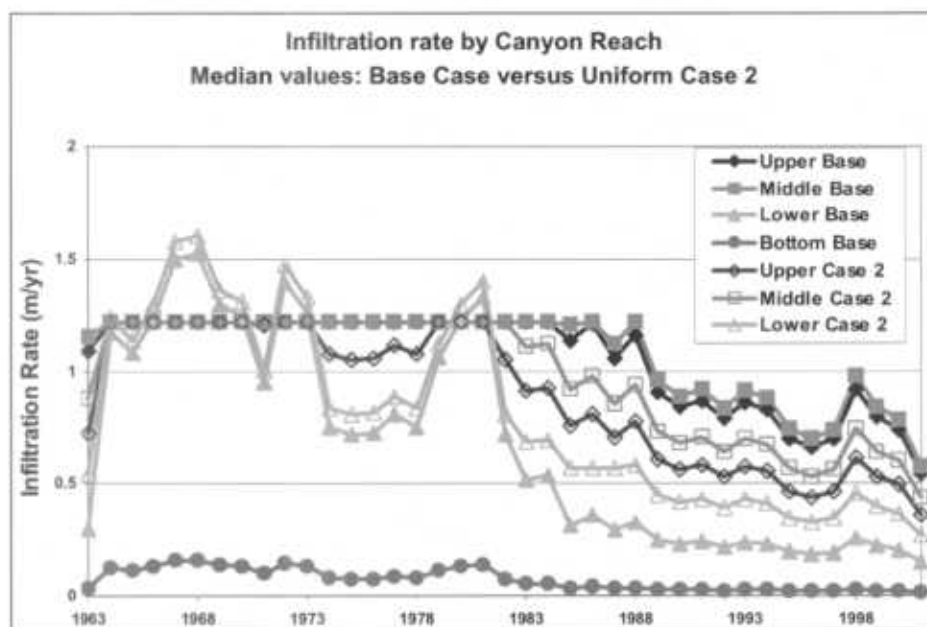
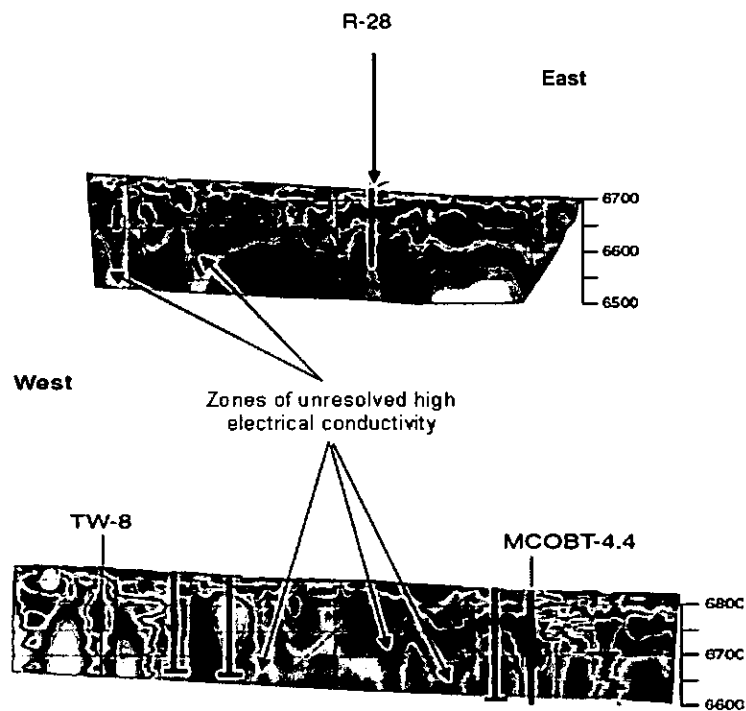


Figure 3.3-3. Comparison of infiltration rates in the upper, middle, lower, and bottom sections of Mortandad Canyon, calculated using the upper/middle-canyon-dominated infiltration model ("Base" in legend) and the lower-canyon-dominated infiltration model ("Case 2" in legend)

### 3.3.2.3 Fast-Path Infiltration

A third conceptual model is also considered in the Tier-3 analysis, which simulates a "short circuit" or fast path through the vadose zone at certain discrete locations along Mortandad Canyon. The fast-path model hypothesizes that three subsurface zones of high conductivity measured in the electrical resistivity survey of Mortandad Canyon are indicative of wet zones that represent faster conduits for groundwater flow directly into the unsaturated tuff beneath the alluvium. Figure 3.3-4 shows portions of the survey where these local regions of low resistivity (or high conductivity) were measured. One interpretation of these measurements is that high electrical conductivity correlates with high moisture content. The fast-path conceptual model simulates these possible wet zones as locations of enhanced infiltration, which causes faster flow paths for groundwater transport compared to the rest of the vadose zone. (Alternatively, high electrical conductivity correlating with high moisture content might indicate a highly water-impermeable zone, such as clay, that holds water but retards its movement.) One conduit is hypothesized for each of the upper, middle, and lower canyon sections with each located near an observed high-conductivity region.



**Figure 3.3-4. Results of resistivity survey in Mortandad Canyon, showing several zones of relatively high electrical conductivity (green to blue)**

In the Tier-3 fast-path model, these three conductive zones are assumed to capture 40% of the infiltration volume that is allocated to the respective canyon section, based on the lower-canyon-dominated uniform infiltration model. The remaining 60% of the infiltration volume is spread uniformly across the remainder of the canyon section for that portion that does not represent a fast path. There is no infiltration in the bottom section of the canyon in the focused infiltration model. The focused infiltration model investigates fast paths occurring alternately and coincidentally in the upper, middle, and/or lower portions of Mortandad Canyon.

Figure 3.3-5 compares the infiltration rates between the lower-canyon-dominated alluvial infiltration models with uniform infiltration and with fast paths. As in Figure 3.3-4, the results shown in the figure are from calculations using the median of the distribution of values for infiltration in the upper canyon ( $I_{upper}$ ) and the median of the distribution of values used for the surface-water multiplication factor.

The total volume of water entering a given canyon section is the same in both the focused flow and uniform infiltration models, but the distribution of that water as infiltration varies. For example, the infiltration rates in the columns representing the fast-flow path in each canyon section are two to three times higher than for the uniform infiltration case. However, infiltration for the nonfast flow paths within the fast-path scenario are correspondingly only about 30% less than for the uniform model.

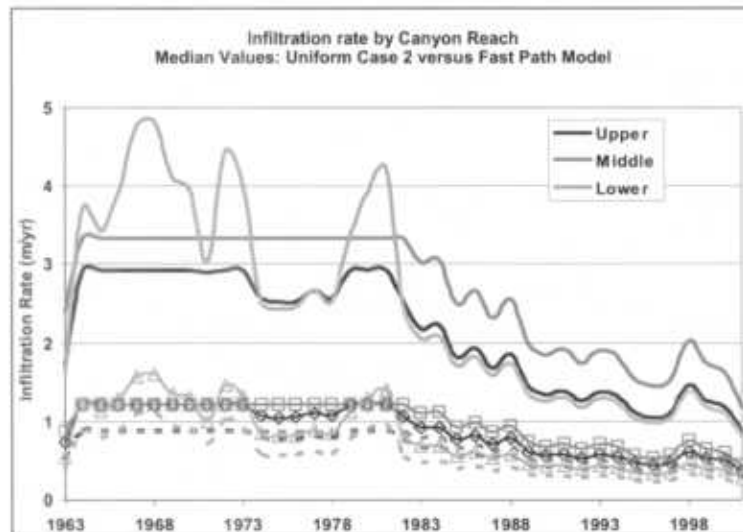


**Figure 3.3-5. Comparison of relative infiltration rates in the upper, middle, and lower sections of Mortandad Canyon using the lower-canyon-dominated uniform infiltration model (solid lines with markers) and the fast-path infiltration model (fast paths represented by solid lines, adjacent nonfast paths represented with dashed lines)**

For the lower-canyon-dominated infiltration model, 1000 simulations were conducted for each contaminant for each of the following fast-path locations:

- Fast path in upper canyon section,
- Fast path in middle canyon section, and
- Fast path in lower canyon section.

Then these simulation results were also combined (but not rerun) to generate further combinations of fast-path simulations as follows:

- Fast paths in upper and middle canyon sections,
- Fast paths in upper and lower canyon sections,
- Fast paths in middle and lower canyon sections, and
- Fast paths in upper, middle, and lower canyon sections.

### 3.3.3 Unsaturated Transport

All unsaturated groundwater transport calculations were run with the FEHM computer code. In the Tier-1 model, the upper, middle, and lower portions of Mortandad Canyon described by Purtymun (1967, 11785) (Table 3.2-1) were represented as three one-dimensional (1-D) columns, as illustrated in Figures 3.2-2 and 3.2-3.

To allow for the analysis of greater spatial variability in infiltration along Mortandad Canyon, the Tier-3 groundwater-transport simulations represented the unsaturated bedrock between the alluvium in the canyon floor and the top of the regional aquifer as 38 1-D columns, as illustrated in Figure 3.3-6. These 38 columns are divided among the four canyon sections that partition infiltrating water, as described in Section 3.3.2 and shown in Figures 2.2-1 and 3.3-6.

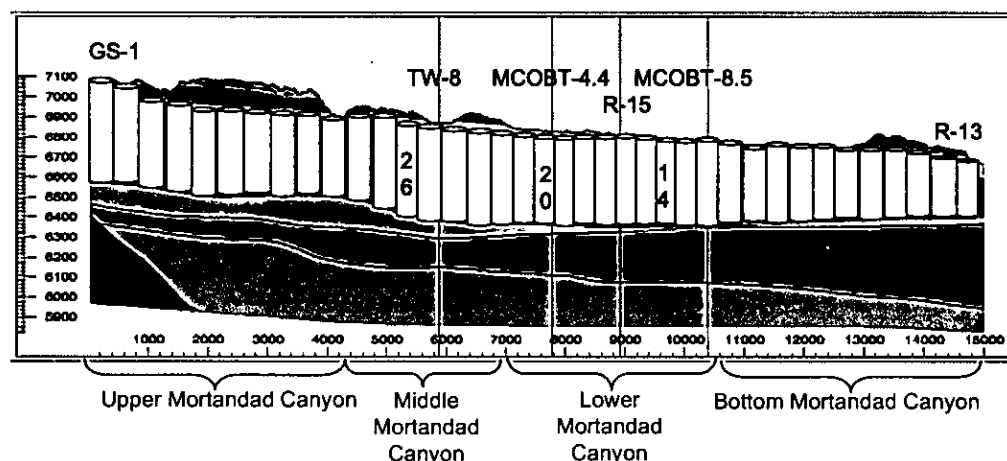


Figure 3.3-6. Illustration of the 38 1-D columns used in the Tier-3 unsaturated transport model, with three columns that are discussed in text

In the Tier-3 analysis, 1000 calculations were conducted for each of the three infiltration boundary conditions. Each of the 1000 calculations used a different set of randomly selected values from distributions representing the source term and infiltration boundary conditions discussed in Sections 3.3.1 and 3.3.2, and from distributions for saturated hydraulic conductivity and porosity of seven stratigraphic layers listed in Table 3.3-3.

Table 3.3-3  
Physical and Hydraulic Parameters and Distributions  
Used in the Tier-3 Unsaturated Transport Model

Stratigraphic Unit	Porosity			Saturated Hydraulic Conductivity (cm/s)		
	Min	Max	Distribution	Min	Max	Distribution
Tshirege Tuff, 1g	0.35	0.67	Normal	3.7e-6	4.0e-3	Log normal
Tsankawi Pumice	0.41	0.55	Normal	3.6e-6	1.2e-2	Log normal
Cerro Toledo	0.41	0.56	Normal	5.4e-6	1.1e-2	Log normal
Otowi Tuff	0.33	0.65	Normal	1.6e-5	2.6e-2	Log normal
Guaje Pumice	0.52	0.84	Normal	1.6e-5	1.2e-2	Log normal
Cerros del Rio Basalt	10 <sup>-5</sup>	10 <sup>-2</sup>	Empirical	1.1e-5	0.1	Log normal
Puye Formation	10 <sup>-5</sup>	0.3	Empirical	3.1e-5	6.2e-2	Log normal

Distributions for Unit 1g, the Tsankawi Pumice, the Cerro Toledo interval, and the Otowi Member were based on an analysis conducted by Springer (2003, 90071), whose tabulated results are included in Appendix B. Hydrologic property distributions developed for the Guaje Pumice, Cerros del Rio basalt, and Puye Formation are based on either small sample sets, field tests, or model calibration, as explained in Appendix B and by Birdsell et al., (2005, in progress).

To represent uncertainty in parameters in the van Genuchten retention model for unsaturated groundwater flow, the Tier-3 groundwater model varied the van Genuchten  $\alpha$  parameter, as recommended by Springer (2003, 90071) and described in Appendix B. Fixed values based on median estimates for the other van Genuchten parameters were used; these values were also used in the Tier-1 analysis. In addition, the Tier-3 unsaturated groundwater transport model evaluated longitudinal (vertical) dispersivity values ranging uniformly between 0.5 and 5.0 m (there is no transverse dispersion because the columns are one-dimensional). A summary of the complete set of final distributions used for the simulations are described and included in the appendix that defines parameter distributions, Appendix B.

### 3.3.3.1 Comparison of Tier-1 and Tier-3 Unsaturated Transport Simulations

Figure 3.3-7 illustrates the difference between the Tier-1 point estimates for the upper and lower canyon locations and the Tier-3 stochastic unsaturated groundwater transport calculations at similar locations, using the upper/middle-canyon-dominated infiltration model. The figures compare the single-point estimate releases over the next 100 yr at the base of the unsaturated zone columns in the Tier-1 model with the first ten of the 1000 stochastic releases in the Tier-3 model. In each case, the flux shown represents the total flux for the appropriate canyon section (integrated over the total area of either the upper or lower canyon section). The ten Tier-3 curves represent ten separate calculations using randomly sampled values from the input distributions identified in Appendix B. The figures indicate that peak flux values are higher in the Tier-1 analysis than the Tier-3 analyses. However, initial arrival times are not necessarily earlier in the Tier-1 analysis, especially in the lower canyon. With the lower-canyon-dominated uniform infiltration model, the Tier-3 releases at the base of the unsaturated zone in the lower canyon have even higher peak values (often double) and first arrival times are more advanced than for the Tier-3 results shown in Figure 3.3-7 (Birdsell et al. 2005, in progress). The general spread in the Tier-3 curves reflects the variability in source releases and in transport rates caused by the variability in parameters between different realizations.

Nitrate mass-flux arrivals at the base of the unsaturated grids are similar to the perchlorate curves in terms of relative peaks and arrival times. The magnitude of the flux is greater because the magnitude of the nitrate source is larger than the perchlorate source. The curves for tritium, however, are different than those for perchlorate, as shown by Birdsell et al. (2005, in progress). The breakthrough curves for tritium are shifted forward in time relative to the perchlorate curves, with no breakthrough after approximately the year 2060 because radioactive decay sufficiently decreases the tritium mass by that time so that virtually no tritium exits the bottom of the vadose zone.

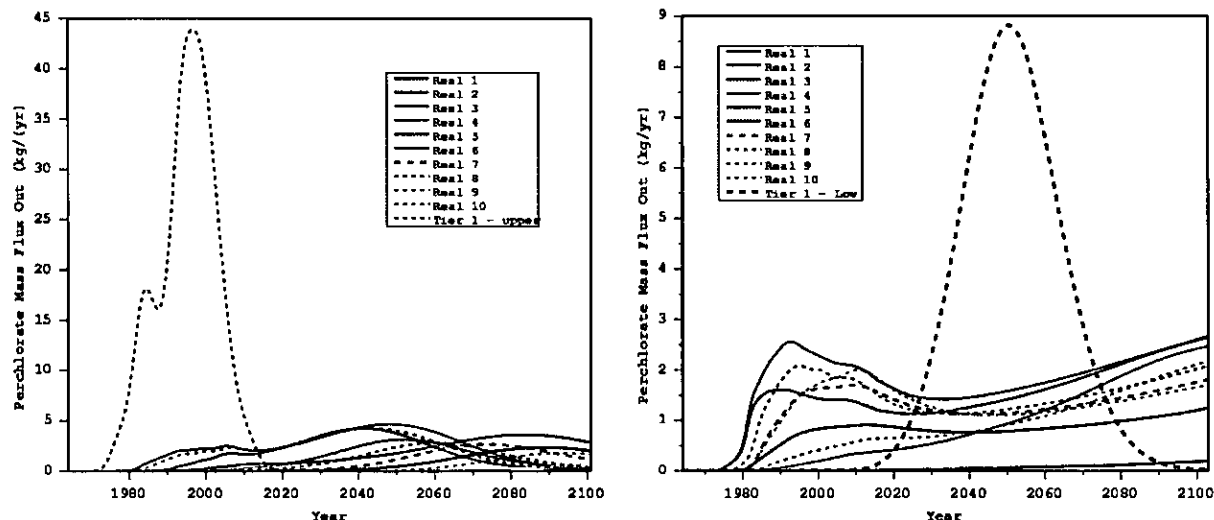


**Figure 3.3-7. Comparison of perchlorate total fluxes exiting the base of the unsaturated zone for the Tier-1 point estimates and 10 realizations of Tier-3 upper/middle-canyon-dominated infiltration simulations. The left figure shows results from the upper-canyon column(s), and the right figure shows results from the lower-canyon column(s).**

### 3.3.3.2 Comparison of Tier-3 Unsaturated Transport Simulations to Field Data

It is useful to compare modeled quantities, such as water content and concentrations, to field data in order to add credence to the simulation setup and results. This process also helps illustrate how the complex coupling of the flow and transport mechanisms with the parameter distributions act together to produce distributions of results. The results presented are from the Tier-3 simulations, using a continuous source that accounts for denitrification and the upper/middle-canyon-dominated infiltration model. Birdsell et al. (2005, in progress) present comparisons between simulation results and data at other locations in the canyon and for other infiltration models.

Figure 3.3-8 compares a time history of alluvial concentrations of nitrate measured in wells MCO-4 and MCO-6 through 1997 to the calculated time history of nitrate concentration entering the unsaturated-zone model. Results for the first 10 stochastic realizations are given. The calculated input concentration is a function of the time-dependent nitrate release stochastically modified to account for denitrification, surface-water mixing, and evapotranspiration. The input nitrate concentration is not influenced by the infiltration conceptual model; therefore, this comparison applies for all infiltration models.

From 1964 through 1980 and again after 1994, the modeled concentrations agree well with the measured concentrations. From 1981 through 1993, the recorded nitrate concentrations released from the RLWTF (Table 2.1-1) were high, but the alluvial well concentrations did not increase correspondingly. One explanation for this is that nitrate degradation within the surface and alluvial waters may have been more efficient in response to the higher nitrate release concentrations during this period. For those same years, the source model, which uses an assumed constant percentage of nitrate degradation, predicts higher input concentrations than recorded in the alluvial wells. The unusually high input concentrations predicted for Realization 5 result from a parameter sampling combination leading to a small fraction of nitrate degradation (large nitrate source) and a small volume of surface flow in the canyon system (little dilution). Birdsell et al. (2005, in progress) show a similar plot for tritium that compares calculated tritium concentration entering the vadose-zone columns to alluvial well data. No such comparison can be made for perchlorate because its concentration has only recently been measured in alluvial wells.

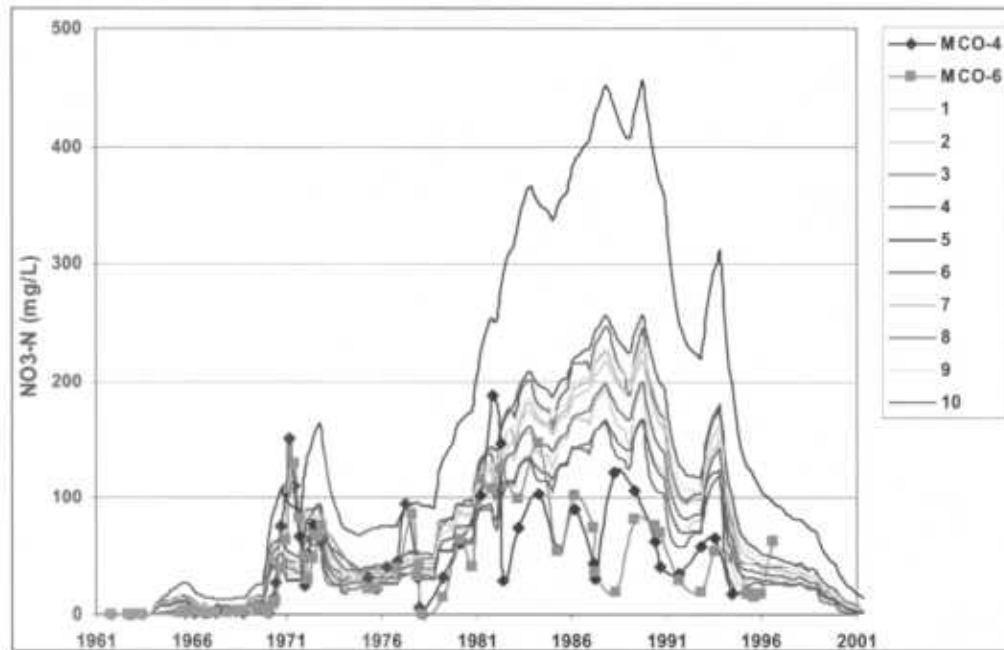


**Figure 3.3-8. Comparison of historical nitrate concentrations in alluvial wells MCO-4 and MCO-6 to simulated input nitrate concentrations for the first ten stochastic realizations**

Figure 3.3-9 shows modeled volumetric water content as a function of elevation calculated for a simulation time representing 1998 for the first 100 stochastic realizations. The profiles are plotted along a single column in the lower-canyon section of the unsaturated transport model and are compared to water-content measurements from core samples collected from boreholes MCOBT-4.4 and MCOBT-8.5 in 2001, and in R-15 in 1998. The column selected for comparison is Column 20, which is located between MCOBT-4.4 and R-15 (Figure 3.3-6). The data for MCOBT-8.5 are adjusted upward to align the base of the alluvium in that well with the top of simulation Column 20 to better compare the three data sets with the calculated water-content profiles.

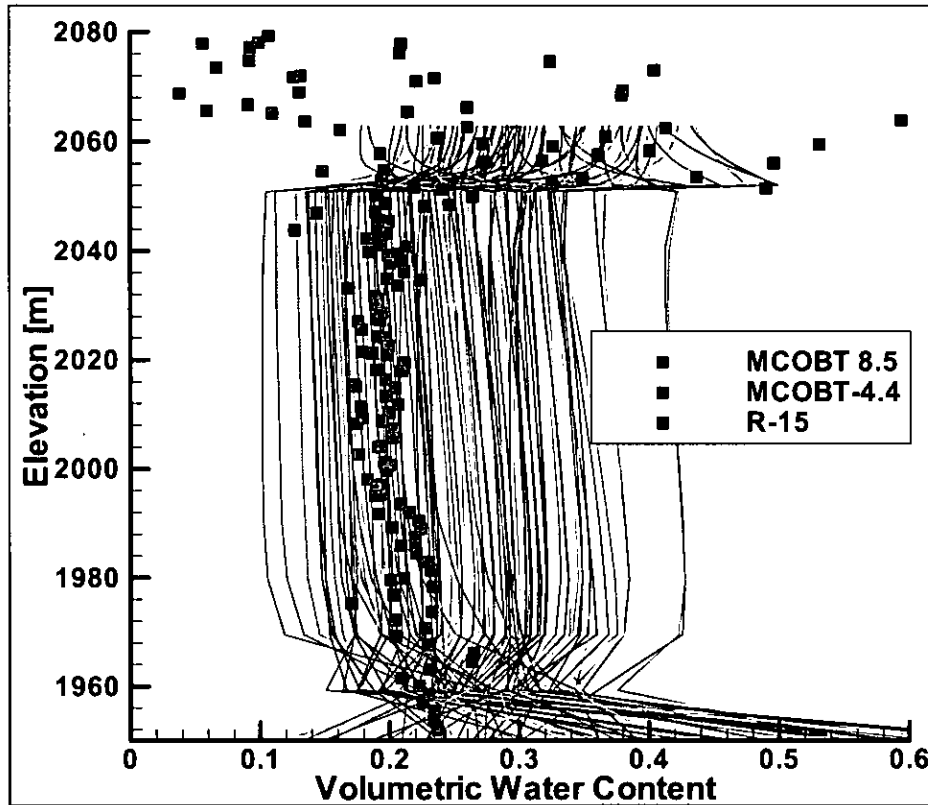


**Figure 3.3-9. Comparison of the first 100 stochastic calculations of water content as a function of elevation, using the upper/middle-canyon-dominated uniform infiltration model, to measured water content from core samples. The simulation column is located between MCOBT-4.4 and R-15 in the lower canyon section.**

The comparison between data and stochastic estimates in Figure 3.3-9 demonstrates a reasonable fit between spatially and temporally discrete measurements and spatially and temporally variable simulations. The data fall within the drier end of the distribution of water contents calculated by the stochastic simulations, especially within the Otowi Member (elevation 1950 to 2051 m in the simulation grid). A comparison of water-content profiles predicted by the model for the middle canyon near well R-1 with R-1 data also show that the data fall within the drier end of the simulated profiles. It should be pointed out that a perfect match with single-point data is not expected with a stochastic analysis. Data like those presented in Figure 3.3-9, and the figures that follow, represent single-point measurements in time and space, with no variability and limited analytical uncertainty. In contrast, stochastic results by design represent broad spatial and temporal scales with the goal of representing not only measurement uncertainty but also the potential spatial and temporal variability.

Figure 3.3-10 compares the first 100 stochastic calculations of perchlorate concentration as a function of elevation in Column 20 of the unsaturated transport model for the upper/middle-canyon-dominated uniform infiltration model with measured concentrations in core samples from boreholes MCOBT-4.4, MCOBT-8.5, and R-15. The elevations for MCOBT-8.5 are again adjusted to align the base of the alluvium with the top of the 1-D simulation column.

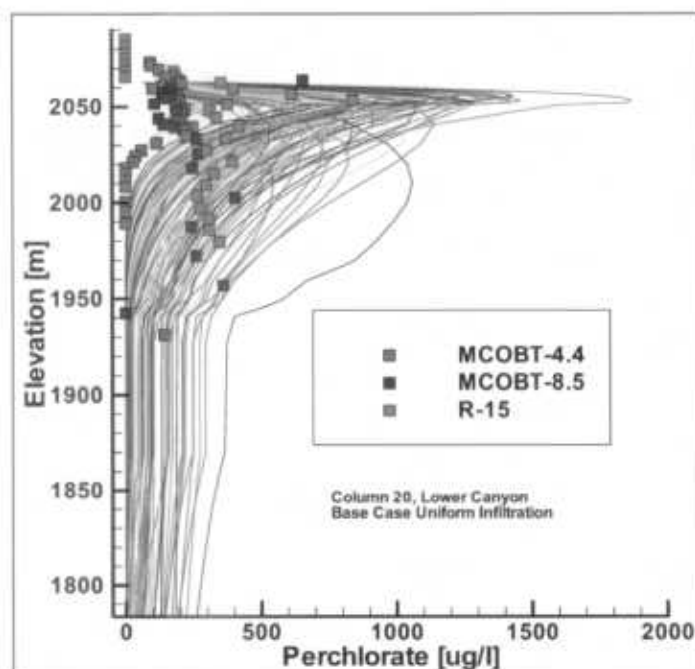


**Figure 3.3-10. Comparison of 100 stochastic calculations of perchlorate concentration as a function of elevation and measured perchlorate concentrations from core samples. The simulation column is located between MCOBT-4.4 and R-15 in the lower canyon section.**

In general, the calculated concentrations are higher than the measurements, indicating that the model may be overestimating contaminant mass in the unsaturated bedrock. Individual profiles can be chosen that compare reasonably well, in terms of their shape and depth, to the measured concentration data. Also, the simulation results bracket the concentration measured in the perched zone found at MCOBT-4.4 at approximately 1930 m. At Column 26, the location represents well R-1 in the middle-canyon section (Figure 3.3-6); the simulation results also bracket the perchlorate concentration data (Birdsell et al., 2005, in progress). Again, however, the calculated concentrations are generally higher than the data.

Figure 3.3-11 compares the first 100 stochastic calculations of unsaturated-zone nitrate concentration as a function of elevation for Column 20 with measured concentrations from boreholes MCOBT-4.4, MCOBT-8.5 (elevation adjusted), and R-15. For nitrate, the calculated concentrations are higher than the measured values, again indicating that the model may be overestimating contaminant mass, in agreement with the measured and calculated alluvial nitrate concentrations shown in Figure 3.3-8. Although these simulated curves have higher peak concentrations than the observations, the elevation of the peaks and the general shape of the measured and simulated concentration profiles are in agreement for most of the simulations. The nitrate concentration data tend toward nondetect values with depth in the three boreholes, which is not the case for perchlorate concentrations in wells MCOBT-8.5 and R-15. Many of the simulations have concentration values below 1950 m that do not tend toward nondetectable concentrations. For nitrate, this appears to be an overprediction of the depth of the contaminant in the lower canyon section. Simulated nitrate concentration profiles for the middle canyon compared to data from well R-1 show that the measured concentrations fall at about the midpoint of the simulated values in terms of magnitude (Birdsell et al. 2005, in progress). However, most of the simulated profiles again spread deeper than do the data.

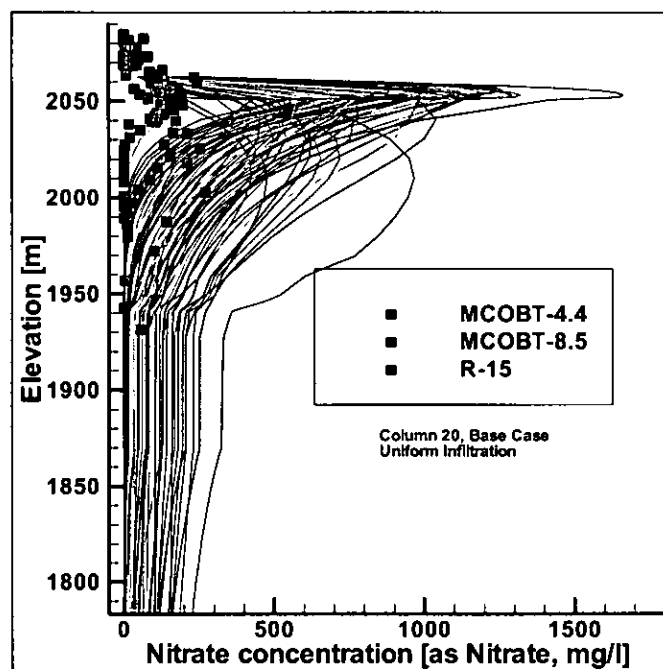


**Figure 3.3-11. Comparison of 100 stochastic calculations of nitrate concentration as a function of elevation with measured nitrate concentrations from core samples. Simulation results are for a column between MCOBT-4.4 and R-15 in the lower canyon section and use the upper/middle-canyon-dominated uniform infiltration model.**

### 3.3.3.3 Comparison of Tier-3 Unsaturated Transport Simulations Using Alternative Infiltration Models

Results for the lower-canyon-dominated uniform infiltration model with continuous release are presented by Birdsell et al. (2005, in progress) and are only briefly summarized here. The results are quite similar to those for the upper/middle-canyon-dominated uniform infiltration models, but they reflect the difference in the distribution of infiltration rates by location, as illustrated in Figure 3.3-3. In comparison to the perchlorate fluxes exiting the unsaturated zone presented in Figure 3.3-7, the fastest releases from the upper canyon are delayed. All releases to the lower canyon are advanced.

At Column 20 in the lower canyon, the larger lower-canyon infiltration rate for this model leads to simulated water content values that are slightly higher than those presented in Figure 3.3-9. However, the data for wells R-1, MCOBT4.4, and MCOBT8.5 still fall within the lower end of the simulated results. Simulated perchlorate and nitrate concentration profiles as a function of depth are deeper than illustrated in Figures 3.3-10 and 3.3-11. The simulations overpredict the depth of the contaminants at MCOBT4.4, where the contaminants are relatively shallow, while still bracketing the value at the perched zone in that well. Concentration data for wells R-15 and MCOBT-8.5 lie within the simulated distributions.

At Column 26 in the middle canyon, the lower-canyon-dominated infiltration model produces lower infiltration rates than does the previous model. Simulated water content profiles are not significantly

different than for the upper/middle-canyon-dominated infiltration model. The water-content data for well R-1 fall within the lower portion of the simulated profiles. Modeled perchlorate and nitrate concentration profiles as a function of depth are shallower and compare well to concentration data for these contaminants measured in well R-1, although the simulated leading edge is again deeper than the data.

Detailed results for the focused infiltration model with continuous release are presented by Birdsell et al. (2005, in progress). This model uses the lower-canyon-dominated infiltration model as its basis with fast flow paths superimposed. As expected, the mass fluxes of contaminants exiting the bases of the columns with focused infiltration occur earlier than in the columns without focused infiltration. Simulated water content profiles are wetter, contaminants migrate deeper in the focused infiltration locations, and these profiles do not compare well to data from wells MCOBT-4.4, MCOBT8.5, R-15 or R-1. Profiles calculated for those columns without focused flow *do* compare well to the data, similar to results in Figures 3.3-9, 3.3-10, and 3.3-11. The simulated water-content profiles are slightly drier, and the contaminant transport with depth is delayed, which actually matches the data better than for the two previous uniform infiltration models. This indicates that lower overall infiltration rates than those used in the two uniform infiltration models may be postulated.

#### 3.3.3.4 Comparison of Tier-3 Unsaturated Transport Simulations Using Continuous and Discontinuous Source Models

Figure 3.3-12 shows results for six of the 1000 stochastic calculations of perchlorate mass fluxes exiting the base of one of the unsaturated-zone columns (Column 14), using the continuous and discontinuous source models. Column 14 lies in the lower canyon (Figure 3.3-6). Curves of the same color but different weight represent stochastic realizations using the same set of random parameter values under the two release conditions, with the continuous (dashed lines) and discontinuous (solid lines) source models. In all cases shown, color-coded sets of curves are similar until the year 2010, revealing the potential impact of residual saturation infiltrating from the alluvium, as modeled. After 2010, the solid curves for the discontinuous source become broader in time, as the result of the reduction in the assumed infiltration rate, than are the dashed curves for the continuous source. The reduction in infiltration rate is assumed to represent decreases in the amount of surface and alluvial waters because the outfall no longer releases surface water. Water and contaminants continue deeper into the system after 2010 as residual pore water equilibrates. Overall, contaminants are transported more slowly, and in lower concentrations, through the unsaturated bedrock when liquid and contaminant input is reduced. With the discontinued source, contaminants are released from the bottom of the unsaturated bedrock (at the top of the regional aquifer) over longer times, with peak mass fluxes reduced by 50% or more.

Time-dependent mass flux at the bottom of the 38 unsaturated transport columns, similar to those shown in Figures 3.3-7 and 3.3-12, provided several thousand separate input boundary conditions for the saturated transport model. Again, 1000 simulations were conducted for each of the 1-D unsaturated-zone columns, for each of three contaminants (nitrate, perchlorate, and tritium), and for each of the alternative infiltration models:

- upper/middle-canyon-dominated infiltration alone (1000 simulations at 38 locations), and
- lower-canyon-dominated infiltration alone (1000 simulations at 27 locations, because the "bottom" canyon is inactive with this conceptual model) and with fast paths in each section of the canyon individually or in combinations (7000 simulations at 27 locations).

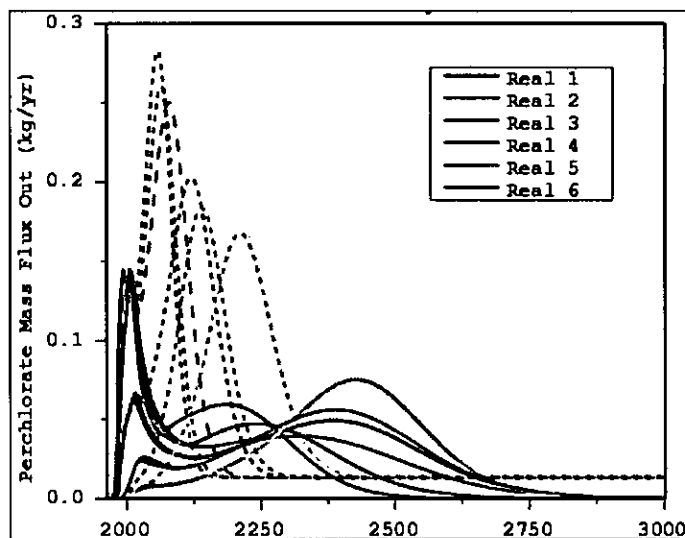


**Figure 3.3-12. Comparison of 6 of 1000 stochastic calculations of perchlorate mass fluxes exiting the base of the unsaturated zone (Column 14 in the lower canyon) for discontinued (solid lines) and continued (dashed lines) releases from the RLWTF**

### 3.3.4 Saturated Transport

There are uncertainties in the conceptual model defining groundwater flow and transport in the regional aquifer. The impacts of conceptual model uncertainties are addressed in the Mortandad Canyon analysis by considering two distinct conceptual models. These alternatives represent approximately two end members on a spectrum of potential flow configurations and therefore capture some of the potential conceptual model uncertainty. The contaminant pathways in the regional aquifer depend heavily on the existence or lack of existence of a phreatic zone in the shallow portion of the regional aquifer. The existence of the phreatic zone depends on the strength of the hydrologic separation of the two shallow and deep compartments of the regional aquifer. This translates into how efficiently the pressure drawdown caused by the pumping wells propagates to the water table. The two alternative conceptual models are as follows:

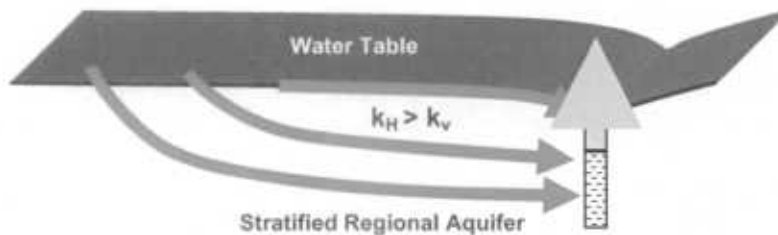
**Model A:** There is no phreatic zone that is hydraulically separated from the rest of the regional aquifer. There is no hydraulic separation between the shallow and deep (pumped) aquifer zones, which allows pumping drawdown to reach the water table. Hydraulic gradients in the phreatic zone are directly affected by the pumping, and contaminants are drawn toward the wells. Here the two compartments are not distinct (do not have different hydrodynamic properties); resistance to downward flow is caused by anisotropic permeability structure (horizontal permeability is greater than vertical permeability). Contaminants are expected to arrive at water supply wells under these conditions.

**Model B:** There is a phreatic zone that is hydraulically separated from the rest of the regional aquifer. There is a strong hydraulic separation between the shallow (phreatic; water-table) and deep (regional aquifer; pumped) zones, which does not allow the pumping drawdowns to reach the water table. Hydraulic gradients in the phreatic zone are unaffected by the pumping. Contaminants are expected to bypass the water-supply wells and will arrive at the springs near the Rio Grande.

We use these end-member conceptual models to establish two numerical models of transport in the regional aquifer. The two models examine the effect of uncertainty in hydraulic separation, as shown in Figure 3.3-13, and create transport pathways that behave similarly to, but not as extreme as, the end members. Both models are run with the computer code FEHM [Zyvoloski et al. 1997, 70147] and use modifications of the Laboratory numerical models of the regional aquifer developed through 2002 [Nylander et al. 2003, 76059; Keating et al. 2000, 90188; Keating et al. 1999, 88746; Vesselinov et al. 2001, 90114).

#### Model "A": Deep Transport Model

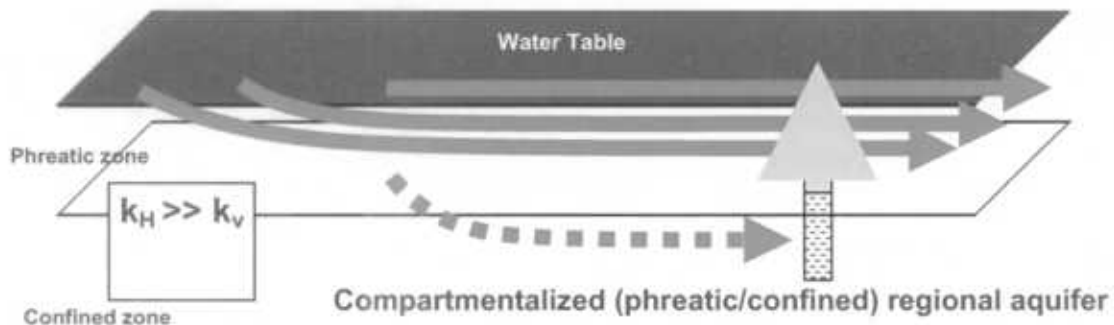
Contaminants migrate toward pumping wells



Anisotropy ratio is low enough so that currently (circa 2002) the existing pumping at depth forms a cone of pressure depression at the water table

#### Model "B": Phreatic Transport Model

Contaminants primarily migrate laterally in phreatic zone toward springs and Rio Grande; very small portion move toward pumping wells



Anisotropy ratio is high enough so that currently (circa 2002) the existing pumping at depth does not form a cone of pressure depression at the water table

Figure 3.3-13. Alternative conceptual models of the saturated zone

It should be noted that recent pumping test data indicate that the regional aquifer is heterogeneous and likely compartmentalized into an upper zone that is phreatic, a relatively impervious lower layer, and another deeper zone that is the regional water-supply aquifer, which is essentially confined. The test data are collected during pumping of PM-2 and PM-4 (McLin 2005, in progress, and McLin 2005, 90073), which makes these conclusions relevant for our site. (To clarify, by "confined here" we mean that the pressure responses to pumping the regional aquifer demonstrate confined conditions. Confined

conditions do not mean that there is no potential for water and contaminants to move between the phreatic and regional aquifer zones.) The upper phreatic zone can be envisioned as a regional "perched" zone, which facilitates lateral groundwater flow and transport. By pumping the deeper portions of the regional aquifer, a portion of phreatic groundwater may be drawn downward toward the water-supply wells by vertical leakance through the relatively impervious layer. Nevertheless, the field data suggest that pumping in the deeper zone has little effect on the water-table elevation. As a result, the pumping has little effect of the directions and rates of hydraulic gradients in the upper phreatic zone as well. Therefore, even if leakance occurs, its impact on the contaminant distribution is likely to be limited, i.e., lateral contaminant movement is likely to occur along the phreatic zone. These observations are also supported by the existing historical records of the groundwater levels in the vicinity of Mortandad Canyon.

In the first numerical implementation (referred to as Model A), the shallow and the deep zones are not hydraulically separated other than by very low values of vertical permeability for the aquifer rocks. As a result, the pumping wells control the spatial distribution of the contaminants entering the regional aquifer at the phreatic surface (water table). By running the numerical model to a future, steady-state condition, this model ensures that most of the contaminants mix deep into the aquifer and are captured by the water-supply wells.

In the second numerical implementation (referred to as Model B), the hydraulic separation between the shallow phreatic zone and the deep confined zones is considered. As a result, most of the contaminants reaching the phreatic zone are transported laterally so that they remain shallow (i.e., close to the water table) and move eastward toward the Rio Grande and the springs that emerge along the river (Vesselinov 2005, 90117). However, some hydraulic connection with the regional aquifer is assumed with this model, and a fraction of the contaminants is pulled toward the pumping wells.

Only Model A is implemented in the Tier-1 analysis, but both models are implemented in the Tier-3 analysis. The contaminant mass fluxes calculated at the bottom of the 38 Tier-3 unsaturated transport columns provide input into 38 cells in the saturated transport grid. The horizontal spatial distribution of the 38 1-D columns in the unsaturated grid coincides with 38 cells in the 3-D saturated transport computational grid.

Table 3.3-4 lists the permeability values for the hydrostratigraphic units represented in the Tier-1 and Tier-3 saturated groundwater-transport models. Both Tier-3 saturated transport models use modified versions of the site-scale 3-D regional-aquifer model described in the Groundwater Annual Status Report for the FY 2002 (Nylander et al. 2003, 76059). Model A uses permeability values obtained by steady-state calibration of the FY 2002 regional model. Model calibration used 2001 pumping data and head responses (data). For Model B, the horizontal permeability values were increased, and the vertical permeability values were decreased for the Puye Formation, the Totavi lentil, and the pumice-rich sediments so that lateral flow in the phreatic zone is achieved (values with an asterisk in Table 3.3-4).

Each grid element along the top of the saturated transport model is assigned one of the three conditions known to occur across the plateau. These boundary conditions are no flow (in grid blocks representing portions of the site where recharge is not thought to occur); specified flux (in grid blocks representing portions of the site where recharge is assumed to occur, in particular beneath canyons); or specified head (in grid blocks representing the Rio Grande, where hydraulic pressure is known and assumed to be constant).

**Table 3.3-4**  
**Permeabilities of Aquifer Materials Evaluated in the Tier-1 and Tier-3 Saturated Transport Model**

Hydrostratigraphic Unit	Permeability log 10 (m <sup>2</sup> )					
	Tier 1		Tier-3 Model A		Tier-3 Model B	
	Horizontal	Vertical	Horizontal	Vertical	Horizontal	Vertical
Pre-Cambrian	-18.00	-18.00	-18.00	-18.00	-18.00	-18.00
Paleozoic/Mesozoic—deep	-13.66	-13.66	-13.66	-13.66	-13.66	-13.66
Paleozoic/Mesozoic—shallow	-12.60	-12.60	-12.60	-12.60	-12.60	-12.60
Pajarito fault zone	-15.01	-15.01	-15.01	-15.01	-15.01	-15.01
Keres Group—deep	-13.66	-13.66	-13.66	-13.66	-13.66	-13.66
Keres Group—shallow	-12.71	-12.71	-12.71	-12.71	-12.71	-12.71
Tschicoma lava flows	-13.75	-13.75	-15.31	-15.31	-15.31	-15.31
Older Miocene basalts (Tb1)	-13.14	-13.14	-12.14	-12.14	-12.14	-12.14
Younger Miocene basalts (Tb2)	-13.14	-13.14	-12.24	-12.24	-12.24	-12.24
Cerros del Rio basalts (Tb4)	-13.14	-13.14	-12.05	-12.05	-12.05	-12.05
Older fanglomerate	-13.72	-14.79	-13.10	-13.51	-13.10	-13.51
Santa Fe Group—shallow	-13.08	-13.08	-12.87	-16.19	-12.87	-16.19
Santa Fe Group—deep	-14.18	-14.18	-16.00	-16.00	-16.00	-16.00
Puye Formation	-12.34	-13.03	-12.85	-16.33	-11.85 <sup>*</sup>	-16.33
Pumice-rich volcanoclastic sediments	-12.34	-13.05	-11.48	-11.48	-10.48 <sup>*</sup>	-16.48 <sup>*</sup>
Totavi lentil	-12.34	-13.03	-12.77	-12.77	-11.77 <sup>*</sup>	-16.77 <sup>*</sup>

\* For Model B, the horizontal permeability values were increased, and the vertical permeability values were decreased for the Puye Formation, the Totavi lentil, and the pumice-rich sediments so that lateral flow in the phreatic zone is achieved.

In the Tier-3 analyses, we use a saturated model representing a range of equally probable future steady-state groundwater flows. Even though currently the actual flow system is far from being at steady state, it can be expected that in the vicinity of the water-supply wells (which includes Mortandad Canyon), a quasi-steady-state regime has been established. Under the quasi-steady state, the hydraulic heads continue to decline in time, but the hydraulic gradients are time invariant and equivalent to the final steady-state estimates. Therefore, the steady-state model provides us with a relatively good estimate of the future hydraulic gradients if we assume invariant future pumping rates. The steady-state model does not allow us to take into account the impact of the known past and the unknown future variations in the pumping rates on the contaminant distribution/capture. Therefore, the ignoring of actual transients in the system might have an important impact on the obtained model predictions, but the impact has not yet been quantified. The impacts of transients on the capture-zone estimates for the water-supply wells in the vicinity of the Mortandad Canyon have been previously analyzed (Vesselinov 2004, 89728; Vesselinov and Keating 2003, 90116; Vesselinov and Keating 2002, 89373; Vesselinov 2005, 90040, 89753). This work demonstrates that the transients in the vicinity of the Mortandad Canyon are important to consider for accurate estimation of the well-capture zones.

To take into account the uncertainty in the constant future pumping rates of the water-supply wells in the Tier-3 analyses, we have assumed that these rates are random but described by the recorded pumping rates of the water-supply wells for the years 1993–2001 (Birdsell et al. 2005, in progress). The pumping rates are given in Table 3.3-5. The production year is chosen as the random variable; each year from 1993 through 2001 has an equal probability of being chosen. The Model A simulations then use the pumping rates for the PM- and O-series wells associated with the chosen year throughout the steady-state simulation. However, for the Model B simulations, the wells are pumped at 10% of the respective annual pumping rates. This pumping condition (along with the enhanced ratio of horizontal-to-vertical permeability values set for the Puye units, Table 3.3-4) was set as an engineering approximation to induce lateral flow and transport in the phreatic zone and cause little deep transport, in accordance with the desired phreatic-zone behavior for conceptual Model B.

**Table 3.3-5  
Variable Well Production Rate (kg/s) Evaluated in the Tier-3 Saturated Transport Models**

Well	Pumping rates [kg/s]											
	1993	1994	1995	1996	1997	1998	1999	2000	2001	Mean	Min	Max
PM-1	7.67	5.21	3.57	4.36	5.73	4.12	6.88	12.79	8.00	6.5	3.6	12.8
PM-2	32.15	35.88	26.13	36.27	19.55	46.36	29.91	40.08	36.41	33.6	19.6	46.4
PM-3	20.23	9.46	19.17	14.22	9.67	26.70	16.20	11.16	11.02	15.3	9.5	26.7
PM-4	29.97	55.64	51.40	24.90	49.75	8.99	13.47	23.14	23.74	31.2	9.0	55.6
PM-5	15.12	18.83	34.93	26.96	11.02	26.74	28.44	22.24	15.11	22.2	11.0	34.9
O-1	na	na	na	na	na	8.05	1.56	6.40	3.02	4.8	1.6	8.1
O-4	34.07	24.69	na	25.16	25.98	28.77	24.07	14.28	43.62	27.6	14.3	43.6

na = not available

The computational grid is uniform (structured) in the vicinity of Mortandad Canyon and the water-supply wells (including beneath the 38 columns for the upper/middle-canyon-dominated infiltration model or 27 columns for the lower-canyon-dominated infiltration model). The Tier-3 saturated transport models were used to calculate 1000 separate simulations of contaminant transport and the resulting concentrations in the regional aquifer at various locations (including production wells, regional observation wells, and Rio Grande/White Rock canyon springs). These calculations addressed variable fluxes of tritium, nitrate, and perchlorate (3000 simulations) from the bottom of the unsaturated transport columns (3000 times 38 [or 27] simulations) for each of the 16 infiltration models (3000 times 38 [or 27] times 16 inputs). In all, more that 750,000,000 calculations of potential contamination levels in well water were conducted to address conceptual model uncertainties and system heterogeneity. In addition, the Tier-3 saturated transport simulations considered the variability in aquifer properties as indicated in Table 3.3-6.

**Table 3.3-6**  
**Aquifer Distributions Evaluated in the Tier-3 Saturated Transport Models**

Parameter	Distribution	Min	Max	Mean
Longitudinal dispersivity (m)	uniform	110	190	150
Transverse dispersivity (m)	1/10 of longitudinal (perfectly correlated)	11	19	15
Santa Fe Group porosity ( $\log_{10} m^3/m^3$ )	log normal	-2	-0.53	-1.2
Basalts porosity ( $\log_{10} m^3/m^3$ )	log normal	-5	-0.2	-3
Tschicoma porosity ( $\log_{10} m^3/m^3$ )	log normal	-5	-0.2	-3
Puye porosity ( $\log_{10} m^3/m^3$ )	log normal	-2	-0.5	-1
Porosity of alternative units (basalts or Puye/Santa Fe Groups) ( $\log_{10} m^3/m^3$ )	log normal	-5	-1	-3

### 3.3.4.1 Comparison of Tier-1 and Tier-3 Saturated Transport Simulations

Figure 3.3-14 compares the concentrations of perchlorate at production well PM-5, calculated using the Tier-1 and Tier-3 saturated transport models. The PM-5 curve on the Tier-1 plot represents the single model prediction; the 1000 curves on the Tier-3 plot represent the uncertainty in the model predictions. The Tier-3 simulations use regional-aquifer Model A and the lower-canyon-dominated infiltration model with fast paths in the upper and middle canyon sections and a continuous source of perchlorate. The differences in the concentration predictions are due to differences between the Tier-1 and Tier-3 models. These differences are related predominantly to (a) contaminant distribution along the canyon (upper-canyon-dominated infiltration model with a very high infiltration rate for Tier-1 versus the lower-canyon-dominated infiltration model for Tier 3), (b) the magnitude of the source term (Tier-3 simulations have less perchlorate mass than the Tier-1 simulation) and (c) assumptions about the unknown post-2001 pumping rates, which control the direction of transport within the aquifer.

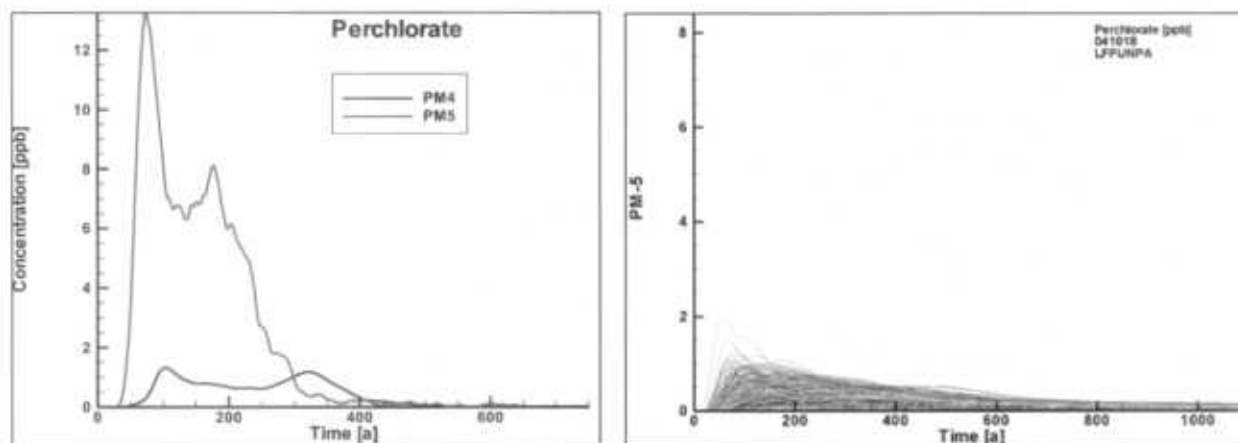


**Figure 3.3-14.** Comparison of Tier-1 (left; green curve) and Tier-3 (right; aquifer Model A and lower-canyon-dominated infiltration model with fast paths in the upper and middle canyons sections) perchlorate concentrations [ppb] in PM-5. (Time = 0 is 1964)

In the Tier-1 groundwater transport simulations, a large percentage of the contamination reaching the supply wells originates from the upper-canyon column in the unsaturated transport model because of the very high, assumed infiltration rate there (Table 3.2-1). This pathway arrives at the regional aquifer in close proximity to PM-5. The pump rates chosen for the Tier-1 analysis set up southerly gradients in the regional aquifer, which cause relatively high concentrations in water pumped from PM-5 for about 200 yr (left). In contrast, a greater volume of water infiltrates in the lower canyon with the Tier-3 model shown, and a high percentage of the Tier-3 saturated-zone simulations use pumping rates that set up easterly gradients in the regional aquifer. This leads to a lower calculated breakthrough at PM-5 as compared to the Tier-1 simulation. However, a large percentage of the Tier-3 simulations that assume aquifer Model A predict concentrations for PM-3 in excess of 1 ppb. The Tier-1 analysis did not predict this result; in fact, the Tier-1 analysis predicted an insignificant breakthrough at PM-3. Therefore, although the PM-5 comparison above shows that the Tier-1 predictions were conservative with respect to that well, the Tier-3 results are conservative with respect to concentrations at PM-3. In addition, for PM-4, the Tier-1 results were conservative; for PM-1, PM-2, O-1, and O-4, the Tier-3 results were conservative, although releases to these wells are predicted to be very minor. PM-3 results are covered in greater detail in the sections that follow.

#### **3.3.4.2 Simulated Contaminant Concentrations in Production Wells**

Generally, when considering regional-aquifer Model A, little difference results in predicted perchlorate and nitrate contaminant concentrations and arrival times to the production wells as a result of the assumed infiltration model. This implies that mixing in the regional aquifer, as affected by pumping, overwhelms transient or variable conditions that more dramatically affect unsaturated transport. Tritium concentrations are somewhat affected by the presence of fast paths through the unsaturated zone, as explained by Birdsell et al. (2005, in progress), because tritium decays quickly (12.3-yr half life) with respect to unsaturated-zone travel times.

Figure 3.3-15 (a, b, and c) presents the 1000 calculated concentrations of perchlorate in water pumped from the PM-1, PM-3, and PM-5 wells, assuming regional-aquifer Model A and the lower-canyon-dominated infiltration scenario with fast paths in the upper- and middle-canyon sections and uniform infiltration in the lower canyon. Each of the 1000 perchlorate-concentration histories is represented by different breakthrough curves, with curve coloring used only to visually distinguish the realizations.

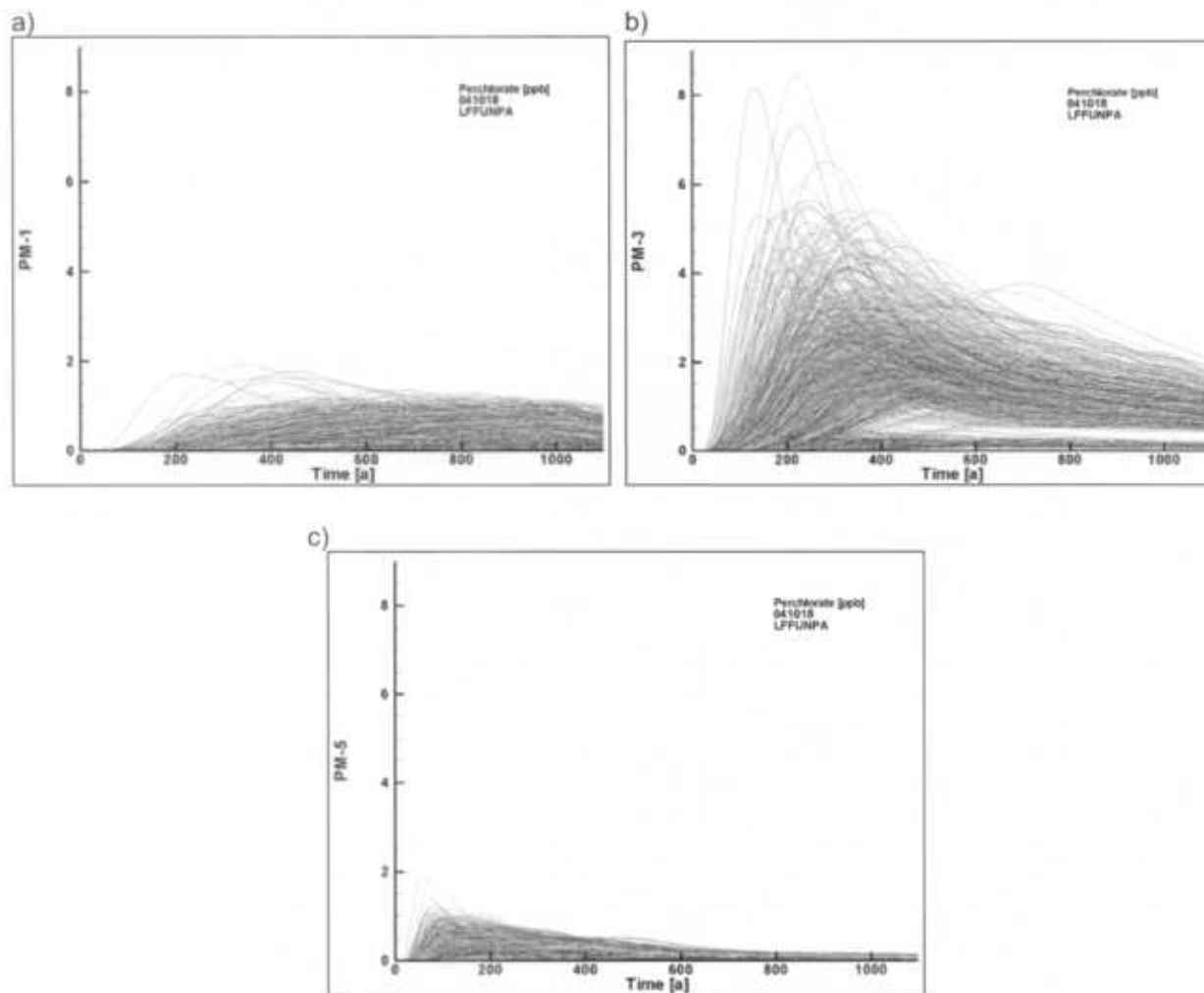


**Figure 3.3-15.** 1000 perchlorate concentration [ppb] histories at water supply wells (a) PM-1, (b) PM-3, and (c) PM-5 for simulated fast-path infiltration in upper and middle Mortandad Canyon and uniform infiltration in lower Mortandad Canyon and regional-aquifer Model A (Time = 0 is 1964).

Perchlorate concentrations at PM-1 (Figure 3.3-15a) remain relatively constant for approximately 700 yr of the 1000-yr simulation period. Arrival times are later at (a) PM-1 than at (b) PM-3 and (c) PM-5, reflecting the fact that (referring back to Figure 2.2-1) PM-1 is farther from the canyon than are PM-3 and PM-5. Supply well PM-5 is nearest to the canyon and is impacted by a relatively short section of the canyon nearest the RLWTF source; consequently, perchlorate concentrations at PM-5 arrive earlier compared to concentrations at PM-1 and PM-3. In fact, a few simulations with the most rapid transport toward PM-5 indicate that perchlorate could currently be at detectable concentrations (in 2005) in pumped water. However, this has not been observed, which indicates that those particular realizations are conservative.

As for PM-1 and PM-5, PM-3 curves reveal generally higher concentrations and more dynamic behavior. A subset of the 1000 curves for PM-3 rests near the horizontal (time) axis showing very low concentrations, but another, larger subset shows much higher concentrations; these two sets of curves are separated by a narrow near-horizontal gap. This split is due to the relative pumping rates of the ensemble of pumping wells (Table 3.3-5), which affect the flow direction. Those simulations that use the

1994 or 1995 production rates have relatively greater pumping at PM-4 and PM-5, which sets up more southerly gradients and yields the lower concentration curves at PM-3. Those simulations with relatively greater pumping at PM-1 and PM-3 drive easterly gradients and lead to the larger subset of higher concentration curves at PM-3.

In addition, some of the PM-3 curves have double peaks. The earlier peaks typically have higher concentrations and spread over a shorter time period; the later peaks typically have lower concentrations and spread over a longer time period. Causes for this “double-hump” behavior are various. The source-term model (and Table 2.1-1) reflects higher-volume effluent releases from the RLWTF at early times (1963 through 1981); however, the largest contaminant mass releases occur later (1981 through 1989). Because the highest effluent volume and contaminant mass releases are out of phase, the time-dependent mass flux into (and out of) the vadose-zone columns has a double-humped character. In addition, the concentrations in the water-supply wells represent contaminants released from different sections of the canyon that have different infiltration models. All of these factors contribute to the dynamic features of the PM-3 concentration history curves.

In Figure 3.3-16, the cumulative peak nitrate concentration reached in each of 1000 calculations for the five PM supply wells is depicted as a single point, plotted at the time when the peak concentration is calculated. Both plots are for simulations that use the lower-canyon-dominated infiltration model and regional-aquifer Model A. The scatter plot on the left shows results with fast-path infiltration in the upper, middle, and lower canyon sections, and the plot on the right shows results for uniform infiltration.

The scatter plots show little difference in peak nitrate concentrations from the two “end-member” lower-canyon-dominated infiltration conceptual models. Under both fast-path and uniform infiltration conditions, the highest concentrations of contaminants occur at PM-3, with lower concentrations of contaminants, arriving earlier, at PM-5 and PM-4. However, the fast-flow paths yield more peak nitrate concentrations occurring at PM-5 in the first 100 yr than do the uniform flow paths. Concentrations at PM-5 are also elevated with the upper/middle-canyon-dominated infiltration model, as described by Birdsell et al. (2005, in progress). As a result, that conceptual model for infiltration does lead to slightly different results for PM-5 but quite similar results for PM-3.

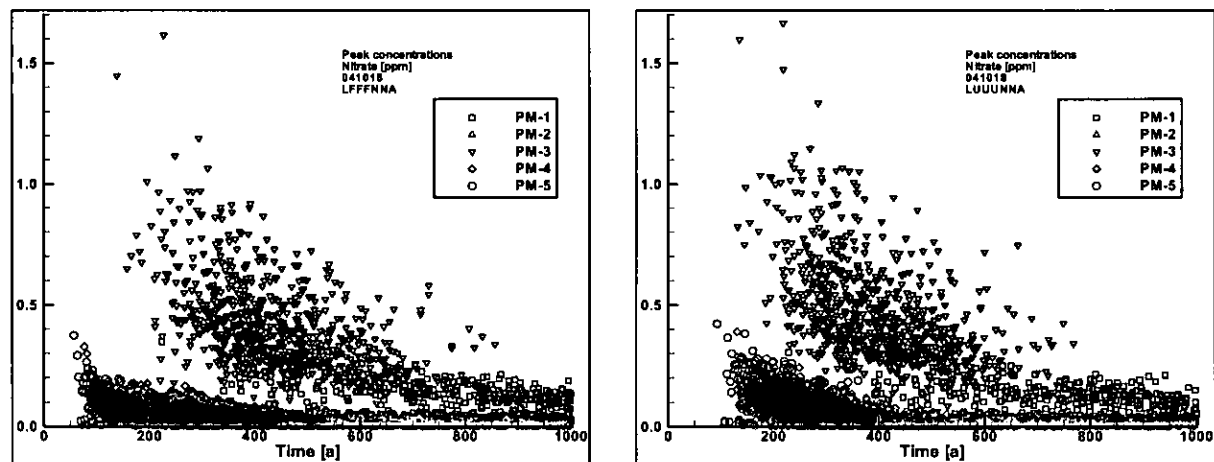
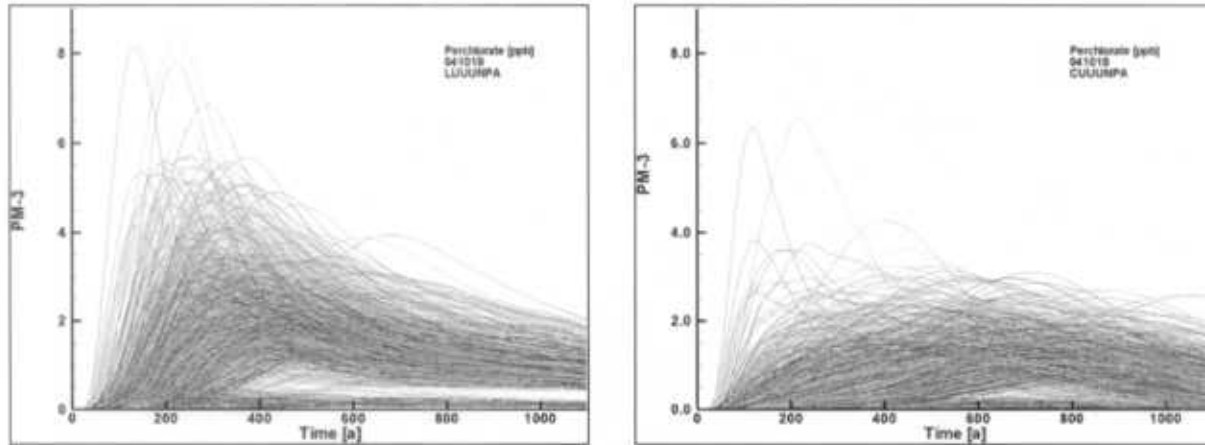


Figure 3.3-16. Peak nitrate concentrations [ppm] and peak arrival times [a] at the water supply wells for fast-path (left) and lower-canyon-dominated uniform infiltration (right) conceptual models with regional-aquifer Model A

Figure 3.3-17 compares the 1000 simulations of perchlorate concentration as a function of time in water pumped from supply well PM-3 calculated for continuous perchlorate releases (plots on left), and discontinued perchlorate releases (plots on right), for the lower-canyon-dominated infiltration model and regional-aquifer Model A.



**Figure 3.3-17. Comparison of perchlorate concentrations [ppb] in PM-3 well water with continuous perchlorate releases (left) and discontinued perchlorate releases (right) for the lower-canyon-dominated uniform infiltration model and regional-aquifer Model A. (Time = 0 is 1964.)**

The most obvious effect of eliminating releases from the RLWTF is a delay in the arrival time of perchlorate at PM-3. Perchlorate concentrations are not significantly reduced by the elimination of discharges, according to these simulations. This indicates that future releases (as modeled) are less important than past releases in determining the ultimate contaminant concentrations at supply wells, which conforms to the vadose-zone data and model results (Figures 3.3-10 and 3.3-12) that show that the majority of the perchlorate mass resides in the pore water in the vadose zone.

### 3.3.4.3 Comparison of Aquifer Models A and B

Figure 3.3-18 shows the portion of the contaminant particles (the particles used in the particle-tracking simulations) from 27 columns (upper-, middle-, and lower-canyon locations) captured in the supply wells included in the simulations for the two different conceptual models of the regional aquifer; assuming predominantly deeper transport and phreatic transport pathways. These results are independent from the unsaturated zone (infiltration model) conceptualizations. The figure shows that for the case of Model A, PM-3, PM-4, and PM-5 capture the largest percentage (68%) of contaminant particles. For Model B, the White Rock springs capture the predominant portion (23%) of the particles. Compared to the Tier-1 calculations, more wells (and the springs) are impacted by releases represented in the Tier-3 analysis.

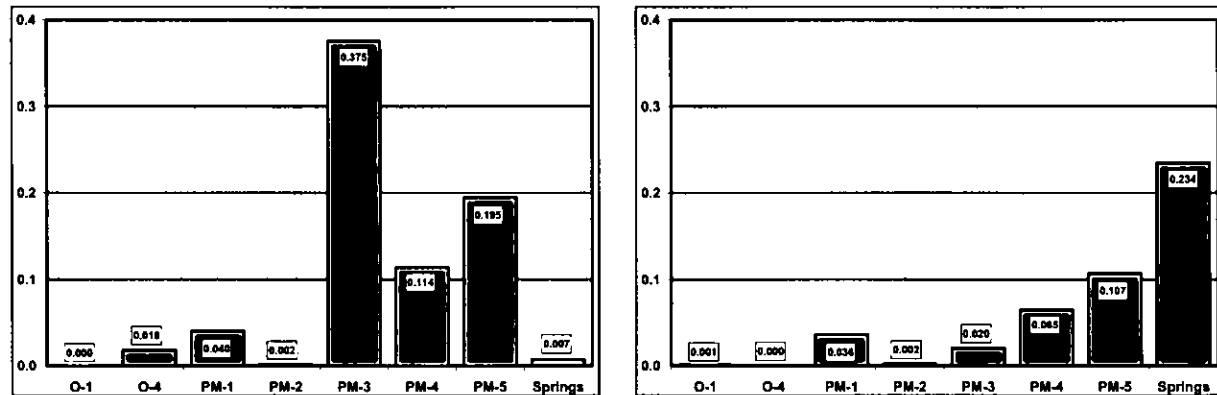


Figure 3.3-18. Portion of the 27,000,000 particles (all 27 release locations, all realizations) captured by the water-supply wells and springs/Rio Grande within 1000 yr for alternative regional aquifer conceptual models: Model A (left) and Model B (right).

Figure 3.3-19 compares the 1000 simulations of perchlorate concentration as a function of time at PM-3 and at the springs using the aquifer Model B. These results assume the lower-canyon-dominated infiltration model with fast flow paths in the upper- and middle-canyon sections and uniform infiltration in the lower canyon. Relative to the PM-3 results for aquifer Model A (shown in Figure 3.3-17), perchlorate concentrations are substantially reduced. The difference is matched by the increased concentrations calculated in spring water starting at about 200 yr. Therefore, less contamination is captured by the water-supply wells with the phreatic aquifer model, and more contamination flows toward the Rio Grande with a relatively longer travel time toward that exposure point.

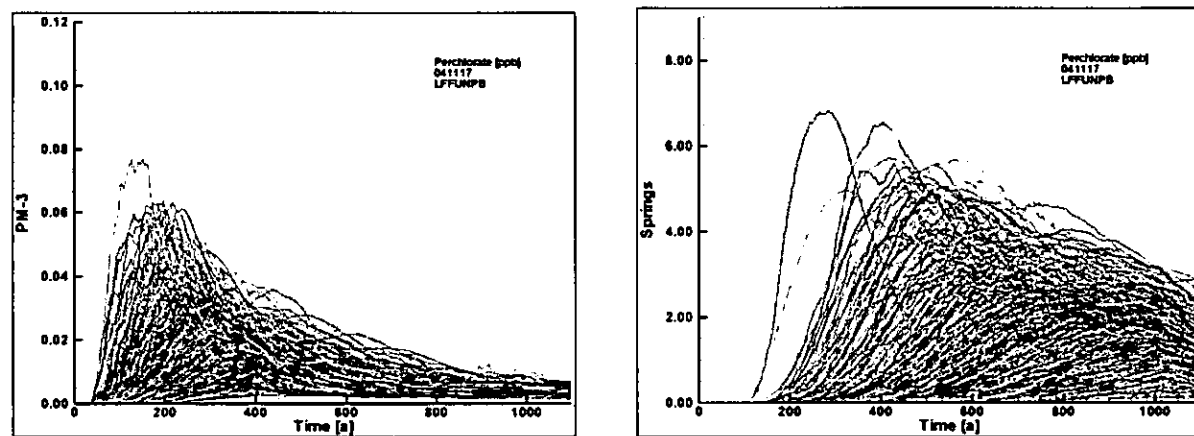


Figure 3.3-19. Perchlorate concentrations [ppb] as a function of time at PM-3 (left) and springs (right) for aquifer Model B (note the different concentration scales) (Time = 0 is 1964).

### 3.4 Tier-3 Human-Health Risk Assessment

As for the Tier-1 risk assessment (Section 3.2), the Tier-3 risk assessments followed EPA's guidance pertaining to chronic drinking-water exposures and calculated values for HI, HQ, and TEDE (EPA IRIS 2005). Adult exposures to nitrate, perchlorate, and tritium were assumed to occur over a 70-yr period, with an ingestion rate of 2 L/day of water pumped exclusively from an individual well. Every pumping well included in the saturated transport simulations was evaluated in the exposure assessment, using the maximum 70-yr average contaminant concentration calculated within the 1000-yr simulation period in the 1000 saturated transport calculations conducted for each infiltration conceptual model. Infant exposures

to nitrate were assumed to occur over a single year, and maximum annual concentrations calculated in the saturated transport simulations were used.

The reference doses used in the adult and infant nitrate toxicity assessments were taken from IRIS/HEAST. The perchlorate toxicity assessments assumed an MCL of 1 ppb, which is the lowest of the proposed drinking-water standards under consideration for perchlorate. The dose assessment for tritium used EPA's 20,000 pCi/L MCL for drinking water.

A probabilistic risk assessment uses the same fundamental exposure and risk equations as do Tier-1 point-estimate approaches. These equations are shown in Figure 3.4-1, which is excerpted from RAGS3 (EPA 2001, 85534).

CANCER AND NONCANCER RISK MODELS	
Exposure Model:	$CDI = \frac{C \times IR \times EF \times ED}{BW \times AT}$
Cancer Risk model:	$Risk = CDI \times CSF$
Noncancer Risk Model:	$HQ = \frac{CDI}{RfD}$
CDI	chronic daily intake of the chemical (mg/kg-day)
C	concentration of the chemical in an exposure medium (e.g., mg/L)
IR	ingestion rate (e.g., L/day for water, mg/day for soil, etc.)
EF	exposure frequency (days/year)
ED	exposure duration (years)
BW	body weight (kg)
HQ	hazard quotient
AT	averaging time (equal to ED × 365 days/year for noncarcinogens and 70 years × 365 days/year for carcinogens)
CSF	cancer slope factor (linear low-dose cancer potency factor) for the chemical (mg/kg-day) <sup>-1</sup>
RfD	reference dose for the chemical for assessing noncancer health effects (mg/kg-day)

**Figure 3.4-1. General equation for calculating human-health risk through drinking water**

In RAGS3 (2001, 85334), EPA states: "In human health risk assessments, probability distributions for risk should reflect variability or uncertainty in exposure." This means that only the exposure assessment portion of the human-health risk assessment is conducted in a probabilistic manner. This is accomplished by using probability distribution functions rather than point estimates to represent uncertainty and variability in exposure-point concentrations (i.e., well-water concentrations). The risk equation in Figure 3.4-1 can be expressed in terms of multiple exposure variables ( $V_i$ ) and a toxicity term:  $Risk = f(V_1, V_2, V_n) \times Toxicity$ . The exposure variables ( $V_i$ ) represent the 1000 simulations of contaminant concentrations in supply wells (conducted for each supply well, for each conceptual model). Numerical techniques (in this case, Monte Carlo sampling) are used to calculate HI or dose values by randomly selecting an exposure-point concentration value ( $V_i$ ) from the concentration distributions calculated in the groundwater transport simulations. This process is repeated 1000 times to produce a probability distribution of HI (or dose) values. Each HI calculation assumes that a hypothetical 70-kg individual drinks 2 L/day of water from a given supply well for 70 yrs.

Each concentration distribution for each supply well is used to compute HQ values (nitrate and perchlorate) for each year using the same default EPA assumptions described in the Tier-1 analysis (Section 3.2). HI is computed adding both components for each year, and the maximum HI value was searched for in the time series. The maximum 70-yr average concentrations for the radioactive element (tritium) is searched and then converted to dose values using the same default EPA assumptions described in the Tier-1 analysis. The output of the risk assessment is 1000 equally likely HI or dose values for each conceptual model treated in the groundwater-transport simulations.

The results of a probabilistic risk assessment are generally presented in the form of a complementary cumulative distribution function (CCDF). A CCDF gives the cumulative probability of HI or dose values, that is, the fraction of the 1000 calculations that produced a specific HI value. The CCDF displays the full range of HI or dose values calculated and the probability that a given HI or dose value will be exceeded. In this case, the CCDF is used to visualize the 95% confidence level for an HI less than 1 and a dose of less than 4 mrem/yr. The results of the risk assessment are given in full in Appendix C, which includes output for all cases (conceptual models and contaminants) over 100-yr and 1000-yr simulation periods. Over the 100-yr period and for all wells, HI is computed to be less than 1, and the dose is less than 4 mrem/yr at a greater than 95% confidence level. Presented below are the results for the full 1000-yr assessment period.

Table 3.4-1 lists the results of the perchlorate and nitrate risk assessments for 1000 yr conducted for several of the groundwater transport conceptual models. Simulation results are shown for both the continuous 1000-yr release and interrupted source-term models. Most of the results presented are for the various vadose-zone infiltration models using regional-aquifer Model A. One result for regional-aquifer Model B is also presented. The table is shaded to show where the calculated HI or HQ had a greater than 5% probability of exceeding a value of 1 (i.e., where more than 50 of the 1000 stochastic HI or HQ calculations for each well exceeded a value of 1).

The first seven entries in Table 3.4-1 give risk-assessment results for various infiltration models using the regional-aquifer Model A. All of these simulations assume that the source and the disposal volumes are continuous over the entire 1000-yr period. Most of the seven supply wells have a very low probability (i.e., less than 5%) of exceeding safe drinking water thresholds (i.e., HI or HQ above 1). The one noteworthy exception is supply well PM-3, which has a greater than 70% probability of exceeding safe drinking-water thresholds in all seven cases, resulting almost entirely from perchlorate in excess of 1 ppb. Maximum HI and HQ values approach 8, generally occurring 250 yr from the present in the simulation. These results also show that the infiltration model assumed for the unsaturated-transport simulations has little effect on the risk calculated for PM-3.

**Table 3.4-1**  
**Results of the Nitrate and Perchlorate Risk Assessment for a 1000-yr Period**

Contaminant(s) Evaluated	Quantity Evaluated	Wells Evaluated	Number of Calculations with HI or HQ >1	Probability of Exceedance of HI or HQ >1	Maximum HQ/HI	Year of Maximum HQ/HI
<b>Upper/middle-canyon-dominated uniform infiltration with regional-aquifer Model A</b>						
Nitrate and Perchlorate	HI	O-1	0	0.0%	0.0169	630
		O-4	0	0.0%	0.5761	247
		PM-1	29	2.9%	1.6626	433
		PM-2	0	0.0%	0.0612	743
		PM-3	744	74.4%	6.9254	179
		PM-4	3	0.3%	1.3597	159
		PM-5	173	17.3%	2.8264	116
<b>Lower-canyon-dominated infiltration with fast paths in the upper, middle, and lower canyons with regional-aquifer Model A</b>						
Nitrate and Perchlorate	HI	O-1	0	0.0%	3.19E-02	590
		O-4	0	0.0%	0.387647	355
		PM-1	45	4.5%	1.83055	423
		PM-2	0	0.0%	6.07E-02	716
		PM-3	754	75.4%	7.643411	265
		PM-4	4	0.4%	1.45586	124
		PM-5	5	0.5%	1.637122	111
<b>Lower-canyon-dominated infiltration with fast paths in the upper and middle canyons with regional-aquifer Model A</b>						
Perchlorate	HQ	O-1	0	0.0%	0.0241	333
		O-4	0	0.0%	0.4287	252
		PM-1	43	4.3%	1.8154	383
		PM-2	0	0.0%	0.0664	719
		PM-3	771	77.1%	7.7959	259
		PM-4	8	0.8%	1.5678	177
		PM-5	4	0.4%	1.6345	112
Nitrate and Perchlorate	HI	O-1	0	0.0%	0.0245	333
		O-4	0	0.0%	0.4355	252
		PM-1	44	4.4%	1.8436	382
		PM-2	0	0.0%	0.0673	719
		PM-3	773	77.3%	7.9236	259
		PM-4	8	0.8%	1.5916	177
		PM-5	5	0.5%	1.6593	112

Table 3.4-1 (continued)

Contaminant(s) Evaluated	Quantity Evaluated	Wells Evaluated	Number of Calculations with HI or HQ >1	Probability of Exceedance of HI or HQ >1	Maximum HQ/HI	Year of Maximum HQ/HI
<b>Lower-canyon-dominated uniform infiltration with regional-aquifer Model A</b>						
Perchlorate	HQ	O-1	0	0.0%	0.0222	926
		O-4	0	0.0%	0.5302	235
		PM-1	41	4.1%	1.9022	393
		PM-2	0	0.0%	0.0651	608
		<b>PM-3</b>	<b>772</b>	<b>77.2%</b>	<b>7.7455</b>	<b>258</b>
		PM-4	12	1.2%	1.7875	170
		PM-5	39	3.9%	1.8516	130
Nitrate and Perchlorate	HI	O-1	0	0.0%	0.0225	926
		O-4	0	0.0%	0.5378	235
		PM-1	43	4.3%	1.9313	393
		PM-2	0	0.0%	0.066	608
		<b>PM-3</b>	<b>774</b>	<b>77.4%</b>	<b>7.8729</b>	<b>258</b>
		PM-4	12	1.2%	1.8137	170
		PM-5	40	4.0%	1.8776	130
<b>Lower-canyon-dominated infiltration with fast path in the lower canyon with regional-aquifer Model A</b>						
Perchlorate	HQ	O-1	0	0.0%	0.031	590
		O-4	0	0.0%	0.4448	245
		PM-1	44	4.4%	1.8593	423
		PM-2	0	0.0%	0.0617	429
		<b>PM-3</b>	<b>750</b>	<b>75.0%</b>	<b>7.4704</b>	<b>266</b>
		PM-4	6	0.6%	1.5107	151
		PM-5	37	3.7%	1.8209	130
Nitrate and Perchlorate	HI	O-1	0	0.0%	0.0319	590
		O-4	0	0.0%	0.4514	245
		PM-1	45	4.5%	1.8879	423
		PM-2	0	0.0%	0.0625	425
		<b>PM-3</b>	<b>754</b>	<b>75.4%</b>	<b>7.5931</b>	<b>266</b>
		PM-4	6	0.6%	1.5332	151
		PM-5	39	3.9%	1.8466	131
<b>Lower-canyon-dominated infiltration with fast path in the middle canyon with regional-aquifer Model A</b>						
Perchlorate	HQ	O-1	0	0.0%	0.0241	333
		O-4	0	0.0%	0.4708	260
		PM-1	44	4.4%	1.848	388
		PM-2	0	0.0%	0.0681	729
		<b>PM-3</b>	<b>773</b>	<b>77.3%</b>	<b>7.7625</b>	<b>258</b>
		PM-4	8	0.8%	1.6502	179
		PM-5	30	3.0%	1.6453	131

Table 3.4-1 (continued)

Contaminant(s) Evaluated	Quantity Evaluated	Wells Evaluated	Number of Calculations with HI or HQ >1	Probability of Exceedance of HI or HQ >1	Maximum HQ/HI	Year of Maximum HQ/HI
<b>Lower-canyon-dominated infiltration with fast path in the middle canyon with regional-aquifer Model A</b>						
Nitrate and Perchlorate	HI	O-1	0	0.0%	0.0245	333
		O-4	0	0.0%	0.4783	260
		PM-1	44	4.4%	1.877	388
		PM-2	0	0.0%	0.069	729
		PM-3	774	77.4%	7.8897	258
		PM-4	8	0.8%	1.6753	167
		PM-5	31	3.1%	1.6704	131
<b>Lower-canyon-dominated infiltration with fast path in the upper canyon with regional-aquifer Model A</b>						
Perchlorate	HQ	O-1	0	0.0%	0.0222	926
		O-4	0	0.0%	0.4979	234
		PM-1	41	4.1%	1.871	377
		PM-2	0	0.0%	0.0638	699
		PM-3	772	77.2%	7.779	259
		PM-4	12	1.2%	1.7183	167
		PM-5	15	1.5%	1.7841	117
Nitrate and Perchlorate	HI	O-1	0	0.0%	0.0225	926
		O-4	0	0.0%	0.5064	234
		PM-1	43	4.3%	1.9006	377
		PM-2	0	0.0%	0.0647	699
		PM-3	773	77.3%	7.9059	259
		PM-4	12	1.2%	1.7456	167
		PM-5	18	1.8%	1.8114	118
<b>Lower-canyon-dominated infiltration with fast paths in the upper and middle canyons with a phreatic regional aquifer model</b>						
Perchlorate	HQ	O-1	0	0.0%	8.72E-03	277
		O-4	0	0.0%	6.69E-04	216
		PM-1	0	0.0%	0.0843	206
		PM-2	0	0.0%	1.05E-03	534
		PM-3	0	0.0%	0.0695	170
		PM-4	0	0.0%	0.0287	239
		PM-5	0	0.0%	0.0960	109
<b>Lower-canyon-dominated uniform infiltration with regional-aquifer Model A and source term interrupted in 2006</b>						
Perchlorate	HQ	O-1	0	0.0%	4.91E-03	630
		O-4	0	0.0%	0.2516	565
		PM-1	3	0.3%	1.0986	618
		PM-2	0	0.0%	0.0412	912
		PM-3	629	62.9%	6.0208	254
		PM-4	0	0.0%	0.7456	140
		PM-5	1	0.1%	1.1109	113

**3.4.1 Risk-Assessment Results for a Continuous Release Scenario, Assuming Regional-Aquifer Model A**

The only other supply well with a greater than 5% probability of exceeding safe drinking water thresholds for nitrate and perchlorate is PM-5, where there is a 17% probability of an HI greater than 1 for a single scenario, the upper/middle-canyon-dominated uniform infiltration model and regional-aquifer Model A. This result is qualitatively consistent with the results of the Tier-1 risk assessment, because with that model, the upper- and middle-canyon sections have high infiltration rates relative to the lower-canyon section causing contaminants to arrive at the regional aquifer close to PM-5. Interestingly, this Tier-3 model is the only scenario in which nitrate has a significant impact on HI.

Table 3.4-2 compares the mean, minimum, maximum, and standard deviation associated with the 1000 HI values calculated for PM-3 for each conceptual model evaluated in the groundwater transport simulations, assuming continuous perchlorate releases throughout the 1000-yr simulation period and assuming that the regional aquifer acts as a well-mixed system with deep transport that generally reaches supply-well screens. On inspection, the statistical parameters (mean, minimum, maximum, and standard deviation) describing the HI distributions appear to be very similar among all conceptual infiltration models.

**Table 3.4-2  
Statistics of HI Distributions Calculated for Perchlorate in Water Pumped from PM-3  
over a 1000-yr Period with Regional-Aquifer Model A and a Continuous Source**

Conceptual Model	Mean HI	Minimum HI	Maximum HI	Standard Deviation
Lower-canyon-dominated infiltration with fast paths in the upper, middle, and lower canyons for perchlorate with regional-aquifer Model A	1.704693	0.070297	7.643411	1.156845
Lower-canyon-dominated infiltration with fast paths in the upper and middle canyons for perchlorate with regional-aquifer Model A	1.887234	0.096496	7.923608	1.255272
Lower-canyon-dominated infiltration with a fast path in the upper canyon for perchlorate with regional-aquifer Model A	1.912401	0.096934	7.905859	1.279627
Lower-canyon-dominated infiltration with a fast path in the middle canyon for perchlorate with regional-aquifer Model A	1.897458	0.096496	7.889667	1.263300
Lower-canyon-dominated infiltration with a fast path in the lower canyon for perchlorate with regional-aquifer Model A	1.730823	0.071004	7.593081	1.179823
Lower-canyon-dominated uniform infiltration for perchlorate with regional-aquifer Model A	1.921613	0.096934	7.872927	1.287188
Upper/middle-canyon-dominated uniform infiltration for perchlorate with regional-aquifer Model A	1.616932	0.059196	6.925407	1.101290

A quantitative analysis shows that the correlation between the HI distributions for each conceptual model range from 0.98 to 1.00, meaning that there is no statistically significant difference in the risk-assessment results for alternative source-term and infiltration models coupled with saturated transport Model A.

Table 3.4-3 lists the statistical parameters describing the HI distributions calculated for PM-5 over the next 1000 yr for different conceptual models of infiltration and assuming that transport within the regional aquifer is deep and moves toward the supply wells (Model A). Even though the risk assessment shows a significant difference in the probability of exceeding an HI of 1 in PM-3 and PM-5, a comparison between Table 3.4-2 and 3.4-3 shows that the HI probability distributions calculated for the two wells are very similar. A statistical analysis of the PM-5 HI parameters shows correlations that range from 0.95 to 1.0 among conceptual models of infiltration.

**Table 3.4-3**  
**Statistics of HI Distributions Calculated for Perchlorate for 1000 Yr**  
**in Water Pumped from PM-5 with Regional-Aquifer Model A and a Continuous Source**

Conceptual Model	Mean HI	Minimum HI	Maximum HI	Standard Deviation
Lower-canyon-dominated infiltration with fast paths in the upper, middle, and lower canyons for perchlorate	0.331494	0.012085	1.637122	0.180272
Lower-canyon-dominated infiltration with fast paths in the upper and middle canyons for perchlorate	0.332942	0.012350	1.659323	0.181206
Lower-canyon-dominated infiltration with a fast path in the upper canyon for perchlorate	0.364866	0.012249	1.811434	0.219947
Lower-canyon-dominated infiltration with a fast path in the middle canyon for perchlorate	0.456497	0.016703	1.670403	0.248006
Lower-canyon-dominated infiltration with a fast path in the lower canyon for perchlorate	0.465825	0.017202	1.846617	0.261774
Lower-canyon-dominated uniform infiltration for perchlorate	0.471758	0.017468	1.877768	0.266194
Upper/middle-canyon-dominated uniform infiltration for perchlorate	0.644288	0.017334	2.826401	0.409099

With respect to the lower-canyon-dominated infiltration models, the focused infiltration conceptual models do not have a significant impact on the calculated risk at any of the wells. Because the lower-canyon-dominated infiltration models resulted in nearly equal risks when using regional-aquifer Model A, detailed results will be provided for individual infiltration models below. The discussions apply equally to all lower-canyon-dominated infiltration models. For completeness, Appendix C describes the risk-assessment results for all of the cases that were evaluated.

Figure 3.4-2 compares the results of the nitrate and perchlorate risk assessment for alternative conceptual models for PM-5 in the form of CCDF. The CCDF is obtained by first ordering all simulations from highest to lowest simulated HI value. A cumulative probability is calculated by starting with the simulation with the second-lowest HI value and adding the probability of the lowest HI value to it to derive a cumulative probability (in this case, 1/1000 plus 1/1000). This procedure is followed for each of the 1000 simulations (for each supply well). The CCDF is then produced by subtracting the probability of each simulation (HI value) from 1.0.

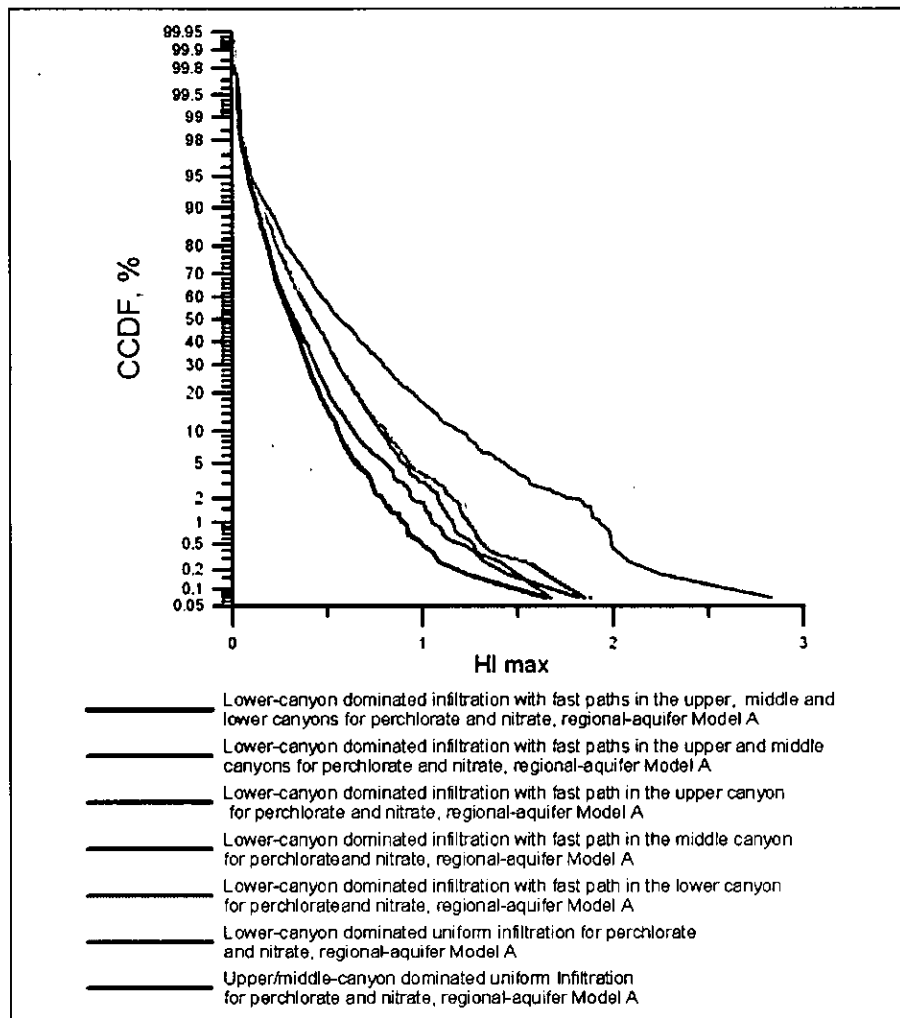


**Figure 3.4-2. Comparison of complementary cumulative distribution functions of HI as a result of perchlorate and nitrate in PM-5 for alternative conceptual infiltration models and a 1000-yr simulation period. All simulations shown assume regional-aquifer Model A.**

Figure 3.4-3 compares CCDFs for nitrate and perchlorate HIs for seven regional supply wells for both the upper/middle-canyon-dominated uniform infiltration model and the lower-canyon-dominated uniform infiltration model, with both assuming regional-aquifer Model A. The CCDF for PM-3 in the top figure of Figure 3.4-3 demonstrates that, for the upper/middle-canyon-dominated uniform infiltration model with the regional-aquifer Model A, there is about a 10% chance that the simulated HI value is greater than 3.0 and a 100% chance that the simulated HI value is less than 7.0. Each curve is generated from the results of 1000 Monte Carlo simulations. In the cases shown, each simulation is assumed to be equally likely. Therefore, the probability of any individual simulation result (HI value) occurring is 1 divided by 1000.

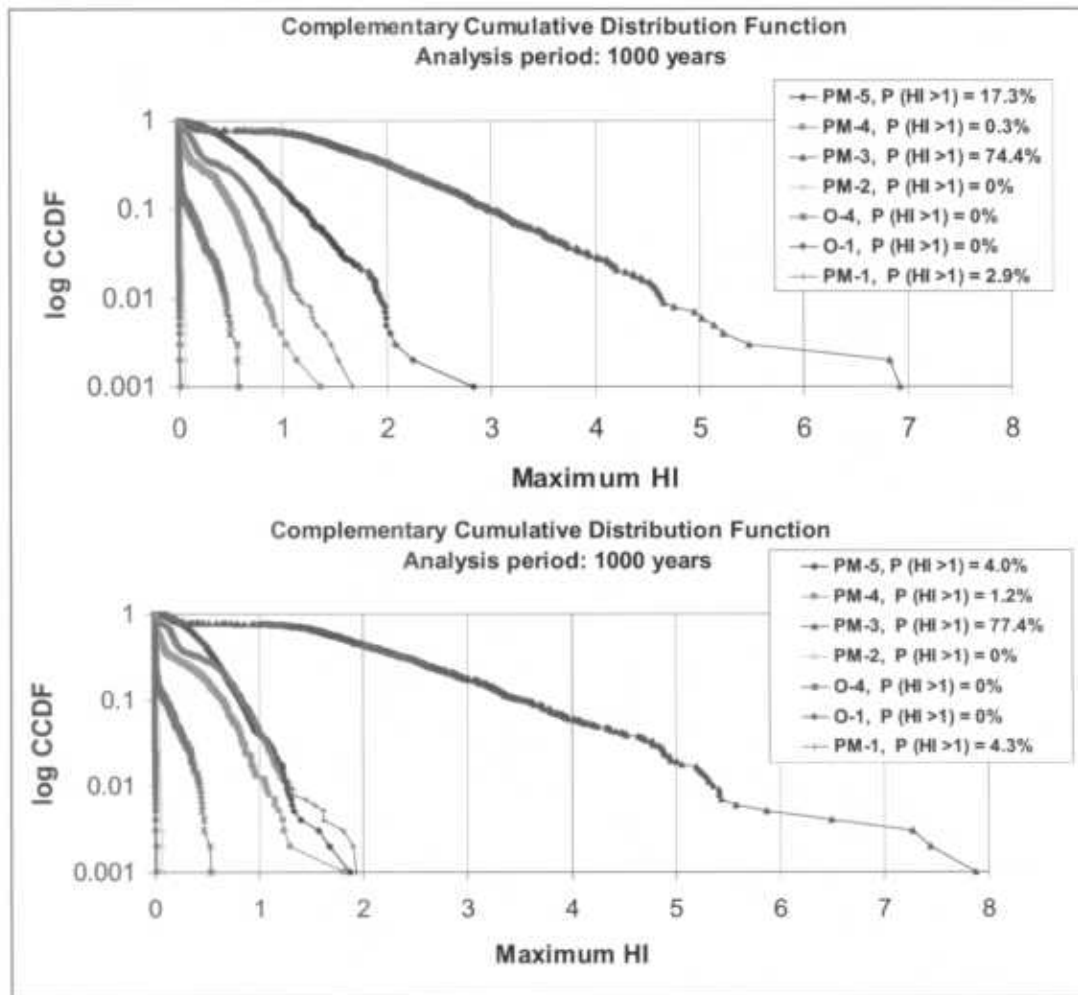
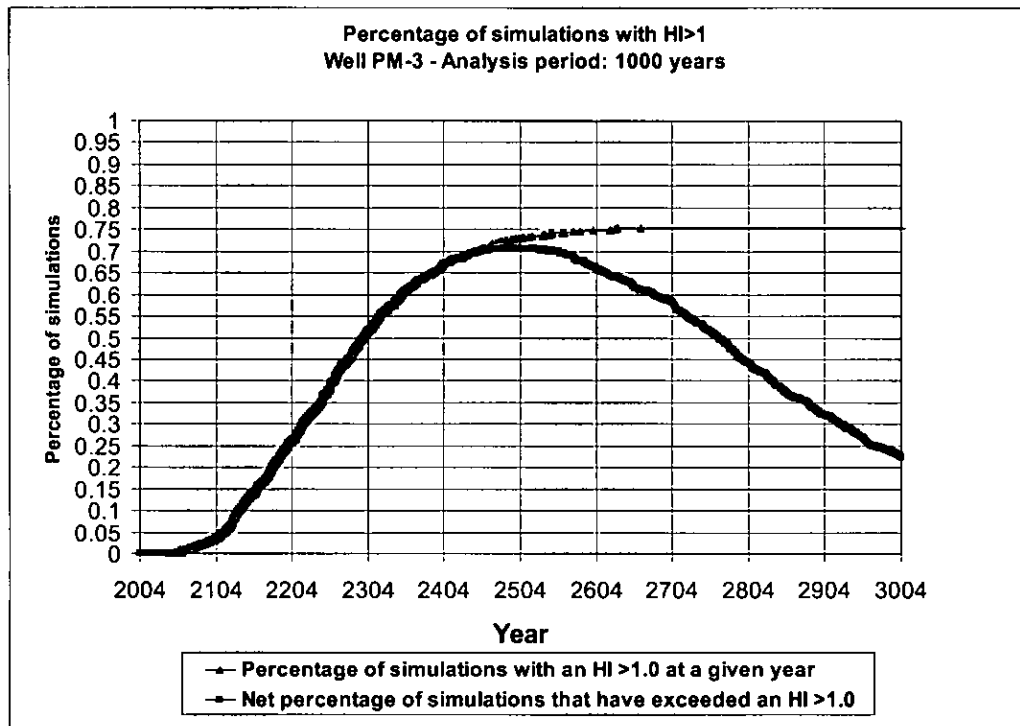


Figure 3.4-3. The CCDF of HI calculated for 1000 equally probable nitrate and perchlorate exposure-point concentrations in water-supply wells for the 1000-yr simulation period for (top) upper/middle-canyon-dominated uniform infiltration model and (bottom) lower-canyon-dominated uniform infiltration model. Both assume regional-aquifer Model A.

Figure 3.4-4 is a plot of perchlorate HI as a function of time for PM-3. Because the HI calculations assume a value of 1 ppb as the MCL in the risk equation shown in Figure 3.4-1, this plot can also be used to understand the perchlorate concentration history in water pumped from PM-3; the case shown features focused flow in the upper three sections of the canyon. The plot demonstrates that over a 100-yr period, the HI for PM-3 meets the stated goals of the risk assessment; that is, HI exceeds 1 in fewer than 5% of the simulations. Greater exceedances are predicted only over longer time frames.



**Figure 3.4-4.** Percentage of 1000 HI calculations that exceed an HI of 1 for perchlorate during any given year of the 1000-yr risk simulation. Lower-canyon-dominated infiltration with fast paths in the upper, middle, and lower canyons for perchlorate and nitrate with regional-aquifer Model A.

Figure 3.4-5 compares the CCDFs for tritium doses for the lower-canyon-dominated infiltration scenario without (top set of curves) and with (bottom set of curves) focused (fast-paths) infiltration in each section of the canyon. These curves cover only a 100-yr period because releases over a longer time period are no greater due to the rapid radioactive decay of tritium. The slightly higher doses calculated with the focused infiltration, bottom figure, reflect the fact that less radioactive decay (and subsequently greater releases of tritium from the unsaturated zone) occurs with shorter transport times. In the uniform infiltration case, top figure, maximum HI values are calculated for supply-well PM-3, but with focused infiltration, maximum HI values are calculated for supply-well PM-5. The reason for the difference is that tritium from the upper portions of the canyon moves faster toward, and decays less before reaching PM-5, which is relatively nearer the upper portion of Mortandad Canyon than the middle or lower portions.

The maximum tritium dose is about 0.04 mrem/yr, calculated for a simulation of 2 L/day ingestion of water exclusively from PM-5 for a 70-yr lifetime. This maximum dose is 100 times below the 4-mrem/yr limit set by the DOE and the EPA for radionuclides in drinking water. Consistent with EPA's methodology, the 4-mrem/yr limit is the dose equivalent of a chronic (i.e., 2 L/day for 70 yr) exposure to 20,000 pCi/L of tritium/L of water, which is the MCL for tritium.

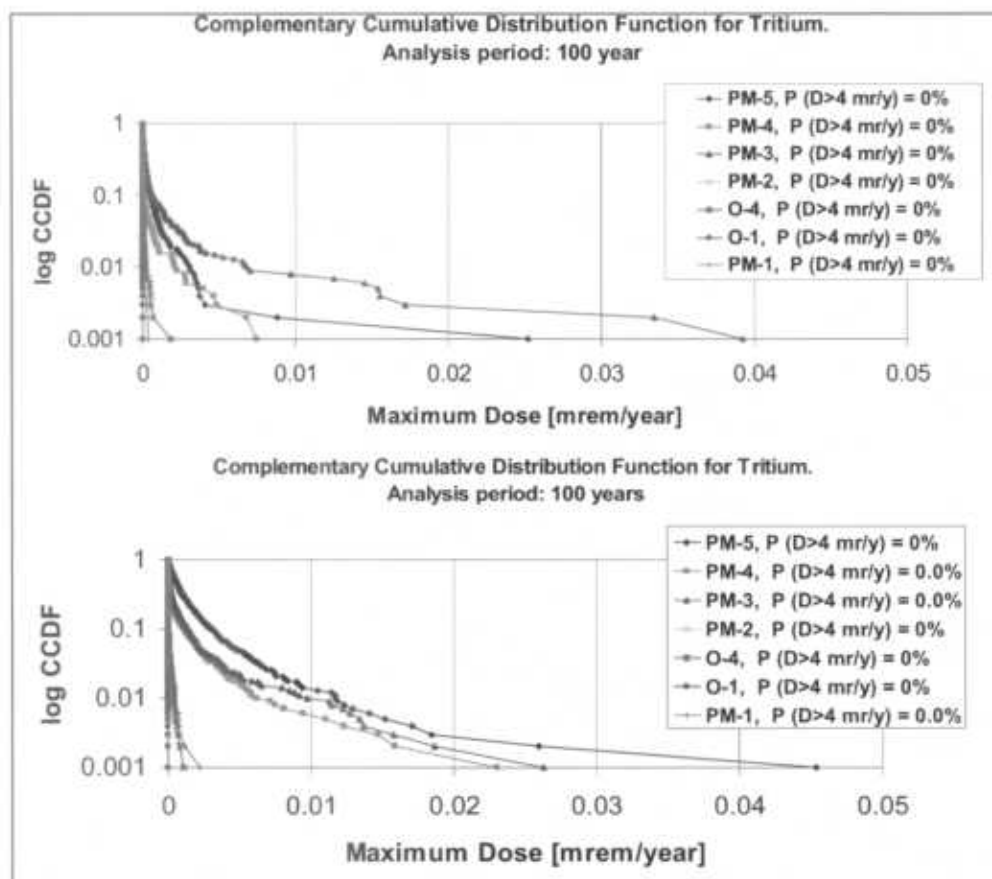


Figure 3.4-5. Complementary cumulative distribution functions of dose calculated for 1000 equally probable tritium exposure-point concentrations in supply wells for (top) lower-canyon-dominated uniform infiltration and (bottom) lower-canyon-dominated infiltration with fast paths in the upper, middle, and lower canyons. Both assume regional-aquifer model A.

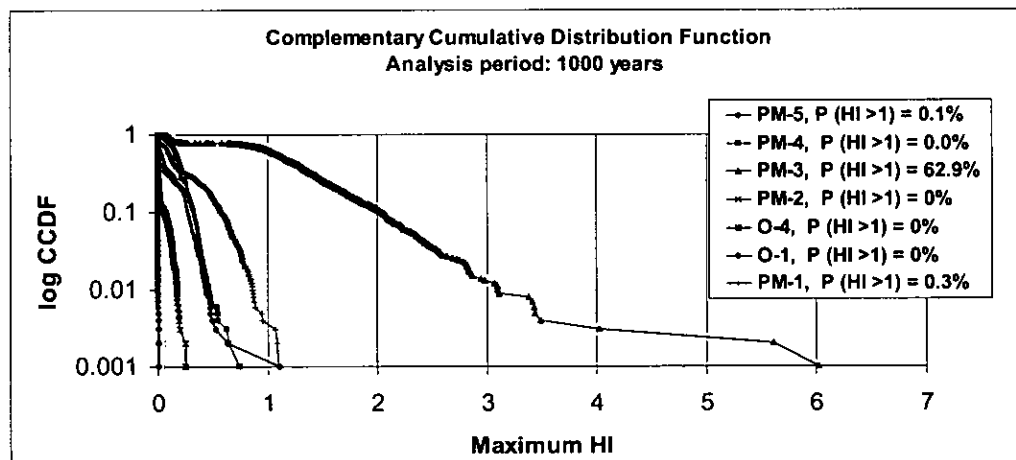
### 3.4.2 Risk-Assessment Results for a Continuous-Release Scenario, Assuming Regional-Aquifer Model B

The eighth entry in Table 3.4-1 gives risk-assessment results for the lower-canyon-dominated infiltration model with fast paths in the upper- and middle-canyon sections, and uniform infiltration in the lower-canyon section using regional-aquifer Model B. The simulation assumes that the source is continuous over the entire 1000-yr period. With this regional aquifer model, none of the seven supply wells has a probability greater than 5% of exceeding safe drinking water thresholds (i.e., HI or HQ above 1). In fact, the water-supply wells have a 0% probability of exceeding an HI of 1 when the regional aquifer is assumed to be a stratified system with little deep mixing of contaminants. Even lower drinking-water concentrations are obtained for the other conceptual models of infiltration with this regional aquifer model, and the HI analysis was not required for those conceptual models. Also, given that this regional aquifer model yields results with no risk to the drinking-water supply wells, a statistical analysis similar to those shown in Tables 3.4-2 and 3.4-3 is not included here. With regional-aquifer Model B, maximum perchlorate concentrations in the springs are predicted to reach values approaching 7 ppb after approximately 250 yr, as described in Section 3.3.4.3. However, HI was not evaluated for the springs because they are not considered to be a viable long-term drinking water source.

### 3.4.3 Risk-Assessment Results for a Discontinued Release Scenario

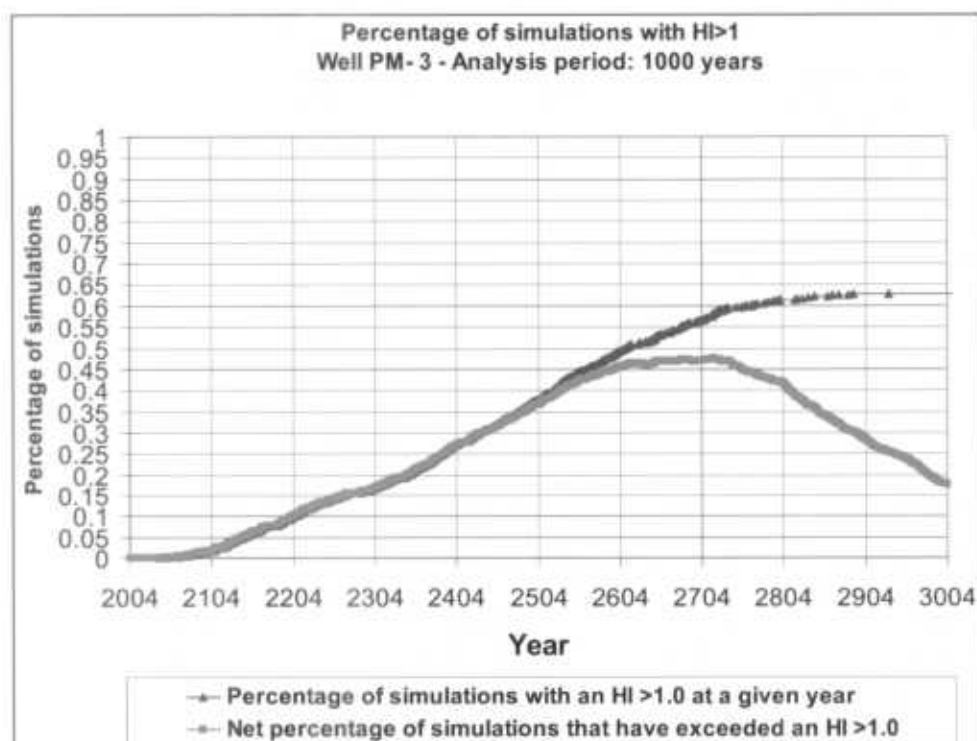
This section presents the results of the risk-assessment calculations conducted for the source-term model that assumes that discharges from the RLWTF will cease in 2006. The last entry in Table 3.4-1 gives the risk-assessment result for perchlorate for this case. The simulation assumes the lower-canyon-dominated, uniform infiltration model and regional-aquifer Model A. When compared to the results in Table 3.4-1 for the same simulation with a continuous perchlorate source, the cessation of effluent disposals decreases exposure at PM-3 slightly. For example, with discontinued discharge, the number of simulations that exceed an HQ of 1.0 decreases from 77.2% to 62.9%, but the maximum HQ for perchlorate decreases from 7.7 to 6.0. This change does not improve exposures to below the desired level of less than 5% of results having an HQ greater than 1.0. Exposures at PM-1, PM-4, and PM-5 do drop from a few percent (1% to 4%) to less than 1% with cessation of the source.

Figure 3.4-6 compares the CCDFs of the maximum HI values calculated for 1000 simulations of perchlorate concentrations in the various water-supply wells, assuming that the RLWTF releases cease in 2006 over the entire 1000-yr simulation. This can be compared to the bottom figure in Figure 3.4-3 to demonstrate the approximate difference resulting from source cessation.



**Figure 3.4-6. Complementary cumulative distribution functions of HI values calculated for 1000 equally probable perchlorate exposure-point concentrations in supply wells over 1000 yr, assuming that RLWTF discharges cease in 2006 (Lower-canyon-dominated uniform infiltration model with regional-aquifer model A)**

Figure 3.4-7 is a plot of the fraction of the 1000 simulations of perchlorate concentrations in water from supply-well PM-3 that resulted in an HI greater than 1 as a function of time. For example, in the first 100 yr of the simulation, approximately 2% of the 1000 simulations (i.e., 20 simulations) resulted in an HI greater than 1, but over the entire 1000-yr simulation period, about 63% of the 1000 simulations resulted in an HI greater than 1. Because the risk assessment assumes a 1 ppb MCL for perchlorate, this plot also shows the evolution of 1 ppb perchlorate concentrations at PM-3. Comparing this figure to Figure 3.4-4 shows the delay of perchlorate breakthrough at well PM-3 caused by cessation of the source. For example, 63% of the simulations reach an HI of 1 in approximately 800 yr with the discontinuous source; 77% of the simulations reach an HI of 1 in approximately 450 yr with the continuous source.



**Figure 3.4-7. Fraction of 1000 simulations with HI > 1 for perchlorate at supply-well PM-3, discontinued release source term, lower-canyon-dominated uniform infiltration model and regional-aquifer Model A**

#### 3.4.4 Risk-Assessment Results for Alternative Perchlorate Limits

Given the fact that the EPA has not promulgated a safe drinking water limit (i.e., an MCL) for perchlorate, and that values between 1 ppb and 24.5 ppb<sup>7</sup> are being considered, risk-assessment calculations were conducted to determine the probability of exceeding an HI of 1 for several assumed MCL values for perchlorate. The results are provided in Table 3.4-4. This analysis indicates that if the MCL for perchlorate were 5 ppb or greater, the potential of exceeding an HI of 1 in drinking water over a 1000-yr period would be less than 5% for all unsaturated-zone and saturated-zone conceptual models.

<sup>7</sup> The National Research Council of the National Academy of Sciences recently proposed a limit of 0.0007 mg/kg/day, which equates to 24.5 ppb for perchlorate in drinking water.

**Table 3.4-4**  
**Probability of Exceeding HI of 1 over 1000 Yr for Several Assumed MCL for Perchlorate**

Conceptual model	Wells	Assumed MCL for Perchlorate [ppb]							
		1	2	3	4	5	6	7	>7
Upper/middle-canyon-dominated uniform infiltration for perchlorate with regional-aquifer Model A	O-1	0.0%	0.0%	0.0%	0.0%	0.0%	0.0%	0.0%	0.0%
	O-4	0.0%	0.0%	0.0%	0.0%	0.0%	0.0%	0.0%	0.0%
	PM-1	2.7%	0.0%	0.0%	0.0%	0.0%	0.0%	0.0%	0.0%
	PM-2	0.0%	0.0%	0.0%	0.0%	0.0%	0.0%	0.0%	0.0%
	PM-3	74.1%	32.9%	9.7%	2.8%	0.5%	0.2%	0.0%	0.0%
	PM-4	0.3%	0.0%	0.0%	0.0%	0.0%	0.0%	0.0%	0.0%
	PM-5	16.7%	0.4%	0.0%	0.0%	0.0%	0.0%	0.0%	0.0%
Lower-canyon-dominated infiltration with fast paths in the upper and middle canyons for perchlorate with regional-aquifer Model A	O-1	0.0%	0.0%	0.0%	0.0%	0.0%	0.0%	0.0%	0.0%
	O-4	0.0%	0.0%	0.0%	0.0%	0.0%	0.0%	0.0%	0.0%
	PM-1	4.3%	0.0%	0.0%	0.0%	0.0%	0.0%	0.0%	0.0%
	PM-2	0.0%	0.0%	0.0%	0.0%	0.0%	0.0%	0.0%	0.0%
	PM-3	77.1%	42.2%	16.5%	5.2%	1.5%	0.4%	0.2%	0.0%
	PM-4	0.8%	0.0%	0.0%	0.0%	0.0%	0.0%	0.0%	0.0%
	PM-5	0.4%	0.0%	0.0%	0.0%	0.0%	0.0%	0.0%	0.0%
Lower-canyon-dominated uniform infiltration for perchlorate with regional-aquifer Model A	O-1	0.0%	0.0%	0.0%	0.0%	0.0%	0.0%	0.0%	0.0%
	O-4	0.0%	0.0%	0.0%	0.0%	0.0%	0.0%	0.0%	0.0%
	PM-1	4.1%	0.0%	0.0%	0.0%	0.0%	0.0%	0.0%	0.0%
	PM-2	0.0%	0.0%	0.0%	0.0%	0.0%	0.0%	0.0%	0.0%
	PM-3	77.2%	43.1%	17.2%	5.8%	1.7%	0.4%	0.3%	0.0%
	PM-4	1.2%	0.0%	0.0%	0.0%	0.0%	0.0%	0.0%	0.0%
	PM-5	3.9%	0.0%	0.0%	0.0%	0.0%	0.0%	0.0%	0.0%
Lower-canyon-dominated infiltration with fast path in the lower canyon for perchlorate with regional-aquifer Model A	O-1	0.0%	0.0%	0.0%	0.0%	0.0%	0.0%	0.0%	0.0%
	O-4	0.0%	0.0%	0.0%	0.0%	0.0%	0.0%	0.0%	0.0%
	PM-1	4.4%	0.0%	0.0%	0.0%	0.0%	0.0%	0.0%	0.0%
	PM-2	0.0%	0.0%	0.0%	0.0%	0.0%	0.0%	0.0%	0.0%
	PM-3	75.0%	37.1%	12.6%	3.6%	0.5%	0.4%	0.1%	0.0%
	PM-4	0.6%	0.0%	0.0%	0.0%	0.0%	0.0%	0.0%	0.0%
	PM-5	3.7%	0.0%	0.0%	0.0%	0.0%	0.0%	0.0%	0.0%
Lower-canyon-dominated infiltration with fast path in the middle canyon for perchlorate with regional-aquifer Model A	O-1	0.0%	0.0%	0.0%	0.0%	0.0%	0.0%	0.0%	0.0%
	O-4	0.0%	0.0%	0.0%	0.0%	0.0%	0.0%	0.0%	0.0%
	PM-1	4.4%	0.0%	0.0%	0.0%	0.0%	0.0%	0.0%	0.0%
	PM-2	0.0%	0.0%	0.0%	0.0%	0.0%	0.0%	0.0%	0.0%
	PM-3	77.3%	42.4%	16.9%	5.4%	1.6%	0.4%	0.2%	0.0%
	PM-4	0.8%	0.0%	0.0%	0.0%	0.0%	0.0%	0.0%	0.0%
	PM-5	3.0%	0.0%	0.0%	0.0%	0.0%	0.0%	0.0%	0.0%

Table 3.4-4 (continued)

Conceptual model	Wells	Assumed MCL for Perchlorate [ppb]							
		1	2	3	4	5	6	7	> 7
Lower-canyon-dominated infiltration with fast path in the upper canyon for perchlorate with regional-aquifer Model A	O-1	0.0%	0.0%	0.0%	0.0%	0.0%	0.0%	0.0%	0.0%
	O-4	0.0%	0.0%	0.0%	0.0%	0.0%	0.0%	0.0%	0.0%
	PM-1	4.1%	0.0%	0.0%	0.0%	0.0%	0.0%	0.0%	0.0%
	PM-2	0.0%	0.0%	0.0%	0.0%	0.0%	0.0%	0.0%	0.0%
	PM-3	77.2%	42.9%	17.1%	5.7%	1.8%	0.4%	0.3%	0.0%
	PM-4	1.2%	0.0%	0.0%	0.0%	0.0%	0.0%	0.0%	0.0%
	PM-5	1.5%	0.0%	0.0%	0.0%	0.0%	0.0%	0.0%	0.0%
Lower-canyon-dominated uniform infiltration for perchlorate with regional-aquifer Model A and source term interrupted in 2006	O-1	0.0%	0.0%	0.0%	0.0%	0.0%	0.0%	0.0%	0.0%
	O-4	0.0%	0.0%	0.0%	0.0%	0.0%	0.0%	0.0%	0.0%
	PM-1	0.3%	0.0%	0.0%	0.0%	0.0%	0.0%	0.0%	0.0%
	PM-2	0.0%	0.0%	0.0%	0.0%	0.0%	0.0%	0.0%	0.0%
	PM-3	62.9%	10.8%	1.2%	0.3%	0.2%	0.1%	0.0%	0.0%
	PM-4	0.0%	0.0%	0.0%	0.0%	0.0%	0.0%	0.0%	0.0%
	PM-5	0.1%	0.0%	0.0%	0.0%	0.0%	0.0%	0.0%	0.0%

#### 4.0 IDENTIFICATION AND EVALUATION OF POTENTIAL RISK-MANAGEMENT ACTIVITIES

This report describes a decision-analysis methodology involving the following steps:

1. the definition and quantification of goals;
2. the definition of the state of knowledge on the nature and extent of contamination and potential pathways leading to human exposure;
3. the calculation of a baseline risk posed by existing contamination; and
4. the identification and evaluation of potential risk-management activities.

Previous chapters presented the results of steps 1–3 for the Mortandad Canyon analysis. This chapter discusses the identification and evaluation of potential risk-management activities. Recall that this report is only a demonstration of this approach and is not the corrective-measures study.

Recall in Chapter 3 that the risks associated with the potential migration of perchlorate to supply wells were acceptable for a 100-yr time period. However, the perchlorate risks were unacceptable for the 1000-yr time period, assuming that the regional aquifer acts as a well-mixed aquifer with transport pathways controlled by supply-well pumping. For this situation, the probabilities that an HI value greater than 1.0 would be realized at PM-3 were around 75% for all infiltration conceptual models and for PM-5 about 15% for one conceptual model using an RfD of 0.00003 milligrams per kilogram per day (mg/kg/day) for perchlorate, which equates to a drinking water concentration of 1 ppb. Therefore, this section investigates potential risk-management activities that could reduce these probabilities to acceptable levels (less than 5%). An analysis of the correlation between the results of the different vadose-zone conceptual models demonstrated a very large correlation between the models (correlation coefficients greater than 90% for all models) and justified the use of almost any conceptual model of infiltration in the following analysis. In addition, the alternative conceptual model for the regional aquifer (Model B) is analyzed and discussed.

#### **4.1 Identifying Potential Risk-Management Activities**

In an optimal situation, the risk-based decision-analysis process would have been completely integrated into the Mortandad Canyon investigation and remedy selection process. However, the risk-based decision-analysis process was being developed as the Mortandad Canyon characterization activities were progressing in parallel. Therefore, although there are a large number of potential risk-management activities that could be employed at Mortandad Canyon, the analysis presented below focuses only on additional characterization with a minimal discussion on groundwater monitoring. As characterization work on Mortandad Canyon proceeds, the baseline risk assessment and, to some degree, the evaluation of risk-management alternatives presented in this document can be used and modified, if need be, to support additional potential risk-management activities. Such activities could include, but are not limited to, contaminant mass removal in the alluvial system, vadose zone, and regional aquifer, wellhead treatment, or monitored natural attenuation.

#### **4.2 Evaluation Process**

Evaluating potential risk-reduction activities involves the following five steps:

1. parameter screening to identify the few parameters that control simulated concentrations and therefore HI values;
2. uncertainty-reduction analysis to determine if the reduction in parameter uncertainty could result in acceptable risk;
3. determination of the likelihood of achieving the required uncertainty reduction (called the likelihood of success);
4. estimation of costs and completion times for the uncertainty-reduction activities; and
5. combining the likelihood of success with costs and completion times in a presentation to decision makers.

As mentioned previously, the Mortandad Canyon risk-based decision analysis occurred in parallel with Mortandad Canyon characterization efforts. Therefore, the decision analysis is not yet fully integrated into the Mortandad Canyon project. In the analysis presented in this document, only steps one and two were completed. These steps are described below.

##### **4.2.1 Parameter Screening**

It is neither practical nor beneficial to evaluate the worth of collecting data on every model parameter. Therefore, parameter screening is used to define a subset of parameters that have the largest impact on calculated HI values (recall that doses from tritium were well below health limits for all simulations). To minimize the chance of excluding an important parameter, two sensitivity analysis methods are used to identify the key parameters that control calculated risks. Those methods are correlation and linear-regression analysis. Correlation and regression analysis were performed using statistical software by StatSoft, Inc. (STATISTICA data-analysis software system, Version 6, [www.statsoft.com](http://www.statsoft.com), 2001). Each method and its associated results are described below.

##### **4.2.2 Correlation Analysis**

The correlation analysis calculates partial correlation coefficients between the distribution of input parameter values used in the groundwater transport simulations and the corresponding HI value calculated in the risk assessment. By definition, correlation coefficients range from -1 to +1 and are dimensionless. The greater the absolute value of the correlation coefficient, the greater the sensitivity of the model output to changes in the value of a specific input parameter. The results of the correlation analysis are summarized in Table 4.2-1, which shades parameters that have an absolute correlation coefficient greater than 0.2 for one or both wells, PM-3 or PM-5.

**Table 4.2-1**  
**Correlation Coefficients Calculated for Input Parameters**  
**and Model-Calculated HI Values for Regional-Aquifer Model A**

Source Term and Infiltration	PM-3	PM-5
Source interpolation factor	0.500	0.001
TA-50 flow to surface-water conversion factor	0.650	0.299
Infiltration rate for the upper canyon	-0.23	0.49
<b>Unsaturated Groundwater Transport</b>		
Longitudinal dispersivity in unsaturated bedrock	-0.08	0.03
Hydraulic conductivity of Guaje Pumice Bed	0.02	0.01
van Genuchten $\alpha$ for Guaje Pumice	0.07	0.02
Porosity of Guaje Pumice	0.01	-0.07
Hydraulic conductivity of Bandelier Tuff Unit 1 g	0.01	-0.03
Porosity of Bandelier Tuff Unit 1 g	0.04	-0.01
van Genuchten $\alpha$ Bandelier Tuff Unit 1 g	0.04	-0.02
Hydraulic Conductivity of Bandelier Tuff Otowi Member	0.04	-0.03
Porosity of Bandelier Tuff Otowi Member	0.02	-0.07
van Genuchten $\alpha$ for Bandelier Tuff Otowi Member	-0.01	0.01
Hydraulic Conductivity of Cerro Toledo	-0.02	0.01
Porosity of Cerro Toledo	-0.04	0.01
van Genuchten $\alpha$ for Cerro Toledo	0.02	-0.00
Hydraulic Conductivity of Tsankawi Pumice	-0.06	-0.00
Porosity of Tsankawi Pumice	0.04	0.00
van Genuchten $\alpha$ for Tsankawi Pumice	-0.01	-0.02
Hydraulic Conductivity of Cerros del Rio Basalt Unit 4	0.01	-0.03
Porosity of Cerros del Rio Basalt Unit 4 (shared with saturated zone)	0.02	-0.02
Hydraulic Conductivity of Puye fanglomerate	0.05	-0.02
van Genuchten $\alpha$ for Puye fanglomerate	0.02	0.01
van Genuchten $n$ for the Puye fanglomerate	-0.01	0.04
Porosity of Puye fanglomerate (shared with saturated zone)	-0.22	-0.06
<b>Saturated Groundwater Transport</b>		
Longitudinal dispersivity of regional aquifer	-0.02	0.13
Supply well production period (1993–2001)	0.50	-0.21
Porosity of the Totavi Lentil	-0.03	0.02
Porosity of the Pumiceous Puye	-0.01	-0.11
Porosity of the Sandy Santa Fe	-0.09	-0.13
Porosity of Tb <sub>2</sub>	-0.03	0.05
Porosity of Tb <sub>2</sub> or Ts	0.03	-0.04
Porosity of the Santa Fe fanglomerate	-0.21	-0.37
Porosity of Puye fanglomerate (shared with unsaturated zone)	-0.22	-0.06
Porosity of the Deepest Basalt Unit	-0.01	0.03
Porosity of the Tschicoma Flows	0.00	-0.01
Porosity of Tb <sub>4</sub> or Tpf	-0.00	0.00
Porosity of Cerros del Rio Basalt Unit 4 (shared with unsaturated zone)	0.02	-0.02

Of the 36 input variables in the groundwater-transport simulations, the following six were found to have the largest correlations with calculated HI values for PM-3:

- TA-50 flow to surface-water conversion factor
- Source interpolation factor
- Supply-well production period during 1993–2001
- Infiltration rate for the upper canyon
- Porosity of the Puye fanglomerate
- Porosity of the Santa Fe fanglomerate

For PM-5, the following four parameters have the largest correlation coefficients:

- Infiltration rate for the upper canyon
- Porosity of the Santa Fe fanglomerate
- TA-50 flow to surface water conversion factor
- Supply-well production period during 1993–2001

#### 4.2.3 Linear Regression Analysis

Another method of identifying sensitive or controlling model parameters is to construct a linear regression between model input parameters and model output, in this case HI values. The output of the regression analysis is a linear equation of the following general form:

$$HI = \text{intercept} + [a1 \times (\text{parameter } 1) + a2 \times (\text{parameter } 2) \dots + aN \times (\text{parameter } N)],$$

In this case, "parameter" is a normalized version of the original sampled parameter,

$$Psc = \frac{P - Pmean}{StdP},$$

where

- Psc* is the normalized value of parameter *P*,
- Pmean* is the mean value of parameter *P*, and
- StdP* is the standard deviation of parameter *P*.

The reason for the normalization is to minimize the effects of the relative magnitude, units of measurement, and range of a given parameter versus another parameter. For example, the porosity of the Bandelier Tuff is dimensionless and ranges from zero to one, but the vadose zone dispersivity has units of 1/m and ranges from 0.5 to 5.0. Therefore, a 10% change in the dispersivity would result in a larger impact on model results than a 10% change in the porosity. In addition, if the units of dispersivity were changed to feet instead of meters, the range of its values would increase, and the absolute model sensitivity would also change.

The resulting regression line provides a basis for predicting HI values and, in some sense, can be seen as a replacement model for the complex set of source term, vadose zone, regional aquifer, and human-behavior models. The coefficients of the regression equation provide a measure of importance of each parameter. Because the goal of the parameter-identification phase of decision analysis is to define a subset of parameters for further investigation, stepwise regression was used to identify the subset of parameters that explains the majority of the variation seen in HI values.

The basic stepwise regression-analysis procedure involves three steps, (1) identifying an initial model; (2) iterating the model of the previous step by adding or removing variables in accordance; and

(3) terminating the iteration when further iteration no longer improves the model. The stepwise linear regression analysis was conducted for PM-3 and PM-5.

Plotted in Figure 4.2-1 is the best-fit regression line for PM-3. In addition, individual plotted points representing, on the x-axis the HI values associated with output from the Tier-3 Monte Carlo analysis (called the observed values), and on the y-axis, points corresponding to the HI values predicted by using the same parameter values in the regression model.

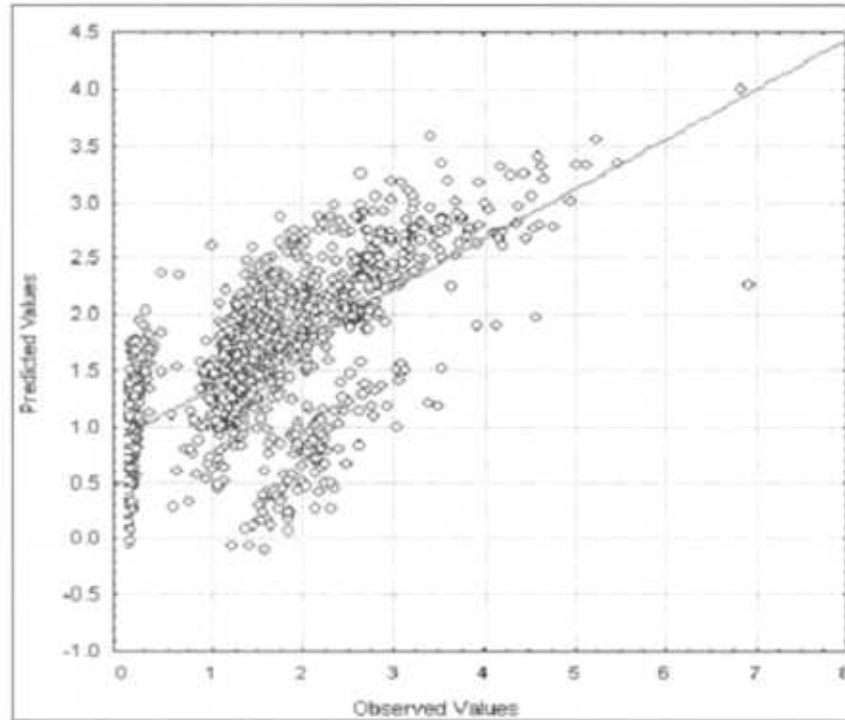


**Figure 4.2-1. Linear-regression analysis results for PM-3 for perchlorate using the upper/middle-canyon-dominated uniform infiltration model and regional-aquifer Model A**

The equation of the line shown in Figure 4.2-1 is

$$\begin{aligned}
 \text{HI} = & 1.6151 \\
 & + 0.55519 \times (\text{Production period during 1993-2001}) \\
 & - 0.2451 \times (\text{Puye fanglomerate porosity}) \\
 & - 0.2413 \times (\text{Santa Fe fanglomerate porosity}) \\
 & - 0.2289 \times (\text{Infiltration rate for the upper canyon}) \\
 & - 0.1799 \times (\text{TA-50 flow to surface-water conversion factor}) \\
 & + 0.12071 \times (\text{Source interpolation factor}) \\
 & - 0.0618 \times (\text{Tsankawi Pumice hydraulic conductivity}) \\
 & - 0.0606 \times (\text{Regional aquifer longitudinal dispersivity}) \\
 & - 0.0532 \times (\text{Vadose zone longitudinal dispersivity})
 \end{aligned}$$

The linear-regression analysis for PM-3 indicates that these nine input variables account for 43.7% of the variability in the HI distribution, but the complete set of all input distributions account for 43.8% of the variability of the HI values. The absolute value of the regression coefficient for each value correlates with the relative importance of the variable, and the sign of the regression coefficient indicates the direction of effect of a given parameter on predicted HI values. This negative regression coefficient indicates that as a parameter value increases, the HI values decrease and vice versa.

As with any linear regression, some indication of how well the predicted values fit the observed, or in this case, model-calculated values, must be provided. Following is a probability plot of the residuals, that is, the difference between model-predicted and regression-predicted HI values (Figure 4.2-2). If the regression provided a perfect fit to the model-predicted values, all residual values would be zero. However, that is not ever the case. Instead, there is a distribution of residuals, and the questions become (1) what is the magnitude of residuals, and (2) how are the residuals distributed? From Figure 4.2-2, one can see that the residuals are distributed over a range of -2 to less than 5. With respect to the distribution of residuals, about 90% are less than an absolute value of 1.0. In addition, there is very little systematic overprediction or underprediction of HI values. On Figure 4.2-2, zero systematic error is shown by the line drawn through the data points. Although there is some deviation of the residuals from the line, deviations occur in less than 1% of the positive residuals and about 5% of the negative residuals. In other words, the linear regression provides a very good fit to the data.

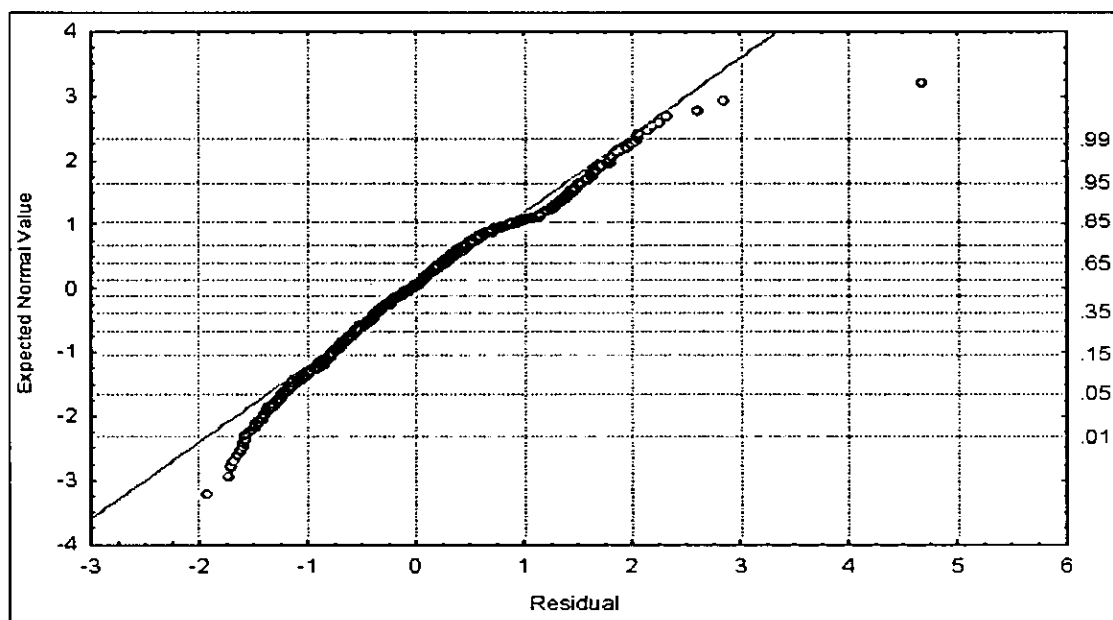


**Figure 4.2-2. Probability plot of residuals for the linear regression of PM-3 data for perchlorate, using the upper/middle-canyon-dominated uniform infiltration model and regional-aquifer Model A.**

The results of the linear regression for PM-5 are shown in Figure 4.2-3.

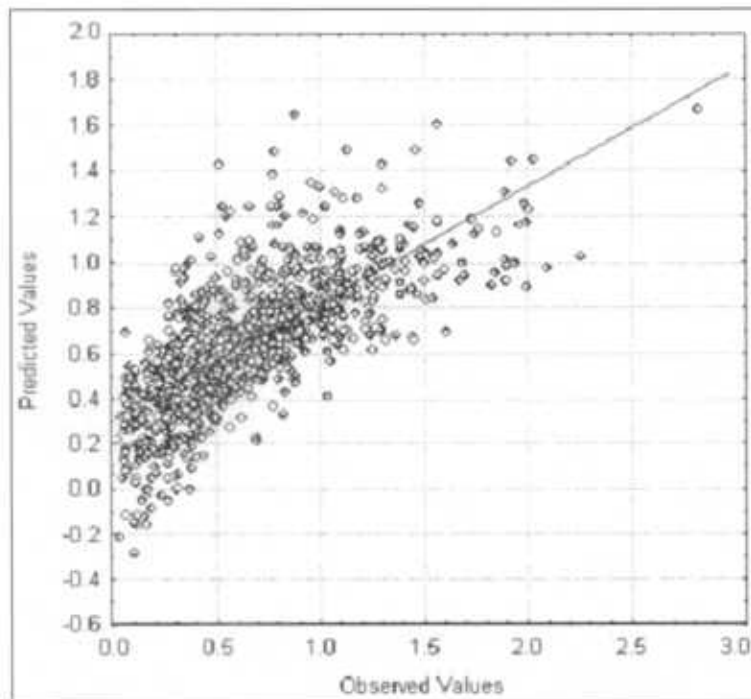


**Figure 4.2-3. Linear regression analysis results for PM-5 for perchlorate, using the upper/middle-canyon-dominated uniform infiltration model and regional-aquifer Model A.**

Regression analysis for PM-5 reveals that 10 input variables are sufficient to provide a reliable prediction of HI, according to the following regression model:

$$\begin{aligned}
 \text{HI} = & 0.64218350 + 0.20766837 \times (\text{Infiltration rate for the upper canyon}) \\
 & - 0.1558593 \times (\text{Porosity of the Santa Fe fanglomerate}) \\
 & - 0.0810868 \times (\text{Porosity of the Sandy Santa Fe}) \\
 & - 0.0795939 \times (\text{Production period during 1993–2001}) \\
 & + 0.06384799 \times (\text{Factor TA-50 flow to surface-water conversion factor}) \\
 & + 0.05425311 \times (\text{Regional Aquifer longitudinal dispersivity}) \\
 & - 0.0454184 \times (\text{Porosity of the Pumiceous Puye}) \\
 & + 0.02261700 \times (\text{Source interpolation factor}) \\
 & - 0.0182292 \times (\text{Bandelier Tuff Otowi Member porosity}) \\
 & - 0.0180355 \times (\text{Puye fanglomerate porosity})
 \end{aligned}$$

The most significant (sensitive) variables are very similar for PM-5 and PM-3. Furthermore, the six sensitive variables identified in the correlation analysis are among the sensitive variables identified in the regression analysis. In a general sense, it appears that the HI values are controlled by dilution and by groundwater and transport velocities. That is, the infiltration rate and the TA-50 flow-to-surface water conversion factor have a direct effect on groundwater velocities. Groundwater velocities and porosities, in

turn, affect contaminant transport velocities. Finally, pumping rates as affected by the production period, the TA-50 flow to surface water conversion factor, and the dispersivity, all affect the dilution of contaminants.

#### **4.2.4 Uncertainty-Reduction Analysis**

The purpose of the uncertainty-reduction analysis is to determine if reducing the uncertainty in one or more of the significant input variables identified in the sensitivity analysis could reduce the risk to acceptable levels. In the case of the Mortandad Canyon analysis, acceptable levels were defined as less than a 5% chance that HI values would exceed a value of 1.0. The uncertainty-reduction analysis itself does not prescribe specific actions, nor does it assert that any action could be effective. Rather, it determines if, and if so, how much, uncertainty reduction would be necessary and sufficient to change the HI distribution (i.e., to reduce the risk).

The general process of uncertainty-reduction analysis is to mine the existing information provided by the Tier-3 Monte Carlo analysis. Specifically, the Monte Carlo analysis provides us with 1000 parameter sets corresponding to 1000 HI values for each of the conceptual models and all wells. Uncertainty-reduction analysis searches these data, one model-input parameter at a time, for new ranges of parameter distributions that would limit the number of HI values that exceed a value of 1.0 to 5% of the total or less. By truncating the parameter values outside this range and their corresponding HI values, a new hypothetical distribution of model input and output is found that meets the exceedance probability. This information is not used in any real risk assessment of the site but is passed on to the next step in the decision-analysis process—estimating the likelihood that such a reduction in parameter uncertainty could occur through future site characterization and/or research.

The specific vadose-zone conceptual model chosen is upper/middle-canyon-dominated uniform infiltration. The regional aquifer is represented with Model A, for which most contaminants are drawn toward the pumping wells. This conceptual model produced a probability of 74.4% of exceeding an HI of 1.0 in PM-3 (which is similar to all other conceptual models) and a 17.3% probability of exceeding an HI of 1.0 in PM-5 (which is the largest exceedance for PM-5 for all the conceptual models).

Reduction in uncertainty in parameters that affect HI values at PM-3 was performed for all of the parameters identified in the previous section except the pumping period. The reason for excluding the pumping period is that this parameter represents variability in past pumping schemes, not uncertainty. In a general sense, variability cannot be reduced. However, a later section will discuss the potential for managing pumping rates or of using characterization to discriminate between conceptual models as a means of achieving a 95% confidence that HI values will be less than 1.0. With regard to the remaining parameters, no amount of uncertainty reduction in any parameter yielded an exceedance probability of less than or equal to 5%. Therefore, no amount of parameter uncertainty reduction through further site characterization or research would cause the PM-3 results to meet project goals for the protection of human health, provided that the conceptual Model A for the regional aquifer holds.

Next, an uncertainty analysis was conducted to determine what level of uncertainty reduction in the 10 sensitive variables identified in the linear regression analysis for PM-5 would be necessary and sufficient to reduce the exceedance probability to less than 5%. Again, PM-5 only exceeds the performance standards when the upper/middle-canyon-dominated uniform infiltration model is combined with regional-aquifer Model A. Shown in Table 4.2-1 are the results of the uncertainty-reduction analysis for PM-5 for this case. These results indicate that reducing uncertainty in 2 of the 10 sensitive input variables could be effective in reducing the probability of exceeding an HI of 1.0 to less than 5%.

**Table 4.2-1**  
**Results of Uncertainty-Reduction Analysis for PM-5**

PM-5 % Exceedance	Condition 1	Condition 2
4.80%	Infiltration rate for the upper alluvium $\leq 1.2$ m/yr	Porosity —Santa Fe fanglomerate $\geq 0.02$
4.04%	Infiltration rate for the upper alluvium $\leq 1.0$ m/yr	—*
4.80%	Porosity of the Santa Fe fanglomerate $\geq 0.1$	—*

\* = There is no second condition.

Table 4.2-1 shows that if future characterization and/or research could prove one of the following: that the maximum infiltration rate in the upper and middle canyon sections (as described by the variable  $I_{upper}$  in the upper/middle-canyon-dominated infiltration model, Section 3.3.2.1) could be shown to be less than or equal to 1.0 m/yr, or that the porosity of the Santa Fe fanglomerate could be demonstrated to be greater than 0.1, then calculated HI values would be lower than 1.0 at the 95% confidence limit. In addition, if joint characterization and/or research on porosity and infiltration could prove that the maximum infiltration rate in the upper and middle canyon sections is less than or equal to 1.2 m/yr and the porosity of the Santa Fe fanglomerate is greater than or equal to 0.02, PM-5 results would comply with the project safety goals.

#### 4.3 Additional Risk-Reduction Possibilities

The previous section identified potential reductions in parameter uncertainty that could lead to compliance with the project goals for discharges to well PM-5. Beyond parameter uncertainty reduction, a few additional risk-reduction activities were identified and are discussed in this section.

##### 4.3.1 Conceptual Model Uncertainty

Recall that for PM-5 only one conceptual model had a probability of less than 95% of an HI value being greater than 1.0. That conceptual model assumed higher infiltration rates in the upper and middle sections of Mortandad Canyon, above the confluence with Ten Site Canyon, than below that confluence. In addition, deep transport within the regional aquifer (Model A) was required. If future site characterization shows that the upper/middle-canyon-dominated infiltration model is untenable, then PM-5 would comply with the stated goals, regardless of the regional-aquifer conceptual model.

It is also very important to point out that the use of the phreatic regional-aquifer model (Model B) resulted in acceptable risk for all wells, including PM-3. Therefore, site-characterization activities should be identified that are capable of distinguishing between the behaviors upon which the two aquifer conceptual models are based.

##### 4.3.2 Discontinuing Discharges into Mortandad Canyon

The original simulations assume that the discharge rate from the RLWTF is continuous from 2002 through 3003 at the 2002 rate of  $1.1 \times 10^7$  L/yr. The perchlorate concentration during that same time was held constant for a given simulation within a range between 51 and 55 ppb. This concentration was based on the nitrate/perchlorate source correlation. However, the current treatment at the RLWTF removes perchlorate to a value below the detection limit of 4 ppb. In addition, Laboratory management could decide to shut off all discharge from the RLWTF. Therefore, simulations were performed to estimate the possible effects of discontinuing discharges from the RLWTF on perchlorate transport through the vadose zone, the regional aquifer, and health indicators at the production wells. This scenario differs from the original sets as described in Section 3.3.1.2. Results of this scenario indicate a probability of exceedance for PM-3 of 62.9% and 0.1% for PM-5, based on the lower-canyon-dominated uniform infiltration model

and Model A for the regional aquifer. In essence, turning off the source does not affect the overall conclusions that releases to PM-3 will still be unacceptable if regional aquifer Model A applies, because the majority of the contaminant mass was released before the assumed management action. This mass predominantly resides in the unsaturated zone and will eventually reach the regional aquifer.

### 4.3.3 Management of Pumping Rates

The importance of the diluting effects of production-well pumping rates on HI values was recognized in the parameter screening (sensitivity analysis) step. At that time, the thought was that pumping, which is required for local water consumption, was not a factor that should be considered as a risk-reduction option. However, upon further reflection, the possibility of controlling the flow from individual wells while maintaining the same overall discharge was analyzed as a potential means of keeping HI values below 1.0.

The variable used in the Tier-3 Mortandad Canyon analysis represented pumping schemes over the past years but did not represent all possible rates or combinations of pumping rates from the different wells. Recognizing that pumping is a variable that can be controlled, that it can have a significant impact on HI values, and that the total volume of water pumped is the main constraint, another sensitivity analysis and uncertainty analysis were performed. These analyses used the pumping rate from each well as the independent variable instead of the pumping scheme associated with a specific year (as done in the original analysis). The dependent parameter in these analyses was the mean HI for PM-3 and PM-5, averaged over seven conceptual models. Next, the sum of HI values (mean HI for PM-5 + mean HI for PM-3) for each simulation was calculated. The final dependent variable was then the logarithm of the sum of HI values.

Shown in Table 4.3-1 are the resulting partial correlation coefficients of the pumping rates at each well and the dependent variable (sum of HI values). Note the strong correlation between the sum of the HI values and the pumping from wells PM-4 and O-4. This is in apparent contradiction to the fact that the HI values at PM-4 and O-4 are consistently very low. The effect of pumping at PM-4 and O-4 appears to be their influence on the direction and rate of flow between the location where contaminants arrive at the water table to the location of wells PM-3 and PM-5 (which have the largest HI values). In contrast, PM-3 and PM-5, the wells with the largest HI values, have the smallest correlation coefficients.

**Table 4.3-1  
Partial Coefficient of Correlation**

Predictor Variables	ln(SumHI)
Q PM-3	0.13
Q PM-5	-0.19
Q PM-4	-0.73
Q PM-1	0.38
Q PM-2	0.21
Q O-1	0.32
Q O-4	0.54

Next, a regression equation was developed, relating the rate of flow from each well to the dependent variable (the logarithm of the sum of average HI values for PM-3 and PM-5). The resulting regression equation is

$$\ln(\text{SumHI}) = 1.902 + .00185*Q\_PM3 + .0013*Q\_PM5 - .029*Q\_PM4 + .0471*Q\_PM1 - .0327*Q\_PM2 - .0024*Q\_O1 + .0166*Q\_O4.$$

The correlation coefficient ( $r$ ) for this equation is 0.86, and the adjusted  $R^2$  is 0.74, which implies that 74% of the variability of the summed and averaged HI values can be explained solely by the pumping rates of the production wells. A comparison of the model-calculated dependent variable (from the Monte Carlo analysis) and the dependent variable produced by the regression equation is shown in Figure 4.3-1.

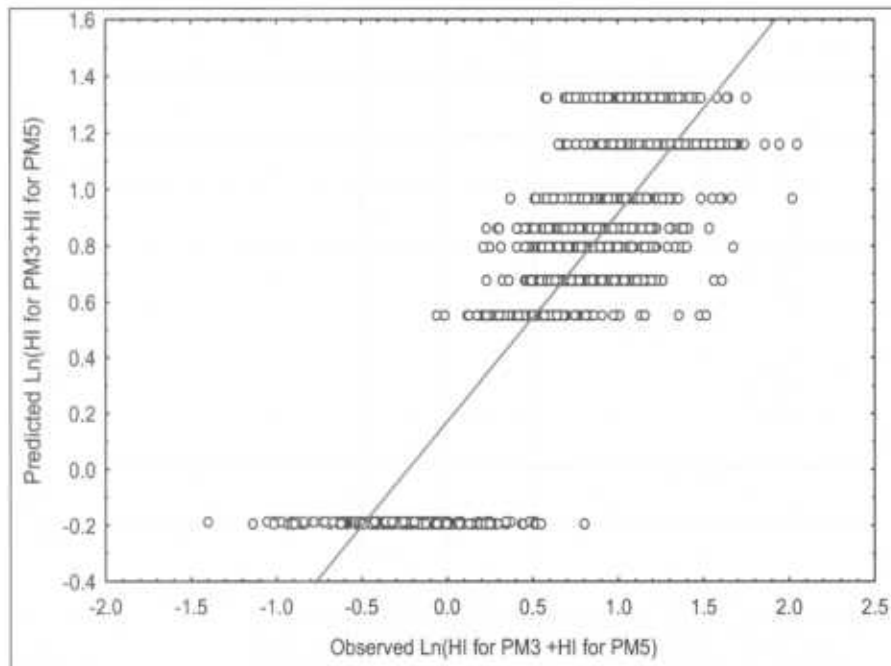


**Figure 4.3-1. Observed and predicted values of the logarithm of the summed averages of HI values for PM-3 and PM-5 for the upper/middle-canyon-dominated uniform infiltration for perchlorate with regional-aquifer Model A**

Given the regression equation relating pumping rates to HI values, the next step was to determine which combination of pumping rates could result in HI values staying below 1.0. To accomplish this, the dependent variable ( $\ln[\text{SumHI}]$ ) is set to less than zero in the regression equation. Next, the regression equation is rescaled to force the total pumping rate to equal 135 kg/s (the average value for the period of 1992–2001) by multiplying all terms by  $135/1.902$ . In doing so, we obtain the following equation for managing the pumping rate:

$$-135 \text{ kg/s} > 0.131 * Q_{\text{PM3}} + 0.092 * Q_{\text{PM5}} - 2.058 * Q_{\text{PM4}} + 3.344 * Q_{\text{PM1}} \\ - 2.321 * Q_{\text{PM2}} - .170 * Q_{\text{O1}} + 1.179 * Q_{\text{O4}}$$

By meeting the constraints of this equation, pumping rates can be adjusted in a manner that ensures that HI values remain below 1.0 while still supplying the total amount of water required for the current supply system. This shows that higher relative pumping rates at PM-2 and PM-4 (which draw the plume in a southerly direction) help minimize HI exceedance; and it also shows that higher relative pumping rates at PM-1 and O-4 (which draw the plume east or northeast) yield higher HI exceedance. As examples, analyses of HI at PM-3 and PM-5 as a function of the production year showed that 1994 and 1995 production rates did not yield HI values greater than 1.0 for more than 5% of the realizations; all other years exceeded the desired HI requirements for PM-3, assuming regional-aquifer Model A. The management equation (given above) is satisfied if the 1994 or 1995 pumping rates (Table 3.3-5) are inserted into the right side of the equation, yielding values of -148 kg/s and -149 kg/s, respectively. In

contrast, the 2000 pump rates (Table 3.3-5) yield a value of -78.6 kg/s for the right side of the equation, which does not satisfy the equation and agrees with the risk-assessment results.

#### **4.4 Summary**

The calculated risk is unacceptable for PM-3 for all but one conceptual model and for PM-5 for one conceptual model based on an RfD of 0.00003 mg/kg/day for perchlorate (equivalent to 1 ppb). This section identified potential reductions in parameter uncertainty and conceptual models that would result in acceptable risks for PM-5. No amount of reduction in parameter uncertainty produced acceptable risks for PM-3.

Two potential risk-management activities could result in acceptable risk at PM-3. The first is to disprove regional-aquifer Model A, which maximizes deeper transport toward the wells, as a viable alternative. Disproving the Model A assumptions for the regional aquifer would leave Model B, which maximizes lateral transport along the phreatic zone and yields acceptable risk for PM-3 and for all of the other water-supply wells. As noted above, these two alternative conceptual models represent near-end members with regards to aquifer behavior, and it would be difficult to "disprove" Model A. The best alternative is to examine available and future sampling and monitoring data from the Mortandad Canyon area to see if contaminants travel laterally near the water table or downward to the well screens. Additionally, acceptable risk at PM-3 could be achieved through optimal management of pumping rates of the production wells.

### **5.0 CONCLUSIONS AND RECOMMENDATIONS**

A risk-based decision-support process has been developed and implemented to assist the Laboratory environmental restoration project in determining what actions are most effective in reducing the potential drinking-water impacts from groundwater contaminants in Mortandad Canyon. Similar implementation of the decision-support process is planned for Los Alamos/Pueblo Canyon, Cañon de Valle, and many of the larger material disposal areas. The risk-based decision-support process implements recommendations from the EPA, the DOE, and the National Academy of Sciences to address environmental contamination problems in the face of inevitable uncertainty. After summarizing the results of the baseline human-health-risk assessment and the associated identification and analyses of potential risk-reduction activities, this chapter discusses several recommended applications of the decision analysis.

#### **5.1 Summary of Results**

The risk-based decision analysis described in this report integrates data, models, and technical expertise within a rational, structured process to support decisions related to characterization, remediation, and monitoring of groundwater contamination that has resulted from discharges into Mortandad Canyon from the RLWTF. Goals set for human health risk include a 95% confidence that HI values are less than 1.0 for perchlorate and nitrate, and the total effective dose equivalent of less than 4.0 mrem/yr for tritium. Of all of the chemicals present in the RLWTF discharge wastewater, these three present the greatest potential hazard to drinking water because of their high solubility, high mobility, and toxicity.

The risk-assessment calculations used EPA's RfDs for nitrate and perchlorate and dose conversion factors defined by DOE and EPA for tritium. At the beginning of the Mortandad Canyon analysis, the EPA had a provisional RfD for perchlorate of 0.00003 mg/kg/day, which is equivalent to a groundwater concentration of 1 ppb. Late in the analysis, EPA changed the RfD for perchlorate to 0.0007 mg/kg/day, which is equivalent to a groundwater concentration of 24.5 ppb. However, the Mortandad Canyon analyses proceeded with the much lower RfD, which, at a minimum, provided an opportunity to demonstrate the process and some potential applications.

Several other assumptions of and/or input to the analyses are conservative despite efforts to define realistic conceptual models and parameter distributions. An updated analysis to further limit these conservatisms would yield even lower HI values than presented in this analysis. First, a smaller source term may be warranted. A broader distribution of the perchlorate and nitrate inventory that shifts the mean and lower bounds to smaller values may be warranted, as described in Sections 3.3.1.1 and 3.3.3.2. Lower maximum infiltration rates may be warranted as well because predictions made with the highest infiltration rates overpredict unsaturated-zone moisture contents and the depths of contaminant profiles (Section 3.3.3.2). With regards to regional-aquifer concentrations, the assumption of constant future pumping rates (over 1000 yr) maximizes transport in a given direction, as controlled by the relative pumping rates of the wells. The wells are not continuously pumped at constant rates, and pumping variability would disperse contaminants. In addition, the current water-supply wells have an expected lifetime of decades rather than centuries, as used in the simulations, and predicted contaminant concentrations at the supply wells over decades do not yield HI values greater than 1.0. With regards to water-supply concentrations, Los Alamos County blends its waters; blending of waters from PM-3 or PM-5 could readily be used to decrease perchlorate concentrations to values less than 1.0 ppb. The updating of these assumptions and input parameters to be more realistic is not recommended at this time. The possible conservative input parameters are noted here for completeness. The discussion of water-supply operations is included because extrapolation of predicted results must be grounded by known operating conditions. The impacts of these conservatisms may be evaluated in the future, if warranted, to help analyze future remedial actions for Mortandad Canyon.

#### 5.1.1 Baseline Risk-Assessment Results

First, a Tier-1 point-estimate calculation of HI was performed that demonstrated that a more realistic analysis was warranted. The Tier-1 analysis yielded a maximum HI of 12, based on an assumed RFD for perchlorate of 1 ppb. Therefore, a Tier-3 or fully probabilistic analysis was performed. The probabilistic analysis demonstrated that nitrate, perchlorate, and tritium do not pose an unacceptable risk to any of the current drinking-water supply wells over the next century. Furthermore, neither nitrate nor tritium concentrations are likely to exceed threshold values over the next millennium. Using the assumed RFD values along with assumptions of continuing discharges from the RLWTF and continued pumping of existing supply wells, perchlorate poses an unacceptable risk within 100 to 1000 yr, with maximum HI values of less than 8.0. For well PM-3, the probability of HI values exceeding 1.0 was well above the 5% confidence limit for all but one conceptual model. Only one conceptual model indicated a possible exceedance probability of greater than 5% for well PM-5. For all other PM- and O-series wells, the probability of HI exceeding 1.0 over 1000 yr was less than 5%.

An interesting result of these analyses was that the Tier-1, supposedly conservative analysis, was not conservative at each pumping well. In the Tier-1 analysis, contaminants arrived at wells PM-4 and PM-5 at concentrations that were higher, and over time scales that were shorter, than in the Tier-3 analysis. The Tier-1 analysis was therefore conservative with respect to wells PM-4 and PM-5. However, in the Tier-1 analysis, contaminant transport to other regional wells did not occur. Particularly in the case of PM-3, the estimated HI values were significantly larger in the Tier-3 probabilistic assessment than they were for the Tier-1 conservative analysis. In fact, PM-3 had no risk in the Tier-1 analysis, but it had the greatest risk of any well in the Tier-3 analysis. This result shows that choosing a conservative scenario is complicated, and not always obvious, in a system that has coupled and competing processes that control contaminant migration. Another interesting result was that including fast flow paths as an unsaturated-zone transport mechanism did not increase the calculated risk at the water-supply wells.

### **5.1.2 Potential Risk-Reduction Activities Analyzed**

The formulation of risk in this risk-based decision analysis incorporates uncertainty in all aspects of groundwater flow and transport. Therefore, risk may be reduced by site characterization and/or research that reduces parameter and/or conceptual model uncertainty.

Only two risk-reduction activities have the potential to decrease the risk at PM-3 to within acceptable limits, assuming the 1 ppb perchlorate RfD. Those activities are (1) to control pumping rates from the production wells; and (2) to show that transport within the regional aquifer is shallow. Risks at PM-5 could be reduced to acceptable levels by (1) showing that infiltration within the lower canyon section is preferred over infiltration into the upper- and middle-canyon sections; (2) to show that transport within the regional aquifer is shallow; (3) reducing uncertainty in the maximum infiltration rate in the upper and middle canyon sections; and (4) reducing uncertainty in the effective porosity of the Santa Fe fanglomerate.

Risk could also be reduced if discharges from the RLWTF are eliminated in the near future. The risk-reduction assessment indicates that maximum HI values would be reduced by a factor of two or three if discharges from the RLWTF were eliminated. However, this activity alone would not lead to acceptable risk, assuming the regional-aquifer Model A and the 1 ppb perchlorate RFD.

## **5.2 Integration with Ongoing Mortandad Canyon Efforts**

In parallel to this risk-based decision analysis, the Laboratory is continuing to characterize the hydrogeology and nature and extent of contamination in Mortandad Canyon mainly through drilling additional boreholes and sampling from the vadose zone and the regional aquifer. In addition, a groundwater-monitoring network for Mortandad Canyon and Laboratory property in general is being designed, and eventually corrective actions will be considered and evaluated. Following is a discussion on the potential use of the results of additional characterization efforts in the risk-based decision framework.

### **5.2.1 Integration with Field and Laboratory Characterization Activities**

The decision-support process is designed to guide site characterization and/or research. In this mode, recommendations for additional characterization and/or research are made if there is a reasonable likelihood that the results of data collection will change a decision and if characterization and/or research are superior alternatives, in terms of additional factors such as cost and time, relative to other risk-management activities such as remediation. In Section 5.1, only a handful of data-collection activities were identified that have the potential to change the decision that something must be done to reduce the risk to PM-3 and PM-5, under the assumptions of this study. However, as mentioned previously, Mortandad Canyon work has been proceeding in parallel with the analyses presented in this report. Therefore, site characterization is proceeding, based on plans made before this decision-analysis work was completed.

In general, ongoing field-characterization work will yield information about the nature and extent of contamination, indirect information on model-input parameters, and information on model assumptions (i.e., conceptual models). Because Mortandad Canyon is the first full application of the risk-based decision-support process, the results of field characterization efforts can also be used to evaluate and refine the process.

It is critical to point out that the goal of the decision-support process is to provide defensible decisions, not to provide model results that perfectly agree with all data, which is not possible anyway. It is very likely

that new data will change model input parameters and/or assumptions, but the question for the risk-based decision process is whether new data change the models in a manner that leads to different risk-management decisions. As it stands, the analysis presented in this report concludes that something must be done to reduce the risk to people drinking water from PM-3 and PM-5 when an RfD of 0.00003 mg/kg/day (1 ppb) is used for perchlorate. In addition, analyses have shown that some new data have the potential to change this decision. Therefore, the results of ongoing, or future, data collection efforts should be viewed in this light. Data that throw into question the decision-support process will be data that either lead to HI values greater than 1.0 at the 95% confidence levels for wells other than PM-3 and PM-5 or at times before 100 yr. The most likely reason for such a change would be an incomplete characterization of uncertainty in our analyses. This is entirely possible because this analysis included only a limited number of people in defining uncertainty, specifically conceptual-model uncertainty. The decision support process calls for the inclusion of all stakeholders (DOE, regulators, public, etc.) in the definition of uncertainty. However, the inclusion of all stakeholders was not possible for these Mortandad Canyon analyses.

In any event, the results of new data collection should be used to update model parameters and assumptions. Given the long-term nature of the risk posed by contamination in Mortandad Canyon and the slow movement of contamination, this updating of model parameters and assumptions does not need to be done at every step of the characterization effort. Instead, we recommend the development of an integrated decision analysis-characterization schedule leading to recommendations for corrective actions.

#### **5.2.2 Use of the Risk-Based Decision-Support Process for Groundwater Monitoring Network Design**

As it stands now, the risk-based decision analysis for Mortandad Canyon cannot be used directly in designing a groundwater-monitoring network for the regional aquifer below Mortandad Canyon. The reason it cannot be used is that the goals of the analysis presented in this report and the goals of a monitoring network may not be the same. The goals of the monitoring network have not been defined but are likely to focus on minimizing the likelihood that a contaminant may migrate beyond Laboratory borders or to a supply well undetected by the monitoring network. Such a goal would necessitate revisiting the conceptual model formulation for both the vadose zone and the regional aquifer. This, in turn, could lead to a reformulation of the models themselves. On the other hand, the majority of the work done in support of this Mortandad Canyon analysis is likely to be very useful in the network design, including, but not limited to, the characterization of the source term, the quantification of parameter uncertainty, and the implementation of the numerical transport models.

#### **5.2.3 Potential Use of the Risk-Based Analysis in Cleanup**

The risk-based decision analysis presented in this report can be used to make general recommendations on corrective measures needed to reduce risk from contaminants in Mortandad Canyon. If the project deems that risk must be reduced through cleanup, then the risk-based decision analysis can identify the amount of contaminant mass that must be reduced and the optimal location of mass reduction. However, more detailed models would need to be constructed to optimize the mass-reduction process.

#### **5.2.4 Potential Use of the Risk-Based Analysis for Monitored Natural Attenuation or Defense of Technical Impracticability**

The results of the risk-based decision analysis for Mortandad Canyon indicate that some action is needed to reduce risk to people drinking water in the future at PM-3 and PM-5, under the assumptions of the study. Therefore, this analysis may provide much of the basis for either monitored natural attenuation (MNA) or a determination of technical impracticability (TI), but additional work and actions are required in both cases. For example, this analysis indicates that MNA alone is not sufficient to control risks

associated with the potential migration of perchlorate to either PM-3 or PM-5. Put another way, natural processes alone are not sufficient to attenuate the perchlorate plume before reaching the PM-3 and PM-5 supply wells. In addition, a TI waiver would require analyses beyond those provided in this report, including but not limited to, remedy feasibility and costs. However, the analyses presented in this report could provide the foundation and starting point for either MNA or a TI waiver.

### **5.3 Concluding Remarks**

The Mortandad Canyon analysis documented in this report has provided an example and test case for the Laboratory risk-based decision process. Application of the risk-based decision process has demonstrated that uncertainties in the nature and extent of contamination and groundwater flow and transport can be quantitatively accounted for in decision making. In addition, this report demonstrated a process for quantifying the link between environmental decision making and the need for additional characterization and/or research. This link provides a quantitative basis for answering the key questions of how much data to collect, what type of data to collect, where to collect it, and most importantly, when data collection is finished. Although not every aspect of the risk-based decision process was exercised for Mortandad Canyon, it is clear that this approach can be used on other Laboratory canyons, material disposal areas (MDAs), as well as sites involving nongroundwater pathways. As envisioned in the integrated technical strategy, risk-based decision analysis will be applied systematically across all transport and exposure media, first one medium and one site/source at a time, then one medium and multiple interacting (cumulative) sites/sources, then multiple media and multiple sources.

### **6.0 REFERENCES**

*The following list includes all documents cited in this document. Parenthetical information following each reference provides the author, publication data, and ER ID number. This information is also included in text citations. ER ID numbers are assigned by the ENV-ERS Records Processing Facility (RPF) and are used to locate the document at the RPF.*

Baltz, E.H., J.H. Abrahams, and W.D. Purtymun, March 1963. "Preliminary Report on the Geology and Hydrology of Mortandad Canyon near Los Alamos, with Reference to Disposal of Liquid Low-Level Radioactive Waste," U.S. Geological Survey Open File Report, Albuquerque, New Mexico. (Baltz et al. 1963, 08402)

Birdsell, K.H., V.V. Vesselinov, B.D. Newman, M.O. Gard, and D.J. Hollis, 2005. "Probabilistic Assessment of Contaminant Transport from Mortandad Canyon," Los Alamos National Laboratory document (in progress), Los Alamos, New Mexico. (Birdsell et al. 2005, in progress)

Broxton, D., and D. Vaniman (2005) "Geologic Framework of a Groundwater System on the Margin of a Rift Basin, Pajarito Plateau, North-Central New Mexico," *Vadose Zone Journal*, Vol. 4, pp. 522-550. (Broxton and Vaniman 2005, 90038)

Broxton D., D. Vaniman, P. Longmire, B. Newman, W. Stone, A. Crowder, P. Schuh, R. Lawrence, E. Tow, M. Everett, R. Warren, N. Clayton, D. Counce, E. Kluk, and D. Bergfeld, 2002. "Characterization Well MCOBT-4.4 and Borehole MCBOT-8.5 Completion Report," Los Alamos National Laboratory report LA-13993-MS, Los Alamos, New Mexico. (Broxton et al. 2002, 76006)

Carey, B., G. Cole, C. Lewis, F. Tasi, R. Warren, and G. WoldeGabriel, 1999. "Revised Site-Wide Geologic Model for Los Alamos National Laboratory (FY99)," Los Alamos National Laboratory document LA-UR-00-2056, Los Alamos, New Mexico. (Carey et al. 1999, 66782)

EPA (U.S. Environmental Protection Agency), December 1989. "Risk Assessment Guidance for Superfund, Vol. I, Human Health Evaluation Manual (Part A)," Interim Final, EPA 540/89/002, Office of Solid Waste and Emergency Response, Washington, D.C. (EPA 1989, 08021)

EPA (U.S. Environmental Protection Agency) December 2001. "U.S. EPA Risk Assessment Guidance for Superfund (RAGS): Volume III, Process for Conducting Probabilistic Risk Assessment, (Part A)" (EPA 540-R-02-002, OSWER 9285.7-45, PB2002 963302). (EPA RAGS3; EPA 2001, 85534)

EPA (U.S. Environmental Protection Agency) Integrated Risk Database (IRIS) web page, 2005. Perchlorate and Perchlorate Salts. (Visited July 2005) ([www.epa.gov/iris/subst/1007.htm](http://www.epa.gov/iris/subst/1007.htm)) [Electronic copy: Perchlorate and Perchlorate Salts, IRIS, Environmental Protection Agency.htm]. (EPA 2005)

Keating, E. H., E.M. Kwicklis, M. Witkowski, and T. Ballantine, 1999. "A Simulation Model for the Regional Aquifer beneath the Pajarito Plateau," Los Alamos National Laboratory report LA-UR-00-1029, Los Alamos, New Mexico. (Keating et al. 1999, 88746)

Keating, E.H., E.M. Kwicklis, V. V. Vesselinov, A. Idar, Z. Lu, G. Zyvoloski, and M. Witkowski, 2000. "A Regional Flow and Transport Model for Groundwater at Los Alamos National Laboratory," A progress report submitted to the Hydrogeologic Characterization Program, Los Alamos National Laboratory document LA-UR-01-2199, Los Alamos, New Mexico. (Keating et al. 2000, 90188)

Keating, E.H., B.A. Robinson, and V.V. Vesselinov, 2005. "Development and Application of Numerical Models to Estimate Fluxes through the Regional Aquifer beneath the Pajarito Plateau," *Vadose Zone Journal*, Vol. 4, pp. 653–671. (Keating et al. 2005, 90039)

Koch, R. J., and D. B. Rogers, 2003. "Water Supply at Los Alamos, 1998–2001," Los Alamos National Laboratory report LA-13985-PR, Los Alamos, New Mexico. (Koch and Rogers 2003, 88425)

Kwickles E., M. Witkowski, K. Birdsell, B. Newman, and D. Walther, 2005. "Development of an Infiltration Map for the Los Alamos Area, New Mexico," *Vadose Zone Journal*, pp. 672–693. (Kwickles et al. 2005, 90069)

LANL (Los Alamos National Laboratory), 1997. "Work Plan for Mortandad Canyon," Los Alamos National Laboratory document LA-UR-97-3291, Los Alamos, New Mexico. (LANL 1997, 56835)

LANL (Los Alamos National Laboratory), 2001. "Groundwater Annual Status Summary Report for Fiscal Year 2000," Los Alamos National Laboratory document ESH-18/WQ&H:01–050. (LANL 2001, 70346)

LANL (Los Alamos National Laboratory), 2002. "Groundwater Annual Status Report for Fiscal Year 2001," Los Alamos National Laboratory document LA-13931-SR, Los Alamos, New Mexico. (LANL 2002, 73113)

LANL (Los Alamos National Laboratory), 2002. "Environmental Surveillance at Los Alamos during 2000, Environmental Surveillance Program: Groups ESH-17, ESH-18, ESH-19, and ESH-20," Los Alamos National Laboratory document LA-13861-ENV, Los Alamos, New Mexico. (LANL 2002, 71301)

LANL (Los Alamos National Laboratory) 2003. "Groundwater Annual Status Report for Fiscal Year 2002, March 2003," Los Alamos National Laboratory document LA-UR-03-0244, Los Alamos, New Mexico. (LANL 2003, 76059)

LANL (Los Alamos National Laboratory), 2004. "Mortandad Canyon Groundwater Work Plan, Revision 1," Los Alamos National Laboratory document LA-UR-04-0165, Los Alamos, New Mexico. (LANL 2004, 82613)

- Longmire, P., D. Broxton, W. Stone, B. Newman, R. Gilkeson, J. Marin, D. Vaniman, D. Counce, D. Rogers, R. Hull, S. McLin, R. Warren, 2001. "Characterization Well R-15 Completion Report," Los Alamos National Laboratory report LA-13749-MS, Los Alamos, New Mexico. (Longmire et al. 2001, 70103)
- Longmire, P., 2002. "Characterization Well R-15 Geochemistry Report," Los Alamos National Laboratory report LA-13896-MS, Los Alamos, New Mexico. (Longmire 2002, 72614)
- McLin, S.G., 2005. "Analyses of the PM-2 Aquifer Test Using Multiple Observation Wells," Los Alamos National Laboratory report LA-14225-MS, Los Alamos, New Mexico. (McLin 2005, 90073)
- McLin, S.G., 2005. Preliminary Analyses of the PM-4 Aquifer Test," Los Alamos National Laboratory report, Los Alamos, New Mexico. (McLin 2005, in progress)
- Nylander, C.L., March 2003. "Groundwater Annual Status Report for Fiscal Year 2002," Los Alamos National Laboratory document LA-UR-03-0244, Los Alamos, New Mexico. (Nylander 2003, 76059)
- Purtymun, W.D., 1967. "The Disposal of Industrial Effluents in Mortandad Canyon, Los Alamos County, New Mexico," U.S. Department of the Interior Geological Survey, Santa Fe, New Mexico. (Purtymun 1967, 11785)
- Purtymun, W.D., 1974. "Dispersion and Movement of Tritium in a Shallow Aquifer in Mortandad Canyon at the Los Alamos Scientific Laboratory," Los Alamos Scientific Laboratory report LA-5716-MS, Los Alamos, New Mexico. (Purtymun 1974, 05476)
- Purtymun, W.D., 1984. "Hydrologic Characteristics of the Main Aquifer in the Los Alamos Area: Development of Ground Water Supplies," Los Alamos National Laboratory report LA-9957-MS, Los Alamos, New Mexico. (Purtymun 1984, 06513)
- Purtymun, W.D., J.R. Buchholz, and T.E. Haksonson, 1977. "Chemical Quality of Effluents and Their Influence on Water Quality in a Shallow Aquifer," *J. Environmental Quality*, Vol. 6, No. 1, pp. 29–32. (Purtymun et al. 1977, 11846)
- Rogers, D., and B. Gallaher, 1995. "The Unsaturated Characteristics of the Bandelier Tuff," Los Alamos National Laboratory report LA-12968-MS, Los Alamos, New Mexico. (Rogers and Gallaher 1995, 55334)
- Rogers, D., B.M. Gallaher, and E.L. Vold, "Vadose Zone Infiltration beneath the Pajarito Plateau at Los Alamos National Laboratory," New Mexico Geological Society, Forty-Seventh Annual Field Conference, September 25–28, 1996. (Rogers et al. 1996, 55543)
- Springer, E.P., 2003. "Qualification for the Hydrologic Property Data," E-mail sent by E.P. Springer on 7/7/03 to Kay Birdsell and Paul Davis. (Springer 2003, 90071)
- van Genuchten, M.T., 1980. "A Closed-Form Solution for Predicting the Hydraulic Conductivity of Unsaturated Soils," *Soil Sci. Soc. Am. J.*, Vol. 44, pp. 892–898. (van Genuchten 1980, 63542)
- Vesselinov, V.V., 2004. "Transient Capture Zone Analysis of Groundwater Supply Wells in the Vicinity of Mortandad Canyon," Los Alamos National Laboratory document LA-UR-05-6877, Los Alamos, New Mexico. (Vesselinov 2004, 89728)
- Vesselinov, V.V., 2004. "On Potential Fast Contaminant Flow Paths to the White Rock Springs through the Regional Aquifer beneath Pajarito Plateau," Los Alamos National Laboratory document LA-UR-05-6871, Los Alamos, New Mexico. (Vesselinov 2004, 90117)

Vesselinov, V.V., 2005. "Logical Framework for Development and Discrimination of Alternative Conceptual Models of Saturated Groundwater Flow beneath the Pajarito Plateau," Los Alamos National Laboratory document LA-UR-05-6876, Los Alamos, New Mexico. (Vesselinov 2005, 89753)

Vesselinov, V.V., 2005. "An Alternative Conceptual Model of Groundwater Flow and Transport in Saturated Zone beneath the Pajarito Plateau," Los Alamos National Laboratory document LA-UR-05-6741, Los Alamos, New Mexico. (Vesselinov 2005, 90040)

Vesselinov, V.V., and E.H. Keating, 2002, "Three-Dimensional Capture Zone Analysis of Groundwater Supply Systems in the Española Basin, Northern New Mexico," GSA Annual Meeting, Denver, Colorado, October 17–30, 2002. (Vesselinov and Keating 2002, 89373)

Vesselinov, V.V., and E.H. Keating, 2003. "On Transient Capture Zone Analysis: The Importance of Dispersion," AGU Meeting, *EOS Trans.*, Vol. 84, p. 46, San Francisco, California, December 8–12, 2003. (Vesselinov and Keating 2003, 90116)

Vesselinov, V.V., E.H. Keating, and J. Doherty, 2001. "Analysis of Uncertainty in Model Predictions of Flow and Transport in the Española Basin Regional Aquifer," Northern New Mexico, AGU Meeting, San Francisco, December 10–14, 2001, *EOS Trans.*, Vol. 82, p. 47. (Vesselinov et al. 2001, 90114)

Zyvoloski, G.A., B.A. Robinson, Z.V. Dash, and L.L. Trease. 1997. "Summary of the Models and Methods for the FEHM Application—a Finite-Element Heat- and Mass-Transfer Code," Los Alamos National Laboratory report LA-13307-MS, Los Alamos National Laboratory, Los Alamos, New Mexico. (Zyvoloski et al. 1997, 70147).

## **Appendix A**

---

*Tier-1 Risk Assessment for Mortandad Canyon Groundwater*

## A-1.0 BACKGROUND AND PURPOSE

To date, no contaminants have been detected in groundwater at supply wells in concentrations that exceed the Environmental Protection Agency's (EPA's) safe drinking water standards.<sup>1</sup> However, alluvial and intermediate groundwater in Mortandad Canyon contains tritium and nitrate at concentrations exceeding their maximum concentration limits (MCLs) and perchlorate exceeding its health advisory level. Although neither alluvial nor intermediate groundwater is used for municipal purposes, both are hydrologically connected to the regional water-supply aquifer, which means that, over time, contaminants in alluvial and intermediate groundwater are expected to reach the regional aquifer. The rate of contaminant transport and the concentration of contaminants (which together describe the flux of contaminants) are important factors in determining appropriate corrective actions to ensure that members of the public are not exposed to unsafe drinking water. Data obtained through (ongoing) site investigations provide information regarding how contaminants moved in the past. These same data also provide information that is used in simulation models that are, in turn, used to provide information regarding how contaminants are expected to move in the future. Simulation models are used to estimate contaminant fluxes and concentrations in water pumped from the regional aquifer. This information is used in exposure and toxicity assessments to evaluate the potential for unsafe concentrations to occur over time.

In this analysis, groundwater transport and supply-well pumping simulations are conducted over a period of 1000 yr, a time frame that captured maximum potential concentrations in production wells. In general, baseline risk assessments for cleanup sites consider a time horizon of up to 100 yr, which is the basis of the objective of the Mortandad Canyon Groundwater Work Plan to characterize the nature and extent of contamination in terms "bounding spatial and temporal (100 yr) uncertainties in contaminant concentrations and distributions. Information obtained from determining the nature and extent of contamination will assist in making decisions regarding characterization, regulatory compliance, pathway analysis, risk assessment, remediation and monitoring" (LANL 2004, 82613).

The approach to this human-health risk assessment is taken from EPA's *Risk Assessment Guidance for Superfund, Volume 3, Part A: Process for Conducting Probabilistic Risk Assessment* (RAGS3; EPA 2000, 85534). Referring back to Figure 1.1-1 of this report, the first step in the risk-assessment process is a simple Tier-1 calculation of risk. EPA (RAGS3; EPA 2000, 85534) defines a Tier-1 assessment as a point estimate of, in our case, hazard index (HI) and dose. The Tier-1 calculation is based on a single set of parameter input values resulting in a single HI or dose value. This point estimate is intended to be biased in the sense that a more complete and realistic analysis would yield lower HI and dose values. This appendix summarizes the Tier-1 risk assessment made for Mortandad Canyon.

The risk-management question that the Tier-1 groundwater pathway risk assessment for Mortandad Canyon was designed to answer is this: Is there a potential for drinking water to be contaminated at unsafe levels resulting from releases from the Radiological Liquid and Waste-Treatment Facility (RLWTF)? The answer to this question is determined by calculating the HIs and hazard quotients (HQs) for nitrate and perchlorate consistent with EPA guidance and then comparing the calculated HI and HQ values with EPA's threshold value of 1.0. If the HQs calculated for either nitrate or perchlorate, or the HI calculated for both nitrate and perchlorate, is less than 1.0, then the answer to the Tier-1 risk-management question is "no," and if calculated HQs and/or HI values are greater than 1.0, then the answer to the risk-management question is "yes." The same question is asked related to tritium exposure

---

<sup>1</sup> Perchlorate has been detected in samples from O-1 in concentrations near 4 ppb; however, O-1 is not being used as a source of drinking water.

when compared to the total effective dose equivalent (TEDE) for radionuclides of 4 mrem/year. If the answer to the risk management question is "yes" for HI, HQ, or TEDE, a more-realistic risk assessment is warranted so that a decision-analysis tool can be developed to assist in addressing subsequent risk-management questions, including those related to data needs, alternative remedies, and long-term monitoring.

### **A-2.0 CONTAMINANT SOURCE, DISTRIBUTION, AND FATE**

Several Laboratory technical areas (TAs) occur along Mortandad Canyon, many of which are (or have been) either direct (through discharge) or indirect (through runoff) sources of surface water. Since 1963, radioactive liquid wastes from Laboratory operations have been collected and treated at the RLWTF at TA-50. Treated wastewater from the RLWTF is discharged into Effluent Canyon, which drains into Mortandad Canyon. The RLWTF is considered to be the greatest single source of surface and groundwater contamination in Mortandad Canyon. The RLWTF remains in operation today and continues to discharge into Mortandad Canyon through Effluent Canyon. Section 2.1, in the main body of this report, discusses the time-dependent discharge volumes and contaminant masses that have been released from the RLWTF since 1964. Discharge volumes have ranged from  $1.36 \times 10^7$  L/yr in 2001 to a high of  $6.03 \times 10^7$  L/yr in 1968. Over the years, treated effluents have included the contaminants tritium, perchlorate, nitrate, uranium, plutonium, and other constituents.

Section 2.2, in the body of this report, discusses the distribution of contaminants within sediments, perched alluvial water, unsaturated-zone pore water, intermediate perched water, and the regional aquifer. Taken as a group, the contaminant distribution data indicate that liquids discharged from the RLWTF flowed along the ephemeral streambed and the underlying alluvial aquifer in Mortandad Canyon. Some of the liquids infiltrated into the unsaturated rock beneath the alluvium to various depths. The observed distribution of contaminants and other supporting data provide the basis for the conceptual model of groundwater transport of contaminants in Mortandad Canyon shown in Figure 2.2-3 (LANL 2004, 82613).

### **A-3.0 TIER-1 GROUNDWATER TRANSPORT SIMULATIONS**

The Tier-1 groundwater transport simulations that were developed to provide contaminant concentrations as input to the Tier-1 risk assessment sequentially integrate the components illustrated in Figure 2.2-3 as follows:

- Source Term: Contaminants are released annually into Mortandad Canyon from the RLWTF.
- Alluvial Transport: Discharges from the RLWTF flow along the streambed and into the near-surface alluvial groundwater in Mortandad Canyon.
- Deep Infiltration: Contaminated alluvial groundwater seeps downward into the unsaturated bedrock.
- Unsaturated Transport: Contaminated groundwater moves downward through unsaturated bedrock under the forces of gravity and capillary suction.
- Saturated Transport: Contaminated groundwater moves from unsaturated rock into saturated rock and sediments and is transported in directions established by natural gradients and those induced by pumping.
- Pumping: Contaminated groundwater in the regional aquifer is drawn into supply wells.

Consistent with EPA guidance on conducting Tier-1 risk assessments, each component of the groundwater transport simulation was considered in a manner that would create the earliest, highest concentrations of contaminants in the regional aquifer while still being consistent with the available data. Release and transport was limited to soluble, mobile contaminants in the RLWTF inventory, namely, tritium, nitrate, and perchlorate.

The Tier-1 groundwater transport simulations do not explicitly account for perching at intermediate depths in the unsaturated zone, which is known to occur at some discrete locations in Mortandad Canyon. However, Tier-1 migration rates through the unsaturated zone are assumed to be sufficiently large to act as rapid flow paths through the unsaturated zone.

### A-3.1 Tier-1 Source Term

The groundwater transport simulations address continuous discharges of wastewater from the RLWTF into Mortandad Canyon between 1964 and 2104. Annual tritium and nitrate releases were based on the discharge records presented previously in Table 2.1-1, with discharges for the 99 yr beyond 2001 held constant at the 2001 rate. Annual perchlorate releases between 1964 and 2001 were inferred from correlations of nitrate and perchlorate measurements in core samples.

Figure 2.2-1, of this report, shows the locations of boreholes from which core samples were analyzed to derive a basis for estimating historic perchlorate releases from the RLWTF. In order of their proximity to the RLWTF outfall, these boreholes are intermediate characterization wells MCOBT-4.4, alluvial observation well MCO-7.2, regional characterization well R-15, and intermediate observation well MCOBT-8.5. Figure A-1 shows plots of perchlorate and nitrate concentrations from core samples from boreholes MCOBT-4.4, MCO-7.2, R-15, and MCOBT-8.5. The plots indicate a strong correlation between perchlorate and nitrate concentrations in the vadose zone at all locations except intermediate observation well MCOBT-8.5. The preferential denitrification of nitrate (rather than perchlorate) is the likely explanation of this exception. Because MCOBT-8.5 is farther from the source of contamination at the RLWTF outfall than MCOBT-4.4, MCO-7.2, and R-15, nitrate in pore water at the location of MCOBT-8.5 has had relatively more time to undergo denitrification through natural microbial processes.

Data shown in Figure A-1 were used in a regression analysis to establish a basis for estimating the time history of perchlorate releases. Specifically, perchlorate and nitrate concentrations at depths between 18 and 141 m below ground surface were analyzed. Data from shallower core samples located in the alluvium (less than approximately 18 m below land surface) were eliminated to remove any bias resulting from individual discharges after 2002, when perchlorate concentrations in treated wastewater were reduced as a result of the reverse osmosis treatment system installed at the RLWTF.

The data associated with core samples from intermediate borehole MCOBT-4.4 revealed the best statistical relationship between nitrate and perchlorate. Therefore, that data set was used to develop a mathematical relationship to estimate perchlorate releases based on the nitrate releases listed in Table 2.1-1. An estimate of the source that represents the 95th percentile upper-bound for the perchlorate source, based on the recorded nitrate source, was derived to be consistent with the Tier-1 approach. This relationship is as follows:

$$\text{Perchlorate } (\mu\text{g/L}) = [\text{Nitrate (mg/L as nitrate)} \times 1.085] + 152.95.$$

Figure A-2 shows the estimated 95th percentile upper-bound history of perchlorate released from the RLWTF based on the correlation with nitrate determined using core sample data from intermediate borehole MCOBT-4.4 in Mortandad Canyon.

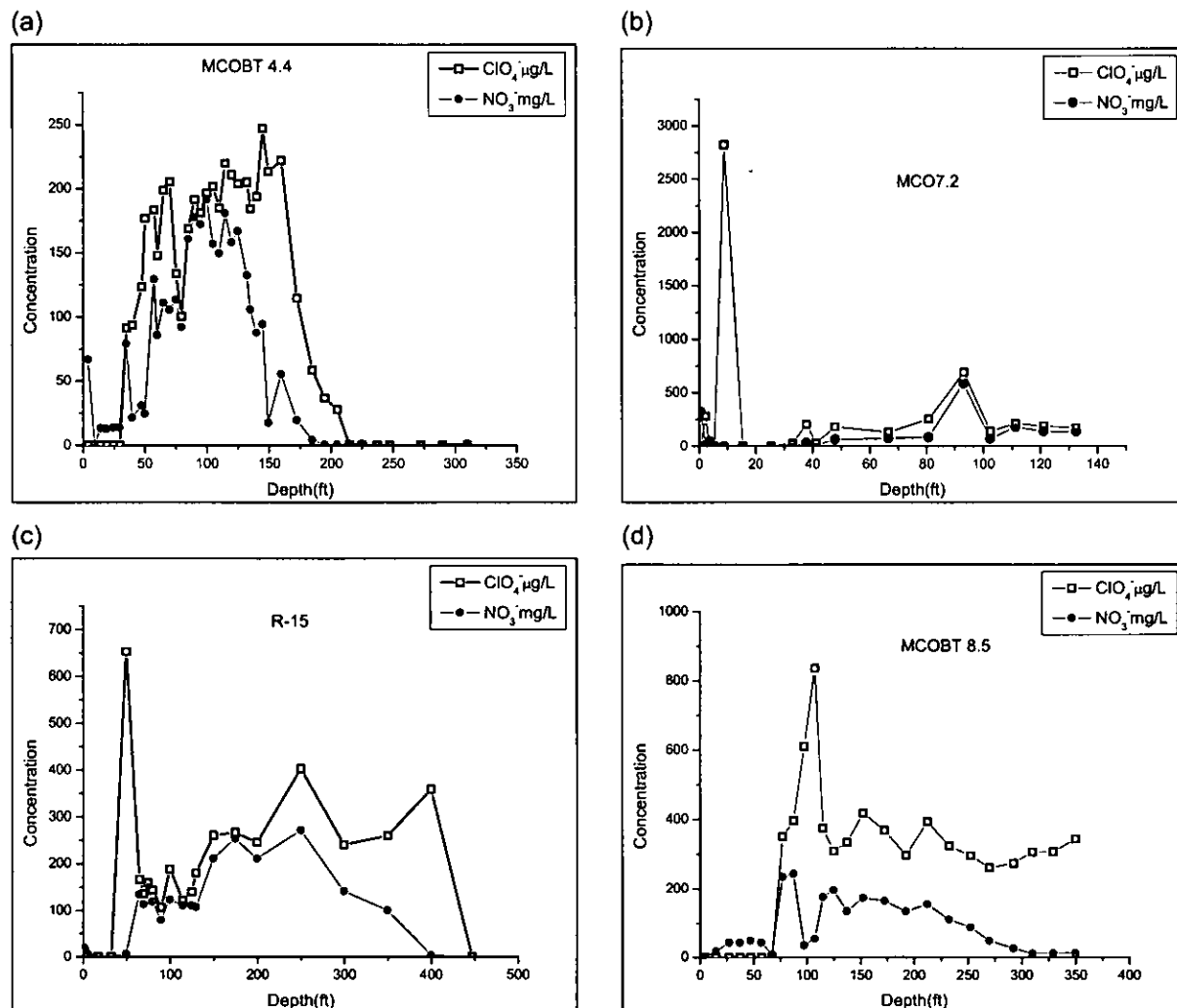


Figure A-1. Perchlorate and nitrate concentrations in pore water from core samples from boreholes in Mortandad Canyon

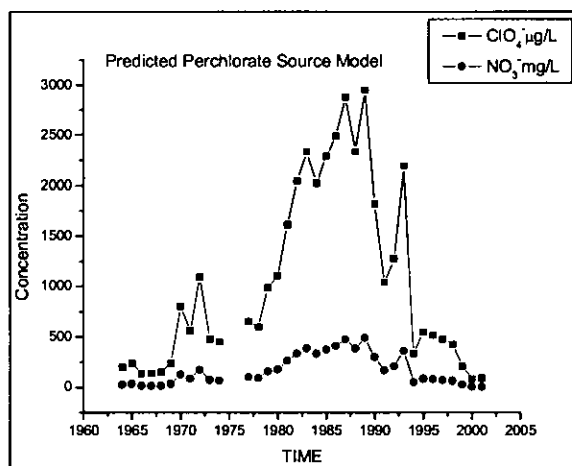


Figure A-2. Annual average estimated release concentrations of perchlorate ( $\mu\text{g/L}$ ) from the RLWTF, based on correlated release concentrations of nitrate ( $\text{mg/L}$ ). The perchlorate release represents a 95th percentile upper boundary for Tier-1 analysis.

### A-3.2 Alluvial-Groundwater Distribution and Infiltration

The annual point estimates of tritium, nitrate, and perchlorate released into Mortandad Canyon in RLWTF surface-water effluent were assumed to be homogeneously mixed with other surface water in the canyon, then to flow along the canyon floor before infiltrating into alluvium. This assumption is supported by gauging station data, which indicate higher surface water flow rates than RLWTF release rates, and also by alluvial nitrate concentration data, which are fairly uniform (i.e., well mixed) throughout the alluvial aquifer. A portion of the combined surface water flowing along Mortandad Canyon infiltrates into alluvial material, creating alluvial groundwater distributed along the canyon. The distribution of alluvial groundwater used in the Tier-1 groundwater transport simulations was based on a study conducted in the early 1960s (Purtymun 1967, 11785).

That study used monthly data from gauging stations, moisture data from alluvial observation wells, and a measure of the hydraulic gradient to estimate the volume of water infiltrating in the three sections along the canyon, which were designated upper, middle, and lower Mortandad Canyon. The spatial delineations established in the Purtymun study are shown in Table A-1. Also shown are the estimated interface areas between the base of the alluvium and the underlying bedrock, and information about the rates and volumes of recharge for each section. The infiltration rates deduced in the Purtymun study for the upper, middle, and lower sections were 6.0, 1.5, and 0.6 m/yr, respectively. It is noteworthy that the estimated infiltration volumes total to  $10 \times 10^7$  L/yr and exceed the discharge volumes recorded at the RLWTF (Table 2.1-1). The difference is attributable to additional sources of surface and alluvial water in Mortandad Canyon between 1963 and 1974.

The Tier-1 infiltration model assumes the steady, effective infiltration rates in Table A-1 as upper bounds, ignoring the general decreasing trend in recent releases to the canyon. In the groundwater transport simulations, the infiltration estimates are used as a continuous annual infiltration rate of contaminated alluvial groundwater into the underlying unsaturated Bandelier Tuff in Mortandad Canyon.

**Table A-1**  
**Infiltration Estimates from the Alluvial Aquifer to the Unsaturated Zone**  
**for Three Sections of Mortandad Canyon (Purtymun 1967, 11785)**

Canyon Section	Location Markers (Figure 2.2-1)	Volume of Infiltrating Water (L/yr)	Effective Infiltration Rate (m/yr)	Area of Section (m <sup>2</sup> )
Upper	TA-50 outfall to MCO-4	$6.0 \times 10^7$ (60%)	6.0	9987
Middle	MCO-4 to MCO-6	$1.8 \times 10^7$ (18%)	1.5	12077
Lower	MCO-6 to Laboratory boundary	$2.2 \times 10^7$ (22%)	0.6	37161

### A-3.3 Unsaturated Transport

Unsaturated groundwater transport calculations were run with the FEHM computer code (Zyvoloski et al. 1997, 70147) for tritium, nitrate, and perchlorate. In the model, the upper, middle, and lower portions of Mortandad Canyon described by Purtymun (1967, 11785) (Table A-1) were represented as three one-dimensional columns, as illustrated in Figure A-3. As the figure indicates, each column was divided into layers representing the appropriate geologic strata between the base of the alluvium and the top of the regional aquifer using data from the site-wide geologic model (Carey et al. 1999, 66782). The cross-sectional area of each column in the unsaturated transport model was equal to the appropriate area in Table A-1, but the corresponding infiltration rate provided the steady, upper boundary condition for the column representing the unsaturated rock beneath Mortandad Canyon. This is illustrated in Figure A-4.

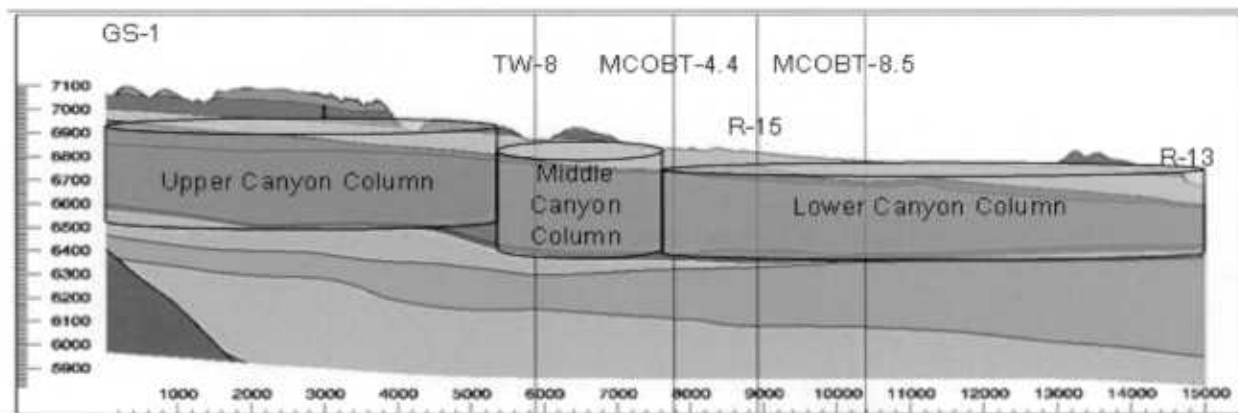


Figure A-3. Illustration of the three 1-dimensional columns used for the Tier-1 unsaturated-zone groundwater transport simulations

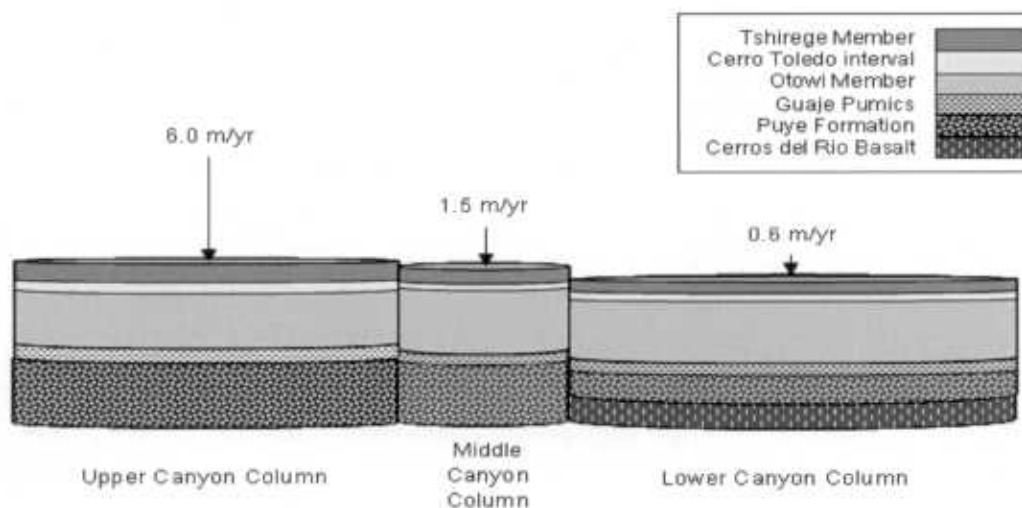


Figure A-4. Steady-state infiltration rates used in the Tier-1 unsaturated groundwater transport model

The hydrogeologic units within each column are assigned material and hydrologic properties (van Genuchten 1980, 63542) derived from site-specific data, as listed in Table A-2. The Cerros del Rio basalt and Tschicoma dacite are assigned very low porosity values representative of fractures to ensure rapid transport through these units, which have a greater likelihood of exhibiting fracture transport than the tuff units. This assumption is consistent with EPA's Tier-1 approach.

**Table A-2**  
**Material Properties and Modeling Parameters Used in**  
**Tier-1 Unsaturated Transport Simulations**

Hydrogeologic Unit	Permeability (m <sup>2</sup> )	Porosity	$\alpha$ m <sup>-1</sup>	$\theta_r$	n
Tshirege member Qbt1v	1.96e-13	0.528	0.44	0.009	1.660
Tshirege member Qbt1g	3.68e-13	0.509	2.22	0.018	1.592
Tsankawi Pumice	1.01e-12	0.473	1.52	0.01	1.506
Cerro Toledo Interval	8.82e-13	0.473	1.52	0.01	1.506
Otowi Member	7.25e-13	0.469	0.66	0.026	1.711
Guaje Pumice Bed	1.53e-13	0.667	0.081	0.01	4.026
Tschicoma dacite	2.96e-13	0.0001	5.00	0.03	1.5
Cerros del Rio Basalt	2.96e-13	0.0001	5.00	0.03	1.5
Puye Formation	4.73e-12	0.35	5.00	0.01	2.68

The total annual masses of nitrate and tritium introduced to the unsaturated zone columns are the recorded annual discharges shown in Table 2.1-1 of the report. The total annual mass of perchlorate is the annual perchlorate concentration estimated using the regression equation presented earlier and shown in Figure A-2, multiplied by the annual discharge volume recorded for the RLWTF (Table 2.1-1). The total annual contaminant mass is distributed into the three canyon sections according to the percentage of the total volume infiltrating to that particular section as given in Table A-1. This approach results in a uniform concentration that varies annually and enters the three unsaturated-zone columns. The total annual contaminant mass was allowed to enter the unsaturated columns the same year that it was released, which in effect yields no residence time in the alluvial groundwater.

Recorded nitrate and tritium mass releases (Table 2.1-1) and correlated perchlorate releases were used in the source term model through 2001, when the Tier-1 calculation was conducted. The 2001 release data were held constant throughout the simulation period to overestimate Tier-1 contaminant releases. In reality, contaminant concentrations are expected to decrease, based on recent history.

Figure A-5 shows nitrate concentration profiles as a function of elevation calculated for the year 2003 for each of the three simulation columns. The calculated nitrate concentrations shown in the figure were compared to field data. Overall, the calculated concentrations in the columns representing the middle and lower canyon approximate measured concentrations in pore water from core samples from those portions of Mortandad Canyon. However, at each location, the calculations produce higher concentrations of contaminants deeper within the columns relative to the field data, which is consistent with the objectives of the Tier-1 analysis. No data exist near the upper canyon column, but the simulated results for the upper canyon show most of the nitrate there being flushed through the column and exiting at the base of the unsaturated zone. This behavior is also consistent with the objectives of the Tier-1 analysis.

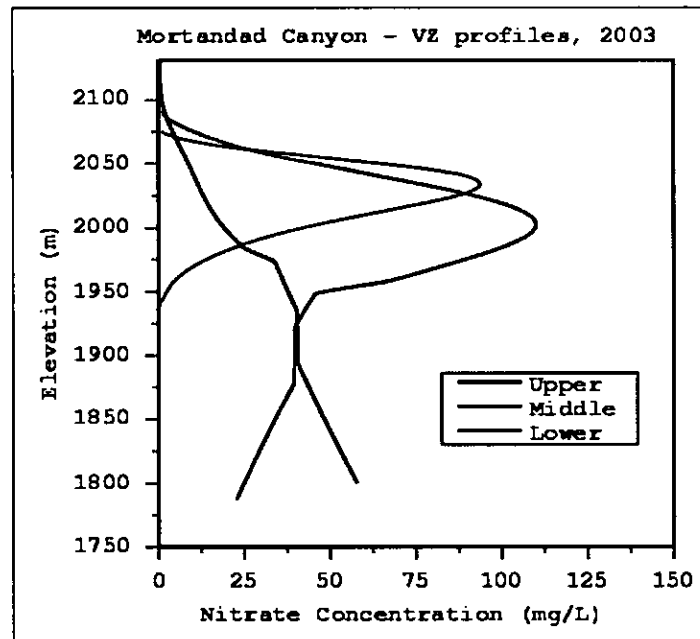


**Figure A-5. Calculated nitrate concentrations at various elevations in the three unsaturated transport columns, Tier-1 model predictions for yr 2003.**

#### A-3.4 Saturated Transport

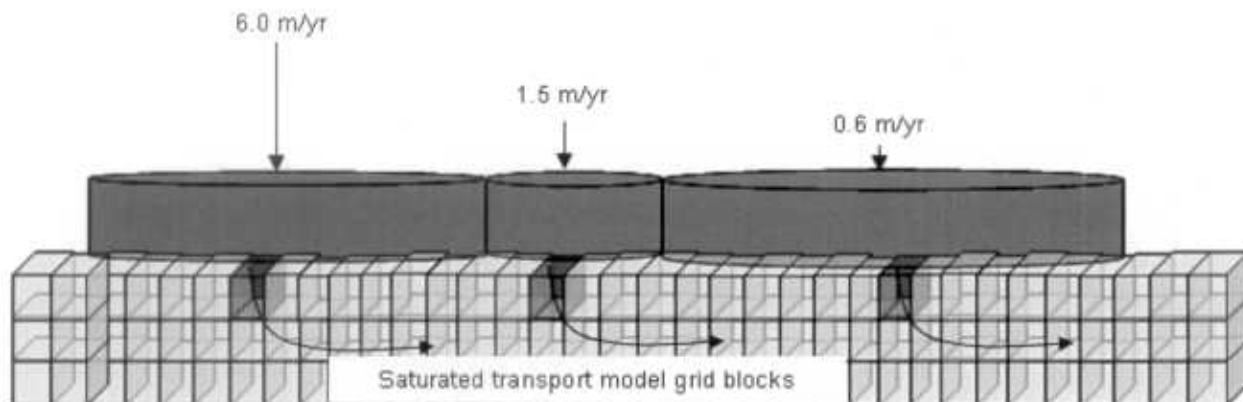
The site-scale version of the regional-aquifer model described in the Groundwater Annual Status Report for Fiscal Year 2002 (LANL 2003, 76059) is used for the Tier-1 saturated groundwater transport simulations. Uniform properties (permeability, porosity) are assigned to each of the zones. Although the units are assumed to be uniform; when combined, they represent a heterogeneous system. The regional aquifer model is calibrated to match measured water levels and measured water fluxes.

Table A-3 lists the permeability values for the hydrostratigraphic units represented in the calibrated, saturated groundwater transport model used for the Tier-1 analysis.

Figure A-6 illustrates the relationship between the three columns in the unsaturated transport model and grid blocks in the saturated transport model. The time-dependent contaminant flux exiting each column in the Tier-1 unsaturated transport model (Figure A-7) is input into a single element at the top of the Tier-1 saturated transport model, coincident with the center of the unsaturated transport column. The saturated transport model then calculates the advective movement of contaminants through the grid elements under transient flow conditions.

**Table A-3**  
**Permeabilities of Aquifer Materials Evaluated in the**  
**Tier-1 Saturated Transport Model**

Hydrostratigraphic Unit	Horizontal Permeability log <sub>10</sub> (m <sup>2</sup> )	Vertical Permeability log <sub>10</sub> (m <sup>2</sup> )
Pre-Cambrian	-18.00	-18.00
Paleozoic/Mesozoic—deep	-13.66	-13.66
Paleozoic/Mesozoic—shallow	-12.60	-12.60
Pajarito fault zone	-15.01	-15.01
Keres Group—deep	-13.66	-13.66
Keres Group—shallow	-12.71	-12.71
Tschicoma lava flows	-13.75	-13.75
Older Miocene basalts (Tb1)	-13.14	-13.14
Younger Miocene basalts (Tb2)	-13.14	-13.14
Cerros del Rio basalts (Tb4)	-13.14	-13.14
Older Fanglomerate	-13.72	-14.79
Santa Fe Group—shallow	-13.08	-13.08
Santa Fe Group—deep	-14.18	-14.18
Puye Formation	-12.34	-13.03
Pumice-rich volcanoclastic sediments	-12.34	-13.05
Totavi lentil	-12.34	-13.03



**Figure A-6.** Illustration of the relationship between the three Tier-1 unsaturated-zone columns and the grid elements used in the Tier-1 saturated-zone model

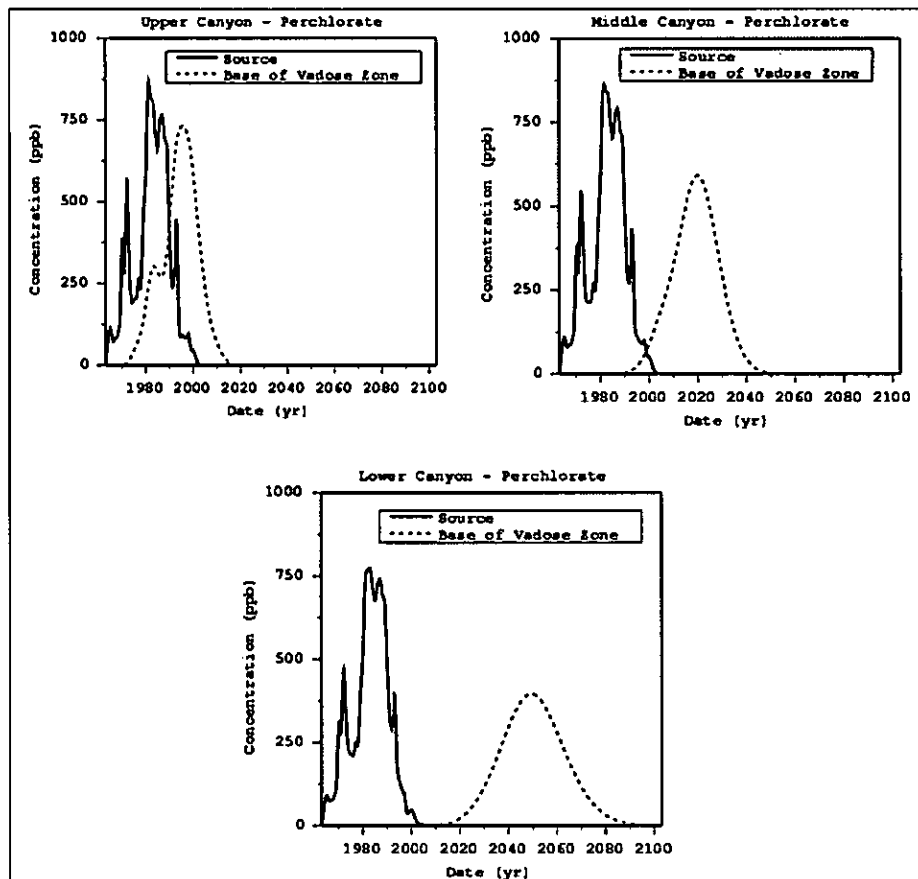


**Figure A-7. Perchlorate concentration versus time at the top and bottom of the three unsaturated-zone grids for the Tier-1 analysis.**

Assumptions in the Tier-1 saturated transport model follow many of the assumptions of regional-aquifer Model A presented in Section 3.3.4 of the main body of this report include the following:

- Within the regional aquifer, the pumping rates control the spatial distribution of contaminants entering the regional aquifer at the water table.
- Groundwater flow is transient. The saturated simulation starts in 1946 to create a transient flow condition that is influenced by pumping rates. Pump rates are averaged over 5-year time periods in the simulation (Figure A-8).
- Pumping rates beyond the year 2000 in the simulation remain unchanged at the average rate for the 1996 to 2000 time period. This sets up a quasi-steady flow field after the year 2000.
- The Puye Formation and the basalts are assumed to behave as uniform porous media.
- The Puye Formation behaves as a uniform, porous sedimentary rock with no preferential flow paths.
- Fracture flow in the basalts is not explicitly defined in the model, but its potential impact is represented by restricting the transport to occur only within 0.0001 of the total volume of rock.
- Dispersion is moderate (10 m longitudinal; 1 m transverse).

The model simulates pumping of water according to 5-year averaged annual production data. Each well penetrates a number of model grid blocks. The model distributes the rate pumped by each water-supply well according to the hydraulic properties of the blocks.

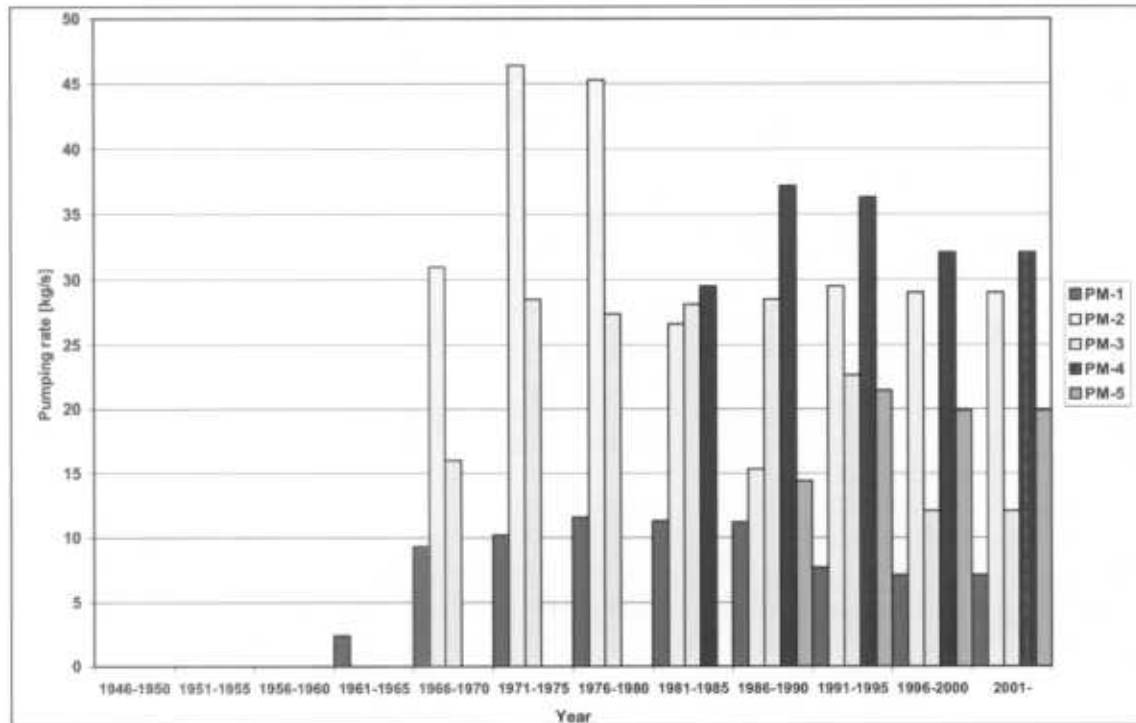


**Figure A-8. Pumping rates used in the model simulations representing a 5-year averaging of the actual pumping rate variability**

Figure A-9 shows the model predicted flow paths from the three locations where contaminants enter the saturated transport model to the supply wells. Contaminants entering the saturated transport model from the upper-canyon column in the unsaturated transport model flow almost directly to PM-5 and do not reach the other PM wells over the simulated time frame. Contaminants from the lower-canyon column flow directly toward PM-4 and do not reach PM-5. Contaminants from the middle-canyon column reach both PM-5 and PM-4. In the Tier-1 groundwater transport simulations, PM-1, PM-2, PM-3, O-1, and O-4 are not impacted by contaminants from the RLWTF released into Mortandad Canyon. This result is dictated by the 1996 to 2000 average pump rates (Figure A-9), which are used during most of the simulation. The high pump rates of PM-2, PM-4, and PM-5 relative to those of PM-1 and PM-3 create a southerly flow that allows PM-4 and PM-5 to capture the contaminants released at the three release locations.

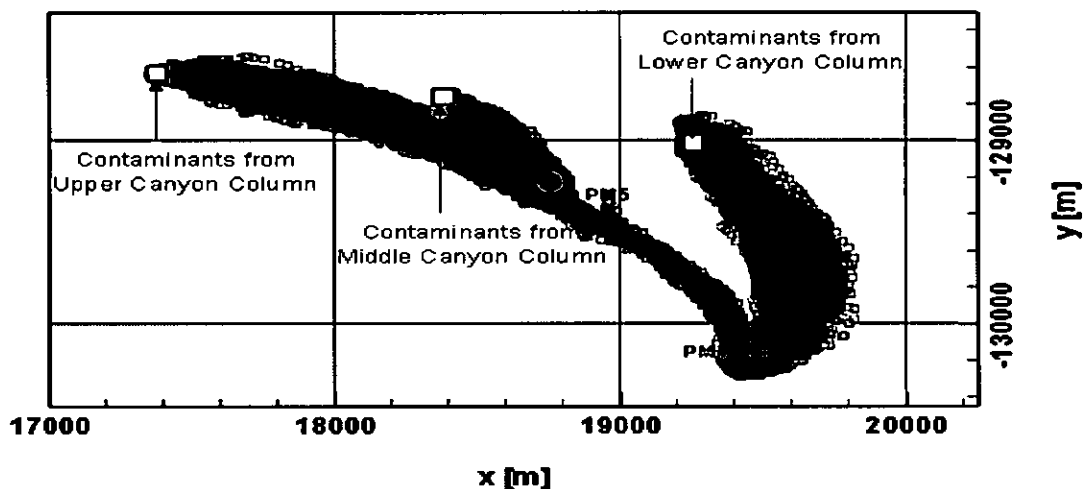


**Figure A-9. Calculated Tier-1 flow paths from Mortandad Canyon to the PM wells in the regional aquifer**

Table A-4 gives contaminant travel-time information for the Tier-1 assessment. The unsaturated-zone travel times represent mean-mass transport times through the upper-, middle-, and lower-canyon columns in the unsaturated transport model. The saturated-zone travel times are mean-mass arrival times for contaminants to reach a supply well upon arrival in the regional aquifer at the water table.

**Table A-4  
Mean-Mass Travel Times for Tier-1 Pathways**

	Unsaturated-Zone Travel Time (yr)	Saturated-Zone Travel Time (yr)	Total Travel Time (yr)
Upper canyon to PM-5	12	152	164
Middle canyon to PM-5	35	33	68
Lower canyon to PM-4	67	7	74

Figure A-10 shows the calculated concentrations of perchlorate in water pumped from PM-4 and PM-5 over the first 750 yr of a 1000-year simulation period, for contamination originating from the upper-, middle-, and lower-canyon columns. Also shown is the cumulative concentration in PM-4 and PM-5 from all three locations. The total mean-mass travel time given in Table A-4 is reflected in the arrival of the peaks in the perchlorate breakthrough curves for PM-4 and PM-5. In the Tier-1 groundwater transport simulations, most of the contamination reaching the supply wells originates from the upper-canyon column in the unsaturated transport model, causing relatively high concentrations in water pumped from PM-5 for about 300 yr (curve a). Releases from the middle-canyon column (curve b) create equally high concentrations in PM-5, but these concentrations are shorter-lived relative to those resulting from the upper-canyon column. Peak perchlorate concentrations reaching PM-4 from the lower canyon (curve c) are almost an order of magnitude lower than at PM-5 for the other canyon sections. These relative concentrations reflect the distribution of contaminants input into each column in the unsaturated transport model. Nitrate concentrations calculated in well water are over 100 times higher than perchlorate concentrations at these same locations, but the curves mimic the shape (concentration vs time) of the perchlorate curves because of the correlation of the perchlorate source term to the nitrate source term, as discussed in Section A.3.

The concentrations of nitrate and perchlorate calculated in supply-well water in the saturated transport model were used in the Tier-1 exposure and toxicity assessment calculations, which are described next. Tritium exposures were not explicitly calculated because radioactive decay during the estimated saturated-zone transport time to wells PM-4 and PM-5 (Table A-4) should be sufficient to reduce tritium concentrations exiting the unsaturated zone (Figure A-11, decayed values) to values less than 20,000 pCi, which is equivalent to the 4-mrem dose threshold for safe drinking water using EPA's toxicity and exposure methodology. The maximum concentration of tritium in pumped water is calculated to be 8000 pCi/L.

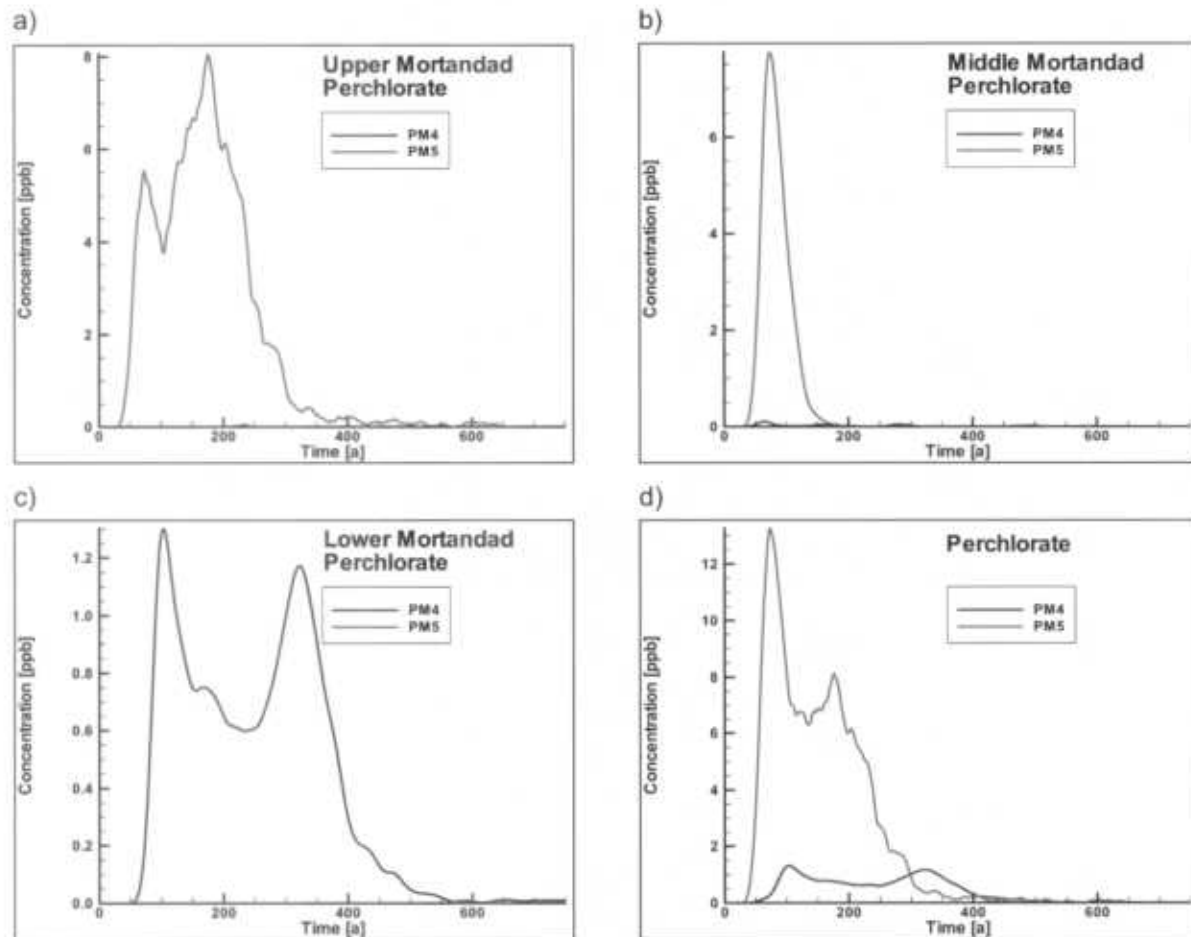
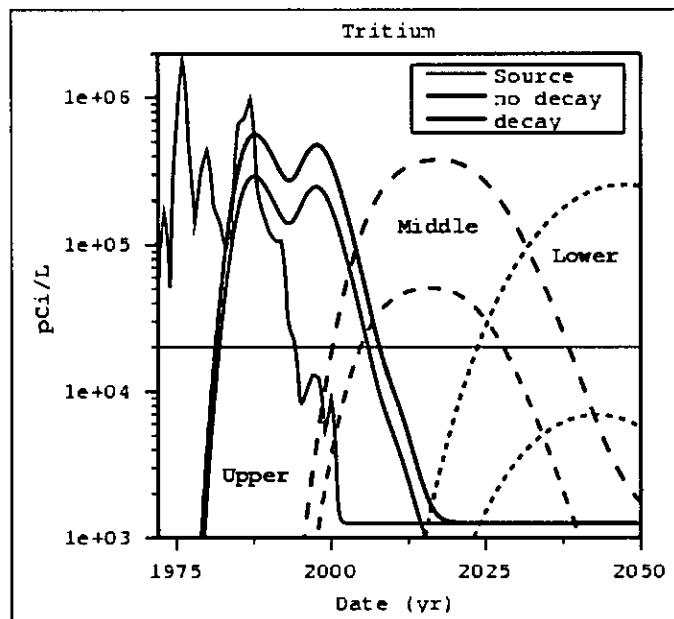


Figure A-10. Tier-1 concentrations of perchlorate from (a) upper, (b) middle, and (c) lower Mortandad Canyon and (d) for the three sections combined in water pumped from PM-4 and PM-5. (Time = 0 represents 1964)



**Figure A-11. Tritium concentration versus time entering (blue line) and leaving (red lines) the three unsaturated-zone columns for the Tier-1 analysis, showing the decrease in concentrations leaving the columns as a result of radioactive decay (black lines compared to red lines).**

#### A-4.0 RISK ASSESSMENT

Following EPA guidance, HQ, and HI values were calculated, assuming hypothetical exposures to nitrate and perchlorate in drinking water at concentrations predicted in the groundwater transport simulations, such as the combined perchlorate concentrations predicted for wells PM-4 and PM-5 shown in Figure A-11(d) resulting from the three unsaturated transport columns combined.

For nitrate, separate HQ values were calculated for infant and adult exposures, using the applicable RfDs from EPA (EPA IRIS, 2005). For perchlorate, HQ values were calculated for hypothetical adult exposures, using a reference dose of 0.00003 mg/kg/day (EPA IRIS, 2005), which is equivalent to an MCL of 1 ppb. Adult HI values were calculated for cumulative exposures to both nitrate and perchlorate.

Adult HQ and HI values were calculated for chronic 70-yr exposures to 2 L/day of contaminated drinking water. The maximum concentrations calculated in any individual well over any continuous 70-yr period were used in the chronic adult exposure toxicity assessments. This implies that a hypothetical member of the public drinks 2 L/day of water drawn exclusively from a single well continuously for 70 yr. All sources of contamination were included in the exposure and toxicity assessment.

Infant HQ values for nitrate were also calculated according to EPA guidance. The infant toxicity assessment assumed a 0.64 L/day ingestion rate over a period of 1 yr, using the maximum annual concentration of nitrate calculated in any single supply well.

Figure A-12 shows the HIs and HQs calculated for hypothetical adult exposures to concentrations of nitrate and perchlorate in water pumped from PM-4 (a) and PM-5 (b). In a general sense, the HI and HQ values follow the trends of the calculated contaminant arrivals at each of the wells. The main difference arises from the use of average 70-year concentrations in the exposure calculations. The HQ and HI values for hypothetical exposures to calculated concentrations of nitrate and perchlorate in waters pumped from PM-4 (a) never exceed 1.0. The HQ values for hypothetical exposures to calculated nitrate concentrations in waters pumped from PM-5 (b) are essentially zero, but the HQ values for hypothetical exposures to perchlorate concentrations in PM-5 are well above 1.0, reaching a maximum of about 8.0. The HI values calculated for both PM-4 and PM-5 exposures are due entirely to perchlorate.

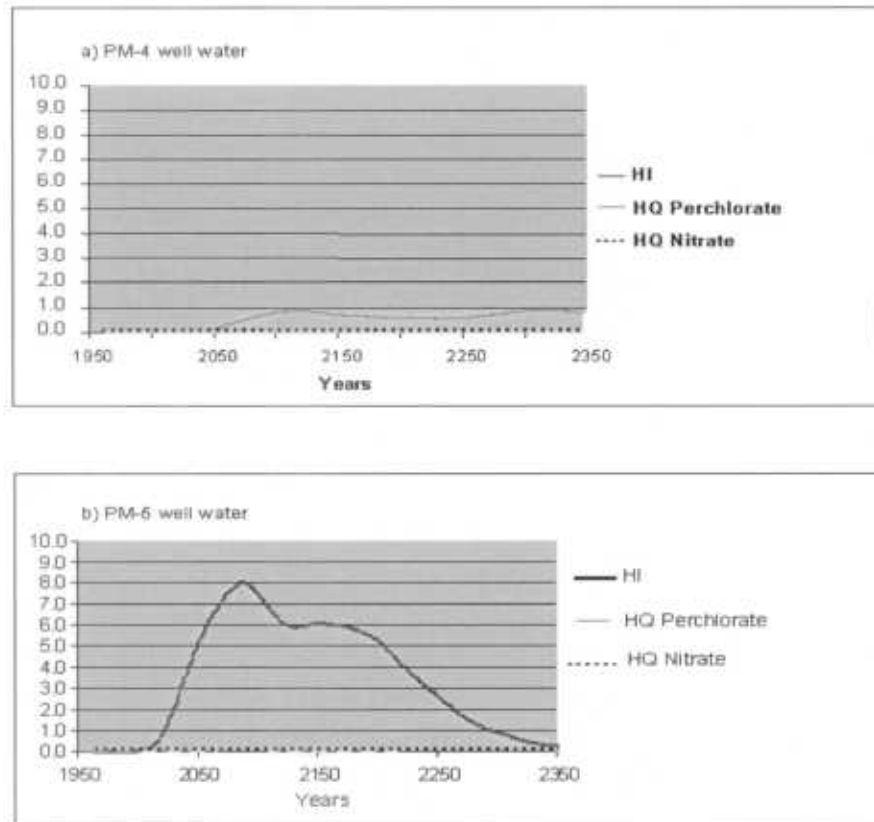


**Figure A-12. Individual nitrate and perchlorate HQs and cumulative HI for adult exposures to concentrations calculated in PM-4 (a) and PM-5 (b) water**

Figure A-13 shows the HQ for hypothetical infant exposures to nitrate concentrations calculated in well water from PM-4 (a) and PM-5 (b). The maximum infant HQ never exceeds the threshold value of 1.

The results of the Mortandad Tier-1 point-estimate risk assessment provide rationale for conducting a higher-tier risk assessment. According to EPA guidance, Tier 2 proceeds with additional data collection, characterizes variability and/or uncertainty, and a more in-depth sensitivity analysis, but more advanced techniques are used in Tier 3 to simultaneously characterize variability and uncertainty. To allow for the development of a decision-analysis tool to aid in decision-making regarding ongoing investigations and imminent corrective-action decisions (including monitoring) for groundwater contamination in Mortandad Canyon, a Tier-3 risk assessment was recommended.

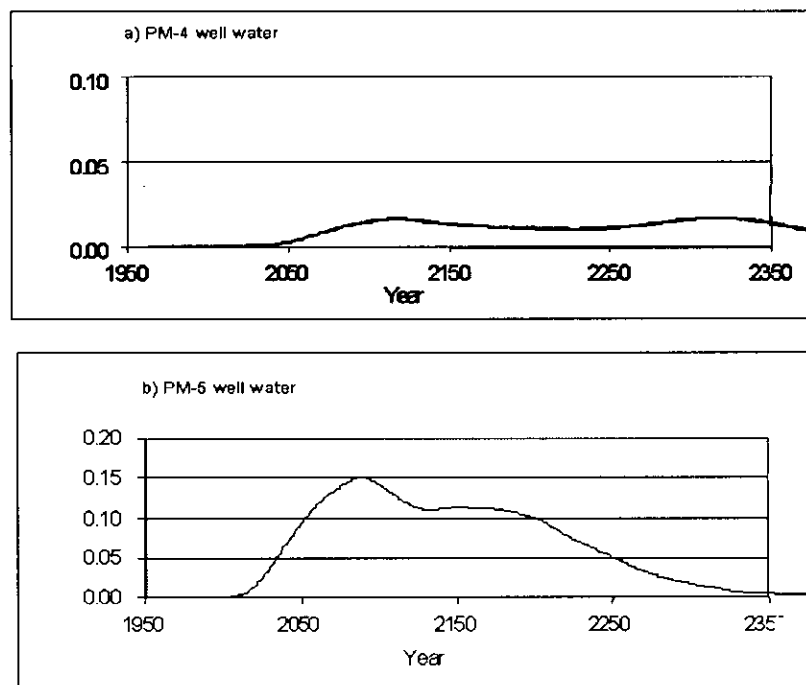


**Figure A-13. Nitrate HQs for infant exposures to concentrations calculated in PM-4 (a) and PM-5 (b) water**

#### A-5.0 REFERENCES

The following list includes all documents cited in this document. Parenthetical information following each reference provides the author, publication data, and ER ID number. This information is also included in text citations. ER ID numbers are assigned by the ENV-ERS Records Processing Facility (RPF) and are used to locate the document at the RPF.

Carey, B., G. Cole, C. Lewis, F. Tasi, R. Warren, and G. WoldeGabriel, 1999. "Revised Site-Wide Geologic Model for Los Alamos National Laboratory (FY99)," Los Alamos National Laboratory document LA-UR-00-2056, Los Alamos, New Mexico. (Carey et al. 1999, 66782)

EPA (Environmental Protection Agency) December 2000. "U.S. EPA Risk Assessment Guidance for Superfund (RAGS) Volume III—Part A: Process for Conducting Probabilistic Risk Assessment," (EPA 540-R-02-002, OSWER 9285.7-45, PB2002 963302). (EPA RAGS3; EPA 2000, 85534).

EPA (Environmental Protection Agency) Integrated Risk Database (IRIS) web page, 2005. Perchlorate and Perchlorate Salts. (visited July 2005) ([www.epa.gov/iris/subst/1007.htm](http://www.epa.gov/iris/subst/1007.htm)) [Electronic copy: Perchlorate and Perchlorate Salts, IRIS, Environmental Protection Agency.htm] (EPA 2005).

LANL (Los Alamos National Laboratory) 2003. "Groundwater Annual Status Report for Fiscal Year 2002, March 2003," Los Alamos National Laboratory document LA-UR-03-0244, Los Alamos, New Mexico. (LANL 2003, 76059)

LANL (Los Alamos National Laboratory), 2004. "Mortandad Canyon Groundwater Work Plan, Revision 1." Los Alamos National Laboratory document LA-UR-04-0165, Los Alamos, New Mexico. (LANL 2004, 82613)

Purtymun, W.D., 1967. "The Disposal of Industrial Effluents in Mortandad Canyon, Los Alamos County, New Mexico," U.S. Department of the Interior Geological Survey, Santa Fe, New Mexico. (Purtymun 1967, 11785)

van Genuchten, M.T., 1980. "A Closed-Form Solution for Predicting the Hydraulic Conductivity of Unsaturated Soils," *Soil Sci. Of Amer. J.*, Vol. 44, pp. 892–898. (van Genuchten 1980, 63542)

Zyvoloski, G.A., B.A. Robinson, Z.V. Dash, and L.L. Trease. 1997, "Summary of the Models and Methods for the FEHM Application—a Finite-Element Heat- and Mass-Transfer Code," Los Alamos National Laboratory report LA-13307-MS, Los Alamos National Laboratory, Los Alamos, New Mexico. (Zyvoloski et al. 1997, 70147).

## **Appendix B**

---

*Parameter Distributions and Parameter Sampling*

## B-1.0 OVERVIEW

This appendix provides a description of the parameter distributions and parameter sampling routine used in the Mortandad Canyon Tier-3 probabilistic risk assessment. The sampled distributions and justifications for each distribution are also provided.

## B-2.0 SAMPLING PROCEDURE

Crystal Ball 7 software developed by Decisioneering, Inc., was used to sample from user-defined probability distributions. Crystal Ball works within Microsoft Excel and offers a variety of sampling schemes for sampling from user-defined probability density functions (pdf). For the Mortandad Canyon Tier-3 risk assessment, 41 model parameters were defined as uncertain. All other parameters were treated deterministically. Probability density functions were defined for each of the uncertain parameters (see Section B.3.0 for pdf definitions). Latin hypercube sampling (LHS) (McKay et al. 1979, 90183) was then used to generate one-thousand stratified random samples of model input for each conceptual model analyzed.

The following discussion of LHS is based on discussions in Wyss and Jorgensen (1998, 90122) and a Rutgers University web publication <http://www.ccl.rutgers.edu/~ssi/srsmreport/node8.html>.

LHS was developed by McKay, Conover, and Beckman (1979, 90183) and has been in use for nuclear-reactor safety and radioactive-waste disposal problems (including for groundwater flow and transport models) since 1975 (Wyss and Jorgensen 1998, 90122). LHS is a stratified sampling scheme that seeks to minimize the number of samples needed to cover the parameter space defined by each pdf. LHS begins by dividing each parameter pdf into  $M$  segments of equal probability. In the Mortandad Canyon Tier-3 risk assessment, each parameter pdf is divided into 1,000 equally probable segments ( $M = 1000$ ). The whole parameter space, consisting of  $N$  parameters (41), is partitioned into  $M^N$  cells ( $1000^{41}$ ), each having equal probability. The following simple example is used to explain how LHS works. Consider a model with just two uncertain parameters, one defined by a normal distribution and the other defined by a uniform distribution. For this example, assume that five samples will be taken from each parameter distribution, resulting in five sets of parameters to use in the model. LHS begins by dividing each parameter pdf into five equally probable segments (Figure B-1). Dividing a pdf into five equally probable segments yields a probability of 0.2 (or 20%) for each segment.

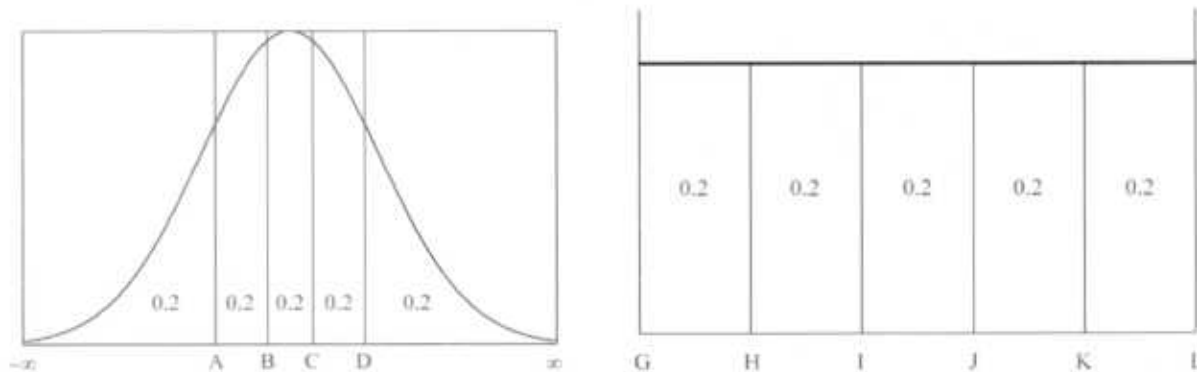


**Figure B-1. Division of the parameter of two hypothetical variables into five equally probable segments**

Next, a random sample is drawn from each probability interval for each parameter. This results in a joint parameter space consisting of two parameters partitioned into five segments each one or  $5^2$  (25) cells (Figure B-2). The next step is to choose five sets of model input where a given set of input is found in one of the 25 cells. For example, cell number (2, 1) indicates that the sample lies in segment 2 with respect to the first parameter and segment 1 with respect to the second parameter. Selection of a specific cell is based on random sampling coupled with the condition that no cell is sampled twice. A possible result of this sampling is shown in Figure B-2.

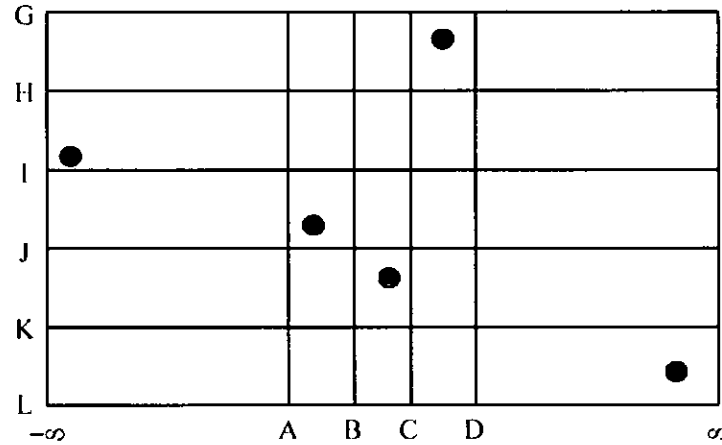
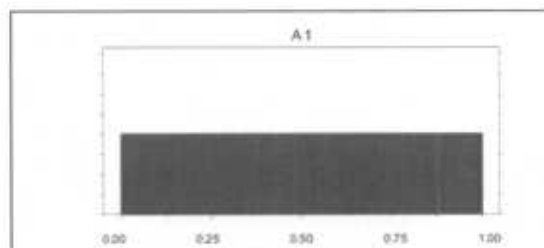


**Figure B-2. Parameter space and LHS sampling selected cells**

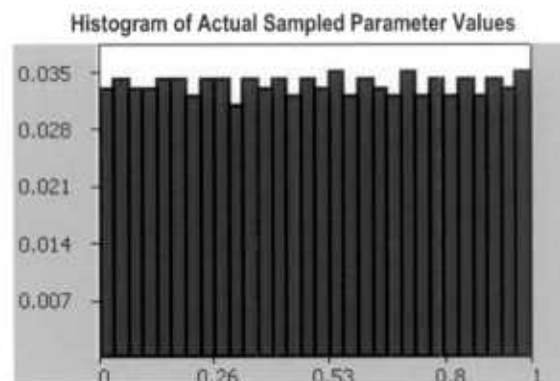
The advantage of this approach is that the random samples are generated from all the possible ranges of values. In contrast to traditional Monte Carlo sampling, the behavior of the model or modeling system is investigated not only across the range of potential parameter values but specifically at the tails of each distribution with relatively few samples.

## B-3.0 PROBABILITY DISTRIBUTION FUNCTIONS

Variable	Source Interpolation Factor [-]
Theoretical Distribution	
Distribution	Uniform
Minimum	0.000
Maximum	1.000



Distribution	Uniform
Minimum	0.0010
Maximum	0.9989
Mean	0.5000
Median	0.5003
Standard Deviation	0.2888



## Justification for Parameter Distribution

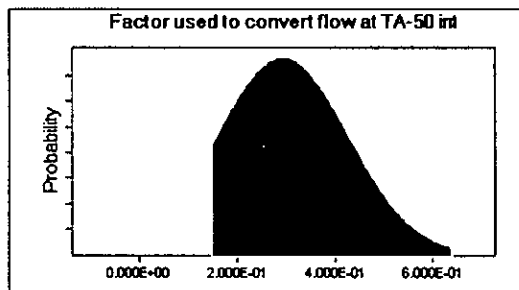
Upper and lower bounds for both the perchlorate source term and the nitrate source term were estimated for this study (Birdsell et al., 2005, in progress). This parameter ranges uniformly between 0 and 1 and is used to interpolate between the upper and lower bound curves. If the parameter is zero, the lower-bound source term is used. If the parameter equals one, the upper-bound source is used. For values between 0 and 1, the source is determined by linearly interpolating between the upper and lower bounds. The source (mass flux versus time) is a boundary condition that is applied to the unsaturated-zone transport simulations. This boundary condition is calculated by the vadose-zone infiltration computer code and within that code.

Background: The source-term bounds assume that nitrate in the environment undergoes denitrification, as explained in Birdsell et al. (2005, in progress). A range of 2% to 30% of the original nitrate source (based on TA-50 outfall records) is estimated to be lost for this study. This range was obtained by estimating nitrate losses using both a mass-balance approach and by comparing the mass ratio of nitrate degradation products to nitrate. Therefore, the upper and lower bounds of the nitrate source are defined simply by accounting for either 2% or 30% less nitrate, respectively.

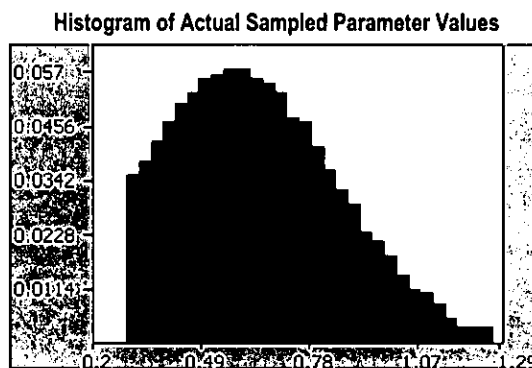
The perchlorate source is derived from the nitrate source based on vadose-zone concentration profiles with depth (see Birdsell et al. 2005, in progress). The nitrate and perchlorate concentration profiles were observed to be correlated. The correlation between the data and the estimate of nitrate degradation was used to derive the upper- and lower-bound estimates of the perchlorate source.

Variable	TA-50 Flow to Surface Flow Conversion Factor [-]
<b>Theoretical Distribution</b>	
<b>Distribution</b>	<b>Truncated Normal</b>
Minimum	0.1489
Maximum	0.6365
Mean	0.2926
Standard Deviation	0.1329

Note: The actual distribution used in the vadose-zone simulations is double that defined in the theoretical distribution.



Distribution	Truncated Normal
Minimum	0.2987
Maximum	1.2723
Mean	0.6500
Median	0.6303
Standard Deviation	0.2091



**Justification for Parameter Distribution**

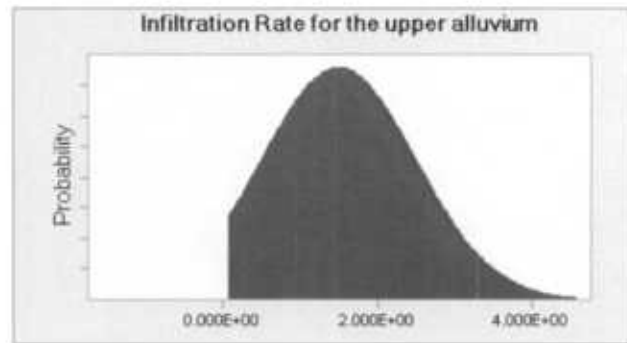
The “actual sampled” distribution for this variable, which was used in the vadose-zone simulations, is double that originally defined by the “theoretical distribution” given above. Therefore, the bottom histogram and the statistics that describe it are twice that shown for the theoretical distribution and its statistics, shown at the top.

This parameter is used to calculate the volumetric flow of water into the modeled section of Mortandad Canyon as a function of the volumetric flow of water released at the TA-50 Radiological Liquid and Waste Treatment Facility (RLWTF). The parameter accounts for two processes to calculate the net dilution or concentration of the RLWTF outfall volume: (1) dilution of the RLWTF outfall by other surface water sources and (2) water lost to evapotranspiration, which acts to concentrate the outfall concentrations. This variable is called fgs1 in the vadose-zone infiltration code. The infiltration model is described in the main body of this report and also in detail by Birdsell et al. (2005, in progress). Birdsell et al. (2005, in progress) also give details about the computer code that implements the vadose-zone infiltration model. For the vadose-zone simulations,

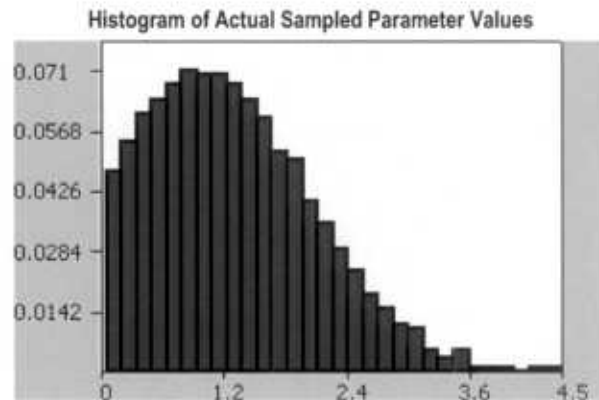
The volumetric flow of water into the canyon = (the volumetric flow of liquid waste from the RLWTF)/fgs1.

The distribution for this parameter was originally developed by comparing nitrate concentrations at alluvial well MCO-4 to reported RLWTF outfall nitrate concentrations for the years 1970 to 1993 (Birdsell 2004, 90121, p. 55). This comparison yields resultant dilution factors of the alluvial aquifer compared to the RLWTF source, which acts as the source of infiltration to the deep vadose zone. However, using this distribution of dilution, the vadose-zone simulation results indicated that the calculated moisture content was much wetter (higher) than that measured in the canyon. The source-term study for nitrate within the canyon estimated that up to half the nitrate could be lost to denitrification (Birdsell et al. 2005, in progress). Using this as an estimate of the nitrate into the system, the distribution (developed by comparing MCO-4 nitrate concentrations to RLWTF nitrate concentrations) is exactly doubled. The doubling of this parameter (which decreases volumetric flow into the canyon by half) yielded better agreement between simulated and measured water contents. It also resulted in better agreement between measured and simulated nitrate concentration profiles and plume depth (Birdsell 2004, 90121, pp. 79–80).

Variable	Infiltration Rate for the Upper Canyon
Theoretical Distribution	
Distribution	Truncated Normal
Minimum	0.050
Maximum	4.47
Mean	1.50
Standard Deviation	1.00



Distribution	Truncated Normal
Minimum	0.0500
Maximum	4.4713
Mean	1.3068
Median	1.2158
Standard Deviation	0.7859

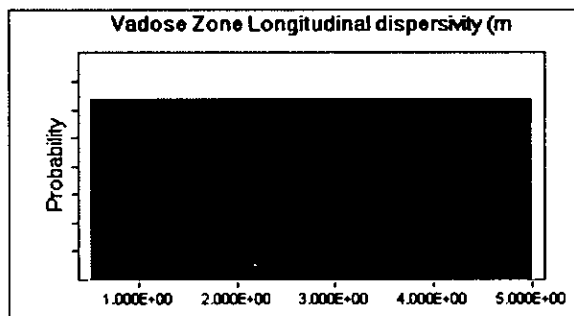


### Justification for Parameter Distribution

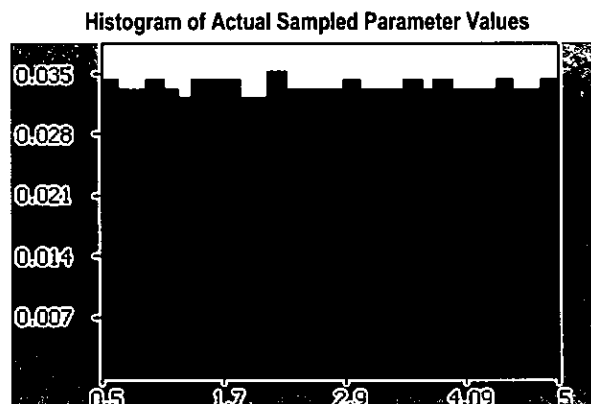
The parameter distribution that defines the "infiltration rate for the upper canyon" actually represents the distribution of maximum infiltration rates in the upper and middle canyon sections for infiltration from the perched alluvial system into the deeper vadose zone. For a particular realization, the vadose-zone infiltration model, which defines the time-dependent infiltration rate to the 38 one-dimensional vadose-zone simulations, maintains the upper and middle canyon infiltration rate as a constant (for the sampled value for a particular computational realization), provided there is sufficient water entering the canyon to both maintain the maximum infiltration rate and to send a minimum percentage of the flow to the next canyon section. The infiltration model and locations of the canyon sections are described in the main body of this report and also in detail by Birdsell et al. (2005, in progress). Birdsell et al. (2005, in progress) also give details about the computer code that implements the vadose-zone infiltration model.

The distribution for the parameter that defines the maximum infiltration rate in the upper and middle canyon sections is based on infiltration and water-balance estimates by Purtymun (1967, 11785), Dander (1998, 88743), Geddis (1992, 31592) and Koenig and McLin (1992, 56029). However, the parameter distribution was updated to the final distribution given above as simulations were performed because very high values (e.g., 6 m/yr) that were originally defined for the upper canyon were not consistent with the evolving conceptual model of infiltration in the canyon or with field data. That is, Purtymun originally thought that the highest infiltration rates occurred in the upper canyon. As field investigations have been completed in the canyon, the conceptual model has evolved so that currently the highest infiltration rates are thought to occur near the sediment traps, which are located in the lower canyon. The time-dependent infiltration model calculates infiltration rates for the upper, middle, lower, and bottom canyon sections using a mass-balance approach, as defined by Birdsell et al. (2005, in progress) and in the vadose-zone section of this report.

Variable	Vadose-Zone Longitudinal (Vertical) Dispersivity [m]
Theoretical Distribution	
Distribution	Uniform
Minimum	0.500
Maximum	5.00



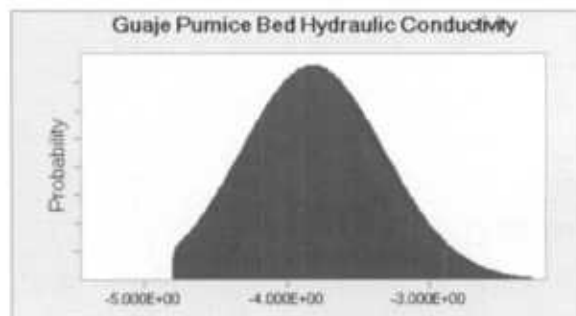
Distribution	Uniform
Minimum	0.5038
Maximum	4.9968
Mean	2.7500
Median	2.7516
Standard Deviation	1.2996



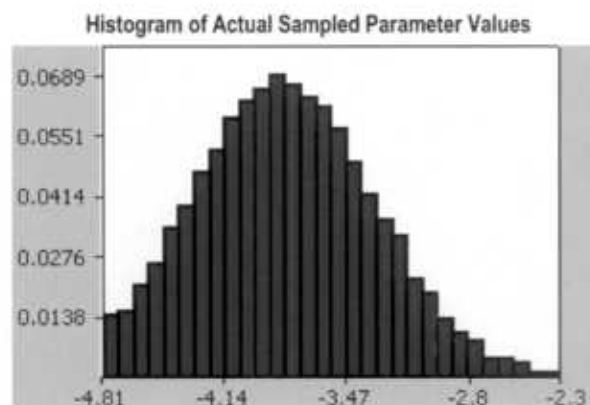
**Justification for Parameter Distribution**

Longitudinal dispersivity is a measure of the spreading of a contaminant front that results from flowing through the tortuous pathways in a porous material. No site data are available for this parameter in the vadose zone. The parameter distribution for the vadose-zone longitudinal (vertical) dispersivity is therefore estimated, based on grid spacing and literature values often used for similar unsaturated-zone studies (Neuman, 1990, 90184).

Variable	Guaje Pumice Bed Hydraulic Conductivity (Log) [cm/s]
Theoretical Distribution	
Distribution	Truncated Log Normal
Minimum	-4.80
Maximum	$\infty$
Mean	-3.820
Standard Deviation	0.500



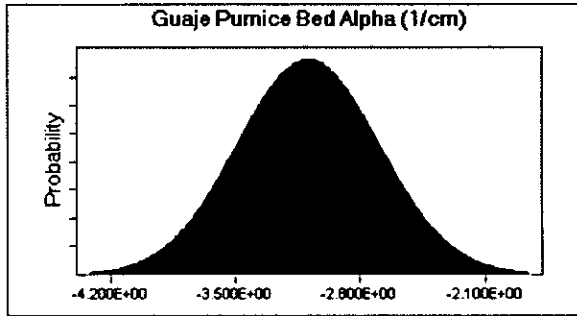
Distribution	Truncated Log Normal
Minimum	-4.7950
Maximum	-1.9218
Mean	-3.7898
Median	-3.8043
Standard Deviation	0.4698



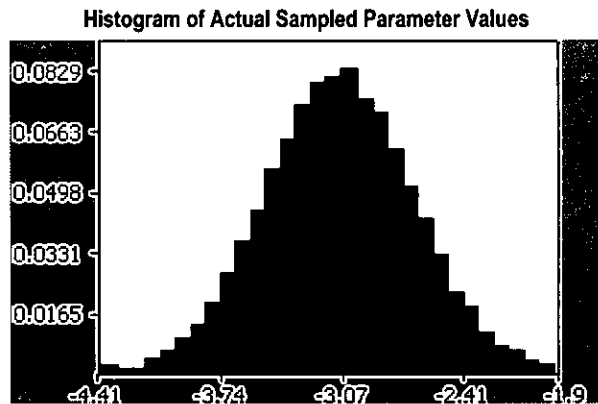
#### Justification for Parameter Distribution

The mean value of the hydraulic conductivity ( $K_s$ ) distribution for the Guaje Pumice is based on the single value measured on a single core sample reported by Springer (1995, 90118) and used for the MDA G Performance Assessment (Birdsell et al. 1999, 69792). Because there is no standard deviation available for this single sample, the standard deviation for the parameter distribution of  $K_s$  is estimated to be similar to those standard-deviation values determined by Springer for Unit 1g, the Otowi Member, and the Tsankawi/Cerro Toledo (See those parameter distributions, as given later in this appendix and in Birdsell, 2003, 90119, p. 149).

Variable	Guaje Pumice Bed Alpha (Log) [1/cm]
Theoretical Distribution	
Distribution	Normal
Minimum	$-\infty$
Maximum	$\infty$
Mean	-3.90
Standard Deviation	0.400



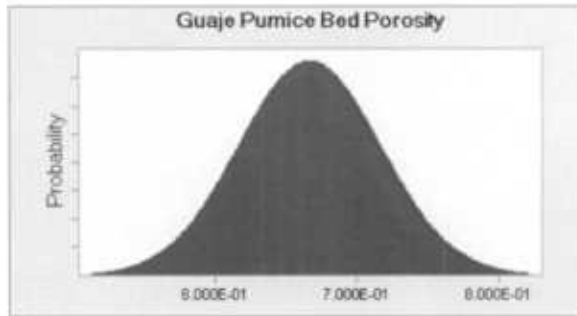
Distribution	Normal
Minimum	-4.3840
Maximum	-1.9071
Mean	-3.0903
Median	-3.0899
Standard Deviation	0.3999



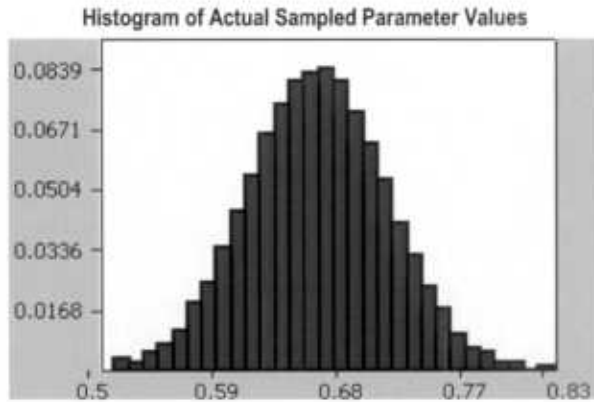
**Justification for Parameter Distribution**

This parameter is the alpha-fitting parameter used in the van Genuchten (1980, 63542 ) formula for the unsaturated water retention curve for the Guaje Pumice bed. The mean value defined for the parameter distribution of alpha for the Guaje Pumice is based on the alpha value derived for a single core sample reported by Springer (1995, 90118) and used for the material disposal area (MDA) G Performance Assessment (Birdsell et al. 1999, 69792). Because no standard deviation was available from the single core sample, the standard deviation value for the distribution, shown above, was estimated for this study to be similar to those determined by Springer for the Units 1g, Otowi Member, and the Tsankawi/Cerro Toledo (as given with those hydrologic units later in the appendix). See those parameter distributions and Birdsell, 2003, 90119, p. 149.

Variable	Guaje Pumice Bed Porosity [-]
Theoretical Distribution	
Distribution	Truncated Normal
Minimum	0.0000
Maximum	0.9970
Mean	0.6670
Standard Deviation	0.0500



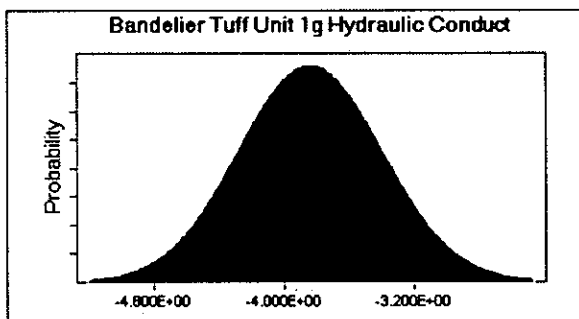
Distribution	Truncated Normal
Minimum	0.5170
Maximum	0.8377
Mean	0.6670
Median	0.6669
Standard Deviation	0.0500



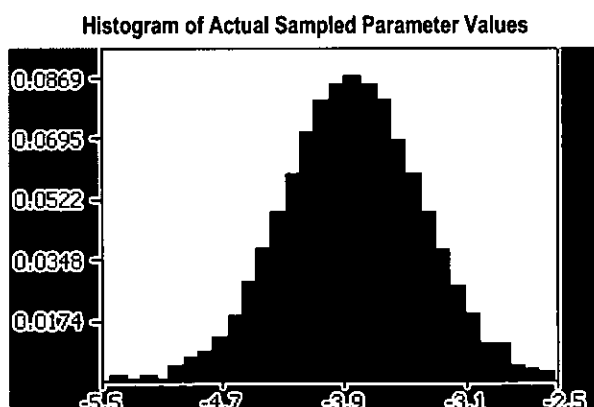
#### Justification for Parameter Distribution

The mean value of the porosity distribution for the Guaje Pumice is based on the single value measured on a single core sample reported by Springer (1995, 90118) and used for the MDA G Performance Assessment (Birdsell et al. 1999, 69792). The standard deviation value is estimated to be similar to those determined by Springer for Unit 1g, the Otowi Member, and the Tsankawi/Cerro Toledo. (See those parameter distributions, as given later in this appendix and in Birdsell, 2003, 90119, p. 149.)

	<b>Bandelier Tuff Unit 1g Hydraulic Conductivity (Log) [cm/s]</b>
<b>Variable</b>	
<b>Theoretical Distribution</b>	
<b>Distribution</b>	<b>Normal</b>
Minimum	-∞
Maximum	∞
Mean	-3.840
Standard Deviation	0.4400
Correlated with	Bandelier Tuff 1g Alpha
Coefficient	0.53



<b>Distribution</b>	<b>Normal</b>
Minimum	-5.4283
Maximum	-2.3983
Mean	-3.8402
Median	-3.8401
Standard Deviation	0.4405



**Justification for Parameter Distribution**

The parameter distribution for the hydraulic conductivity ( $K_s$ ) for Unit 1g comes from the distribution for  $\text{Log}_{10} K_s$  given below in Table B-1. Table B-2 shows the correlation between parameters for Unit 1g.

**Table B-1  
Bandelier Tuff Unit 1g Statistical Analyses of Hydrologic Properties**

Note: Estimated by Springer (2003, 90071), using core samples

Property	Canyon-Mesa Interaction	Distribution	Mean	Standard Deviation
Bulk Density	No	—*	1.17	0.11
$\theta_s$	Yes	Normal	0.50	0.06
$\theta_r$	Yes	—*	0.02	0.03
$\text{Log}_{10} K_s$	No	Normal	-3.84	0.44
N	No	Normal	1.60	0.21
$\text{Log}_{10} \alpha$	No	—*	-2.08	0.39
Porosity	Not tested	—*	0.52	0.05

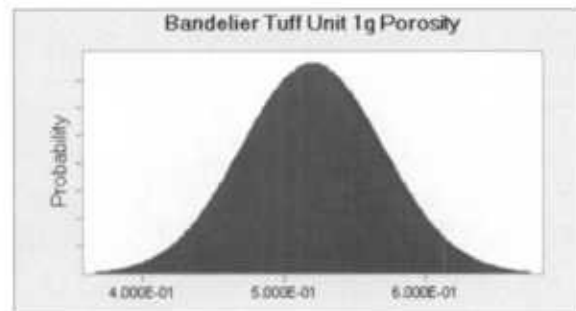
\*The distribution is unknown.

**Table B-2**  
Correlation between Parameters for Unit 1g

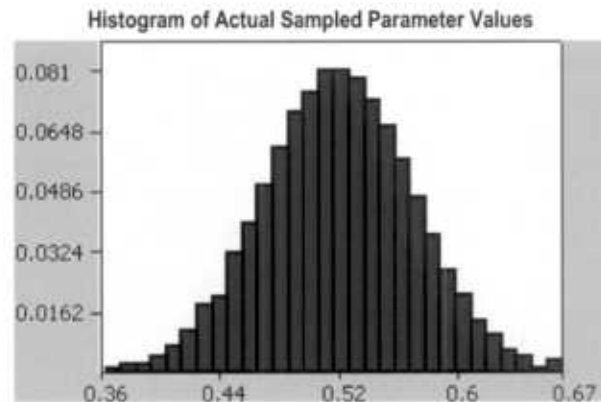
Property	Bulk Density	$\theta_s$	$\theta_r$	$\text{Log}_{10} K_s$	N	$\text{Log}_{10} \alpha$
Bulk Density	1.0	-0.15	0.19	-0.33 <sup>a</sup>	-0.26	0.14
$\theta_s$	-0.15	1.0	0.08	0.47 <sup>a</sup>	-0.39 <sup>a</sup>	0.46 <sup>a</sup>
$\theta_r$	0.19	0.08	1.00	-0.09	0.10	0.01
$\text{Log}_{10} K_s$	-0.33 <sup>a</sup>	0.47 <sup>a</sup>	-0.09	1.0	-0.39 <sup>a</sup>	0.53 <sup>a</sup>
N	-0.26	-0.39 <sup>a</sup>	0.10	-0.39 <sup>a</sup>	1.0	-0.82 <sup>a</sup>
$\text{Log}_{10} \alpha$	0.14	0.46 <sup>a</sup>	0.01	0.53 <sup>a</sup>	-0.82 <sup>a</sup>	1.0

<sup>a</sup> Indicates significant correlation at the 0.05 level.

Variable	Bandelier Tuff Unit 1g Porosity [-]
Theoretical Distribution	
Distribution	Truncated Normal
Minimum	0.000
Maximum	1.000
Mean	0.520
Standard Deviation	0.050



Distribution	Normal
Minimum	0.3522
Maximum	0.6700
Mean	0.5200
Median	0.5200
Standard Deviation	0.0500

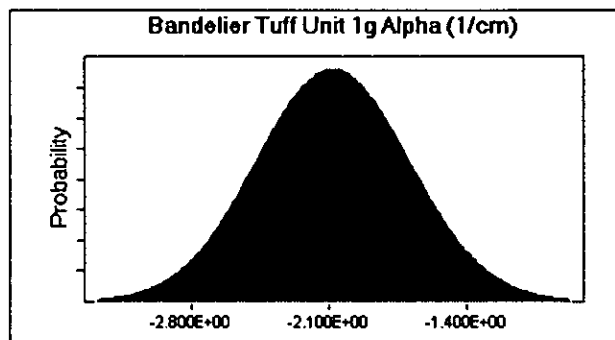


#### Justification for Parameter Distribution

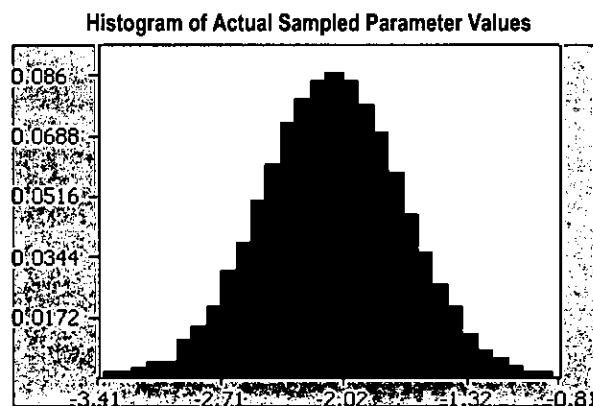
The parameter distribution for the porosity of Unit 1g comes from the distribution estimated by Springer (2003, 90071), using core samples.

See Table B-1 on page B-10 under the parameter distribution for Bandelier Tuff Unit 1g Hydraulic Conductivity information.

Variable	Bandelier Tuff Unit 1g Alpha (Log) [1/cm]
<b>Theoretical Distribution</b>	
Distribution	Normal
Minimum	$-\infty$
Maximum	$\infty$
Mean	-2.080
Standard Deviation	0.3900
Correlated with Coefficient	Bandelier Tuff Unit 1 g Hydraulic Conductivity 0.53



Distribution	Normal
Minimum	-3.3715
Maximum	-0.7953
Mean	-2.0800
Median	-2.0803
Standard Deviation	0.3903

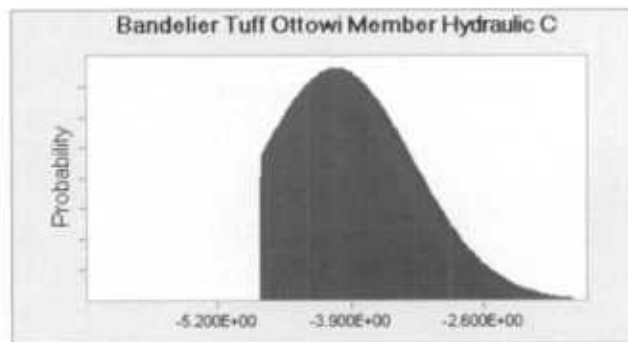


**Justification for Parameter Distribution**

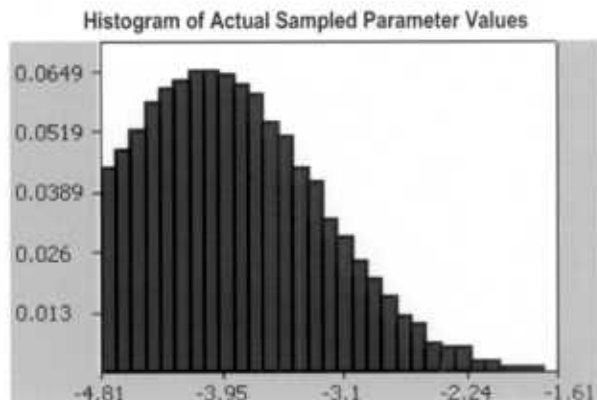
This parameter is the alpha-fitting parameter used in the van Genuchten (1980, 63542) formula for the unsaturated water-retention curve for Unit 1g. The parameter distribution for alpha comes from the distribution estimated by Springer (2003, 90071), using core samples of Unit 1g tuff. The alpha parameter is correlated to the hydraulic conductivity.

See Tables B-1 and B-2 above under the parameter distribution for Bandelier Tuff Unit 1g Hydraulic Conductivity information.

Variable	Bandelier Tuff Otowi Member Hydraulic Conductivity (Log) [cm/s]
Theoretical Distribution	
Distribution	Truncated Normal
Minimum	-4.800
Maximum	$\infty$
Mean	-4.050
Standard Deviation	0.7500



Distribution	Truncated Normal
Minimum	-4.7967
Maximum	-1.5911
Mean	-3.8342
Median	-3.8998
Standard Deviation	0.5958



### Justification for Parameter Distribution

The parameter distribution for the hydraulic conductivity ( $K_s$ ) for the Otowi Member comes from the distribution for  $\text{Log}_{10} K_s$  given below (Tables B-3 and B-4).

**Table B-3**  
**Bandelier Tuff Otowi Member Statistical Analyses of Hydrologic Properties**

(Note: Hydrologic properties estimated by Springer (2003, 90071), using core samples. Minimum  $K_s$  truncated so that the Otowi Member would not saturate in simulations with the highest infiltration rates.)

Property	Canyon-Mesa Interaction	Distribution	Mean	Standard Deviation
Bulk Density	No	—*	1.21	0.11
$\theta_s$	No	Normal	0.44	0.06
$\theta_r$	Yes	—*	0.00	0.02
$\text{Log}_{10} K_s$	Yes	—*	-4.05	0.75
N	No	—*	1.90	0.50
$\text{Log}_{10} \alpha$	No	—*	-2.39	0.38
Porosity	Not tested	—*	0.48	0.05

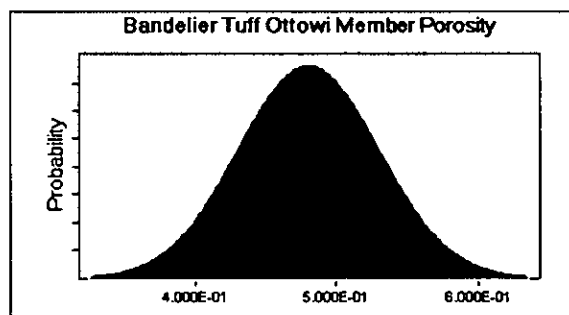
\* The distribution is unknown.

**Table B-4**  
**Correlation between Parameters for Otowi Member**

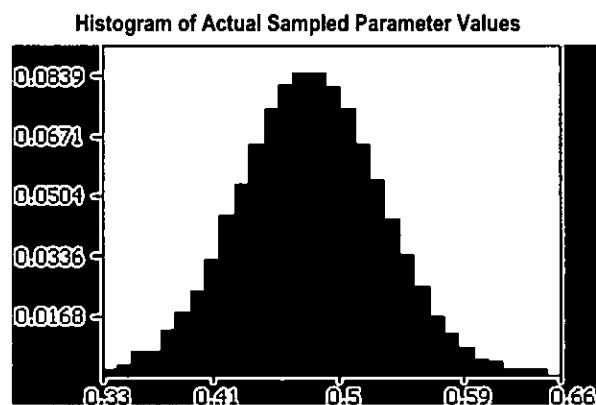
Property	Bulk Density	$\theta_s$	$\theta_r$	$\text{Log}_{10} K_s$	N	$\text{Log}_{10} \alpha$
Bulk Density	1.0	-0.59*	0.08	-0.49*	0.22	-0.34*
$\theta_s$	-0.59*	1.00	0.24	0.68*	-0.47	0.61*
$\theta_r$	0.08	0.24	1.0	0.39*	-0.02	0.09
$\text{Log}_{10} K_s$	-0.49*	0.68*	0.39*	1.00	-0.44	0.28
N	0.22	-0.47*	-0.02	-0.44*	1.0	-0.85*
$\text{Log}_{10} \alpha$	-0.34*	0.61*	0.09	0.28	-0.85*	1.0

\* Indicates significant correlation at the 0.05 level.

Variable	Bandelier Tuff Otowi Member Porosity [-]
<b>Theoretical Distribution</b>	
<b>Distribution</b>	Truncated Normal
Minimum	0.000
Maximum	1.000
Mean	0.4800
Standard Deviation	0.0500



Distribution	Normal
Minimum	0.3293
Maximum	0.6502
Mean	0.4800
Median	0.4800
Standard Deviation	0.0500

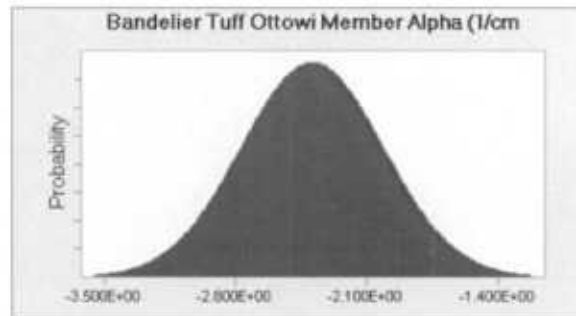


**Justification for Parameter Distribution**

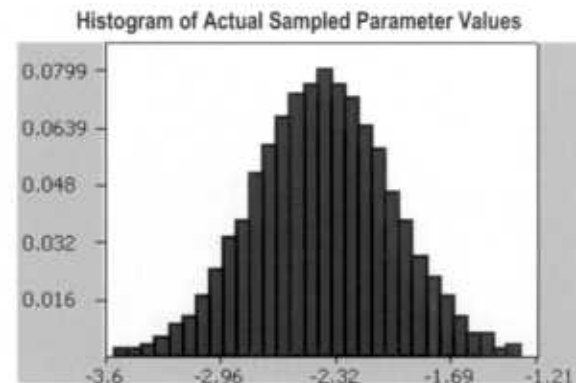
The parameter distribution for the porosity of the Otowi Member comes from the distribution estimated by Springer (2003, 90071), using core samples.

See Table B-3 under the parameter distribution for Bandelier Tuff Otowi Member Hydraulic Conductivity information.

Variable	Bandelier Tuff Otowi Member Alpha (Log) [1/cm]
Theoretical Distribution	
Distribution	Normal
Minimum	$-\infty$
Maximum	$\infty$
Mean	-2.390
Standard Deviation	0.3800



Distribution	Normal
Minimum	-3.5411
Maximum	-1.2779
Mean	-2.3900
Median	-2.3901
Standard Deviation	0.3791

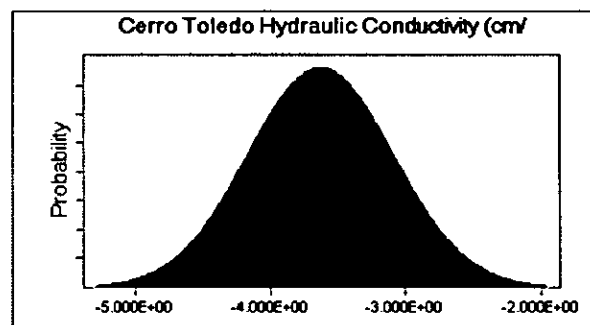


#### Justification for Parameter Distribution

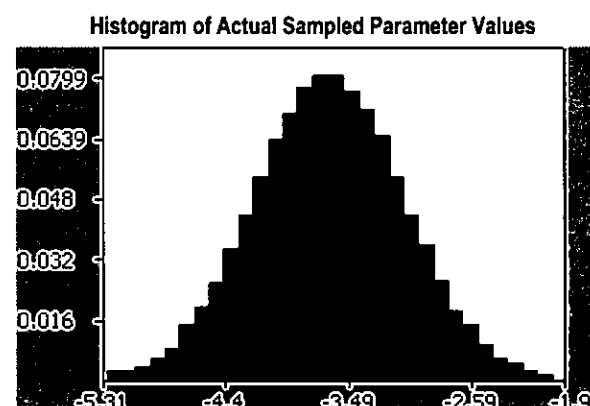
This parameter is the alpha-fitting parameter used in the van Genuchten (1980, 63542) formula for the unsaturated water-retention curve for the Otowi Member. The parameter distribution for alpha comes from the distribution estimated by Springer (2003, 90071), using core samples of Otowi Member tuff. The alpha parameter is correlated to the hydraulic conductivity.

See Tables B-3 and B-4 above under the parameter distribution for Bandelier Tuff Otowi Member Hydraulic Conductivity information.

Variable	Cerro Toledo Hydraulic Conductivity (Log) [cm/s]
<b>Theoretical Distribution</b>	
<b>Distribution</b>	Normal
Minimum	$-\infty$
Maximum	$\infty$
Mean	-3.630
Standard Deviation	0.5400
Correlated with Coefficient	Cerro Toledo Alpha 0.67



Distribution	Normal
Minimum	-5.2675
Maximum	-1.9674
Mean	-3.6298
Median	-3.6298
Standard Deviation	0.5391



**Justification for Parameter Distribution**

The parameter distribution for the hydraulic conductivity ( $K_s$ ) for the Cerro Toledo interval comes from the distribution for  $\text{Log}_{10} K_s$  given below (Tables B-5 and B-6).

**Table B-5**  
**Cerro Toledo/Tsankawi Statistical Analyses of Hydrologic Properties**

(Note: Estimated by Springer (2003, 90071), using core samples)

Property	Distribution	Mean	Standard Deviation
Bulk Density	—	1.22	0.22
$\theta_s$	—	0.48	0.09
$\theta_r$	—	0.01	0.02
$\text{Log}_{10} K_s$	Normal	-3.63	0.54
N	Normal	1.48	0.19
$\text{Log}_{10} \alpha$	Normal	-1.93	0.52
Porosity	—	0.48	0.02

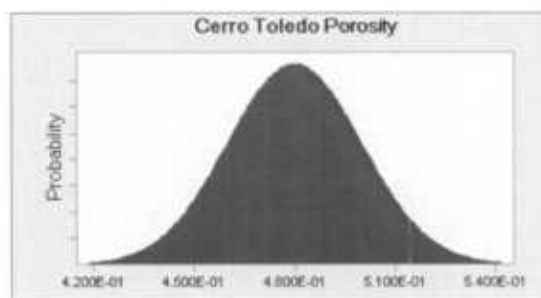
\* The distribution is unknown.

**Table B-6**  
**Correlation between Parameters for Cerro Toledo/Tsankawi**

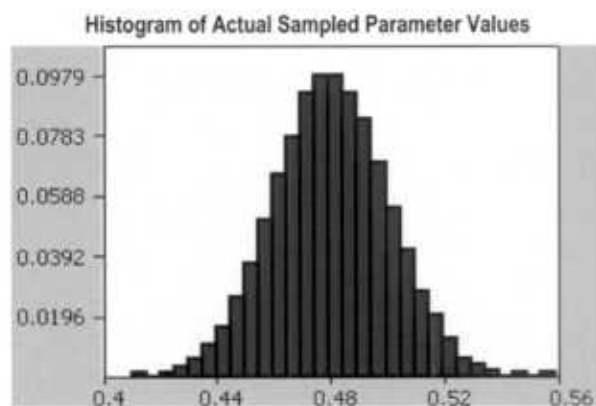
Property	Bulk Density	$\theta_s$	$\theta_r$	$\text{Log}_{10} K_s$	N	$\text{Log}_{10} \alpha$
Bulk Density	1.0	-0.41	-0.35	-0.07	0.16	-0.21
$\theta_s$	-0.41	1.0	-0.10	0.21	-0.75*	0.33
$\theta_r$	-0.35	-0.10	1.0	0.41	0.21	0.22
$\text{Log}_{10} K_s$	-0.07	0.21	0.41	1.0	0.0	0.67*
N	0.16	-0.75*	0.21	0.0	1.0	-0.27
$\text{Log}_{10} \alpha$	-0.21	0.33	0.22	0.67*	-0.27	1.0

\* Indicates significant correlation at the 0.05 level.

Variable	Cerro Toledo Porosity [-]
Theoretical Distribution	
Distribution	Truncated Normal
Minimum	0.000
Maximum	1.000
Mean	0.4800
Standard Deviation	0.0200



Distribution	Normal
Minimum	0.4052
Maximum	0.5585
Mean	0.4800
Median	0.4800
Standard Deviation	0.0201

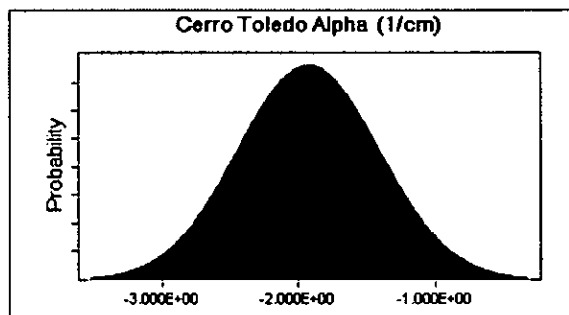


#### Justification for Parameter Distribution

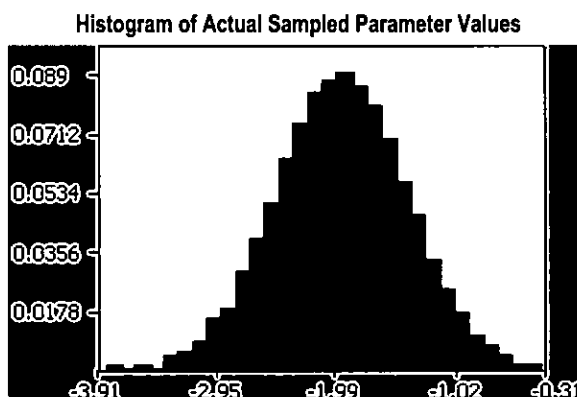
The parameter distribution for the porosity of the Cerro Toledo interval comes from the distribution estimated by Springer (2003, 90071), using core samples.

See Table B-5 under the parameter distribution for the Cerro Toledo interval Hydraulic Conductivity information.

Variable	Cerro Toledo Alpha (Log) [1/cm]
<b>Theoretical Distribution</b>	
<b>Distribution</b>	<b>Normal</b>
Minimum	$-\infty$
Maximum	$\infty$
Mean	-1.930
Standard Deviation	0.520
Correlated with Coefficient	Cerro Toledo Hydraulic Conductivity 0.67



Distribution	Normal
Minimum	-3.8203
Maximum	-0.1231
Mean	-1.9300
Median	-1.9300
Standard Deviation	0.5210

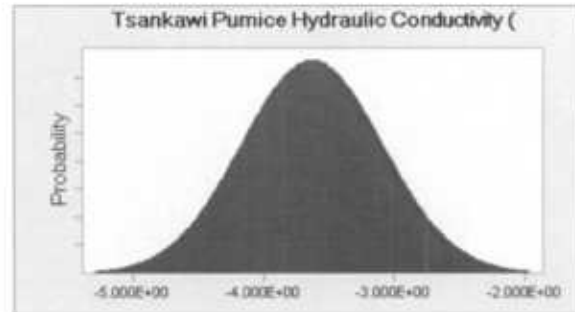


**Justification for Parameter Distribution**

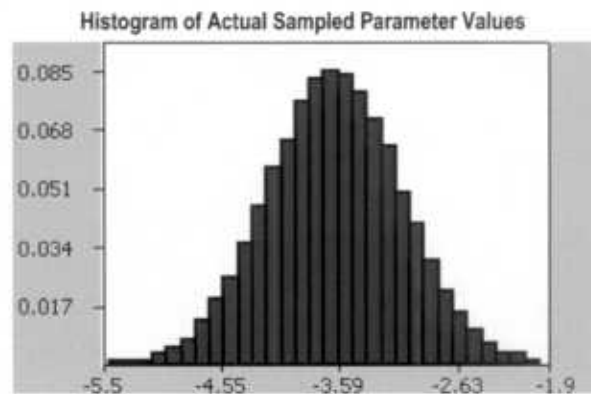
This parameter is the alpha-fitting parameter used in the van Genuchten (1980, 63542) formula for the unsaturated water-retention curve for the Cerro Toledo interval. The parameter distribution for alpha comes from the distribution estimated by Springer (2003, 90071), using core samples of material from the Cerro Toledo interval and the Tsankawi Pumice. The alpha parameter is correlated to the hydraulic conductivity.

See Tables B-5 and B-6 under the parameter distribution for Cerro Toledo interval hydraulic conductivity information.

Variable	Tsankawi Pumice Hydraulic Conductivity (Log) [cm/s]
<b>Theoretical Distribution</b>	
<b>Distribution</b>	<b>Normal</b>
Minimum	$-\infty$
Maximum	$\infty$
Mean	-3.630
Standard Deviation	0.5400
Correlated with Coefficient	Tsankawi Pumice Alpha 0.67



Distribution	Normal
Minimum	-5.4446
Maximum	-1.9235
Mean	-3.6301
Median	-3.6300
Standard Deviation	0.5401



### Justification for Parameter Distribution

The parameter distribution for the hydraulic conductivity ( $K_s$ ) for the Tsankawi Pumice comes from the distribution for  $\text{Log}_{10} K_s$  given below (Tables B-7 and B-8).

**Table B-7**  
**Cerro Toledo/Tsankawi Statistical Analyses of Hydrologic Properties**

(Note: Estimated by Springer (2003, 90071), using core samples)

Property	Distribution	Mean	Standard Deviation
Bulk Density	—*	1.22	0.22
$\theta_s$	—*	0.48	0.09
$\theta_r$	—*	0.01	0.02
$\text{Log}_{10} K_s$	Normal	-3.63	0.54
N	Normal	1.48	0.19
$\text{Log}_{10} \alpha$	Normal	-1.93	0.52
Porosity	—*	0.48	0.02

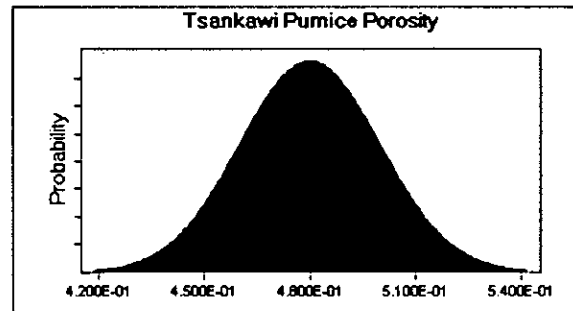
\* The distribution is unknown.

**Table B-8**  
**Correlation between Parameters for Cerro Toledo/Tsankawi**

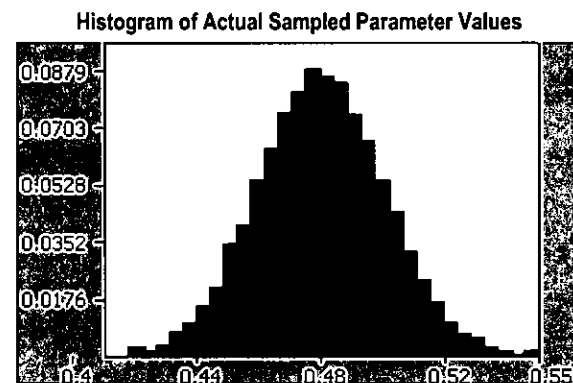
Property	Bulk Density	$\theta_s$	$\theta_r$	$\text{Log}_{10} K_s$	N	$\text{Log}_{10} \alpha$
Bulk Density	1.0	-0.41	-0.35	-0.07	.016	-0.21
$\theta_s$	-0.41	1.0	-0.10	0.21	-0.75*	0.33
$\theta_r$	-0.35	-0.10	1.0	0.41	0.21	0.22
$\text{Log}_{10} K_s$	-0.07	0.21	0.41	1.0	0.0	0.67*
N	0.16	-0.75*	0.21	0.0	1.0	-0.27
$\text{Log}_{10} \alpha$	-0.21	0.33	0.22	0.67*	-0.27	1.0

\*Indicates significant correlation at the 0.05 level.

Variable	Tsankawi Pumice Porosity [-]
Theoretical Distribution	
Distribution	Truncated Normal
Minimum	0.000
Maximum	1.000
Mean	0.480
Standard Deviation	0.020



Distribution	Truncated Normal
Minimum	0.4062
Maximum	0.5497
Mean	0.4800
Median	0.4800
Standard Deviation	0.0200

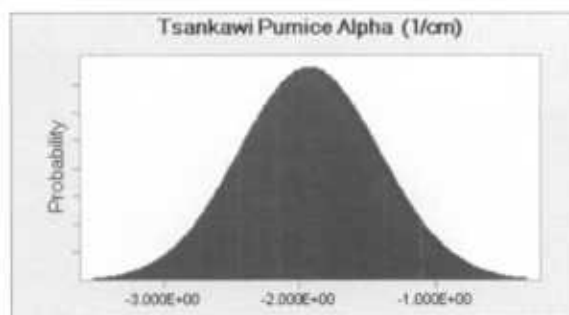


**Justification for Parameter Distribution**

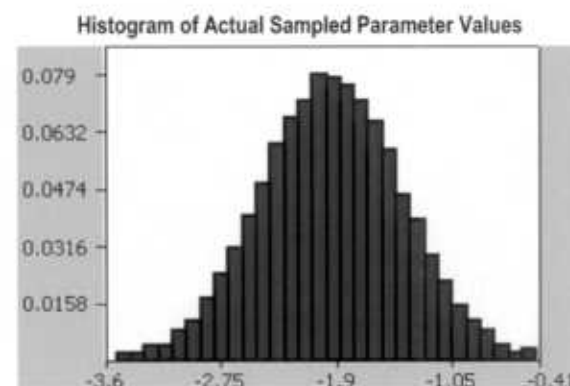
The parameter distribution for the porosity of the Tsankawi Pumice comes from the distribution estimated by Springer (2003, 90071), using core samples.

See Table B-7 under the parameter distribution for Tsankawi Pumice hydraulic conductivity information.

Variable	Tsankawi Pumice Alpha (Log) [1/cm]
<b>Theoretical Distribution</b>	
Distribution	Normal
Minimum	-∞
Maximum	∞
Mean	-1.930
Standard Deviation	0.520
Correlated with Coefficient	Tsankawi Pumice Hydraulic Conductivity 0.67



Distribution	Normal
Minimum	-3.5118
Maximum	-0.3354
Mean	-1.9300
Median	-1.9305
Standard Deviation	0.5192

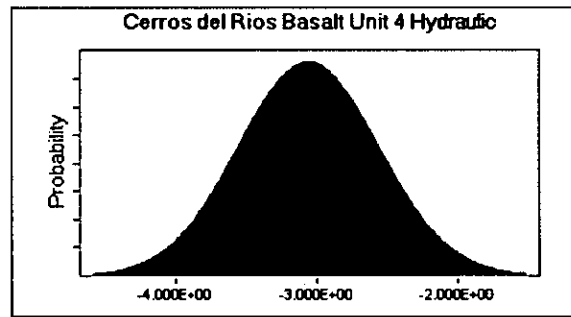


### Justification for Parameter Distribution

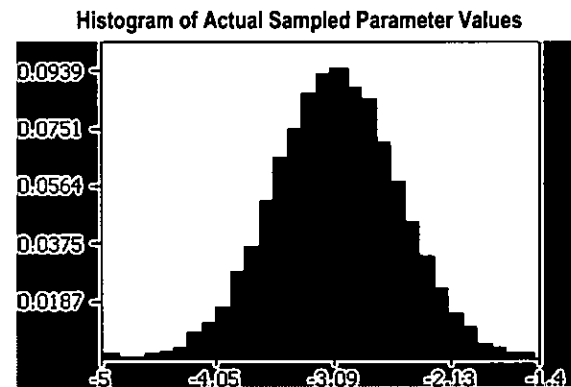
This parameter is the alpha-fitting parameter used in the van Genuchten (1980, 63542) formula for the unsaturated-water retention curve for the Tsankawi Pumice. The parameter distribution for alpha comes from the distribution estimated by Springer (2003, 90071), using core samples of the Cerro Toledo interval and Tsankawi Pumice. The alpha parameter is correlated to the hydraulic conductivity.

See Tables B-7 and B-8 under the parameter distribution for Tsankawi Pumice Hydraulic Conductivity information.

Variable	Cerros del Rio Basalt Unit 4 Hydraulic Conductivity (Log) [cm/s]
<b>Theoretical Distribution</b>	
<b>Distribution</b>	Log Normal
Minimum	$-\infty$
Maximum	$\infty$
Mean	-3.060
Standard Deviation	0.500



Distribution	Log Normal
Minimum	-4.9742
Maximum	-0.9931
Mean	-3.0598
Median	-3.0598
Standard Deviation	0.5029



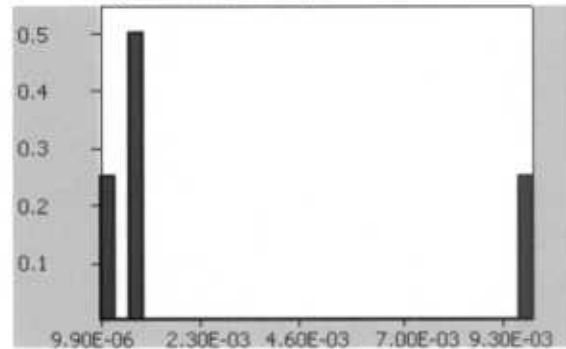
**Justification for Parameter Distribution**

The estimate is based on field tests (pump tests and injection tests) performed in the regional aquifer. The estimate is based on 2002 knowledge (Nylander et al. 2003, 76059) and also agrees with the calibration of field data by Stauffer and Stone (2005, 90037) at the Los Alamos Canyon weir site, where appropriate hydraulic conductivity values are  $10^{-2}$  and  $10^{-3}$  cm/s (-2 to -3 for Log[K<sub>s</sub>]). See also Birdsell, 2003, 90119, p. 149.

Variable	Cerros del Rio Basalt Unit 4 (Tb4) Porosity [-]
Theoretical Distribution	
Distribution	Empirical (Custom)
Value	Probability
1.000E-05	0.05
1.000E-04	0.20
1.000E-03	0.50
1.000E-02	0.25

Distribution	Empirical (Custom)
Minimum	0.00001
Maximum	0.010
Mean	0.0030
Median	0.0010
Standard Deviation	0.00405

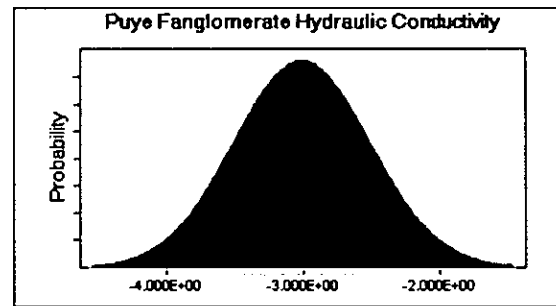
Histogram of Actual Sampled Parameter Values



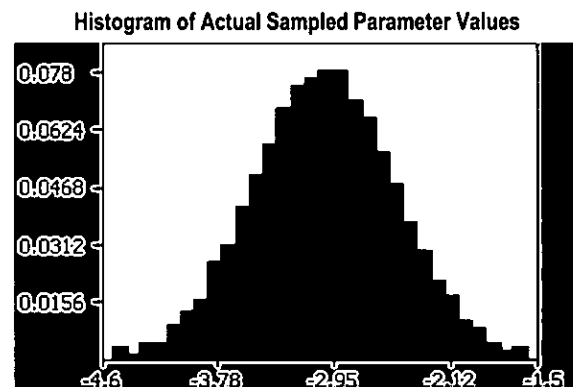
#### Justification for Parameter Distribution

This discrete distribution for porosity was developed to treat the Cerros del Rio Basalt unit as a fractured medium for purposes of the contaminant transport simulations. Stauffer and Stone (2005, 90037) modeled a bromide tracer test at the Los Alamos Canyon weir site and found that a porosity range of 0.001 to 0.01 for the Cerros del Rio Basalt unit yielded a good model fit to the observed bromide transport. These two discrete porosity values were chosen to represent 75% of the distribution. The lower values of 1E-04 and 1E-05 represent the remaining 25% in order to account for possible very rapid transport. See Birdsell, 2004, 90121, p. 63.

Variable	Puye Fanglomerate Hydraulic Conductivity Log [cm/s]
Theoretical Distribution	
Distribution	Log Normal
Minimum	$-\infty$
Maximum	$\infty$
Mean	-3.010
Standard Deviation	0.500



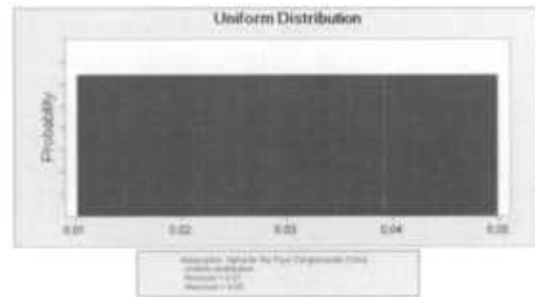
Distribution	Log Normal
Minimum	-4.5146
Maximum	-1.2147
Mean	-3.0097
Median	-3.0104
Standard Deviation	0.4996



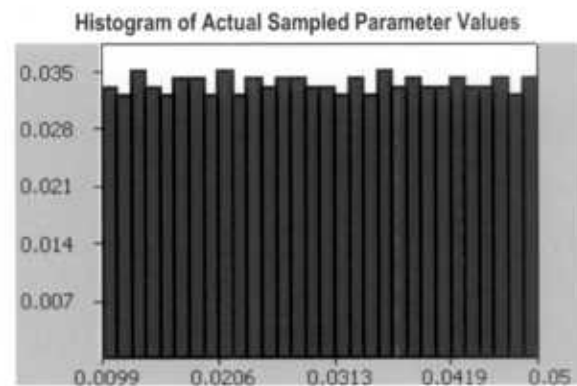
**Justification for Parameter Distribution**

This estimate was based on field tests (pump tests and injection tests) performed in the regional aquifer and on an estimate based on 2002 knowledge (Nylander et al. 2003, 76059). See also Birdsell 2003, 90119; pp. 142 and 149.

Variable	Alpha for the Puye Fanglomerate (Log) [1/cm]
Theoretical Distribution	
Distribution	Uniform
Minimum	0.010
Maximum	0.050



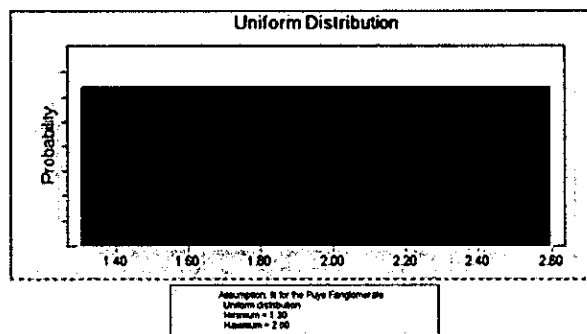
Distribution	Uniform
Minimum	0.0100
Maximum	0.0500
Mean	0.0300
Median	0.0300
Standard Deviation	0.0116



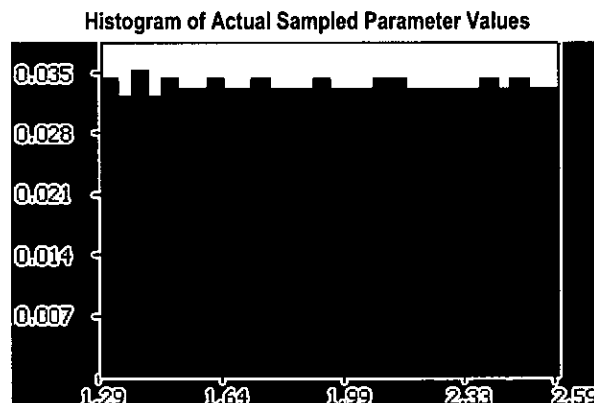
### Justification for Parameter Distribution

This parameter is the alpha-fitting parameter used in the van Genuchten (1980, 63542) formula for the unsaturated-water retention curve for the Puye fanglomerate. No measurements have been made on Puye fanglomerate samples in order to estimate the alpha parameter. Therefore, to treat this parameter as variable, a distribution was estimated. The distribution for alpha is based on parameter values measured on like materials as reported in the literature. A range in alpha parameters corresponding to a clay/silt material (van Genuchten et al. 1991, 65419) was chosen to account for the smallest pore sizes of the Puye fanglomerate. The estimate was further refined through calibration of the vadose-zone simulations to field data (predominantly concentration versus depth profiles in the Mortandad Canyon Observation (MCO) Bandelier Tuff (BT) wells and in R-15, see Birdsell 2004, 90121, pp. 117–120).

Variable	N for the Puye Fanglomerate [-]
Theoretical Distribution	
Distribution	Uniform
Minimum	1.300
Maximum	2.600



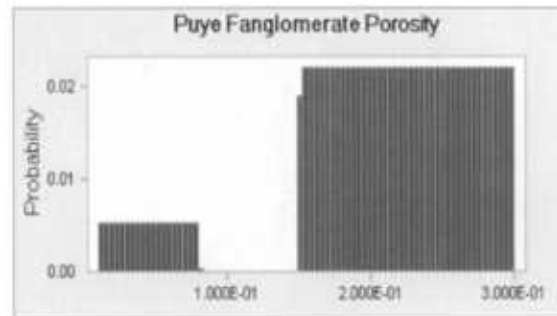
Distribution	Uniform
Minimum	1.3007
Maximum	2.6000
Mean	1.9500
Median	1.9502
Standard Deviation	0.3755



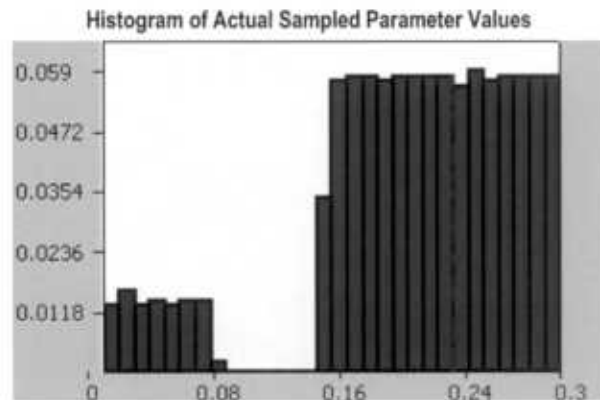
**Justification for Parameter Distribution**

This parameter is the N-fitting parameter used in the van Genuchten (1980, 63542) formula for the unsaturated water-retention curve for the Puye fanglomerate. No measurements have been made on Puye fanglomerate samples in order to estimate the N parameter. Therefore, to treat this parameter as variable, a distribution was estimated. The distribution for N is based on parameter values measured on like materials as reported in the literature. A range in N parameters corresponding to a coarse soil material (van Genuchten et al. 1991, 65419) was chosen to account for the large-size distribution of the Puye fanglomerate. The estimate was further refined through calibration of the vadose-zone simulations to field data (predominantly concentration versus depth profiles in the MCOBT wells and in R-15, see Birdsell 2004, 90121, pp. 117–120).

Variable	Puye Faglglomerate Porosity [-]	
Theoretical Distribution		
Distribution		Custom
Minimum	Maximum	Probability
1.000E-02	8.000E-02	0.10
1.500E-01	3.000E-01	0.90



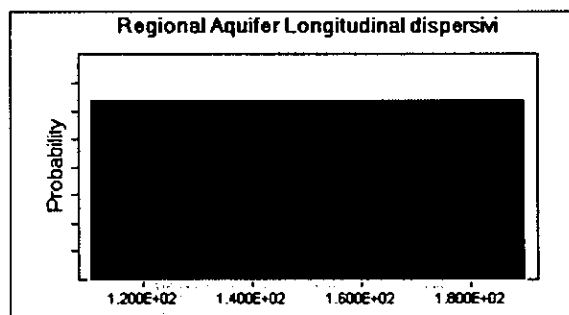
Distribution	Empirical (Custom)
Minimum	0.0109
Maximum	0.3000
Mean	0.2070
Median	0.2166
Standard Deviation	0.0682



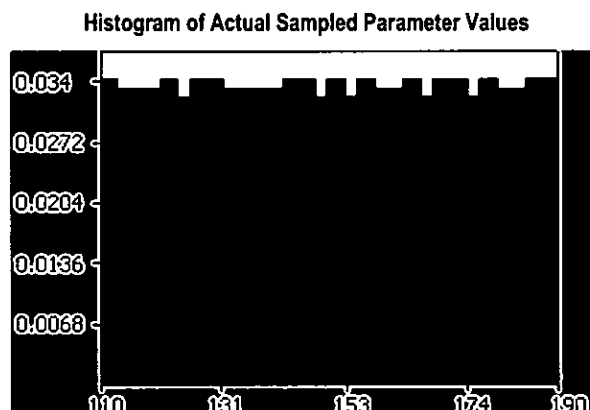
### Justification for Parameter Distribution

This discrete distribution for porosity was developed to treat the Puye fanglomerate as both a matrix medium and a fractured medium for purposes of the contaminant-transport simulations. The portion (90%) of the distribution between 0.15 and 0.3 represents a matrix material and is based on bulk porosity values measured in the saturated zone (personal communication with Elizabeth Keating). The portion (10%) of the distribution between 0.01 and 0.08 is meant to simulate possible preferential or fracture flow paths. Because the Puye fanglomerate is a mixture of rocks of different sizes rather than a massive unit, like some of the basalts on the plateau, extremely low porosity values (i.e.,  $<.01$ ) were not estimated. See Birdsell 2004, 90121, p. 5.

Variable	Regional Aquifer Longitudinal Dispersivity [m]
<b>Theoretical Distribution</b>	
Distribution	Uniform
Minimum	110.0
Maximum	190.0



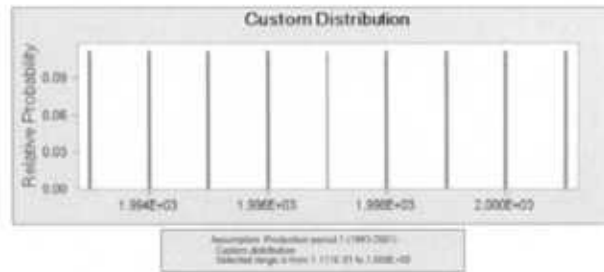
Distribution	Uniform
Minimum	110.02
Maximum	189.937
Mean	150.001
Median	149.9655
Standard Deviation	23.1078



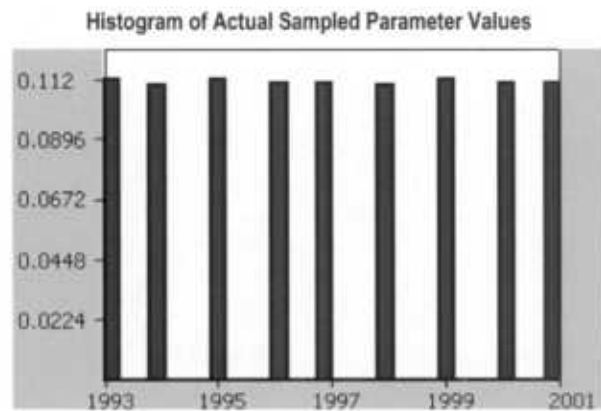
**Justification for Parameter Distribution**

The aquifer dispersivity (macrodispersion) is a parameter that depends on the properties of the flow medium and on the scale at which groundwater transport occurs. No field data are available indicating the values and their uncertainty for this parameter. Based on literature data, it was assumed that longitudinal dispersivity varies uniformly in the selected range from 110 to 190 m (Neuman 1990, 90184). The transverse dispersivity is selected to be 1/10 of the longitudinal random values based on literature data (Freeze and Cherry 1979, 64057).

Variable	Production Period 3 (1993-2001)
<b>Theoretical Distribution</b>	
Distribution	Custom
Minimum	1993
Maximum	2001
Probability	1
Step	1



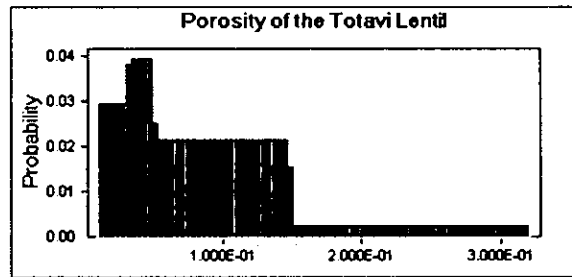
Distribution	Discrete Uniform
Minimum	1993
Maximum	2001
Mean	1996.998
Median	1997
Standard Deviation	2.5847



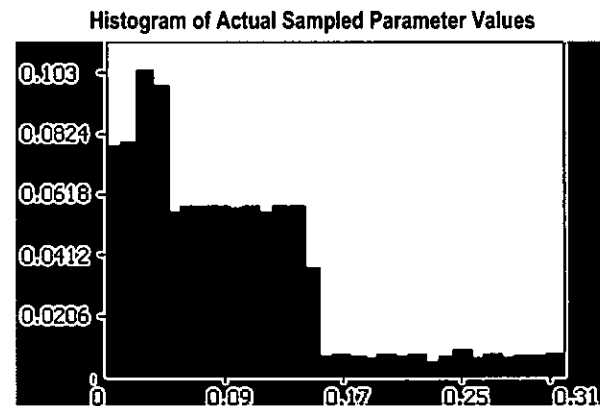
### Justification for Parameter Distribution

Annually averaged pumping rates for the period from 1993 to 2001 are selected to represent potential future pumping regimes. Since 1993, all the existing water-supply wells are operating. Only data collected since 2001 were included in the analysis when the study started in 2002. That is why the pre-1993 and post-2001 data are not included. The distribution is defined to be discrete and uniform where each yearly pumping regime is equally probable. This random variable defines which of the pumping regimes from 1993 to 2001 are selected as a future pumping regime.

Variable	Porosity of the Totavi Lentil [-]	
Theoretical Distribution		
Distribution		Custom
Minimum	Maximum	Probability
1.000E-02	3.000E-02	0.15
3.000E-02	5.000E-02	0.20
5.000E-02	1.500E-01	0.55
1.500E-01	3.200E-01	0.10



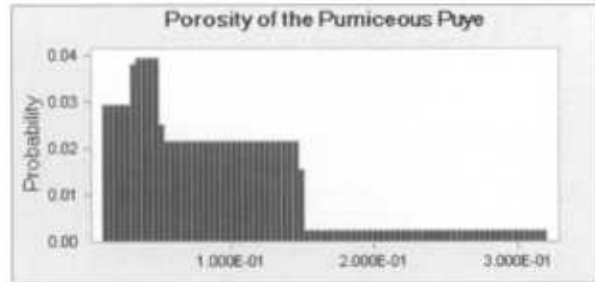
Distribution	Empirical (Custom)
Minimum	0.0100
Maximum	0.3184
Mean	0.0895
Median	0.0772
Standard Deviation	0.0641



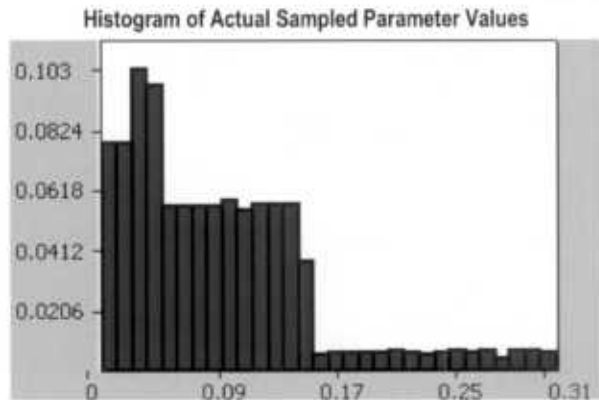
**Justification for Parameter Distribution**

Totavi Lentil river deposits (embedded in the Puye Formation) are porous media with relatively high permeability and relatively high porosity. The distribution is based on literature data for properties of a porous medium (Freeze and Cherry 1979, 64057). It represents a truncated normal distribution with a range from 0.01 to 0.15, where the most probable value is on the order of 0.05. Higher and lower values are less probable and ranked lower as described above.

Variable		Porosity of the Pumiceous Puye [-]
Theoretical Distribution		
Distribution		Custom
Minimum	Maximum	Probability
1.000E-02	3.000E-02	0.15
3.000E-02	5.000E-02	0.20
5.000E-02	1.500E-01	0.55
1.500E-01	3.200E-01	0.10



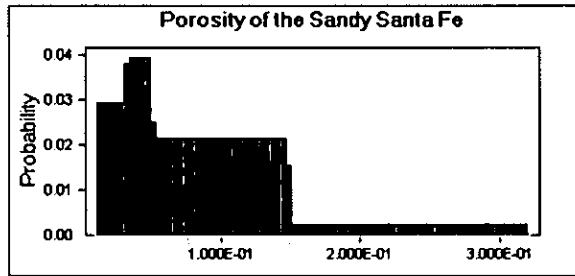
Distribution	Empirical (Custom)
Minimum	0.0100
Maximum	0.3182
Mean	0.0895
Median	0.0772
Standard Deviation	0.0641



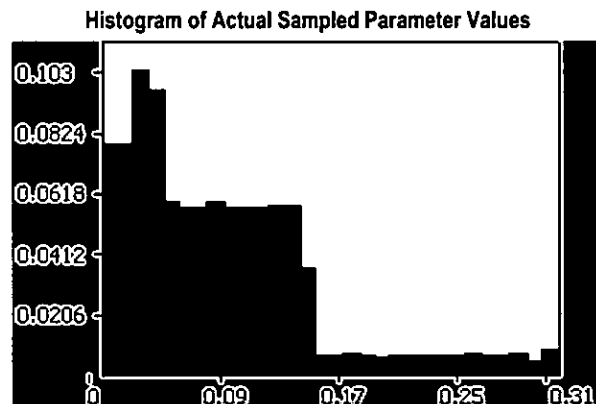
#### Justification for Parameter Distribution

Puye Formation deposits are porous medium with relatively high permeability and relatively high porosity. The distribution is based on literature data for properties of a porous medium (Freeze and Cherry 1979, 64057). It represents a truncated normal distribution. The most probable porosity values are defined to be on the order of 0.1.

Variable	Porosity of the Sandy Santa Fe [-]	
<b>Theoretical Distribution</b>		
<b>Distribution</b>		<b>Custom</b>
<b>Minimum</b>	<b>Maximum</b>	<b>Probability</b>
1.000E-02	3.000E-02	0.15
3.000E-02	5.000E-02	0.20
5.000E-02	1.500E-01	0.55
1.500E-01	3.200E-01	0.10



Distribution	Empirical (Custom)
Minimum	0.0100
Maximum	0.3184
Mean	0.0895
Median	0.0773
Standard Deviation	0.0641

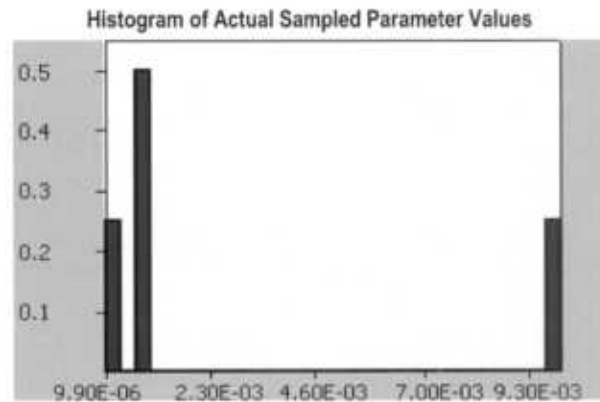


**Justification for Parameter Distribution**

The Santa Fe group is a porous medium with relatively high permeability and relatively high porosity. The distribution is based on literature data for properties of a porous medium (Freeze and Cherry 1979, 64057). It represents a truncated normal distribution. The most probable porosity values are defined to be on the order of 0.1.

Variable	Porosity of Tb2 [-]
<b>Theoretical Distribution</b>	
<b>Distribution</b>	<b>Custom</b>
<b>Value</b>	<b>Probability</b>
1.000E-05	0.05
1.000E-04	0.20
1.000E-03	0.50
1.000E-02	0.25

Distribution	Empirical (Custom)
Minimum	1.00E-05
Maximum	0.0100
Mean	0.0030
Median	0.0010
Standard Deviation	0.0040



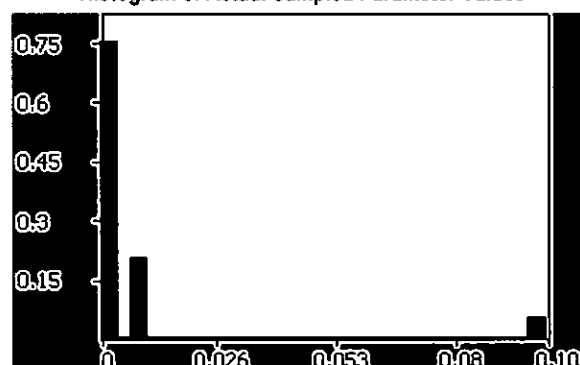
#### Justification for Parameter Distribution

The basalt deposits of Tb2 are a potential fast-flow path for groundwater transport as a result of existing fractures. No site-specific data are available for this parameter. A distribution equivalent to the distribution for Tb4 was used.

Variable	Porosity of Tb2 or Ts [-]
<b>Theoretical Distribution</b>	
Distribution	Custom
Value	Probability
1.000E-05	0.05
1.000E-04	0.20
1.000E-03	0.50
1.000E-02	0.20
1.000E-01	0.05

Distribution	Empirical (Custom)
Minimum	1.00E-05
Maximum	0.10
Mean	0.0075
Median	0.0010
Standard Deviation	0.0216

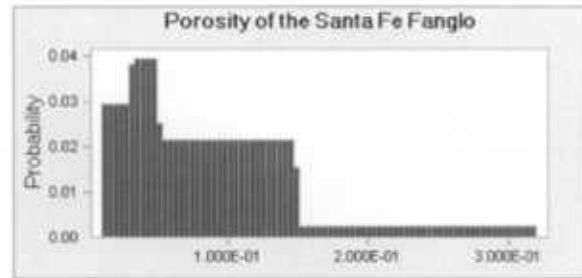
Histogram of Actual Sampled Parameter Values



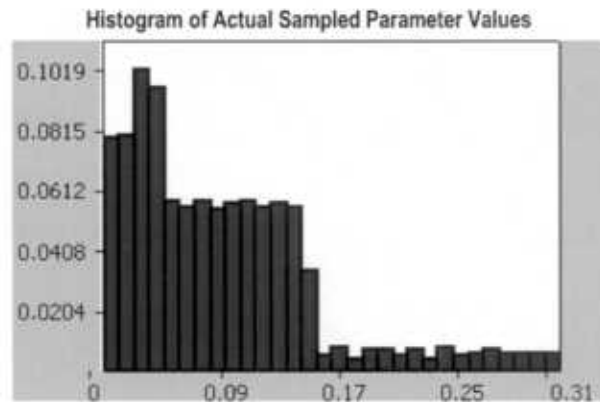
**Justification for Parameter Distribution**

The hydrostratigraphic unit “Tb2 or Ts” represents some of the uncertainties that currently exist in the Laboratory 3-D geologic model. The existing data do not define the spatial extent of Tb2 basalts. The selected porosity ranges represent this uncertainty. The distribution is defined in a way to resemble a truncated log-normal distribution. It is established using literature data for properties of porous and fractured mediums (Freeze and Cherry 1979, 64057). Some mixture of contaminant flow through both porous and fractured media (represented by porosity values on the order of  $10^{-3}$ ) is defined to be the most probable.

Variable		Porosity of the Santa Fe Fanglomerate [-]
Theoretical Distribution		
Distribution		Custom
Minimum	Maximum	Probability
1.000E-02	3.000E-02	0.15
3.000E-02	5.000E-02	0.20
5.000E-02	1.500E-01	0.55
1.500E-01	3.200E-01	0.10



Distribution	Empirical (Custom)
Minimum	0.0102
Maximum	0.3199
Mean	0.0895
Median	0.0773
Standard Deviation	0.0641



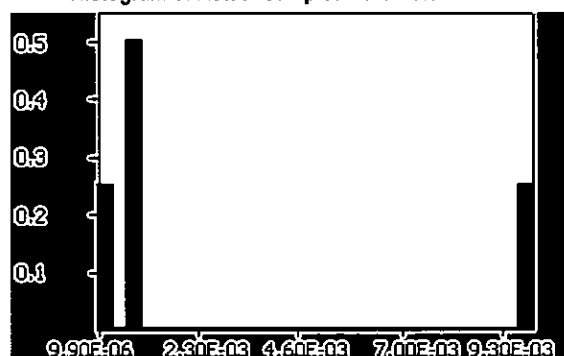
### Justification for Parameter Distribution

Santa Fe fanglomerate is a porous medium with relatively high permeability and relatively high porosity. The distribution is based on the general literature data for properties of a porous medium (Freeze and Cherry 1979, 64057). It represents a truncated normal distribution. The most probable porosity values are defined to be on the order of 0.1.

Variable	Porosity of the Deepest Basalt Unit [-]
<b>Theoretical Distribution</b>	
<b>Distribution</b>	<b>Custom</b>
<b>Value</b>	<b>Probability</b>
1.000E-05	0.05
1.000E-04	0.20
1.000E-03	0.50
1.000E-02	0.25

Distribution	Empirical (Custom)
Minimum	0.00001
Maximum	0.0100
Mean	0.0030
Median	0.0010
Standard Deviation	0.00405

Histogram of Actual Sampled Parameter Values



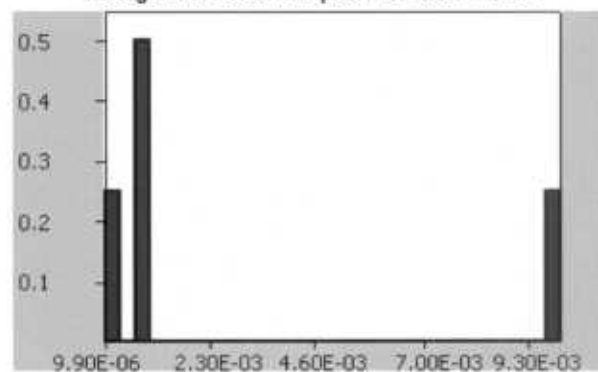
**Justification for Parameter Distribution**

Deep basalt units are a potential fast-flow path for groundwater transport because of existing fractures. No site-specific data for this parameter are available; therefore, a distribution equivalent to the distribution for Tb4 is used.

Variable	Porosity of the Tschicoma Flows [-]
Theoretical Distribution	
Distribution	Custom
Value	Probability
1.000E-05	0.05
1.000E-04	0.20
1.000E-03	0.50
1.000E-02	0.25

Distribution	Empirical (Custom)
Minimum	0.00001
Maximum	0.0100
Mean	0.0030
Median	0.0010
Standard Deviation	0.0040

Histogram of Actual Sampled Parameter Values



#### Justification for Parameter Distribution

Tschicoma Flow deposits are considered to be a potential fast-flow path for groundwater transport resulting from existing fractures. No site-specific data for this parameter are available; therefore, a distribution equivalent to the distribution for Tb4 is used.

Variable	Porosity of Tb4 or Tpf [-]
<b>Theoretical Distribution</b>	
Distribution	Custom
Value	Probability
1.000E-05	0.05
1.000E-04	0.20
1.000E-03	0.50
1.000E-02	0.20
1.000E-01	0.05

Distribution	Empirical (Custom)
Minimum	0.00001
Maximum	0.1000
Mean	0.0075
Median	0.0010
Standard Deviation	0.0216

Histogram of Actual Sampled Parameter Values



**Justification for Parameter Distribution**

The hydrostratigraphic unit Tb4 or Tpf represents some of the uncertainty that exists in the Laboratory 3-D geologic model. The existing data do not define the spatial extent of Tb4 basalts. The selected porosity range represents this uncertainty. The distribution is defined to resemble a truncated log-normal distribution. It is established using literature data for properties of porous and fractured mediums (Freeze and Cherry 1979, 64057). Some mixture of a contaminant flow through both porous and fractured media (represented by porosity values on the order of  $10^{-3}$ ) is defined to be the most probable.

#### B-4.0 SAMPLE CONVERGENCE

In a Monte Carlo analysis, there is always the question of how many samples are required to adequately cover the pdf for all parameters. LHS minimizes the number of samples required by means of the stratified sampling. However, there is no predefined number of samples and no analytical solution to define the number of samples required to completely cover the pdf of each parameter. Instead, convergence testing involves repeated sampling using more and more samples and checking for changes in the distribution of model output. Using such an approach, Schuyler (1997, 90120) found that "instead of a 10,000 trial (traditional) run, about the same degree of accuracy can be achieved with LHS in only 100 trials" for single-parameter sampling and "4% as many trials as would be required using conventional Monte Carlo sampling" for multiple-parameter sampling.

Convergence testing for the Mortandad Canyon Tier-3 analysis was performed by sampling subsets from the original 1,000 samples, estimating the new probability of exceedance, and comparing it to the original probability of exceedance. These subsets were sampled using LHS. Complementary cumulative distribution functions (CCDFs) and corresponding exceedance probabilities for the 100, 200, 300, 400, and 750 sample subsets for wells PM-3 and PM-5 are shown in Figures B-3 and B-4.

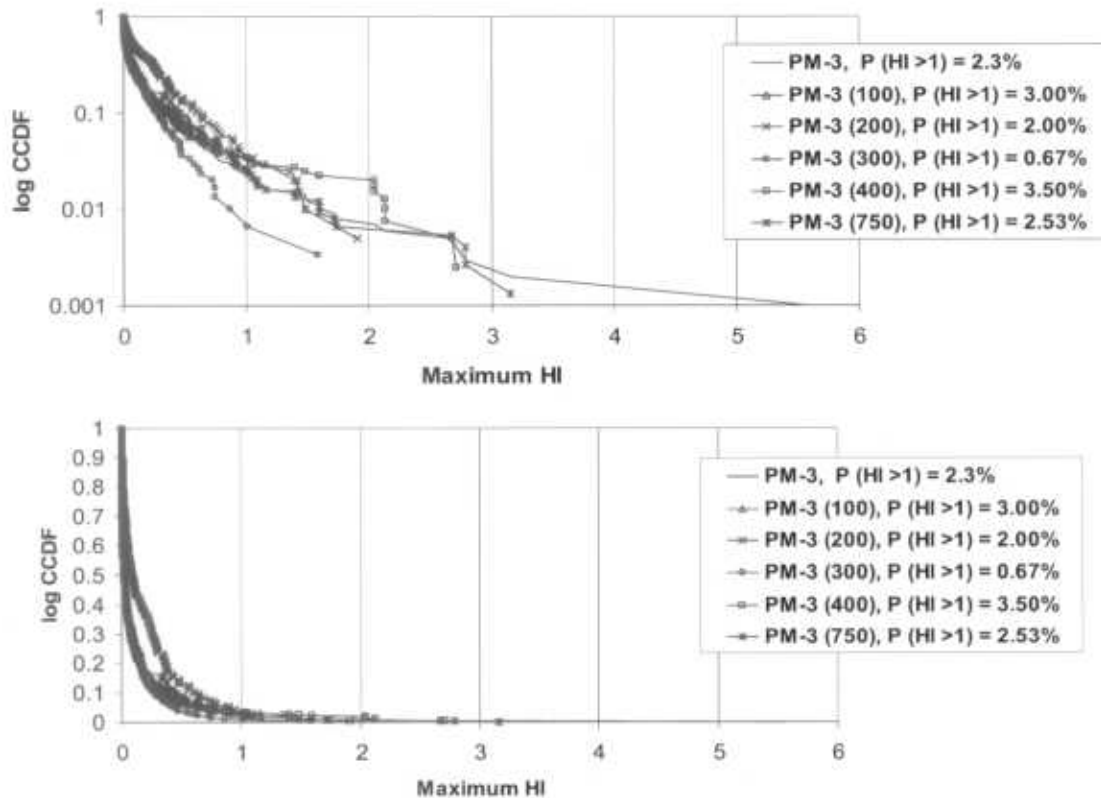
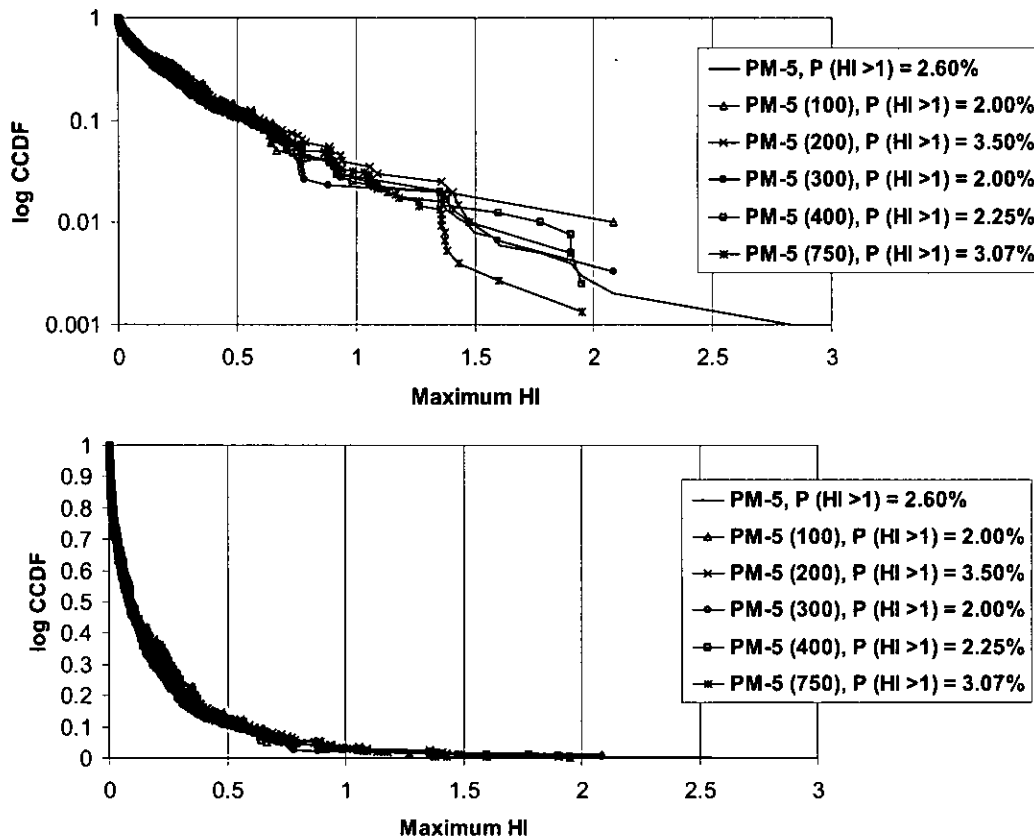
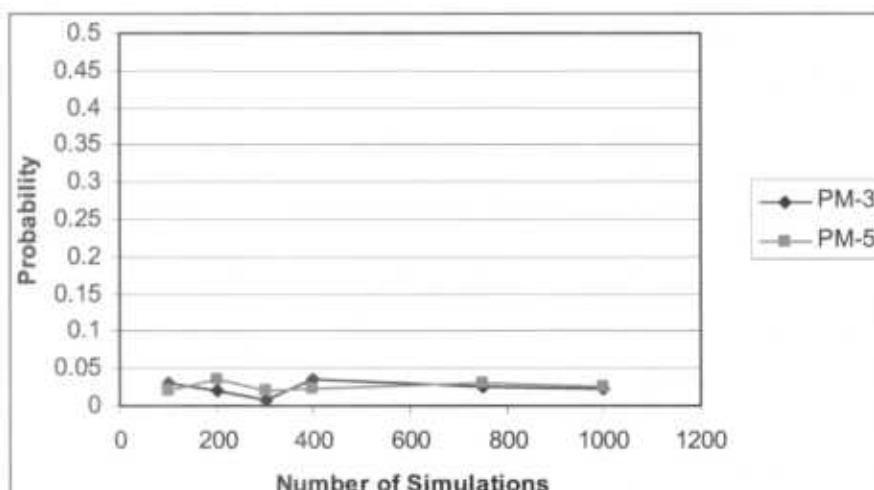


Figure B-3. Comparison of CCDF and the probability of exceedance of HI for PM-3 using random subsets of simulation results (100, 200, 300, 400, and 750 simulations from a total of 1000). The log scale (upper graphic) is provided for better differentiation of the lower portion of the curves.



**Figure B-4. Comparison of CCDF and the probability of exceedance of HI for PM-5 using random subsets of simulation results (100, 200, 300, 400, and 750 simulations from a total of 1000). The log scale (upper graphic) is provided for better differentiation of the lower portion of the curves.**

CCDFs presented in the Figures B-3 and B-4 demonstrate that a CCDF created with as few as 100 samples is virtually identical to the CCDF created with 1000 samples. However, it could be argued that the original 1000 samples did not cover all of the combined parameter space, and therefore none of the subsamples would be expected to find extremes of parameter combinations. This issue cannot truly be addressed without taking more samples (2000, 3000, etc.). Nevertheless, we are not regulating or making decisions based on the most extreme possible model behavior. Instead, 95% has been defined as the acceptable level of confidence. Shown in the following graph, Figure B-5 is the change in exceedance probability as a function of the sample number. Note that the exceedance probability is barely fluctuating, that all fluctuations are about an order of magnitude below the 95% confidence (5% exceedance) level, and that convergence has been achieved by about 600 samples.



**Figure B-5. Probability of exceedance versus number of sampled simulations**

Therefore, taking more than 1000 samples may produce simulations with slightly larger HI values but shouldn't change the probability of exceedance.

#### B-5.0 REFERENCES

The following list includes all documents cited in this document. Parenthetical information following each reference provides the author, publication data, and ER ID number. This information is also included in text citations. ER ID numbers are assigned by the ENV-ERS Records Processing Facility (RPF) and are used to locate the document at the RPF.

Birdsell, K., 2003. "Scientific Notebook Pertaining to Mortandad Canyon Modeling of Vadose-Zone Flow and Transport," Los Alamos National Laboratory, Los Alamos, New Mexico. (Birdsell 2003, 90119)

Birdsell, K., 2004. "Scientific Notebook Pertaining to Mortandad Canyon Modeling of Vadose-Zone Flow and Transport," Los Alamos National Laboratory, Los Alamos, New Mexico. (Birdsell 2004, 90121)

Birdsell, K.H., W.E. Soll, K.M. Bower, A.V. Wolfsberg, T. Orr, and T.A. Cherry, 1999. "Simulations of Groundwater Flow and Radionuclide Transport in the Vadose and Saturated Zones beneath Area G, Los Alamos National Laboratory," Los Alamos National Laboratory report LA-13299-MS, Los Alamos, New Mexico. (Birdsell et al. 1999, 69792)

Birdsell, K. H., V.V. Vesselinov, B.D. Newman, D. Hollis, M.O. Gard, G. Cole, and J.W. Carey, 2005. "Probabilistic Assessment of Contaminant Transport from Mortandad Canyon," Los Alamos National Laboratory report, Los Alamos, New Mexico. (Birdsell et al. 2005, in progress)

Dander, D., 1998. "Unsaturated Groundwater Flow beneath Upper Mortandad Canyon, Los Alamos, New Mexico," Los Alamos National Laboratory document LA-UR-4759, Los Alamos, New Mexico. (Dander 1998, 88743)

Freeze, R.A., and J.A. Cherry, 1979. *Groundwater*, Prentice-Hall, Inc., Englewood Cliffs, New Jersey. (Freeze and Cheery 1979, 64057)

Geddis, A.M., 1992. "Preliminary Modeling of Moisture Movement in the Tuff beneath Mortandad Canyon, Los Alamos National Laboratory," Los Alamos National Laboratory document LA-UR-92-2577, Los Alamos, New Mexico. (Geddis 1992, 31592)

Koenig, E., and S. McLin, 1991. "Application of a Lumped-Parameter Model toward Understanding the Behavior of the Mortandad Canyon Perched Alluvial Aquifer System," Los Alamos National Laboratory report, Los Alamos, New Mexico. (Koenig and McLin 1991, 56029)

McKay, M.D., R. J. Beckman, and W.J. Conover, 1979. "A Comparison of Three Methods for Selecting Values of Input Variables in the Analysis of Output from a Computer Code" *Technometrics*, Vol. 42(1), pp. 55–61. (McKay et al. 2000, 90183)

Neuman, S.P., 1990. "Universal Scaling of Hydraulic Conductivities and Dispersivities in Geologic Media," *Water Resources Research*, Vol. 26, pp. 1749–1758. (Neuman 1990, 90184)

Nylander, C.L., K.A. Bitner, G. Cole, E.H. Keating, S. Kinkead, P. Longmire, B. Robinson, D.B. Rogers, and D. Vaniman, 2003. "Groundwater Annual Status Report for Fiscal Year 2002," Los Alamos National Laboratory document LA-UR-03-0244, GPP-03-011, Los Alamos, New Mexico. (Nylander et al. 2003, 76059)

Purtymun, W.D., 1967. "The Disposal of Industrial Effluents in Mortandad Canyon, Los Alamos County, New Mexico," U.S. Department of the Interior Geological Survey, Santa Fe, New Mexico. (Purtymun 1967, 11785)

Schuyler, J.R., 1997. "#25 Monte Carlo Simulation Stopping Rule with Latin Hypercube Sampling," <http://maxvalue.com/tip025.htm>. (Schuyler 1997, 90120)

Springer, E.P., 1995, Hydrologic Properties for Guaje Pumice, A Single Core Sample, [Personal Communication for Guaje properties]. (Springer 1995, 90118)

Springer, E.P. 2003, "Hydrologic Properties," e-mail (informal communication). (Springer 2003, 90071)

Stauffer, P.H., and W.J. Stone, 2005. "Surface Water/Groundwater Connection at the Los Alamos Canyon Weir Site, Part II: Modeling of Tracer Test Results," available at [www.vadosezonejournal.org](http://www.vadosezonejournal.org). *Vadose Zone J.* (Stauffer and Stone 2005, 90037)

van Genuchten M.Th., 1980. "A Closed-Form Equation for Predicting the Hydraulic Conductivity of Unsaturated Soils," *Soil Sci. Soc. Am. J.*, Vol. 44, pp. 892–898. (van Genuchten 1980, 63542)

van Genuchten, M.Th., F.J. Leij, and S.R. Yates, 1991. "The RETC Code for Quantifying the Hydraulic Functions of Unsaturated Soils," U.S. Environmental Protection Agency report EPA/600/2-91/065. (Van Genuchten et al. 1991, 65419)

Wyss, G.D, and K.H. Jorgensen, 1998. "A User's Guide to LHS: Sandia's Latin Hypercube Sampling Software," Sandia National Laboratories report SAND 98-0210, Albuquerque, New Mexico. (Wyss and Jorgensen 1998, 90122)

# Appendix C

---

*Risk-Assessment Results*

## C-1.0 OVERVIEW

This appendix presents the conversion of concentrations to human-health-related indicators; hazard index, hazard quotient (HI, HQ, and dose); the results of the Mortandad Canyon Tier-3 probabilistic-risk assessment; and the relation between the calculations and Environmental Protection Agency (EPA) drinking water standards, reference doses, and maximum concentrations levels (MCLs), and the Department of Energy's (DOE's) dose standard for tritium. Exposure and toxicity models and the selection of the corresponding exposure parameters are also provided.

The only existing groundwater exposure pathway for contaminants in Mortandad Canyon is from surface discharges through the vadose zone to the regional aquifer and to existing production wells. Therefore, indicators of potential human-health effects were calculated at each production well.

Tier 3 is a probabilistic risk assessment using Monte Carlo methods for propagating uncertainty, resulting in 1000 equally probable health indicators for each production well. Complementary cumulative distribution functions (CCDFs) were used to display simulation results for both 100- and 1000-yr analysis periods. Tables with the resulting probabilities of exceedance are provided (Tables C-1.1, C-1.2, and C-1.3). Additionally, for cases whose HI values exceed 1.0 at the 95% confidence limit, graphs of the percentage of the results that exceed an HI of 1.0 are plotted as a function of time (Figures C-1.1 to C-1.9). Finally, shown in Table C-1.4 are probabilities of exceedance for less-restrictive reference doses (concentration limits) for perchlorate.

**Table C-1.1**  
**Probabilities of Exceedance of HI Greater than 1 and Maximum HIs for 100-Yr Analysis**

Contaminant(s) Evaluated	Quantity Evaluated	Wells Evaluated	Number of Maximum HIs or HQs Calculations	Number of Calculations with HI or HQ >1	Probability of Exceedance of HI or HQ >1	Maximum HQ/HI Round off?
<b>Upper/middle-canyon-dominated uniform infiltration with regional-aquifer Model A</b>						
Perchlorate	HQ	O-1	1000	0	0.0%	4.55E-10
		O-4	1000	0	0.0%	0.302
		PM-1	1000	0	0.0%	0.511
		PM-2	1000	0	0.0%	1.58E-04
		PM-3	1000	23	2.3%	5.551
		PM-4	1000	1	0.1%	1.242
		PM-5	1000	26	2.6%	2.784
Nitrate and Perchlorate	HI	O-1	1000	0	0.0%	7.11E-10
		O-4	1000	0	0.0%	0.31
		PM-1	1000	0	0.0%	0.53
		PM-2	1000	0	0.0%	1.71E-04
		PM-3	1000	24	2.4%	5.70
		PM-4	1000	1	0.1%	1.27
		PM-5	1000	28	2.8%	2.83

Table C-1.1 (continued)

Contaminant(s) Evaluated	Quantity Evaluated	Wells Evaluated	Number of Maximum HIs or HQs Calculations	Number of Calculations with HI or HQ >1	Probability of Exceedance of HI or HQ >1	Maximum HQ/Hi Round off?
<b>Lower-canyon-dominated infiltration with fast paths in the upper, middle, and lower canyons with regional-aquifer Model A</b>						
Perchlorate	HQ	O-1	1000	0	0.0%	1.72E-08
		O-4	1000	0	0.0%	0.213
		PM-1	1000	0	0.0%	0.776
		PM-2	1000	0	0.0%	5.49E-05
		PM-3	1000	35	3.5%	5.647
		PM-4	1000	3	0.3%	1.434
		PM-5	1000	4	0.4%	1.041
Nitrate and Perchlorate	HI	O-1	1000	0	0.0%	2.35E-08
		O-4	1000	0	0.0%	0.22
		PM-1	1000	0	0.0%	0.80
		PM-2	1000	0	0.0%	7.27E-05
		PM-3	1000	35	3.5%	5.80
		PM-4	1000	3	0.3%	1.46
		PM-5	1000	5	0.5%	1.64
<b>Lower-canyon-dominated infiltration with fast paths in the upper and middle canyons with regional-aquifer Model A</b>						
Perchlorate	HQ	O-1	1000	0	0.0%	1.06E-06
		O-4	1000	0	0.0%	0.22
		PM-1	1000	0	0.0%	0.61
		PM-2	1000	0	0.0%	1.92E-04
		PM-3	1000	34	3.4%	6.27
		PM-4	1000	2	0.2%	1.35
		PM-5	1000	4	0.4%	1.63
<b>Lower-canyon-dominated infiltration with fast paths in the upper and middle canyons with regional-aquifer Model A (cont.)</b>						
Nitrate and Perchlorate	HI	O-1	1000	0	0.0%	1.54E-06
		O-4	1000	0	0.0%	0.23
		PM-1	1000	0	0.0%	0.65
		PM-2	1000	0	0.0%	2.19E-04
		PM-3	1000	38	3.8%	6.50
		PM-4	1000	2	0.2%	1.39
		PM-5	1000	5	0.5%	1.66
<b>Lower-canyon-dominated uniform infiltration with regional-aquifer Model A</b>						
Perchlorate	HQ	O-1	1000	0	0.0%	1.06E-06
		O-4	1000	0	0.0%	0.19
		PM-1	1000	0	0.0%	0.60
		PM-2	1000	0	0.0%	1.92E-04
		PM-3	1000	30	3.0%	6.16
		PM-4	1000	3	0.3%	1.46
		PM-5	1000	4	0.4%	1.85

Table C-1.1 (continued)

Contaminant(s) Evaluated	Quantity Evaluated	Wells Evaluated	Number of Maximum HIs or HQs Calculations	Number of Calculations with HI or HQ >1	Probability of Exceedance of HI or HQ >1	Maximum HQ/Hi Round off?
<b>Lower-canyon-dominated uniform infiltration with regional-aquifer Model A (continued)</b>						
Nitrate and Perchlorate	HI	O-1	1000	0	0.0%	1.54E-06
		O-4	1000	0	0.0%	0.20
		PM-1	1000	0	0.0%	0.64
		PM-2	1000	0	0.0%	2.19E-04
		PM-3	1000	31	3.1%	6.40
		PM-4	1000	3	0.3%	1.51
		PM-5	1000	7	0.7%	1.88
<b>Lower-canyon-dominated infiltration with fast path in the lower canyon with regional-aquifer Model A</b>						
Perchlorate	HQ	O-1	1000	0	0.0%	1.24E-08
		O-4	1000	0	0.0%	0.16
		PM-1	1000	0	0.0%	0.75
		PM-2	1000	0	0.0%	4.82E-05
		PM-3	1000	29	2.9%	5.48
		PM-4	1000	4	0.4%	1.49
		PM-5	1000	4	0.4%	1.82
Nitrate and Perchlorate	HI	O-1	1000	0	0.0%	2.35E-08
		O-4	1000	0	0.0%	0.18
		PM-1	1000	0	0.0%	0.79
		PM-2	1000	0	0.0%	7.25E-05
		PM-3	1000	31	3.1%	5.70
		PM-4	1000	4	0.4%	1.52
		PM-5	1000	7	0.7%	1.85
<b>Lower-canyon-dominated infiltration with fast path in the middle canyon with regional-aquifer Model A</b>						
Perchlorate	HQ	O-1	1000	0	0.0%	1.06E-06
		O-4	1000	0	0.0%	0.21
		PM-1	1000	0	0.0%	0.61
		PM-2	1000	0	0.0%	1.92E-02
		PM-3	1000	33	3.3%	6.24
		PM-4	1000	2	0.2%	1.33
		PM-5	1000	3	0.3%	1.65
Nitrate and Perchlorate	HI	O-1	1000	0	0.0%	1.54E-06
		O-4	1000	0	0.0%	0.22
		PM-1	1000	0	0.0%	0.65
		PM-2	1000	0	0.0%	2.19E-04
		PM-3	1000	36	3.6%	6.47
		PM-4	1000	2	0.2%	1.37
		PM-5	1000	3	0.3%	1.67

Table C-1.1 (continued)

Contaminant(s) Evaluated	Quantity Evaluated	Wells Evaluated	Number of Maximum HIs or HQs Calculations	Number of Calculations with HI or HQ >1	Probability of Exceedance of HI or HQ >1	Maximum HQ/HI Round off?
<b>Lower-canyon-dominated infiltration with fast path in the upper canyon with regional-aquifer Model A</b>						
Perchlorate	HQ	O-1	1000	0	0.0%	1.06E-06
		O-4	1000	0	0.0%	0.20
		PM-1	1000	0	0.0%	0.60
		PM-2	1000	0	0.0%	1.92E-04
		PM-3	1000	30	3.0%	6.19
		PM-4	1000	3	0.3%	1.47
		PM-5	1000	8	0.8%	1.78
Nitrate and Perchlorate	HI	O-1	1000	0	0.0%	1.54E-06
		O-4	1000	0	0.0%	0.21
		PM-1	1000	0	0.0%	0.64
		PM-2	1000	0	0.0%	2.19E-04
		PM-3	1000	33	3.3%	6.43
		PM-4	1000	3	0.3%	1.53
		PM-5	1000	8	0.8%	1.81
<b>Lower-canyon-dominated infiltration with fast paths in the upper and middle canyons with regional-aquifer Model B</b>						
Perchlorate	HQ	O-1	1000	0	0.0%	1.59E-03
		O-4	1000	0	0.0%	3.82E-05
		PM-1	1000	0	0.0%	0.06
		PM-2	1000	0	0.0%	6.47E-05
		PM-3	1000	0	0.0%	0.06
		PM-4	1000	0	0.0%	0.02
		PM-5	1000	0	0.0%	0.10
<b>Lower-canyon-dominated uniform infiltration with regional-aquifer Model A and source term interrupted in 2006</b>						
Perchlorate	HQ	O-1	1000	0	0.0%	1.28E-06
		O-4	1000	0	0.0%	0.15
		PM-1	1000	0	0.0%	0.53
		PM-2	1000	0	0.0%	2.04E-04
		PM-3	1000	18	1.8%	5.30
		PM-4	1000	0	0.0%	0.75
		PM-5	1000	1	0.1%	1.11

**Table C-1.2**  
**Doses and Probabilities of Exceedance of Dose\* >4 mrem/yr for 100 Years**

\*Doses were computed according to 40CFR141.66 maximum contaminant level for radionuclides, Table A

Contaminant(s) Evaluated	Quantity Evaluated	Wells Evaluated	Number of Maximum Dose Calculations	Number of Doses >4 mrem/yr	Probability of Exceedance of Dose >4 mrem/yr	Maximum Dose Round off?	Year of Maximum Dose
<b>Lower-canyon-dominated infiltration with fast paths in the upper, middle, and lower canyons with regional-aquifer Model A</b>							
Tritium	Dose	O-1	1000	0	0.0%	3.39E-12	141
		O-4	1000	0	0.0%	1.12E-3	103
		PM-1	1000	0	0.0%	2.28E-3	113
		PM-2	1000	0	0.0%	1.38E-08	141
		PM-3	1000	0	0.0%	0.03	106
		PM-4	1000	0	0.0%	0.02	93
		PM-5	1000	0	0.0%	0.05	86
<b>Lower-canyon-dominated infiltration with fast paths in the upper and middle canyons with regional-aquifer Model A</b>							
Tritium	Dose	O-1	1000	0	0.0%	2.75E-10	141
		O-4	1000	0	0.0%	2.41E-3	105
		PM-1	1000	0	0.0%	3.7E-4	106
		PM-2	1000	0	0.0%	8.15E-08	141
		PM-3	1000	0	0.0%	0.04	104
		PM-4	1000	0	0.0%	7.64E-3	102
		PM-5	1000	0	0.0%	0.05	86
<b>Lower-canyon-dominated uniform infiltration with regional-aquifer Model A</b>							
Tritium	Dose	O-1	1000	0	0.0%	2.75E-10	141
		O-4	1000	0	0.0%	1.83E-3	103
		PM-1	1000	0	0.0%	3.69E-4	105
		PM-2	1000	0	0.0%	8.16E-08	141
		PM-3	1000	0	0.0%	0.04	104
		PM-4	1000	0	0.0%	7.46E-3	102
		PM-5	1000	0	0.0%	0.03	94
<b>Lower-canyon-dominated infiltration with fast path in the lower canyon with regional-aquifer Model A</b>							
Tritium	Dose	O-1	1000	0	0.0%	3.39E-12	141
		O-4	1000	0	0.0%	4.19E-4	119
		PM-1	1000	0	0.0%	2.22E-3	113
		PM-2	1000	0	0.0%	1.38E-08	141
		PM-3	1000	0	0.0%	0.03	106
		PM-4	1000	0	0.0%	0.02	91
		PM-5	1000	0	0.0%	0.03	94

Table C-1.2 (continued)

Contaminant(s) Evaluated	Quantity Evaluated	Wells Evaluated	Number of Maximum Dose calculations	Number of Doses >4 mrem/yr	Probability of Exceedance of Dose >4 mrem/yr	Maximum Dose Round off?	Year of Maximum Dose
<b>Lower-canyon-dominated infiltration with fast path in the middle canyon with regional-aquifer Model A</b>							
Tritium	Dose	O-1	1000	0	0.0%	2.75E-10	141
		O-4	1000	0	0.0%	2.36E-3	105
		PM-1	1000	0	0.0%	3.7E-4	106
		PM-2	1000	0	0.0%	8.15E-08	141
		PM-3	1000	0	0.0%	0.04	104
		PM-4	1000	0	0.0%	7.63E-3	102
		PM-5	1000	0	0.0%	0.04	87
<b>Lower-canyon-dominated infiltration with fast path in the upper canyon with regional-aquifer Model A</b>							
Tritium	Dose	O-1	1000	0	0.0%	2.75E-10	141
		O-4	1000	0	0.0%	1.98E-3	104
		PM-1	1000	0	0.0%	3.69E-4	105
		PM-2	1000	0	0.0%	8.16E-08	141
		PM-3	1000	0	0.0%	0.04	104
		PM-4	1000	0	0.0%	7.47E-3	102
		PM-5	1000	0	0.0%	0.03	92

Table C-1.3  
HIs and Probabilities of Exceedance of HI >1 for 1000 years

Contaminant(s) Evaluated	Quantity Evaluated	Wells Evaluated	Number of Maximum HIs or HQs Calculations	Number of Calculations with HI or HQ >1	Probability of Exceedance of HI or HQ >1	Maximum HQ/HI Round off?	Year of Maximum HQ/HI
<b>Upper/middle-canyon-dominated uniform infiltration with regional-aquifer Model A</b>							
Perchlorate	HQ	O-1	1000	0	0.0%	0.02	630
		O-4	1000	0	0.0%	0.57	247
		PM-1	1000	27	2.7%	1.65	433
		PM-2	1000	0	0.0%	0.06	744
		PM-3	1000	741	74.1%	6.81	179
		PM-4	1000	3	0.3%	1.34	159
		PM-5	1000	167	16.7%	2.78	116
Nitrate and Perchlorate	HI	O-1	1000	0	0.0%	0.02	630
		O-4	1000	0	0.0%	0.58	247
		PM-1	1000	29	2.9%	1.66	433
		PM-2	1000	0	0.0%	0.06	743
		PM-3	1000	744	74.4%	6.93	179
		PM-4	1000	3	0.3%	1.36	159
		PM-5	1000	173	17.3%	2.83	116

Table C-1.3 (continued)

Contaminant(s) Evaluated	Quantity Evaluated	Wells Evaluated	Number of Maximum HIs or HQs Calculations	Number of Calculations with HI or HQ >1	Probability of Exceedance of HI or HQ >1	Maximum HQ/Hi Round off?	Year of Maximum HQ/Hi
<b>Lower-canyon-dominated infiltration with fast paths in the upper, middle and lower canyons with regional-aquifer Model A</b>							
Perchlorate	HQ	O-1	1000	0	0.0%	3.14E-02	590
		O-4	1000	0	0.0%	0.38	355
		PM-1	1000	41	4.1%	1.8	423
		PM-2	1000	0	0.0%	5.99E-02	716
		PM-3	1000	751	75.1%	7.52	265
		PM-4	1000	3	0.3%	1.43	124
		PM-5	1000	4	0.4%	1.61	111
Nitrate and Perchlorate	HI	O-1	1000	0	0.0%	3.19E-02	590
		O-4	1000	0	0.0%	0.39	355
		PM-1	1000	45	4.5%	1.83	423
		PM-2	1000	0	0.0%	6.07E-02	716
		PM-3	1000	754	75.4%	7.64	265
		PM-4	1000	4	0.4%	1.46	124
		PM-5	1000	5	0.5%	1.64	111
<b>Lower-canyon-dominated infiltration with fast paths in the upper and middle canyons with regional-aquifer Model A</b>							
Perchlorate	HQ	O-1	1000	0	0.0%	0.02	333
		O-4	1000	0	0.0%	0.43	252
		PM-1	1000	43	4.3%	1.82	383
		PM-2	1000	0	0.0%	0.07	719
		PM-3	1000	771	77.1%	7.80	259
		PM-4	1000	8	0.8%	1.57	177
		PM-5	1000	4	0.4%	1.63	112
Nitrate and Perchlorate	HI	O-1	1000	0	0.0%	0.02	333
		O-4	1000	0	0.0%	0.44	252
		PM-1	1000	44	4.4%	1.84	382
		PM-2	1000	0	0.0%	0.07	719
		PM-3	1000	773	77.3%	7.92	259
		PM-4	1000	8	0.8%	1.59	177
		PM-5	1000	5	0.5%	1.66	112
<b>Lower-canyon-dominated uniform infiltration with regional-aquifer Model A</b>							
Perchlorate	HQ	O-1	1000	0	0.0%	0.02	926
		O-4	1000	0	0.0%	0.53	235
		PM-1	1000	41	4.1%	1.90	393
		PM-2	1000	0	0.0%	0.07	608
		PM-3	1000	772	77.2%	7.75	258
		PM-4	1000	12	1.2%	1.79	170
		PM-5	1000	39	3.9%	1.85	130

Table C-1.3 (continued)

Contaminant(s) Evaluated	Quantity Evaluated	Wells Evaluated	Number of Maximum HIs or HQs Calculations	Number of Calculations with HI or HQ >1	Probability of Exceedance of HI or HQ >1	Maximum HQ/HI Round off?	Year of Maximum HQ/HI
<b>Lower-canyon-dominated uniform infiltration with regional-aquifer Model A (continued)</b>							
Nitrate and Perchlorate	HI	O-1	1000	0	0.0%	0.02	926
		O-4	1000	0	0.0%	0.54	235
		PM-1	1000	43	4.3%	1.93	393
		PM-2	1000	0	0.0%	0.07	608
		PM-3	1000	774	77.4%	7.87	258
		PM-4	1000	12	1.2%	1.81	170
		PM-5	1000	40	4.0%	1.88	130
<b>Lower-canyon-dominated infiltration with fast path in the lower canyon with regional-aquifer Model A</b>							
Perchlorate	HQ	O-1	1000	0	0.0%	0.03	590
		O-4	1000	0	0.0%	0.44	245
		PM-1	1000	44	4.4%	1.86	423
		PM-2	1000	0	0.0%	0.06	429
		PM-3	1000	750	75.0%	7.47	266
		PM-4	1000	6	0.6%	1.51	151
		PM-5	1000	37	3.7%	1.82	130
Nitrate and Perchlorate	HI	O-1	1000	0	0.0%	0.03	590
		O-4	1000	0	0.0%	0.45	245
		PM-1	1000	45	4.5%	1.89	423
		PM-2	1000	0	0.0%	0.06	425
		PM-3	1000	754	75.4%	7.59	266
		PM-4	1000	6	0.6%	1.53	151
		PM-5	1000	39	3.9%	1.85	131
<b>Lower-canyon-dominated infiltration with fast path in the middle canyon with regional-aquifer Model A</b>							
Perchlorate	HQ	O-1	1000	0	0.0%	0.02	333
		O-4	1000	0	0.0%	0.47	260
		PM-1	1000	44	4.4%	1.84	388
		PM-2	1000	0	0.0%	0.068	729
		PM-3	1000	773	77.3%	7.76	258
		PM-4	1000	8	0.8%	1.65	179
		PM-5	1000	30	3.0%	1.65	131
Nitrate and Perchlorate	HI	O-1	1000	0	0.0%	0.02	333
		O-4	1000	0	0.0%	0.48	260
		PM-1	1000	44	4.4%	1.88	388
		PM-2	1000	0	0.0%	0.07	729
		PM-3	1000	774	77.4%	7.89	258
		PM-4	1000	8	0.8%	1.68	167
		PM-5	1000	31	3.1%	1.67	131

Table C-1.3 (continued)

Contaminant(s) Evaluated	Quantity Evaluated	Wells Evaluated	Number of Maximum HIs or HQs Calculations	Number of Calculations with HI or HQ >1	Probability of Exceedance of HI or HQ >1	Maximum HQ/HI Round off?	Year of Maximum HQ/HI
<b>Lower-canyon-dominated infiltration with fast path in the upper canyon with regional-aquifer Model A</b>							
Perchlorate	HQ	O-1	1000	0	0.0%	0.02	926
		O-4	1000	0	0.0%	0.50	234
		PM-1	1000	41	4.1%	1.87	377
		PM-2	1000	0	0.0%	0.06	699
		PM-3	1000	772	77.2%	7.78	259
		PM-4	1000	12	1.2%	1.72	167
		PM-5	1000	15	1.5%	1.78	117
Nitrate and Perchlorate	HI	O-1	1000	0	0.0%	0.02	926
		O-4	1000	0	0.0%	0.51	234
		PM-1	1000	43	4.3%	1.90	377
		PM-2	1000	0	0.0%	0.06	699
		PM-3	1000	773	77.3%	7.91	259
		PM-4	1000	12	1.2%	1.75	167
		PM-5	1000	18	1.8%	1.81	118
<b>Lower-canyon-dominated infiltration with fast paths in the upper and middle canyons with regional-aquifer Model B</b>							
Perchlorate	HQ	O-1	1000	0	0.0%	8.72E-03	277
		O-4	1000	0	0.0%	6.69E-04	216
		PM-1	1000	0	0.0%	0.08	206
		PM-2	1000	0	0.0%	1.05E-03	534
		PM-3	1000	0	0.0%	0.07	170
		PM-4	1000	0	0.0%	0.03	239
		PM-5	1000	0	0.0%	0.10	109
<b>Lower-canyon-dominated uniform infiltration with regional-aquifer Model A and source term interrupted in 2006</b>							
Perchlorate	HQ	O-1	1000	0	0.0%	4.91E-03	630
		O-4	1000	0	0.0%	0.25	565
		PM-1	1000	3	0.3%	1.10	618
		PM-2	1000	0	0.0%	0.04	912
		PM-3	1000	629	62.9%	6.02	254
		PM-4	1000	0	0.0%	0.75	140
		PM-5	1000	1	0.1%	1.11	113

**Table C-1.4**  
**Probability of Exceedance for Perchlorate HQs for**  
**Higher Perchlorate Maximum Concentration Limits**

Conceptual Model	Wells	Probability of Exceedance for 1000 years (additional 0.0% are not shown)								
		Potential Maximum Concentration Level for Perchlorate [ug/L]								
		1	2	3	4	5	6	7	8	24.5
Upper/middle-canyon-dominated uniform infiltration for perchlorate with regional-aquifer Model A	O-1	0.0%								
	O-4	0.0%								
	PM-1	2.7%	0.0%							
	PM-2	0.0%								
	PM-3	74.1%	32.9%	9.7%	2.8%	0.5%	0.2%	0.0%		
	PM-4	0.3%	0.0%							
	PM-5	16.3%	0.4%	0.0%						
Lower-canyon-dominated infiltration with fast paths in the upper and middle canyons for perchlorate with regional-aquifer Model A	O-1	0.0%								
	O-4	0.0%								
	PM-1	4.3%	0.0%							
	PM-2	0.0%								
	PM-3	77.1%	42.2%	16.5%	5.2%	1.5%	0.4%	0.2%	0.0%	
	PM-4	0.8%	0.0%							
	PM-5	0.4%	0.0%							
Lower-canyon-dominated uniform infiltration for perchlorate with regional-aquifer Model A	O-1	0.0%								
	O-4	0.0%								
	PM-1	4.1%								
	PM-2	0.0%								
	PM-3	77.2%	43.1%	17.2%	5.8%	1.7%	0.4%	0.3%	0.0%	
	PM-4	1.2%	0.0%							
	PM-5	3.9%	0.0%							
Lower-canyon-dominated infiltration with fast path in the lower canyon for perchlorate with regional-aquifer Model A	O-1	0.0%								
	O-4	0.0%								
	PM-1	4.4%	0.0%							
	PM-2	0.0%								
	PM-3	75.0%	37.1%	12.6%	3.6%	0.5%	0.4%	0.1%	0.0%	
	PM-4	0.6%	0.0%							
	PM-5	3.7%	0.0%							
Lower-canyon-dominated infiltration with fast path in the middle canyon for perchlorate with regional-aquifer Model A	O-1	0.0%								
	O-4	0.0%								
	PM-1	4.4%	0.0%							
	PM-2	0.0%								
	PM-3	77.3%	42.4%	16.9%	5.4%	1.6%	0.4%	0.2%	0.0%	
	PM-4	0.8%	0.0%							
	PM-5	3.0%	0.0%							

Table C-1.4 (continued)

Conceptual Model	Wells	Probability of Exceedance for 1000 years (additional 0.0% are not shown)								
		Potential Maximum Concentration Level for Perchlorate [ug/L]								
		1	2	3	4	5	6	7	8	24.5
Lower-canyon-dominated infiltration with fast path in the upper canyon for perchlorate with regional-aquifer Model A	O-1	0.0%								
	O-4	0.0%								
	PM-1	4.1%	0.0%							
	PM-2	0.0%								
	PM-3	77.2%	42.9%	17.1%	5.7%	1.8%	0.4%	0.3%	0.0%	
	PM-4	1.2%	0.0%							
	PM-5	1.5%	0.0%							
Lower-canyon-dominated infiltration with fast paths in the upper and middle canyons for perchlorate with regional-aquifer Model B	O-1	0.0%								
	O-4	0.0%								
	PM-1	0.0%								
	PM-2	0.0%								
	PM-3	0.0%								
	PM-4	0.0%								
	PM-5	0.0%								
Lower-canyon-dominated uniform infiltration for perchlorate with regional-aquifer Model A and source term interrupted in 2006	O-1	0.0%								
	O-4	0.0%								
	PM-1	0.3%	0.0%							
	PM-2	0.0%								
	PM-3	62.9%	10.8%	1.2%	0.3%	0.2%	0.1%	0.0%		
	PM-4	0.0%								
	PM-5	0.1%	0.0%							

FIGURES OF PERCENTAGE OF SIMULATIONS WITH HI GREATER THAN 1 VS TIME

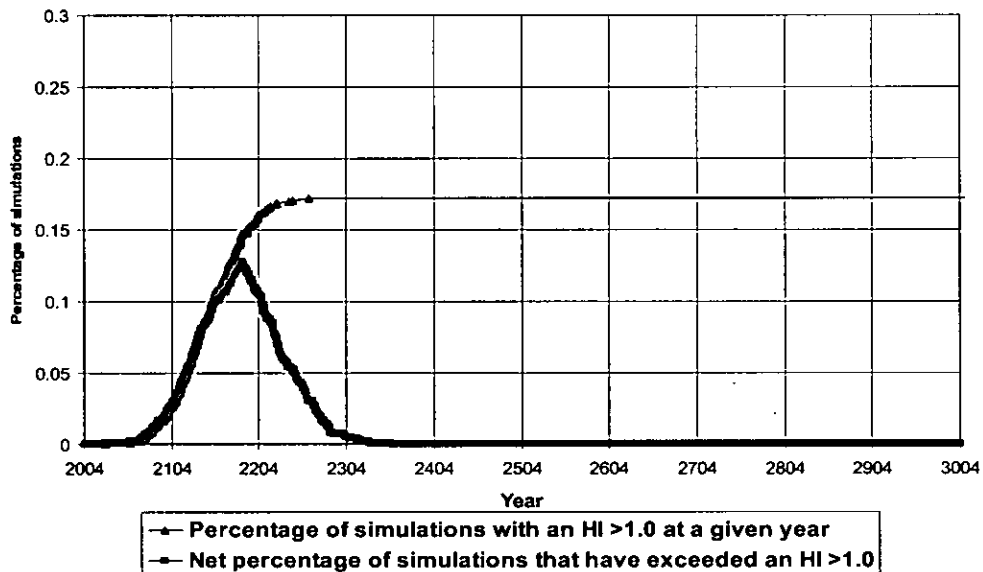


Figure C-1.1. Percentage of simulations with HI > 1 for upper/middle-canyon-dominated uniform infiltration for perchlorate and nitrate with regional-aquifer Model A for PM-5 and a 1000-yr analysis period

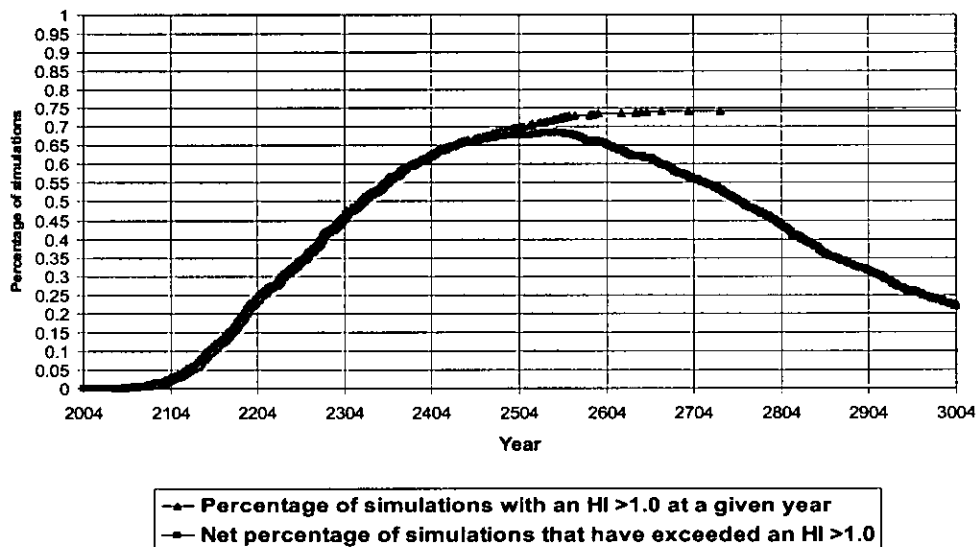


Figure C-1.2. Percentage of simulations with HI > 1 for upper/middle-canyon-dominated uniform infiltration for perchlorate and nitrate with regional-aquifer Model A for PM-3 and a 1000-yr analysis period

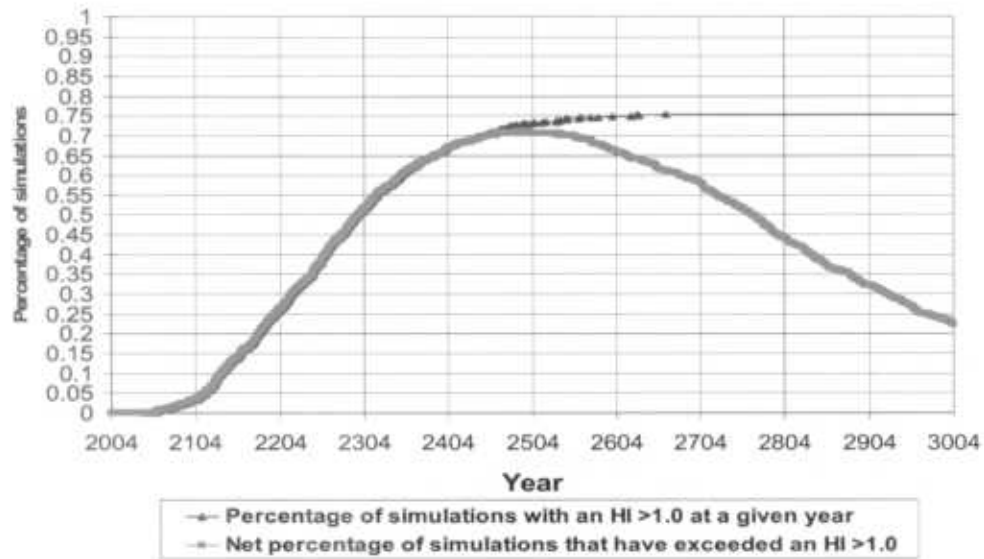


Figure C-1.3. Percentage of simulations with HI > 1 for lower-canyon-dominated infiltration with fast paths in the upper, middle, and lower canyons for perchlorate and nitrate with regional-aquifer Model A for PM-3 and a 1000-yr analysis period

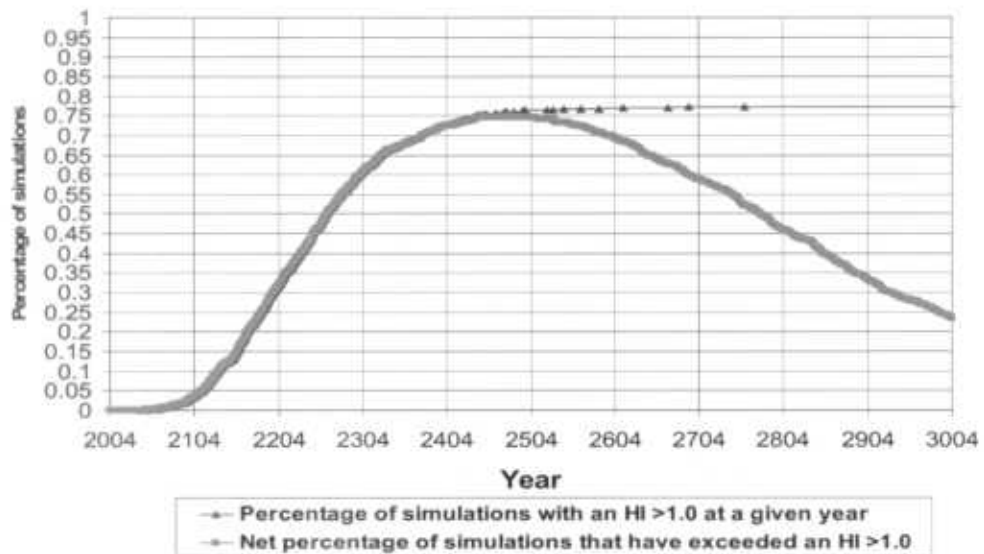
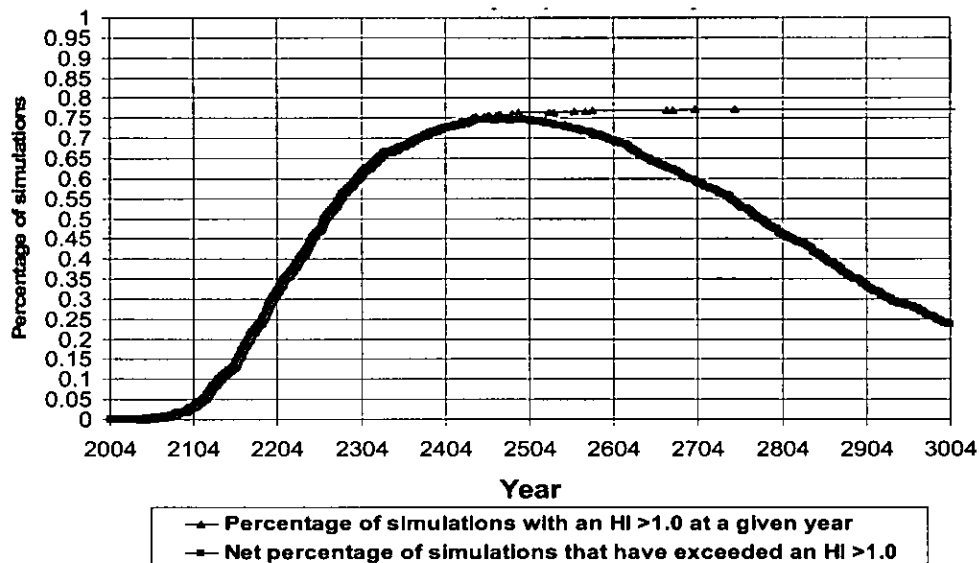
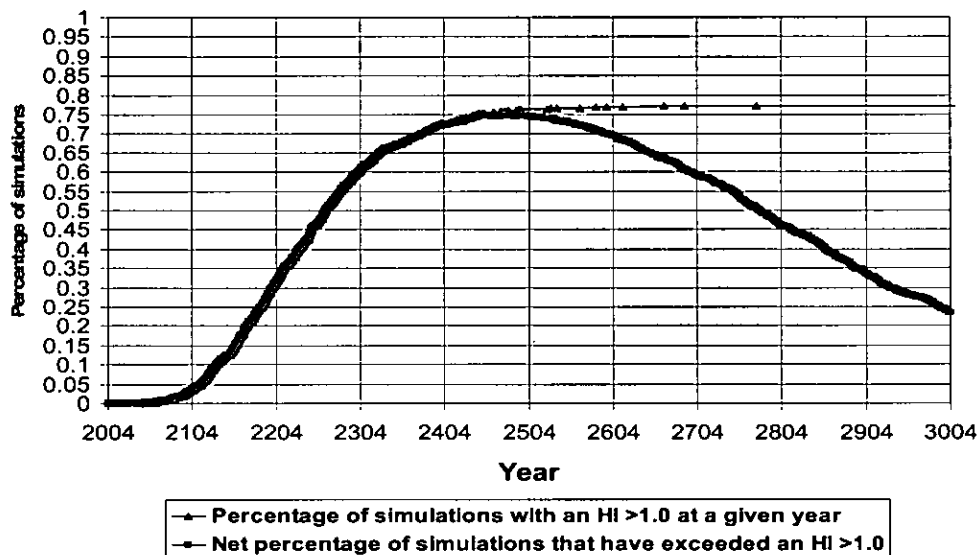


Figure C-1.4. Percentage of simulations with HI > 1 for lower-canyon-dominated infiltration with fast paths in the upper and middle canyons for perchlorate and nitrate with regional-aquifer Model A for PM-3 and a 1000-yr analysis period



**Figure C-1.5.** Percentage of simulations with HI >1 for lower-canyon-dominated infiltration with a fast path in the upper canyon for perchlorate and nitrate with regional-aquifer Model A for PM-3 and a 1000-yr analysis period



**Figure C-1.6.** Percentage of simulations with HI >1 for lower-canyon-dominated infiltration with a fast path in the middle canyon for perchlorate and nitrate with regional-aquifer Model A for PM-3 and a 1000-yr analysis period

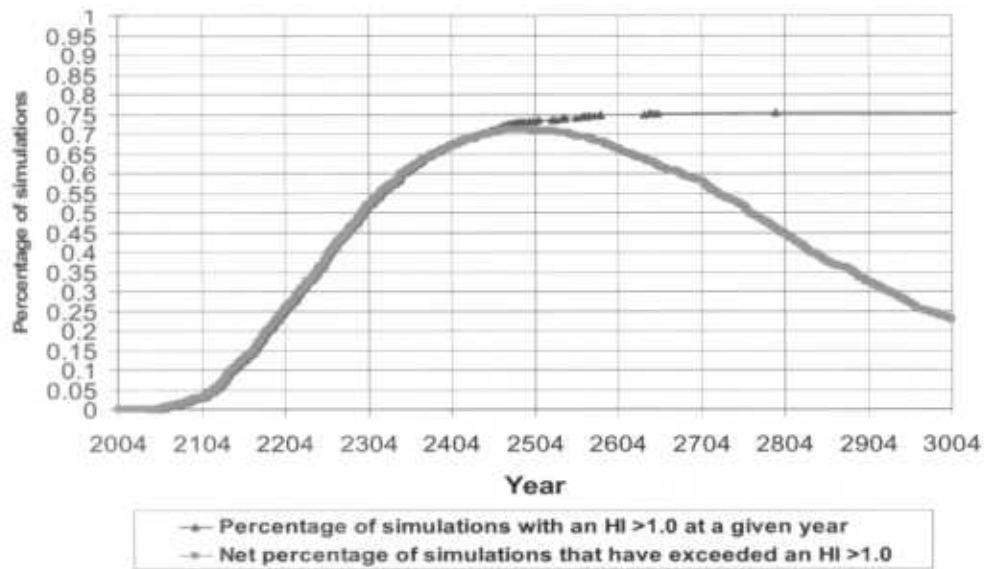


Figure C-1.7. Percentage of simulations with HI > 1 for lower-canyon-dominated infiltration with fast path in the lower canyon for perchlorate and nitrate with regional-aquifer Model A for PM-3 and a 1000-yr analysis period

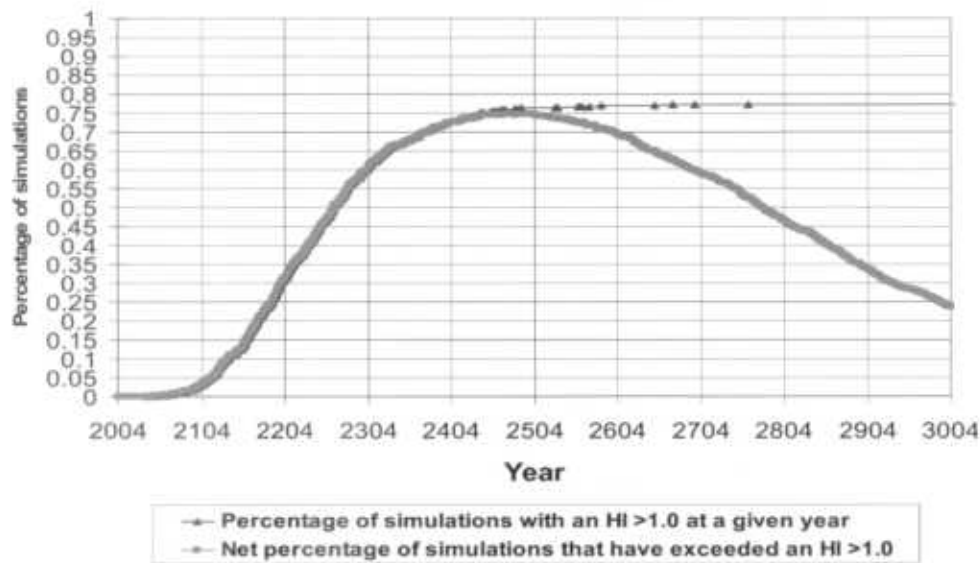
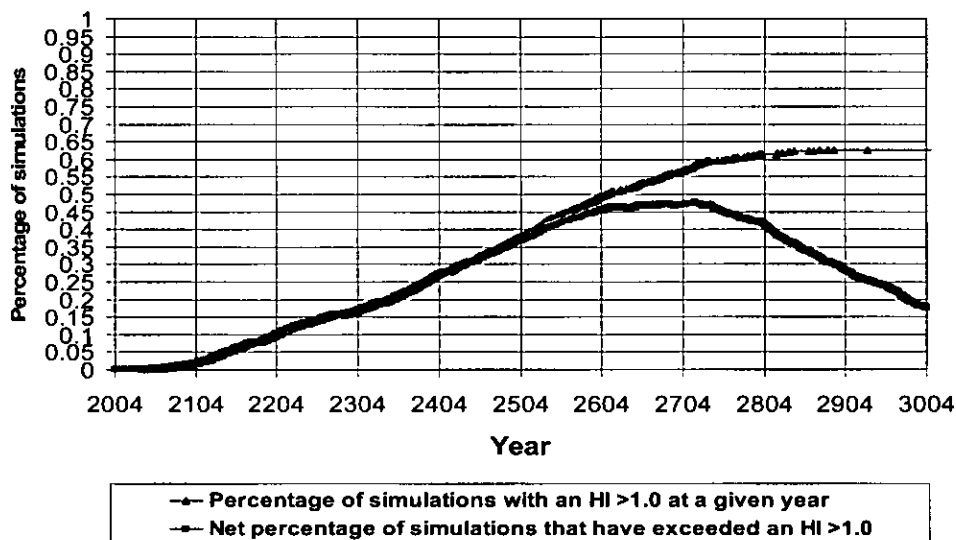


Figure C-1.8. Percentage of simulations with HI > 1 for lower-canyon-dominated uniform infiltration for perchlorate and nitrate with regional-aquifer Model A for PM-3 and a 1000-yr analysis period



**Figure C-1.9. Percentage of simulations with HI > 1 for lower-canyon-dominated uniform infiltration for perchlorate with regional-aquifer Model A and source term interrupted in 2006 for PM-3 and a 1000-yr analysis period**

### C-2.0 RISK-ASSESSMENT CALCULATIONS

The term “risk” in environmental restoration is often only used to describe the chance of an individual getting cancer after being exposed to a contaminant. In the Mortandad Canyon Tier-3 risk assessment, risk is used to indicate the likelihood of exceeding an EPA health indicator (HQ and/or HI values) because perchlorate and nitrate are not classified as carcinogens. In addition, the likelihood of exceeding the DOE-specified drinking-water dose standard (DOE Order 5400.5, 90190) was used to evaluate potential health effects from tritium-contaminated groundwater.

The calculation of HI, HQ, and total equivalent dose effective (TEDE) for assessing drinking-water exposures follows the EPA guidance (EPA 1989, 08021). Each production well was evaluated in the exposure assessment using a moving 70-yr average contaminant concentration calculated within the analysis period(s) (100 and 1000 yr for HQ/HI and 100 yr for dose).

#### C-2.1 Exposure Model

Following EPA guidance (EPA 1989, 08021), adult exposures to nitrate, perchlorate, and tritium were assumed to occur over a 70-yr period, with an ingestion rate of 2 L/day of water pumped exclusively from an individual well. EPA’s exposure model was used to compute the chronic daily intake (CDI) as follows:

$$CDI [mg/(kg/day)] = (C_{70} [mg/L] \times CR [L/day] \times EF [day/yr] \times ED [y]) / (BW [kg] \times AT [day]) ,$$

where

- CDI chronic daily intake of the chemical in mg/kg/day);
- $C_{70}$  average concentration of the chemical over 70 yr in mg/L;
- CR contact rate: water ingestion rate of 2 L/day;
- EF exposure frequency, 365 days/yr;
- ED exposure duration: 70 yr;
- BW body weight: 70 kg; and

AT averaging time: ED × 365 days/yr for noncarcinogens.

Model output concentrations were obtained in moles/L and were converted to mg/L, using the following equation:

$$C_{70} [\text{mg/L}] = C_{70} [\text{moles/L}] \times \text{MW} [\text{g/moles}] \times 1000 \text{ mg/g} ,$$

where

MW atomic or molecular weight in g/mole.

The CDI was computed for each year, based on the average calculated concentrations for the previous 69 yr plus the current year.

### C.2.2 Hazard Quotient and Hazard Index Computation

The HI is the summation of the HQ for each chemical assessed. The HQ is computed in the following manner:

$$\text{HQ} = \text{CDI} [\text{mg}/(\text{kg}/\text{day})] / \text{RfD} [\text{mg}/(\text{kg}/\text{day})] ,$$

where

HI dimensionless number; and

RfD reference dose for the chemical for assessing noncancerous health effects (mg/kg/day).

If only one constituent is evaluated, then HIs are equivalent to HQs and reported as HIs. When both nitrate and perchlorate are included, HI is computed as

$$\text{HI} = \Sigma (\text{HQ}_{\text{NO}_3} + \text{HQ}_{\text{ClO}_4}) .$$

For all cases, HQ/HI is computed for each simulation year based on a concentration averaged over a moving 70-yr period. Once all HIs were computed for a given simulation, its maximum HI was chosen for use in all further analyses.

### C-2.3 Radioactive Dose Computation

The annual radioactive dose equivalent for ingestion of water contaminated with radionuclides is calculated as

$$\text{Dose} [\text{mrem}/\text{yr}] = C_{70} [\text{pCi}/\text{L}] \times \text{CR} [\text{L}/\text{day}] \times \text{EF} [\text{day}/\text{yr}] \times \text{DCF} [\text{mrem}/\text{pCi}] ,$$

where

Dose annual dose equivalent in mrem/yr;

$C_{70}$  moving average radionuclide concentration over 70 yr in pCi/L;

CR contact rate: water ingestion rate of 2 L/day;

DCF dose conversion factor for radionuclide ingestion in mrem/pCi; and

EF exposure frequency, 365 days/yr.

Model output concentration, in moles/L, was converted to pCi/L, using the following equation:

$$C_{70} [\text{pCi}/\text{L}] = C_{70} [\text{moles}/\text{L}] \times \text{NA} \times [1/\text{moles}] \times \text{Conv. factor} [\text{pCi}/\text{Bq}] [\text{yr}/\text{s}] \times \ln(2) / \text{Tmed} [\text{yr}] ,$$

where

NA	Avogadro's number (6.02 E+23 [1/moles]);
Tmed	Half-life [yr]; and
Conversion factor	27.027 pCi/Bq-yr/(31,536,000 s) = 8.5702E-07 pCi-yr/(Bq-s).

Incorporating the conversion factor into the above equation yields

$$C_{70} [\text{pCi/L}] = C_{70} [\text{moles/L}] \times 3.57613E + 17 [\text{pCi-yr/moles}] / T_{\text{med}}[\text{yr}].$$

### C-3.0 TOXICITY PARAMETERS CALCULATION AND SELECTION

This section includes two parts: the first uses perchlorate as an example of how EPA determines an RfD and the associated MCL for a chemical; the second one explains the selection of nitrate and perchlorate RfDs and the tritium dose conversion factor (DCF) for the Mortandad Canyon Tier-3 analysis.

#### C-3.1 EPA's Reference Dose

The EPA's RfD is an estimate of the daily intake of a contaminant that is likely to be without any appreciable risk of deleterious effects during a person's lifetime. The RfD is based on the assumption that thresholds exist for certain toxic effects. RfDs are expressed in units of mg/kg/day. The following discussion uses perchlorate as an example of how an RfD is set by EPA and how it relates to MCLs.

Perchlorate has recently become a national regulatory and public health concern. In early 1997, the existence of widespread groundwater contamination with perchlorate in the United States was realized with the development of an analytical method for quantifying perchlorate concentrations at a detection limit of 4 µg/L (EPA 2003, 90507). In 1998, perchlorate was placed on the EPA's Contaminant Candidate List for consideration for possible regulation. In 1999, EPA required drinking water monitoring for perchlorate under the Unregulated Contaminant Monitoring Rule (Laboratory Perchlorate Issues, Laboratory Interim Draft, May 2003).

In 2002, EPA concluded that the potential human-health risks of perchlorate exposures could include effects on the developing nervous system and thyroid tumors. This assessment included a draft RfD that was intended to be protective for both types of effects. The draft RfD, 0.00003 mg/kg/day (EPA 2003, 90505), was based on perceived changes in infant rat brain structure (PerchlorateNews.com, October 23, 2003).

Using the draft RfD along with EPA standard exposure assumptions for a 70-kg body weight and 2-L/day drinking water consumption yields an equivalent MCL of 1 µg/L (EPA 2003, 90505).

Recently, EPA changed the RfD for perchlorate based on a study by Greer et al. (2002, 90189). The Greer et al. study (2002, 90189) used iodide uptake inhibition as a key biochemical event that precedes all potential thyroid-mediated effects of perchlorate exposure. Exposure levels obtained in this manner are referred to as no-observed-effect levels (NOEL) by EPA because iodide uptake inhibition is not an adverse effect but a biochemical change that precedes health effects. The use of a NOEL in setting an RfD is more conservative and health-protective than traditional methods based on observed health effects. Using the NOEL approach and the Greer et al. study (2002, 90189), EPA defined the RfD for perchlorate as 0.007 mg/kg/day. Accounting for variability in responses among humans, specifically the fetuses of pregnant women who might have hypothyroidism or iodide deficiency, EPA assigned an intraspecies uncertainty factor of 10, resulting in an RfD of 0.0007 mg/kg/day, which is the equivalent of an MCL of 24.5 mg/kg/day (EPA's Integrated Risk Iris Database [IRIS], 2005, 90508).

At the time the Mortandad Canyon Tier-3 risk assessment was performed, the EPA RfD for perchlorate was 0.00003 mg/kg/day. This value was used in all Tier-3 assessments and corresponds to a perchlorate MCL of 1 µg/L.

The RfD for nitrate for the Mortandad Canyon Tier-3 assessment was taken from EPA's IRIS (<http://www.epa.gov/iris/subst/0076.htm>). The RfD for oral exposure to nitrate in water is 1.6 mg/kg/day.

### C-3.2 DOE Radioactive Dose Limit

The dose assessment for tritium used DOE's 4 mrem/yr (DOE order 5400.5, 90190) dose-concentration guideline (DCG) for drinking water. To convert model-produced concentrations to dose, a DCF for tritium was adopted from 40 CFR141.66 (MCLs for radionuclides) Table A, where it is assumed that a drinking water concentration of 20,000 pCi/L yields a dose of 4 mrem/yr.

### C-4.0 RISK-ASSESSMENT RESULTS

The results of a probabilistic risk assessment are generally presented in the form of a CCDF. A CCDF displays the full range of HQs/HIs or doses calculated and the probability that a given HQ/HI or dose will be exceeded.

The CCDF for HIs or dose are computed in the following way. (HI will be used in the explanation as an example.)

HIs are sorted from smallest to largest.

For each HI, a probability is assigned; for our case, the same probability is assigned to each value. This probability is the sampling probability of  $1/N$ , with  $N$  being the total number of simulations (1000 for the Mortandad Tier-3 analysis)

The cumulative distribution function (CDF) is computed for each HI. The value corresponding to one HI is the summation of its probability and the probability from all lower HIs. For example, a probability of  $1/N$  is assigned to the smallest HI. The cumulative probability of  $1/N + 1/N$ , or  $2/N$  is assigned to the next largest HI and so on. The largest HI ends up having a probability of 1.0 ( $N/N$ ). The cumulative probabilities are the probability of obtaining a value lower or equal to the selected HI, i.e., the probability of finding an HI lower or equal to maximum HI equals 1, but the probability of finding a value lower or equal to the minimum HI is  $1/N$ .

The CCDF is obtained by computing the complement to the CDF. This is done by subtracting the CDF cumulative probabilities from 1.0. The smallest HI value will now have a probability of  $(N-1)/N$  and corresponds to the probability of obtaining a value greater than the smallest HI. In a CCDF, the probability is zero for obtaining an HI greater than the largest value.

CCDFs are used in the Mortandad Canyon assessment to visualize the 95% confidence level in relation to calculated HIs and doses.

The first step in the Mortandad Canyon Tier-3 risk assessment was to compute HIs for perchlorate and nitrate for all conceptual models for a 100-yr analysis period. In Table C-1.1, a summary of computed probabilities of HIs exceeding 1.0 and the maximum HIs are presented for each well. PM-3 has the maximum probability of exceedance for all conceptual models except for the phreatic-transport regional aquifer Model B, where the probability of exceedance for all conceptual models is zero for all wells. All probabilities of exceedance are below the 5% limit for 100 yr. Within 100 yr, the maximum HI for PM-3 is about 6.5. CCDFs for this case are shown in Figures C.4-1 to C.4-18.

The radioactive doses associated with potential tritium exposure were computed for each conceptual model for the 100-yr analysis period (see Figures C.4-19 to C.4-30). The probabilities of exceeding a radioactive dose of 4 mrem/yr (i.e., an MCL of 20,000 pCi/L) were computed and are shown in Table C-1.2. Table C-1.2 also presents the maximum calculated doses for all wells and a variety of conceptual models. All doses are below the dose limit of 4 mrem/yr, and therefore the probability of exceeding a dose limit is zero. The wells that show the largest doses are PM-3 and PM-5, with maximum doses of less than 0.05 mrem/yr.

The HI analyses were also conducted for a 1000-year simulation period. A summary of exceedance probabilities and maximum HIs are presented in Table C-4.3. Corresponding CCDFs are shown in Figures C-4.31 to C-4.48. The probabilities of an HI exceeding 1.0 for PM-3 for regional-aquifer conceptual Model A are approximately 75%. However, HIs for the 1,000-yr period of analysis are only slightly larger than the maximum HI for the 100-yr analysis with all HIs being less than 8.0. PM-5 has probabilities of exceedance below 5% for all conceptual models except for the upper/middle-canyon-dominated uniform infiltration for perchlorate and nitrate with regional-aquifer conceptual Model A. This conceptual model has a 17% probability of exceeding an HI of 1.0. The maximum HI is about 2.8 for this conceptual model.

For conceptual models whose exceedance probabilities are above 5%, curves showing the time dependence of the percentage of simulations with HIs greater than 1.0 are shown in Figures C-1.1 to C-1.9. For well PM-3, all conceptual models have a percentage of HIs exceeding 1.0 within the 500 yr. For the one conceptual model where PM-5 has a 17% probability of exceedance, this percentage is reached in about 200 yr.

The Mortandad Canyon Tier-3 analysis was based on a perchlorate RfD of 0.00003 mg, which is equivalent to an MCL of 1.0 µg/L. At the same time, EPA was considering new evidence relating to the perchlorate RfD. Therefore, an analysis of alternative RfD values was performed (Table C-1.4). In summary, the probabilities of exceedance are zero for all conceptual models for an assumed RfD of 0.00024 mg/kg/day, which is equivalent to a concentration limit of 8 µg/L. Note that the EPA has recently published an RfD of 0.0007 mg/kg/day for perchlorate. This RfD is equivalent to a groundwater concentration limit of 24.5 µg/L. (EPA's Integrated Risk Database [IRIS], 2005, 90508).

### FIGURES OF COMPLEMENTARY CUMULATIVE DISTRIBUTION FUNCTION FOR HI FOR 100 YEARS ANALYSIS

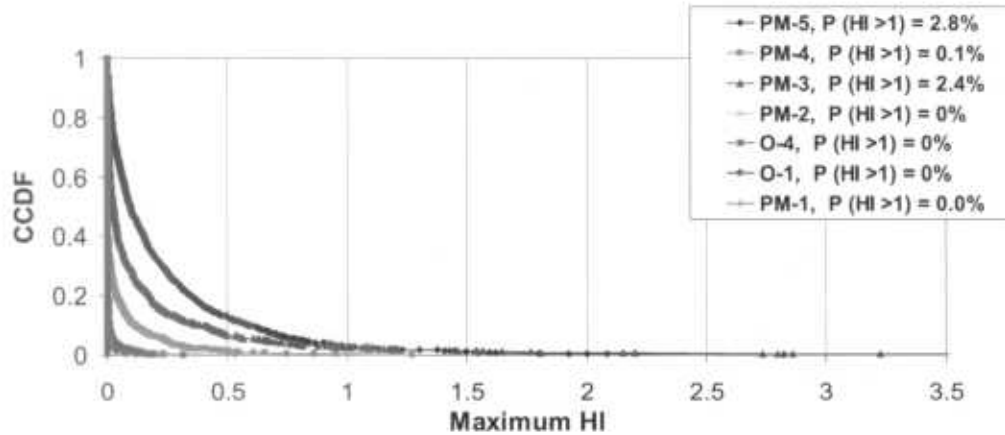


Figure C-4.1. CCDF for upper/middle-canyon-dominated uniform infiltration for perchlorate and nitrate with regional-aquifer Model A for a 100-yr analysis period (linear scale)

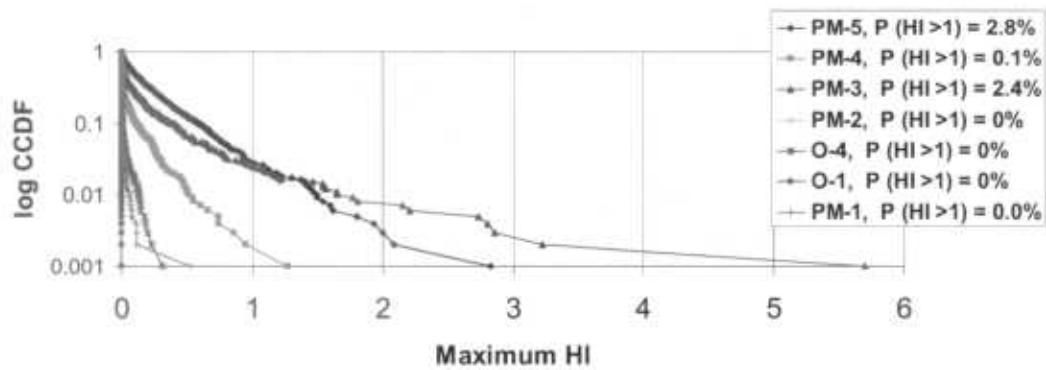


Figure C-4.2. CCDF for upper/middle-canyon-dominated uniform infiltration for perchlorate and nitrate with regional-aquifer Model A for a 100-yr analysis period (log scale)

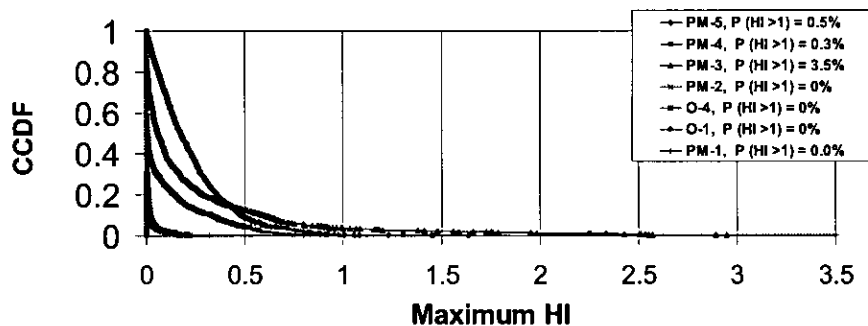


Figure C-4.3. CCDF for lower-canyon-dominated infiltration with fast paths in the upper, lower, and middle canyons for perchlorate and nitrate with regional-aquifer Model A for a 100-yr analysis period (linear scale)

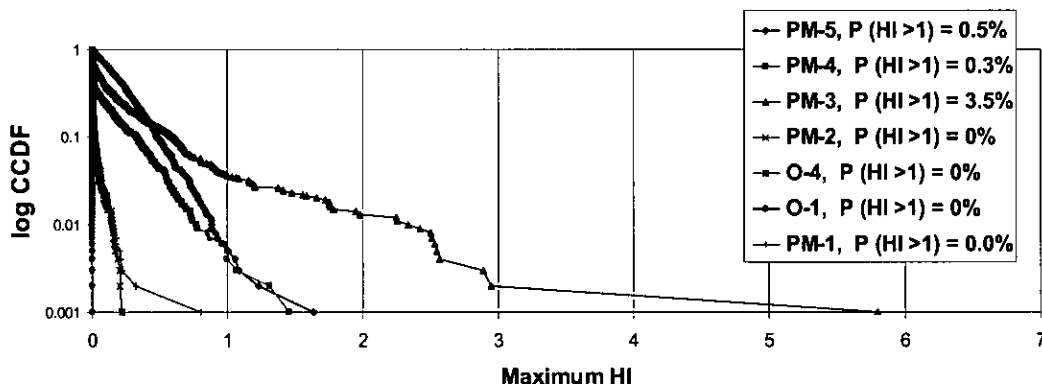


Figure C-4.4. CCDF for lower-canyon-dominated infiltration with fast paths in the upper, lower, and middle canyons for perchlorate and nitrate with regional-aquifer Model A for a 100-yr analysis period (log scale)

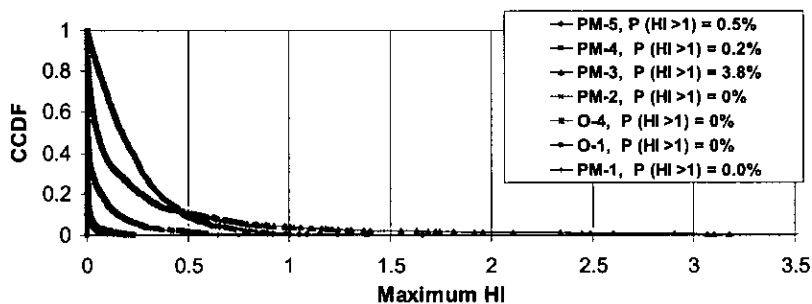


Figure C-4.5. CCDF for lower-canyon-dominated infiltration with fast paths in the upper and middle canyons for perchlorate and nitrate with regional-aquifer Model A for a 100-yr analysis period (linear scale)

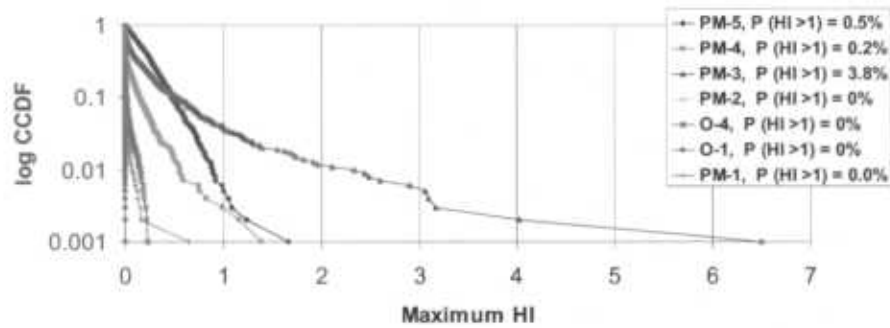


Figure C-4.6. CCDF for lower-canyon-dominated infiltration with fast paths in the upper and middle canyons for perchlorate and nitrate with regional-aquifer Model A for a 100-yr analysis period (log scale)

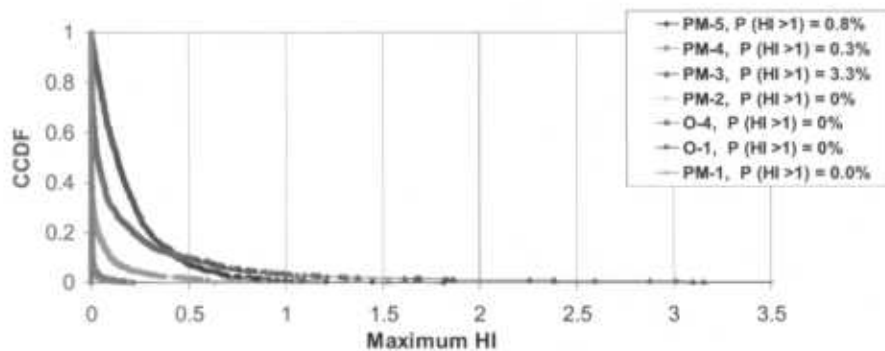


Figure C-4.7. CCDF for lower-canyon-dominated infiltration with fast path in the upper canyon for perchlorate and nitrate with regional-aquifer Model A for a 100-yr analysis period (linear scale)

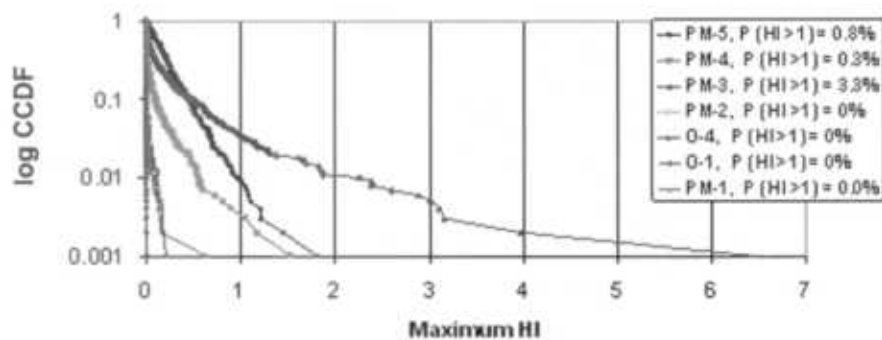


Figure C-4.8. CCDF for lower-canyon-dominated infiltration with fast path in the upper canyon for perchlorate and nitrate with regional-aquifer Model A for a 100-yr analysis period (log scale)

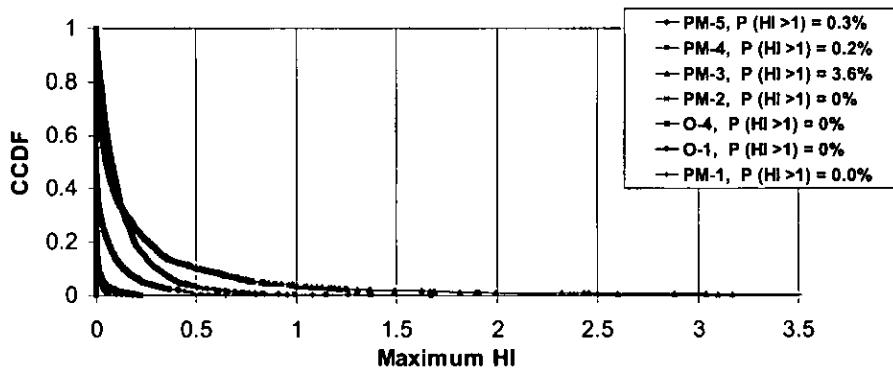


Figure C-4.9. CCDF for lower-canyon-dominated infiltration with fast path in the middle canyon for perchlorate and nitrate with regional-aquifer Model A for 100-yr analysis period (linear scale)

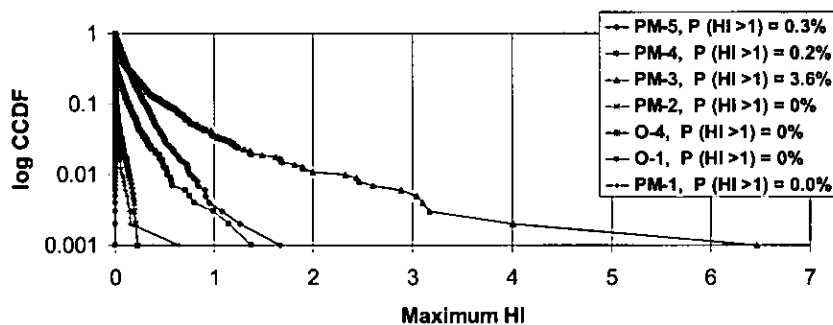


Figure C-4.10. CCDF for lower-canyon-dominated infiltration with fast path in the middle canyon for perchlorate and nitrate with regional-aquifer Model A for a 100-yr analysis period (log scale)

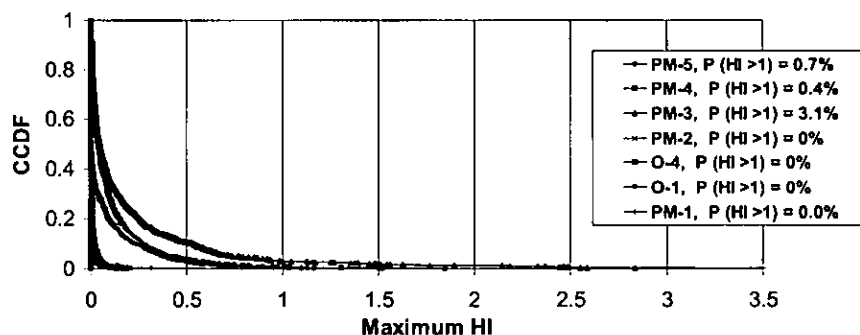


Figure C-4.11. CCDF for lower-canyon-dominated infiltration with fast path in the lower canyon for perchlorate and nitrate with regional-aquifer Model A for a 100-yr analysis period (linear scale)

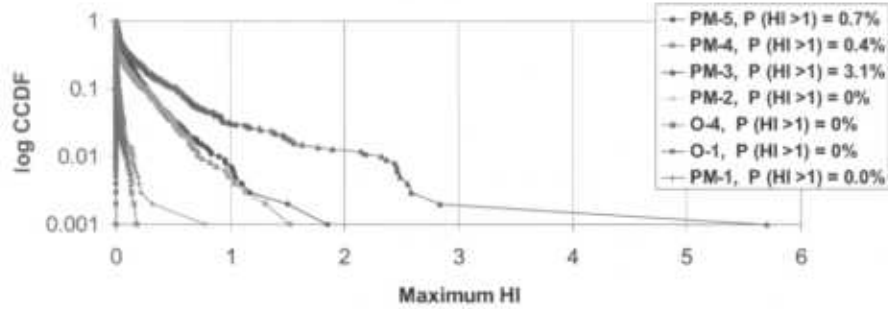


Figure C-4.12. CCDF for lower-canyon-dominated infiltration with fast path in the lower canyon for perchlorate and nitrate with regional-aquifer Model A for a 100-yr analysis period (log scale)

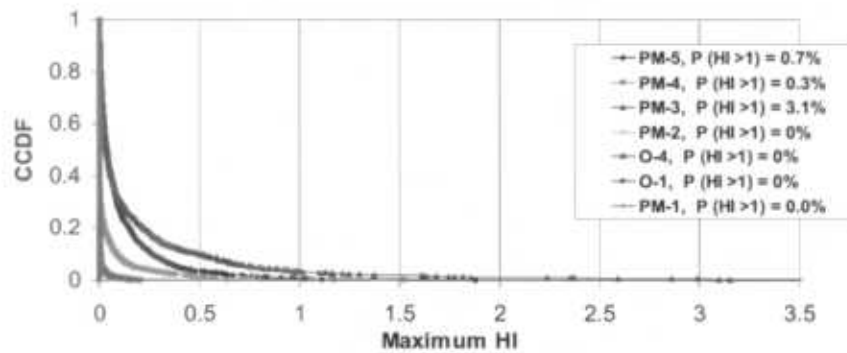


Figure C-4.13. CCDF for lower-canyon-dominated uniform infiltration for perchlorate and nitrate with regional-aquifer Model A for a 100-yr analysis period (linear scale)

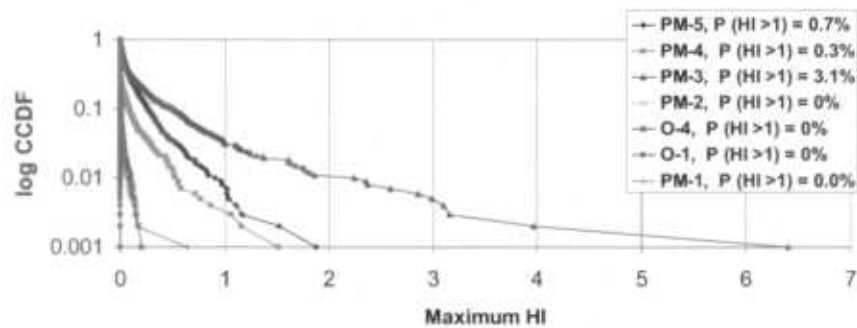


Figure C-4.14. CCDF for lower-canyon-dominated uniform infiltration for perchlorate and nitrate with regional-aquifer Model A for a 100-yr analysis period (log scale)

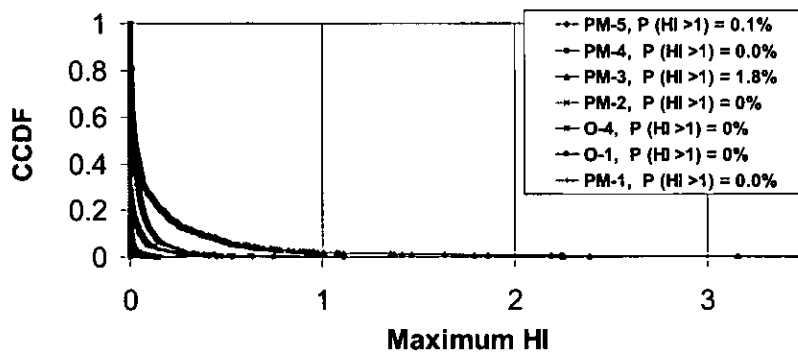


Figure C-4.15. CCDF for lower-canyon-dominated uniform infiltration for perchlorate with regional-aquifer Model A and source term interrupted in 2006, for a 100-yr analysis period (linear scale)

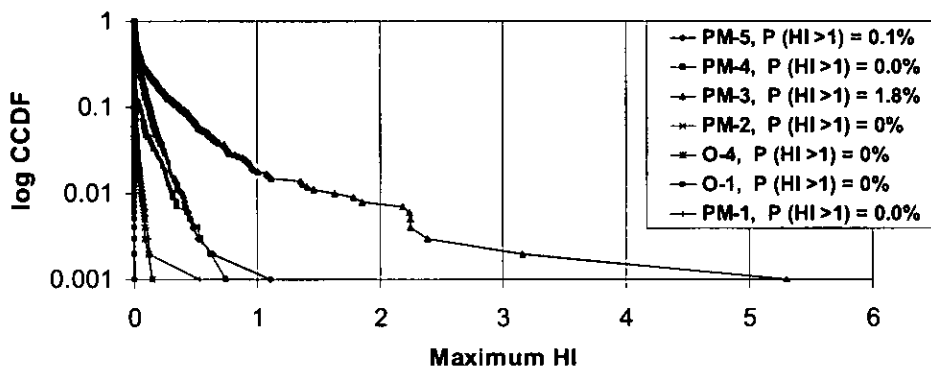


Figure C-4.16. CCDF for lower-canyon-dominated uniform infiltration for perchlorate with regional-aquifer Model A and source term interrupted in 2006, for a 100-yr analysis period (log scale)

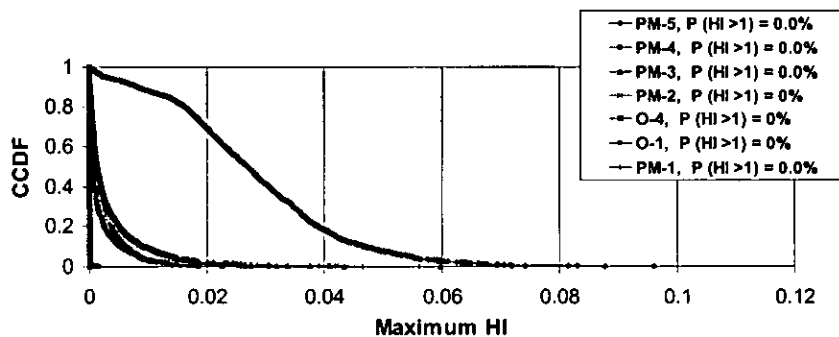


Figure C-4.17. CCDF for lower-canyon-dominated infiltration with fast paths in the upper and middle canyon for perchlorate with regional-aquifer Model B for a 100-yr analysis period (linear scale)

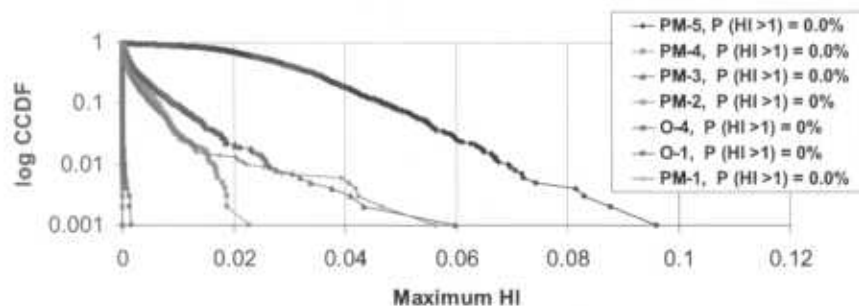


Figure C-4.18. CCDF for lower-canyon-dominated infiltration with fast paths in the upper and middle canyon for perchlorate with regional-aquifer Model B for a 100-yr analysis period (log scale)

### FIGURES OF COMPLEMENTARY CUMULATIVE DISTRIBUTION FUNCTION FOR TRITIUM DOSE FOR 100 YEARS ANALYSIS

(Doses were computed according to 40CFR141.66 maximum contaminants level for radionuclides, Table A.)

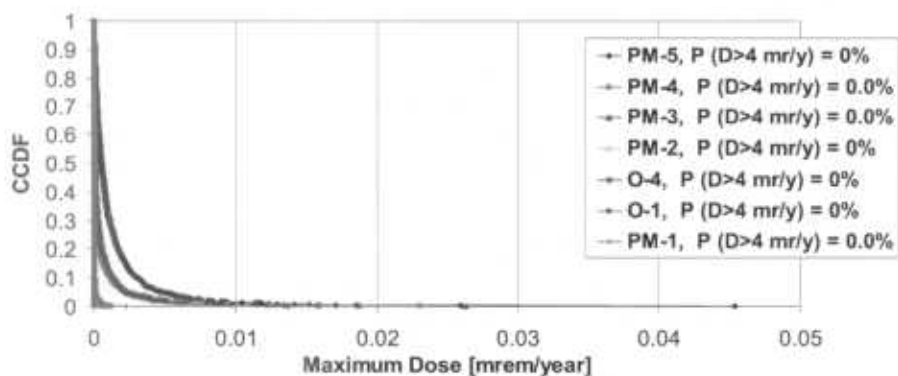


Figure C-4.19. CCDF for lower-canyon-dominated infiltration with fast paths in the upper, middle, and lower canyons for tritium with regional-aquifer Model A for a 100-yr analysis period (linear scale)

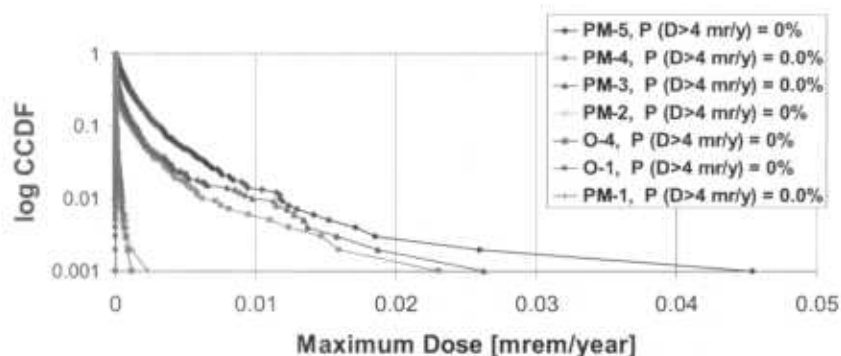


Figure C-4.20. CCDF for lower-canyon-dominated infiltration with fast paths in the upper, middle, and lower canyons for tritium with regional-aquifer Model A for a 100-yr analysis period (log scale)

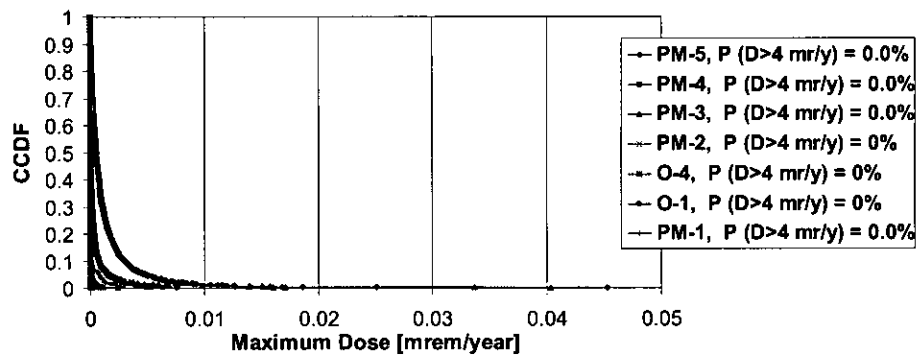


Figure C-4.21. CCDF for lower-canyon-dominated infiltration with fast paths in the upper and middle canyons for tritium with regional-aquifer Model A for a 100-yr analysis period (linear scale)

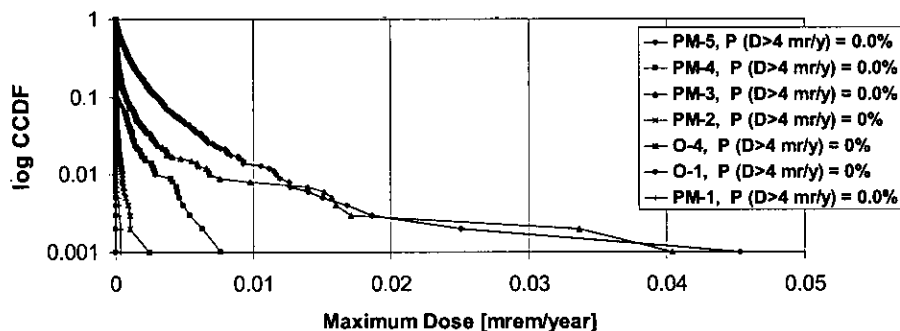


Figure C-4.22. CCDF for lower-canyon-dominated infiltration with fast paths in the upper and middle canyons for tritium with regional-aquifer Model A for a 100-yr analysis period (log scale)

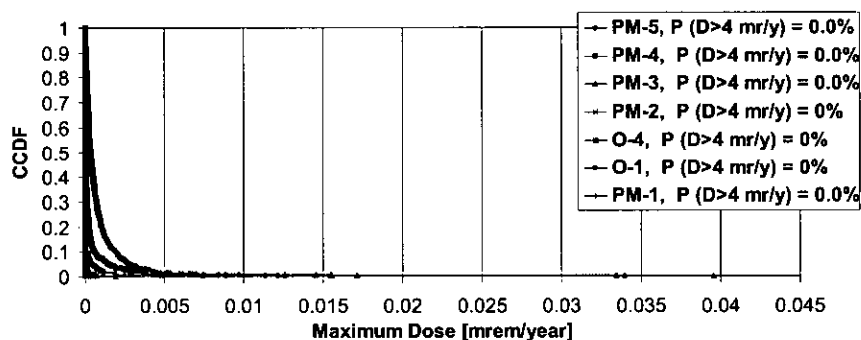


Figure C-4.23. CCDF for lower-canyon-dominated infiltration with fast path in the upper canyon for tritium with regional-aquifer Model A for a 100-yr analysis period (linear scale)

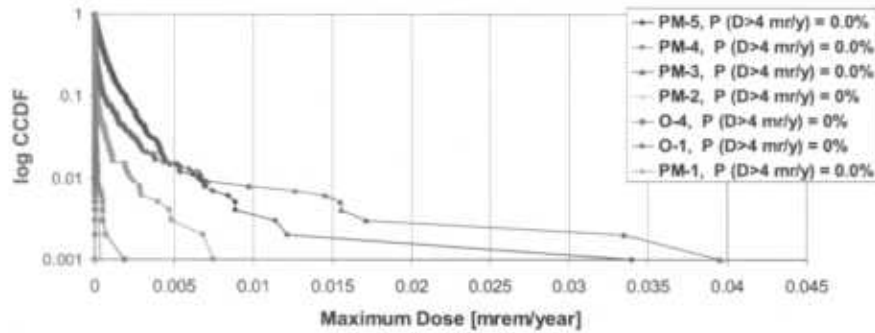


Figure C-4.24. CCDF for lower-canyon-dominated infiltration with fast path in the upper canyon for tritium with regional-aquifer Model A for a 100-yr analysis period (log scale)

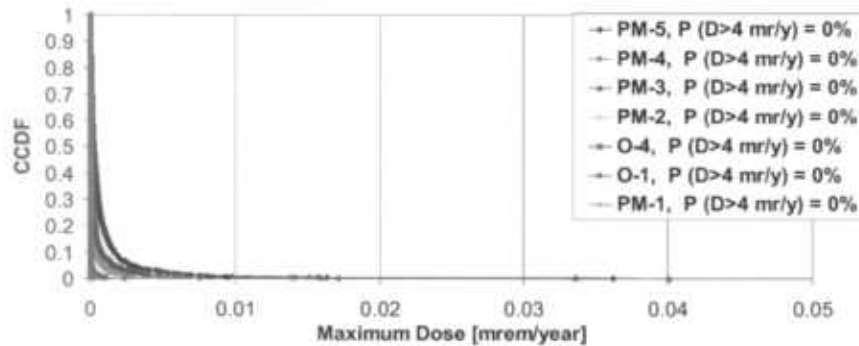


Figure C-4.25. CCDF for lower-canyon-dominated infiltration with fast path in the middle canyon for tritium with regional-aquifer Model A for a 100-yr analysis period (linear scale)

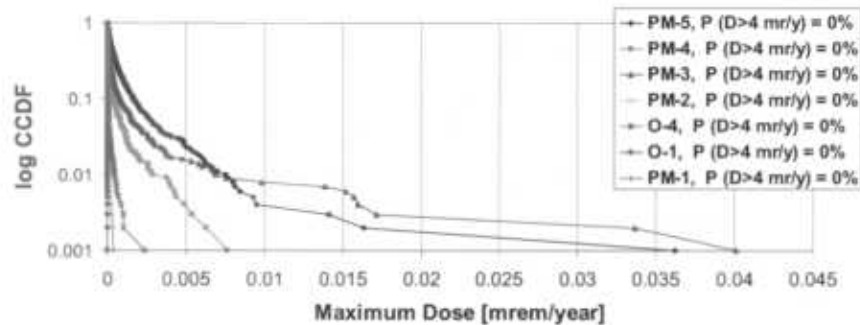


Figure C-4.26. CCDF for lower-canyon-dominated infiltration with fast path in the middle canyon for tritium with regional-aquifer Model A for a 100-yr analysis period (log scale)

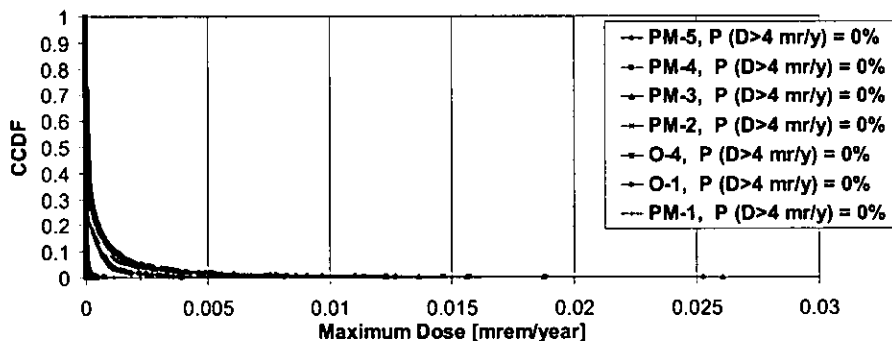


Figure C-4.27. CCDF for lower-canyon-dominated infiltration with fast path in the lower canyon for tritium with regional-aquifer Model A for a 100-yr analysis period (linear scale)

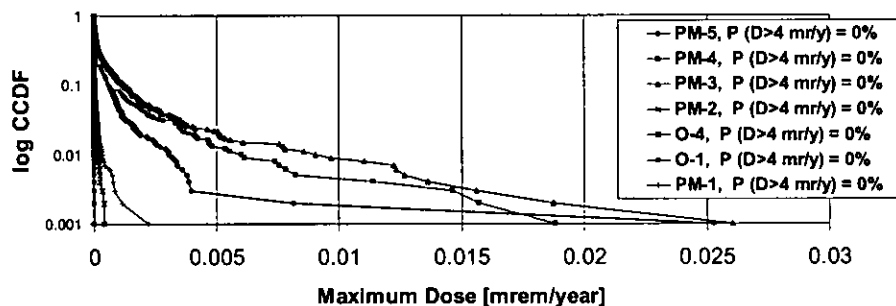


Figure C-4.28. CCDF for lower-canyon-dominated infiltration with fast path in the lower canyon for tritium with regional-aquifer Model A for a 100-yr analysis period (log scale)

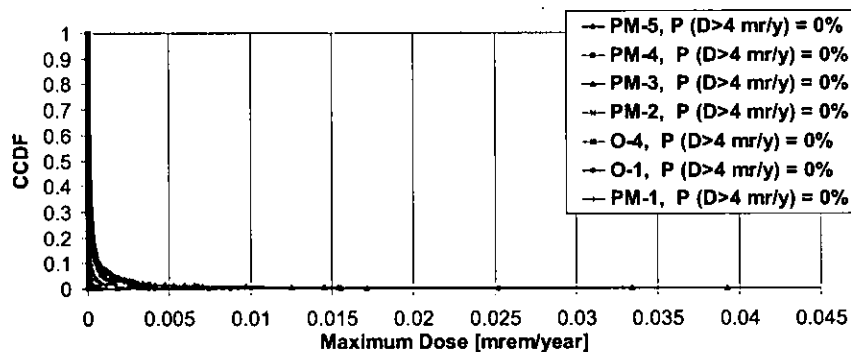


Figure C-4.29. CCDF for lower-canyon-dominated uniform infiltration for tritium with regional-aquifer Model A for a 100-yr analysis period (linear scale)

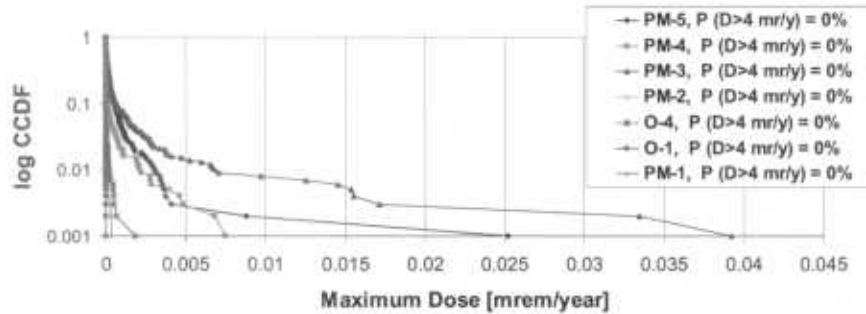


Figure C-4.30. CCDF for lower-canyon-dominated uniform infiltration for tritium with regional-aquifer Model A for a 100-yr analysis period (log scale)

FIGURES OF COMPLEMENTARY CUMULATIVE DISTRIBUTION FUNCTION FOR HI FOR 1000-YR ANALYSIS

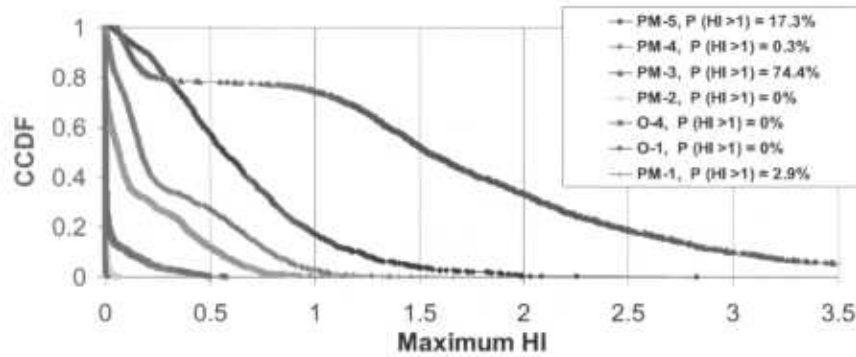


Figure C-4.31. CCDF for upper/middle-canyon-dominated uniform infiltration for perchlorate and nitrate with regional-aquifer Model A for a 1000-yr analysis period (linear scale)

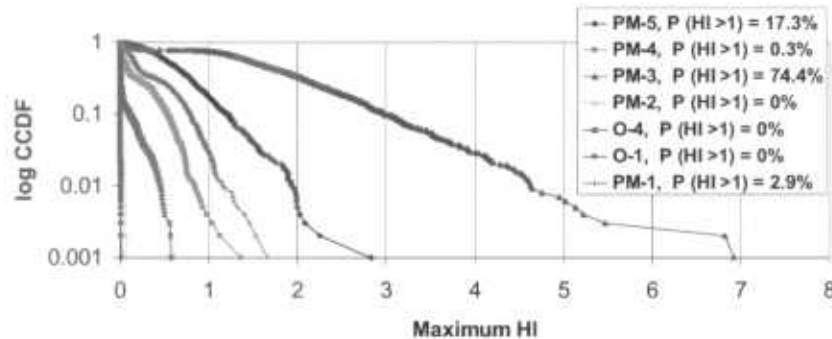


Figure C-4.32. CCDF for upper/middle-canyon-dominated uniform infiltration for perchlorate and nitrate with regional-aquifer Model A for a 1000-yr analysis period (log scale)

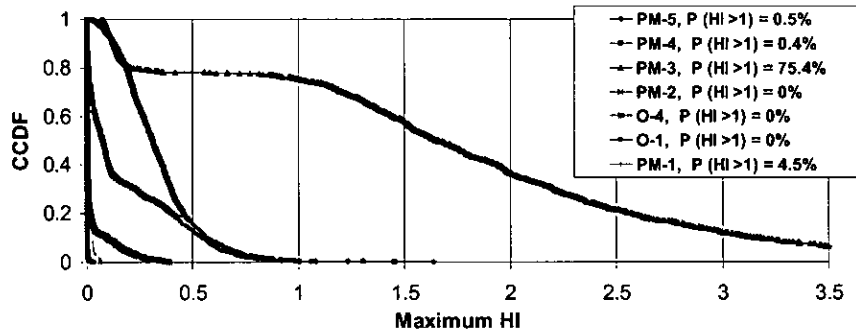


Figure C-4.33. CCDF for lower-canyon-dominated infiltration with fast paths in the upper, middle, and lower canyons for perchlorate and nitrate with regional-aquifer Model A for a 1000-yr analysis period (linear scale)

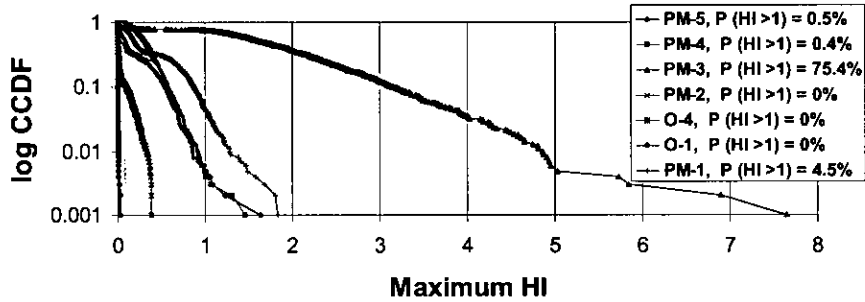


Figure C-4.34. CCDF for lower-canyon-dominated infiltration with fast paths in the upper, middle, and lower canyons for perchlorate and nitrate with regional-aquifer Model A for a 1000-yr analysis period (log scale)

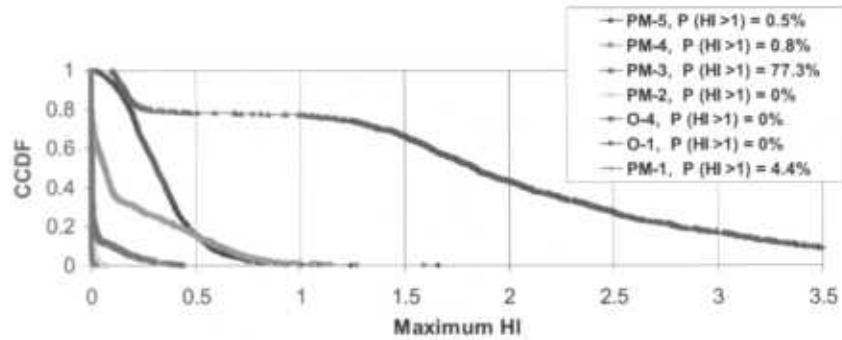


Figure C-4.35. CCDF for lower-canyon-dominated infiltration with fast paths in the upper and middle canyons for perchlorate and nitrate with regional-aquifer Model A for a 1000-yr analysis period (linear scale)

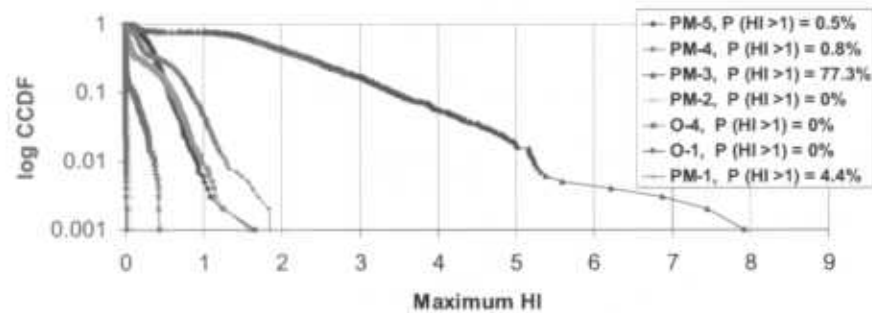


Figure C-4.36. CCDF for lower-canyon-dominated infiltration with fast paths in the upper and middle canyons for perchlorate and nitrate with regional-aquifer Model A for a 1000-yr analysis period (log scale)

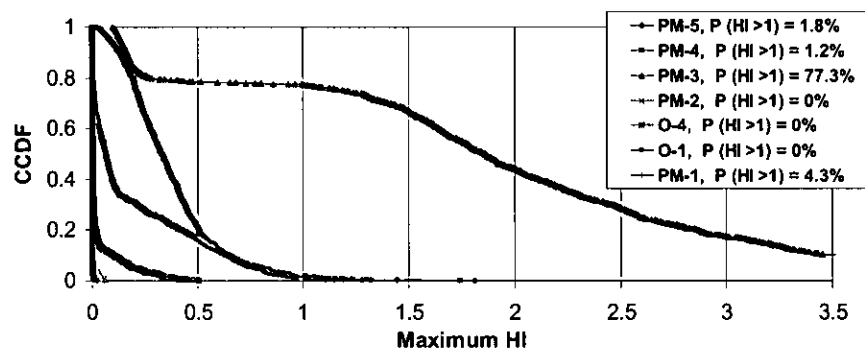


Figure C-4.37. CCDF for lower-canyon-dominated infiltration with fast path in the upper canyon for perchlorate and nitrate with regional-aquifer Model A for a 1000-yr analysis period (linear scale)

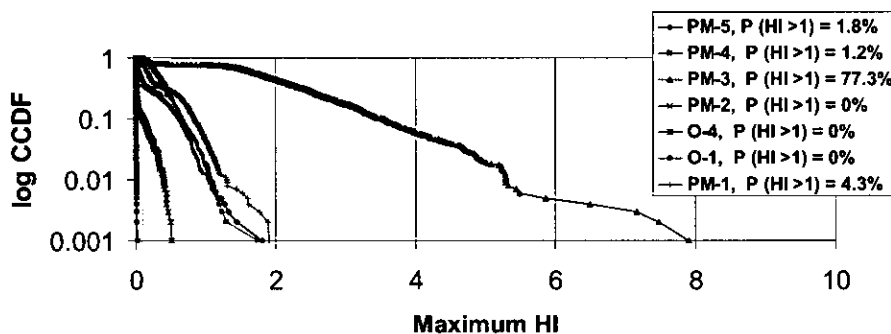


Figure C-4.38. CCDF for lower-canyon-dominated infiltration with fast path in the upper canyon for perchlorate and nitrate with regional-aquifer Model A for a 1000-yr analysis period (log scale)

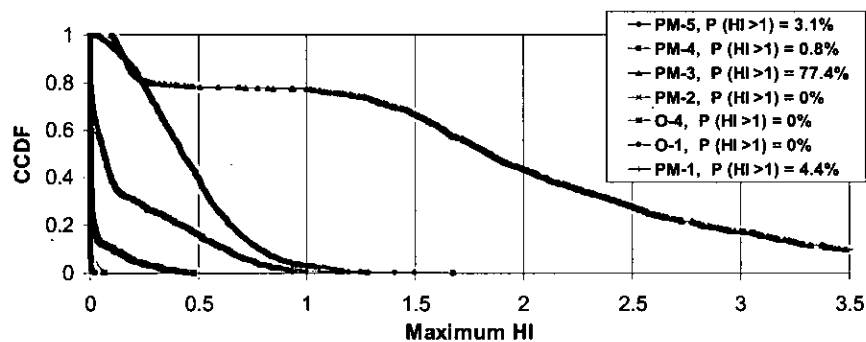


Figure C-4.39. CCDF for lower-canyon-dominated infiltration with fast path in the middle canyon for perchlorate and nitrate with regional-aquifer Model A for a 1000-yr analysis period (linear scale)

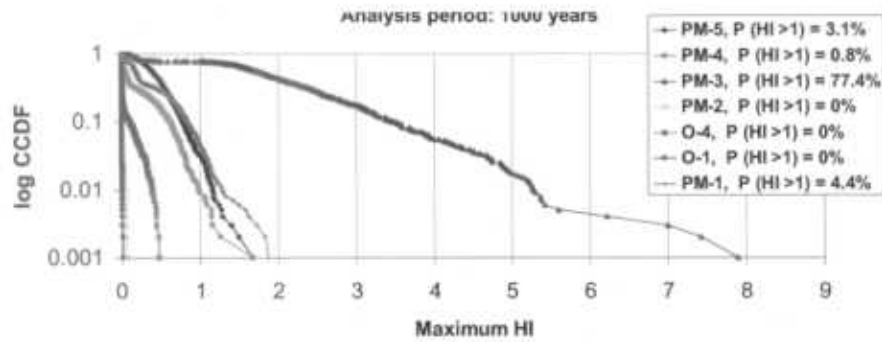


Figure C-4.40. CCDF for lower-canyon-dominated infiltration with fast path in the middle canyon for perchlorate and nitrate with regional-aquifer Model A for 1000-yr analysis period (log scale)

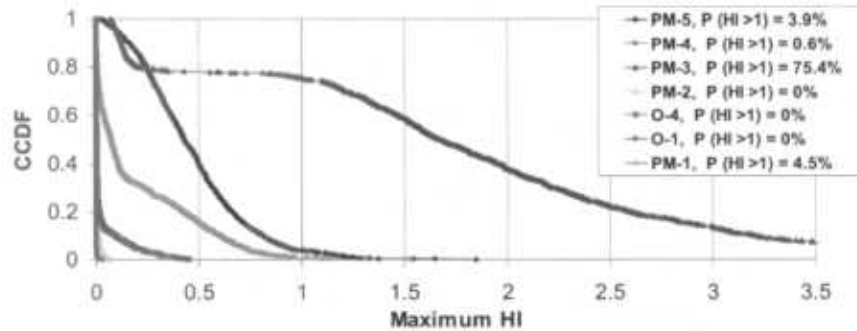


Figure C-4.41. CCDF for lower-canyon-dominated infiltration with fast path in the lower canyon for perchlorate and nitrate with regional-aquifer Model A for a 1000-yr analysis period (linear scale)

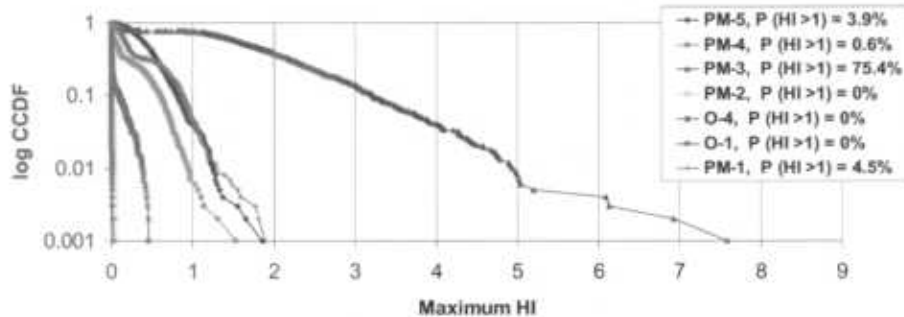


Figure C-4.42. CCDF for lower-canyon-dominated infiltration with fast path in the lower canyon for perchlorate and nitrate with regional-aquifer Model A for a 1000-yr analysis period (log scale)

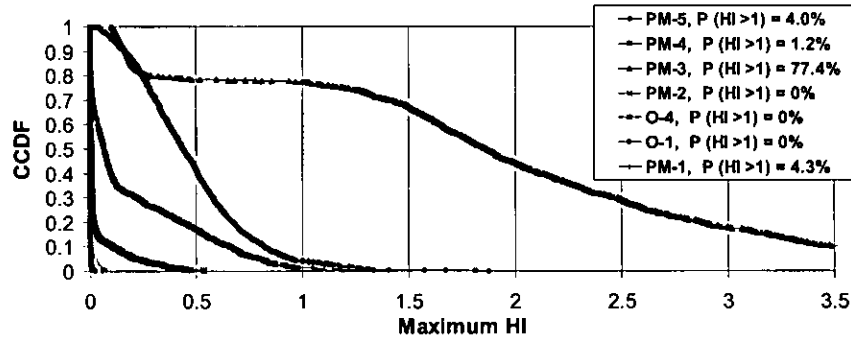


Figure C-4.43. CCDF for lower-canyon-dominated uniform infiltration for perchlorate and nitrate with regional-aquifer Model A for a 1000-yr analysis period (linear scale)

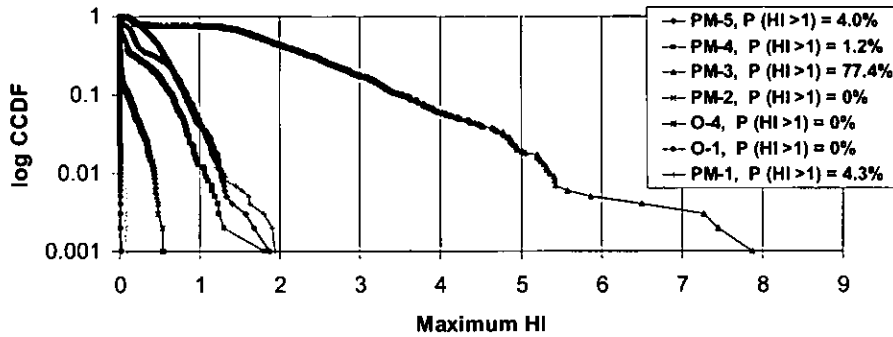


Figure C-4.44. CCDF for lower-canyon-dominated uniform infiltration for perchlorate and nitrate with regional-aquifer Model A for a 1000-yr analysis period (log scale)

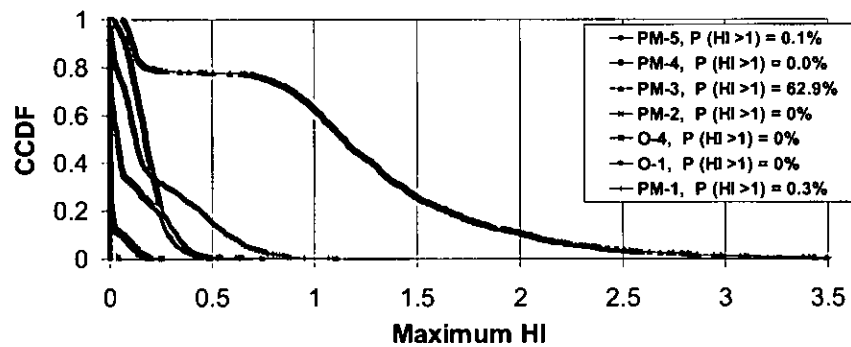


Figure C-4.45. CCDF for lower-canyon-dominated uniform infiltration for perchlorate with regional-aquifer Model A and source term interrupted in 2006 for a 1000-yr analysis period (linear scale)

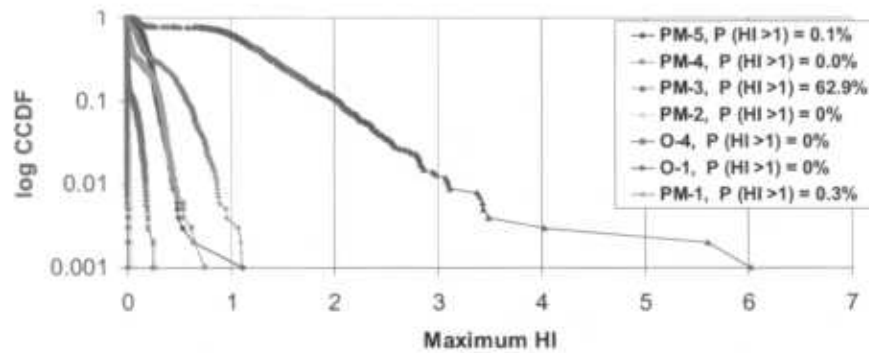


Figure C-4.46. CCDF for lower-canyon-dominated uniform infiltration for perchlorate with regional-aquifer Model A and source term interrupted in 2006 for a 1000-yr analysis period (log scale)

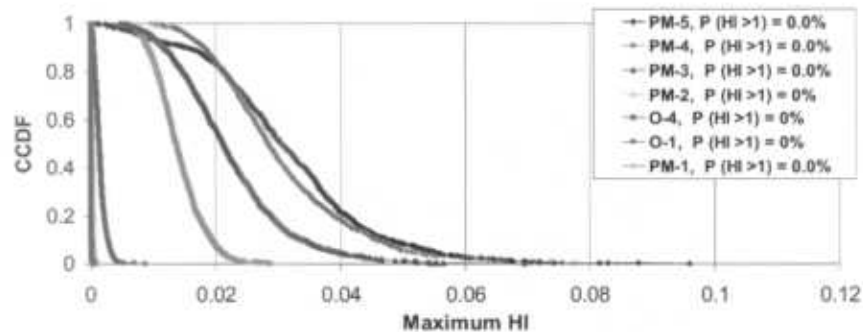


Figure C-4.47. CCDF for lower-canyon-dominated infiltration with fast paths in the upper and middle canyons for perchlorate with regional-aquifer Model B for a 1000-yr analysis period (linear scale)

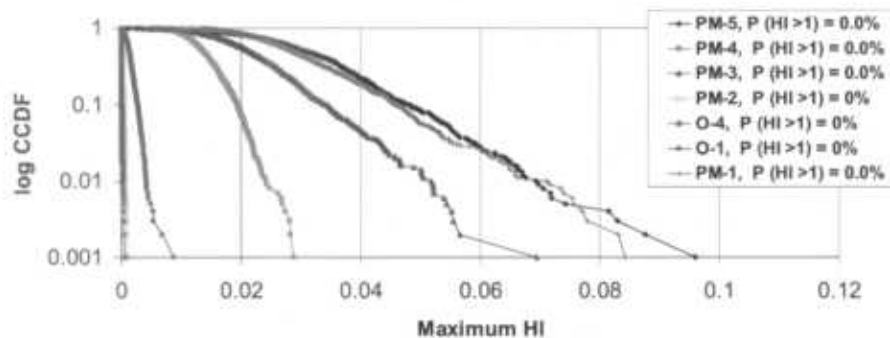


Figure C-4.48. CCDF for lower-canyon-dominated infiltration with fast paths in the upper and middle canyons for perchlorate with regional-aquifer Model B for a 1000-yr analysis period (log scale)

### C-5.0 SUMMARY OF RESULTS

The analysis for the 100-yr simulation period results in a confidence level of more than 95% that HI are less than 1.0 and that doses are less than 4 mrem/yr for all conceptual models. The maximum HI obtained for all wells and conceptual models is about 6.5 and corresponds to PM-3 for the lower-canyon-dominated infiltration with fast paths in the upper and middle canyons for perchlorate and nitrate with regional-aquifer Model A. Maximum HIs for PM-3 are greater than 1.0 for all conceptual models except for regional-aquifer conceptual Model B. Maximum HIs are also greater than 1.0 for PM-4 and PM-5 for the 100-yr period.

The Tier-3 risk assessment was performed for a 1000-yr simulation period only for HQs and HIs, because the maximum tritium doses occurred within the first 100-yr period because of tritium's short half life (12.3 yr).

Regional-aquifer conceptual Model B has no HIs greater than 1.0 for any production well. However, regional-aquifer conceptual Model A has a probability of exceedance of between 74.4% and 77.4% for PM-3 for all conceptual models, except when the source term is interrupted in 2006. This conceptual model has a 62.9% probability of exceedance for PM-3. The maximum HI for all PM-3 simulations is below 8.0. PM-5 has a probability of exceedance of 17.3% only for the upper/middle-canyon-dominated uniform infiltration for perchlorate and nitrate with regional aquifer Model A. Exceedance probabilities are below 5% for PM-5 for all other conceptual models. The maximum HI for PM-5 for all simulations is 2.8.

An analysis of the effect of larger perchlorate RfDs indicates that the probability that an HI will exceed 1.0 is zero if an RfD of 0.00024 mg/kg/day is assumed. This RfD is equivalent to an MCL of 8 µg/L. The EPA had recently published an RfD for perchlorate of 0.0007 mg/kg/day, which is equivalent to an MCL of 24.5 µg/L (EPA's Integrated Risk Iris Database (IRIS), 2005, 90508).

### C-6.0 REFERENCES

*The following list includes all documents cited in this document. Parenthetical information following each reference provides the author, publication data, and ER ID number. This information is also included in text citations. ER ID numbers are assigned by the ENV-ERS Records Processing Facility (RPF) and are used to locate the document at the RPF.*

DOE (U.S. Department of Energy) Order 5400.5, Change 2, 1993. "Radiation Protection of the Public and the Environment," U.S. DOE, Washington, D.C. [Electronic copy: Folder "RagsV1A" L by chapters in 19 pdf files]. (DOE 1993, 90190)

EPA (U.S. Environmental Protection Agency), 1989. Risk Assessment Guidance for Superfund (RAGS): Volume I. *Human Health Evaluation Manual. (Part A. Baseline Risk Assessment). Interim Final.* Office of Emergency and Remedial Response, Washington, DC. EPA/540/1-89/002, December 1989. (EPA 1989, 08021)

EPA (U.S. Environmental Protection Agency) (web page), September 2003. "Perchlorate Environmental Contamination: Toxicological Review and Risk Characterization," (2002 External Review Draft) [Electronic copy: National Center for Environmental Assessment—EIMS Record Results.htm]. (EPA 2003, 90507)

EPA, (U.S. Environmental Protection Agency) (web page), May 2003. Groundwater and Drinking Water. Perchlorate. [Electronic copy: EPA Ground Water & Drinking Water Perchlorate.htm]. (EPA, 2003, 90505)

EPA (U.S. Environmental Protection Agency) Integrated Risk Iris Database (IRIS) web page, 2005. Perchlorate and Perchlorate Salts. (Visited July 2005) ([www.epa.gov/iris/subst/1007.htm](http://www.epa.gov/iris/subst/1007.htm)) [Electronic copy: Perchlorate and Perchlorate Salts, IRIS, Environmental Protection Agency.htm]. (EPA 2005, 90508)

Greer, M.A., Goodman, G., Pleuss, R.C., and Greer, S.E., 2002. "Health Effect Assessment for Environmental Perchlorate Contamination: The Dose Response for Inhibition of Thyroidal Radioiodide Uptake in Humans," *Environ. Health Perspective*, Vol. 110, pp. 927–937. (Greer et al. 2002, 90189)

**RRES-RS Document Signature Form** Read/Write Access Person Making Entry is WIN/106229/Unknown (Created on 8/8/2005)


Printable Page

**Document Catalog Number ER2005-0580** (Please prefix the name of all electronic versions of this document with this number.)

\* Required Field

<b>*Document Title / Subject</b>	Decision Anaylsis for Addressing Groundwater Contaminants from the Radioactive LiquidWaste Treatment Facility Released into Mortandad Canyon	
<b>PRs</b>	None	
<b>Associated Document Catalog Number(s)</b>	None	
<b>*Author</b>	Echohawk, John (Chris) C <input type="checkbox"/> 667-9049	echohawk@lanl.gov
<b>*Author Organization</b>	Analysis & Assessment <input type="checkbox"/>	
<b>Document Team</b>	Amador, Mable I Editor 665-0528	amador@lanl.gov
	Moore, Randi L. Compositor 665-7268	randim@lanl.gov
<b>*Document Type</b>	Technical Papers/Report, Journa Article <input type="checkbox"/>	<b>Former OU</b> N/A <input type="checkbox"/>
<b>Date Due</b>	<b>Date Final Complete</b>	<b>Date Sent to DOE</b>
<b>Date Sent to NMED</b>	<b>Date Sent to RPF (Paper &amp; Electronic)</b>	
<b>Received Per RPF</b>	<b>RPF ER ID Number</b>	
<b>CT No</b>	<b>LA-UR Number</b>	
<b>Performance Measure No</b>		
<b>AA Deliverable</b> <input type="checkbox"/>	<b>Certification Required</b> <input type="checkbox"/>	<b>Force Peer Review</b> <input type="checkbox"/>
<b>Distribution TO:</b>		
<b>Distribution FROM:</b>		
<b>Distribution COPY:</b>		
<b>Distribution THRU:</b>		
<b>Attachment Notes</b>		
<b>Status/Comments</b>		

**Reviewer Signatures:** (By signing, the reviewer indicates that he/she reviewed and approves the document.)

Reviewer (Print reviewer's name under title)	Signature	Date
Author CHRIS ECHOHAWK	<i>J. Chris Echowawk</i>	1/23/06
Peer Review Chair DAVE BROXTON	<i>David Broxton</i>	1/24/06
Solid Waste Regulatory Compliance (SWRC) N/A	_____	_____
LANL Legal Reviewer		
DOE/LASO Reviewer N/A	_____	_____
Project Leader CHRIS ECHOHAWK	<i>J. Chris Echowawk</i>	
Program Manager JEAN DEWART	<i>Jean Dewart</i>	2/3/06

Document Catalog Number ER2005-0580

Top

DOC SIG FORM FOR DOCUMENT: DECISION ANALYSIS FOR  
ADDRESSING GROUNDWATER  
... MORTANDAD CANYON